JOHANNES GUTENBERG UNIVERSITÄT MAINZ

Elucidating the role of the transcription factor interferon regulatory factor 4 in differentiated T helper 17 and regulatory T cells

---

Dissertation for the degree

Doctor of Natural Sciences (Dr. rer. nat.)

Department of Biology

Johannes Gutenberg-University, Mainz

Anna Maria Christina Gabele

born 20.02.1992 in Regensburg

Mainz, 2024

Dean: Prof. Dr. Eckhard Thines

1. Examiner:

2. Examiner:

Day of oral examination: 19.12.2024

TABLE OF CONTENT

LIST OF FIGURES

LIST OF TABLES

ABBREVIATION

°C	Degree Celsius
µL	Microlitre
A3AR	Adenosine A3 receptor
AHR	Aryl hydrocarbon receptor
AICE	AP-1-IRF composit element
APC	Antigen presenting cell
ATL	Adult T cell leukemia/lymphoma
BATF	Basic leucine zipper ATF-like transcription factor
BirA	Biotin ligase BirA
Blimp-1	B lymphocyte-induced maturation protein 1
bp	Base pair
CD	Cluster of differentiation
ChIP-seq	Chromatin immune precipitation followed by sequencing
CLL	Chronic lymphocytic leukemia
CML	Chronic myeloid leukemia
CTL	Cytotoxic lymphocytes
DBD	DNA-binding domain
DIA	Data independent acquisition
DMSO	Dimethyl sulfoxide
DNA	Deoxyribonucleic acid
DSP	Dithiobis(succinimidylpropionate)
DTT	1,4-Dithiothreitol
EAE	Experimental autoimmune encephalomyelitis
EICE	Ets-IRF composit element
EMSA	Electrophoretic mobility shift assay
FACS	Fluorescent activated cell separation/sorting
FICZ	6-Formylindolo [3,2-b] carbazole
FLI1	Friend leukemia virus integration 1
Fosl2	Fos-related antigen 2
FoxP3	Foxhead box protein 3
Fwd	Forward
GO	Gene ontology
GRK2	G-protein-coupled receptor kinase 2
HIF1α	Hypoxia-inducible factor 1α
HPO	Horseradish peroxidase
IAA	Iodoacetamide
IAD	IRF-associated domain
IBD	Inflammatory dowel disease
ICOS	Inducible T cell co-stimulator

IFN-γ	Interferon gamma
IgG	Immunoglobulin G
IKZF	Ikaros family zinc finger protein
IL	Interleukin
IRF(4)	Interferon regulatory factor (4)
ISRE	Interferon stimulated response elements
ITK	IL-2 inducible T cell kinase
JAK3	Janus kinase
kDa	Kilo Dalton
LPS	Lipopolysaccharides
MACS	Magnetic activated cell sorting
MAR	Missing at random
MHC	Major histocompatibility complex
min	Minutes
mL	Millilitre
MM	Multiple Myeloma
MNAR	Missing not at random
mRNA	messenger ribonucleic acid
mTOR	Mammalian target of rapamycin
NaCl	Sodium chloride
nd	Not determined
NFAT	Nuclear factor of activated T cells
nL	Nanolitre
ns	Not significant
PD1	Programmed cell death protein 1
PIC	Protease inhibitor cocktail
PMA	Phorbol-12-myristat-13-acetate
PP6	Protein phosphatase 6
PSSM	Position specific scoring matrix
qPCR	Quantitative polymerase chain reaction
RA	Rheumatoid arthritis
Rev	Reverse
RFX1	Regulatory factor X 1
RORγ	RAR-related orphan receptor gamma
rpm	Rounds per minute
Runx	Runt-related transcription factor
s	Seconds
SATB1	Special AT-rich sequence binding protein 1
SLE	Systemic lupus erythematosus
SNP	Single nucleotide polymorphism
SP3	Single-pot solid-phase-enhanced sample preparation

STAT	Signal transducer and activator of transcription
TCDD	2,3,7,8-Tetrachlorodibenzo-p-dioxin
TCR	T cell receptor
TGF-β	Transforming growth factor beta
Th	T helper cell
TIGIT	T cell immunoreceptor with immunoglobulin and ITIM domain
TLR	Toll-like receptor
Treg	Regulatory T cell
TSS	Transcription start site
USP	Ubiquitin specific peptidase
UTR	Untranslated region

I. INTRODUCTION

1.1 Development of CD4$^+$ T cells

An immune response is a complex interplay of different immune cells that fights infiltrating pathogens to subsequently eliminate the invader. Innate immune cells, such as mast cells, dendritic cells, granulocytes and macrophages, are among the first line of defence and exert a broad and less specific immune response. In contrast, cells of the adaptive immune system, such as the bone marrow-derived B lymphocytes (B cells) and the thymus-derived T lymphocytes (T cells), exert a specified response against a pathogen. As T and B cells proliferate only after engagement of the antigen, the adaptive response has a delayed onset and is only triggered temporarily. However, some cells can develop an immunological memory, which leads to a faster immune response and clearance after re-encountering the same invader. T cells are the cellular part of the adaptive immune response while B cells are considered the humoral part. All T cells express a specific T cell receptor (TCR), which recognizes and interacts with antigens presented on major histocompatibility complexes (MHC), and non-covalent attached CD3 (cluster of differentiation) molecules, which are essential for the intracellular signalling and activation of downstream processes. Based on the expression of the co-receptor, T lymphocytes can be further divided into two subtypes: CD8$^+$ cytotoxic T cells (around one third) and CD4$^+$ T helper cells (two thirds). As the name suggests, CD4$^+$ T helper cells 'help' and support the elimination of mainly extracellular bacteria through the secretion of particular cytokines or activation of specific immune cells, while cytotoxic T cells mostly eliminate virus infected cells (Chaplin, 2010; Luckheeram et al., 2012; Murphy et al., 2016).

The generation of immune cells takes place in the primary lymphatic tissue, e.g. bone marrow or thymus, while the activation and differentiation of immune cells occurs in secondary lymphatic tissue, such as lymph nodes, spleen or Peyer's patches. A total a three signals, including the close interaction of T cells and antigen-presenting cells (APCs), the so called the immunological synapse, are required to induce effector T cell differentiation. First, naïve T cells have to encounter the matching antigen-peptide for their receptor presented on an MHC molecule of an antigen-presenting cell (APC), which are mostly dendritic cells, to become activated. CD4$^+$ T cells detect antigens on MHCII molecules while CD8$^+$ T cells match with peptides presented on MHCI molecules. The second signal is a co-stimulatory signal which promotes the survival and proliferation of the cell. The third and last signal is derived from the cytokine milieu in which the naïve cell encounters the antigen, simultaneously defining the subset of helper cell to which the cells differentiate. The concentration of antigens as well as the type of APC also influences the outcome of T cell activation. In the CD4$^+$ T helper compartment, T helper 1 (Th1), T helper 2 (Th2), T helper 9 (Th9), T helper 17 (Th17) and regulatory T cells (Tregs) are the major subsets to which a naïve T cell can differentiate. Each subtype is characterized by the expression of a particular transcription factor (TF), the secretion of a characteristic cytokine set and its effector function (see Figure 1).

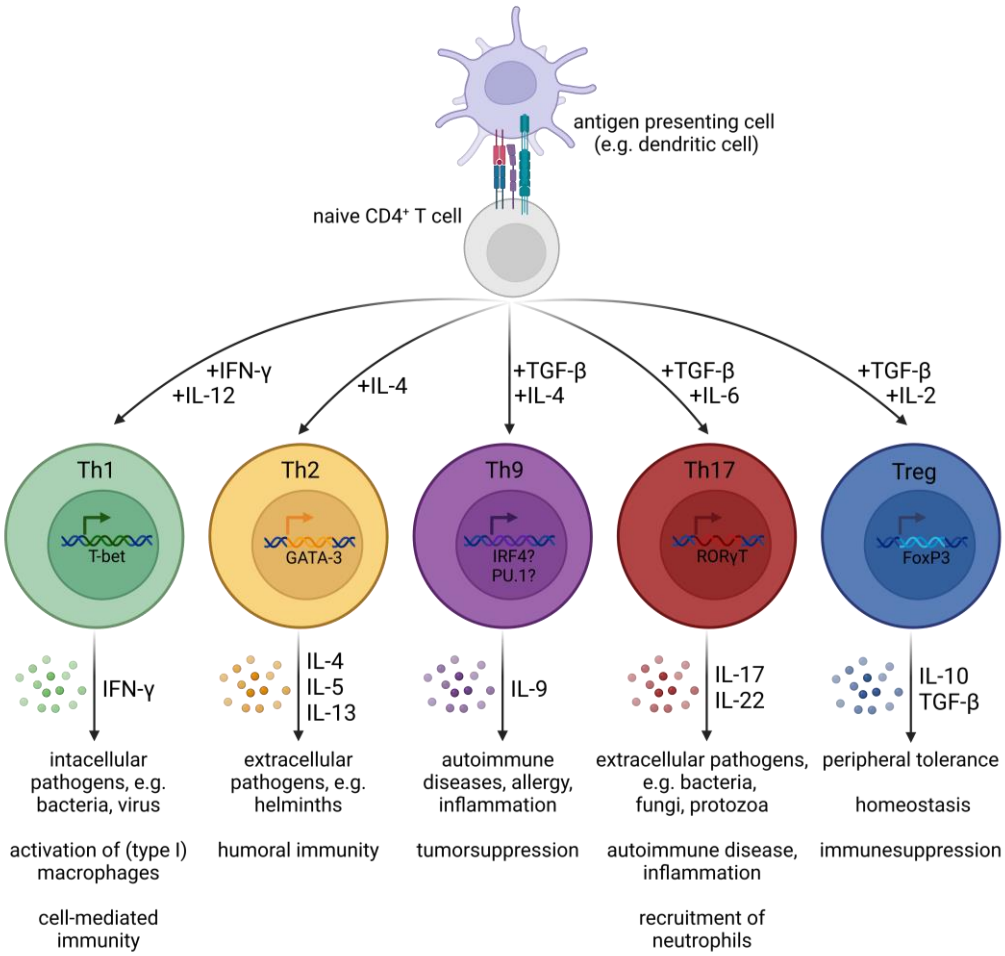

Figure 1: Overview of different CD4⁺ T cell subtypes. Upon stimulation, naïve CD4⁺ T cells can differentiate into different T cell subtypes. The figure above shows important cytokines for T cell fate. In addition, the master transcription factors, characteristic secreted cytokines and main effector functions of differentiated effector cells are summarized.

IFNγ-secreting Th1 cells express the master transcription factor T-bet and activate type I macrophages for the defence of intracellular pathogens, e.g. bacteria or viruses. The Th2 subset is characterized by expressing the transcription factor GATA3 and secreting interleukin (IL)-4 to protect from large extracellular pathogens, e.g. helminths. The production of IL-9 is typical of the Th9 subset, which, however, lacks a lineage-specific transcription factor. A number of TFs, including PU.1, IRF4, GATA3, STAT6 and ETV5, are involved in the development of Th9 cells and contribute to the debated inflammatory and anti-tumoral nature (Cui, 2019; Kaplan, 2013). Th17 cells are a subset involved in the defence of extracellular bacteria, fungi and some protozoa. They secrete IL-17A, IL-17F, IL-22 and express the master transcription factor RORγT (RAR-related orphan receptor gamma). Treg cells, on the other hand, are important for maintaining immune tolerance and preventing autoimmune/inflammatory diseases through the secretion of anti-inflammatory cytokines such as IL-10 or transforming growth factor (TGF-β). The characteristic transcription factor of Tregs is forkhead box protein 3 (FoxP3) (Chaplin, 2010; Cui, 2019; Luckheeram et al., 2012; Murphy et al., 2016; Zhu & Zhu, 2020). Further detailed information about Th17 and Treg cells can be found in chapters 1.2 and 1.3.

1.2 T helper 17 cells (Th17)

In 2005, Th17 cells were discovered to be pro-inflammatory cells that are important for defending against extracellular bacteria and fungi. However, Th17 cells have also been described in the context of inflammatory diseases, autoimmune disorders, tumorigenesis and transplant rejection. In humans, the chemokine receptor CCR6 is a unique marker that distinguishes $CCR6^+$ $CXCR3^-$ Th17 cells from $CCR6^-$ $CXCR3^+$ Th1 cells. CCR6 mediates skin and mucosal tissue homing of T cells, causing the infiltration of pathogenic cells and inducing inflammatory diseases, such as psoriasis or inflammatory bowel disease (IBD), in these tissues (Tesmer et al., 2008; X. Zhu & Zhu, 2020). *In vivo*, the secretion of IL-1β, IL-6 and IL-23 by APCs is needed to induce and enhance the development and effector functions of Th17 cells while *in vitro* the cytokines IL-6, IL-21 and TGF-β are used (Tesmer et al., 2008; Zhou & Littman, 2009). Downstream of the cytokine receptors, signal transducer and activator of transcription 3 (STAT3) is induced, which further activates the expression of interferon regulatory factor 4 (IRF4) and the master transcription factor RORγT. The NFAT/NF-κB/AP-1 pathway downstream of the TCR can also induce the expression of RORγT. In cooperation with IRF4, basic leucine zipper ATF-like transcription factor (BATF) and Runt-related transcription factor 1 (Runx1), the master transcription factor RORγT promotes the expression of Th17-characteristic genes, such as *Il17a*, *Il17f, Il21* or *Il22* (Bandini et al., 2018; Tesmer et al., 2008; Zhou et al., 2009). Animals lacking RORγT have a dysregulated T cell compartment, strong down-regulation of Th17 differentiation, no lymph nodes or Payer's patches and delayed onset of autoimmune disorders, e.g. experimental autoimmune encephalomyelitis (EAE). In addition, these mice are prone to developing lymphoma (Ivanov et al., 2006; Liljevald et al., 2016; Ruan et al., 2011; X. Zhu & Zhu, 2020). Other diseases are also described in the context of non-functional Th17 cells: patients with chronic candidiasis have a mutation in the *Rorc* gene (coding for RORγT) that is also connected with a lack of Th17 cells. Mutations in the *Stat3* (coding for the corresponding protein) or *Dock8* gene are described in many patients with hyper-IgE syndrome, a primary immunodeficiency disorder, who also have a deficiency in Th17 cells (Tesmer et al., 2008; X. Zhu & Zhu, 2020). In addition, murine studies show that if STAT3 is absent, cells fail to differentiate into Th17 cells (no IL-17 secretion) and do not induce EAE (Barbi et al., 2013). On the other hand, strong secretion of IL-17 or expression of other Th17 cell characteristics is associated with several autoimmune and inflammatory diseases: for example, rheumatoid arthritis (RA) is an IL-17 (and IL-23)-driven disease characterized by chronic inflammation in different joints. Psoriasis, a chronic inflammatory disease of the skin, shows elevated levels of IL-17A and IL-17F in the inflamed tissue as well as the serum. In a phase II clinical study, interference of the IL-23 signalling pathway indicated promising results to treat psoriasis patients. IL-17 has also been shown to be a pathogenic factor for the development of multiple sclerosis, clinically manifested by the demyelination of neurons, in different studies where the absence of Th17 cells prevented the development of EAE in mice. Ultimately, using antibodies to interfere with the development of Th17 cells or the secretion of their effector cytokines is a promising therapy target or has already proven to be a successful treatment for Th17-associated diseases (Tesmer et al., 2008; X. Zhu & Zhu, 2020).

1.3 Regulatory T cells (Tregs)

Regulatory T cells (Tregs) are a subset of anti-inflammatory $CD4^+$ T cell subset, which was first described in 1995 by Sakaguchi and his colleagues (Sakaguchi et al., 1995). This cell type plays an important role in the maintenance of self-tolerance and prevention of autoimmune/inflammatory diseases and cancer development. In 2003, the master transcription factor of the formerly described $CD25^+$ T cells, FoxP3, was identified. FoxP3 is essential for the specific development of Treg cells and needs to be maintained for suppressive function (X. Li & Zheng, 2015). Two different types of Treg cells can be distinguished: naturally thymus-derived Treg cells (tTregs or nTregs) and inducible Treg (iTreg) or peripheral Treg (pTreg) cells that differentiate from naïve T cells (*in vitro* studies give rise to iTregs while pTregs develop outside the thymus, especially in the gut, *in vivo*). nTreg cells mainly recognize self-antigens and control self-reactive effector T cells, whereas pTregs also identify non-self-antigens and therefore also maintain the mucosal tolerance in the gut. No explicit markers to discriminate nTreg from pTreg have been found, but in the gut $ROR\gamma T^+$ Treg cells are thought to be pTregs while $GATA3^+$ Treg cells are assumed to be nTregs. To initiate i/pTreg development, the cytokines IL-2 and TGF-β are essential and activate STAT5 (signal transducer and activator of transcription 5) and SMAD2/3 (SMAD family member 2/3), which promote the expression of FoxP3 downstream (X. Li & Zheng, 2015; X. Zhu & Zhu, 2020). FoxP3 is important for the repressive character of Treg cells and the induction of other genes that exert immune-suppressive functions (Barbi et al., 2013). Similar to the Th17 cells, the master transcription factor for Treg cells can be activated through TCR-induced stimulation of the NFAT/NF-κB/AP-1 pathway. Runx1, Nrfa2, Foxo1 and other Foxo family members, SATB1 and Helios are some examples of other transcription factors that can also influence the differentiation and function of Treg cells. The regulatory function of Treg cells is discussed as being due to various mechanisms: 1) expression of regulatory and inhibitory cytokines, e.g. IL-10, TGF-β or IL-35; 2) consumption of IL-2, the motor for other $CD4^+$ T cells to survive and proliferate; 3) expression of negative signal transduction receptors, e.g. CTLA-4, CD39 or CD73; 4) expression of perforin and granzyme B (cytotoxicity); and 5) removal of p:MHCII molecules on APCs in an antigen-specific manner (Alvisi et al., 2020; X. Zhu & Zhu, 2020).

Autoimmune disorders are not only associated with Th17 cells or mutations in Th17-specific genes, but can also be due to mutations in Treg-specific genes or not-fully-functional Treg cells. Mutations in the *Foxp3* gene can lead to severe diseases (IPEX syndrome – often associated with symptoms of autoimmune disorders) or less severe conditions (Th2-related diseases) in humans. Mice (*scurfy* mice) can develop strong symptoms of autoimmunity or multi-organ inflammation, which can be lethal, when carrying a mutation in the gene for the master transcription factor (X. Zhu & Zhu, 2020). Loss of suppressive function and Treg-characteristic gene expression is seen in Treg cells that do not express FoxP3 expression (Williams & Rudensky, 2007). A lethal autoimmune syndrome is also observed when FoxP3 is ablated in the germline (X. Li & Zheng, 2015). In addition, mutations have been observed in other murine genes coding for proteins that are involved in carrying out the repressive function of Treg cells, e.g. IRF4, Blimp-1, Bach2, Ezh2 and SATB1 (X. Zhu & Zhu, 2020). Treg cells with defective suppressor functions have been described in the context of autoimmune diseases, such as multiple

sclerosis, type I diabetes and psoriasis. Decreased levels of Treg cells have been detected in patients suffering from allergies or asthmatic diseases. On the other hand, high amounts of Treg cells were involved in chronic virus infection, where Treg cells probably inhibit the active antiviral immune response. A similar mechanism could be involved in cancer development when Treg cells prevent a good immunological reaction to tumour antigens. The induction of anti-inflammatory cytokines and the transfer of *ex vivo* generated and expanded Treg cells are currently being investigated intensively and could be future therapy approaches (Taams et al., 2006).

1.4 T cell plasticity

T cell plasticity can be defined as the "ability of a single cell to take on characteristics of many T cell subsets simultaneously, or at different times, during the course of its life cycle" (Goldsmith et al., 2021). Loss of cell plasticity is a characteristic of ageing cells, but can also prevent the development of diseases such as autoimmune disorders or tumorigenesis, which could be due to the change in cell fate. T cell plasticity has been described for almost all $CD4^+$ T cell subsets, but especially Th17 cells are reported to be unstable and highly plastic. Th17 cells tend to convert into Th1-like cells, but intermediate phenotypic cells have also been described. Single cell sequencing has revealed a pathogenic-to-regulatory nature of Th17 cells, which were assumed to be a homogenous T cell population. Mechanisms behind the instability of Th17 cells, the so-called "dichotomous nature" (Stockinger & Omenetti, 2017) of Th17 cells, are not fully understood. Alterations in metabolism, e.g. nutrients, oxygen levels or energy sources, have been recently discussed as influencing $CD4^+$ T cell plasticity. However, environmental factors such as sodium chloride, microbiota and angiogenesis, as well as epigenetic changes with subsequent differences in gene expression profiles, are also debated to influence cell plasticity. An example is the *Foxp3* promoter in Th17 cells, which is not epigenetically repressed and therefore could allow these cells to convert into Treg cells. Glutamine metabolism, for example, is mentioned in the context of Th17-Th1 plasticity as well as Th1-Treg plasticity. CD5 antigen-like (CD5L) regulates fatty acid metabolism in Th17 cells and can contribute to both pathogenic and regulatory activity in these cells. A positive regulator of glycolysis, the transcription factor hypoxia-inducible factor 1α (HIF1α), is also described with opposite roles in the development of Th17 and Treg cells: Treg cells prevent the expression of HIF1α, whereas it is important to Th17 cells as it directly induces the expression of RORγT and consequently the Th17 fate. In line with this, HIF1α deficiency impairs Th17 development while promoting Treg differentiation. Inhibition of the glycolytic pathway showed the same effect on Th17 and Treg development (Corcoran & O'Neill, 2016; Goldsmith et al., 2021; Shi et al., 2011; X. Zhu & Zhu, 2020). Gerriets et al. demonstrated that Treg cells mainly use pyruvate oxidation (OXPHO) for ATP generation while Th17 cells rely on aerobic glycolysis and glutamine oxidation (Gerriets et al., 2015; L. Sun et al., 2017). But it is not only Th17 cells that show an unstable phenotype. Treg cells have also been described as converting into Th17 cells (or other T helper subsets): studies describe IL-17 secreting $FoxP3^+$ cells in humans and mice, which can transdifferentiate from iTreg or nTreg cells (X. O. Yang et al., 2008b). In the presence of IL-6 or the absence of TGF-β and in combination with IL-6, Treg cells secreted IL-17 and also showed up-regulated expression of RORγT and down-regulation of FoxP3. In addition, IL-17^+ Treg cells showed reduced suppressive activity

(Tesmer et al., 2008; L. Xu et al., 2007; X. O. Yang et al., 2008b; J. Zhu & Paul, 2010). Knockout studies of STAT3 and RORγ in T cells demonstrated that STAT3 is the critical driver of FoxP3 down-regulation (X. O. Yang et al., 2008a). Interestingly, cell fate experiments revealed that many effector cells, including IL-17$^+$ cells, derive from Treg cells as it could be shown that they used to express FoxP3 (Barbi et al., 2013; J. Zhu & Paul, 2010). The functional flexibility and plasticity of Treg cells to respond properly to their surrounding microenvironment is assumed to be important, on the one hand for tailoring their suppressive function and on the other hand for maintaining immunological homeostasis (X. Li & Zheng, 2015). Understanding and exploiting this immune imbalance may be an opportunity to re-program differentiated cells into a desired cell type for treating immune-related diseases (J. Zhu & Paul, 2010).

1.5 Interferon Regulatory Factor 4 (IRF4)

Interferon regulatory factor 4 (IRF4), also known as PIP (PU.1-interacting partner), MUM1 (multiple myeloma oncogene 1) or LSIRF (lymphocyte-specific interferon regulatory factor), is a member of the family of interferon regulatory factors (IRFs). For mice and humans there are nine members described, namely IRF1 to IRF9. As transcription factors, all IRFs regulate gene expression and various aspects of innate and adaptive immune responses (M. Huber & Lohoff, 2014; P. Li et al., 2012; Nam & Lim, 2016; Yanai et al., 2012). IRFs are not only important for the induction of type I interferons (IFN-α and -β) but also for the development and function of different immune cells such as T or B lymphocytes, dendritic cells and macrophages (Jefferies, 2019; Nam & Lim, 2016). Just like its homolog IRF8, the expression of IRF4 is restricted to immune cells, and it is the only member of the family of IRFs which is not induced by type I or II interferons, toll-like receptors (TLRs) or pattern recognition receptors (PRRs) (P. Li et al., 2012). Instead, IRF4 is induced by the binding of antigen receptors (e.g. T/B cell receptors) or by stimulation with lipopolysaccharides (LPS), IL-4 or CD40. Expression of IRF4 following TCR signalling is mediated via the NF-κB pathway (Grumont & Gerondakis, 2000; Ruan et al., 2011; Wong et al., 2022) , especially by c-Rel, which binds to the *Irf4* promoter. In healthy T cells, IRF4 is only transiently expressed upon TCR stimulation and *Irf4* mRNA expression represents the strength of T cell receptor activation, making its expression dose-dependent (Wong et al., 2022). It is known that IRF4 is a crucial player for the development, activation and effector function of different immune cells as it is involved in the induction of cell type specific genes. On the other hand, IRF4 is also considered an oncogene (J. Lu et al., 2023; Wong et al., 2022) because abnormal expression of it, e.g. loss, amplification or mutations (Vanderbilt University Medical Center, 2023), is associated with different types of cancer, e.g. B cell chronic lymphocytic leukaemia (CLL), adult T cell leukaemia/lymphoma (ATL) or multiple myeloma (MM). However, dysregulation of IRF4 has also been described as associated with the development of autoimmune diseases such as multiple sclerosis, type I diabetes and Crohn's disease (S. Sundararaj & Casarotto, 2021; W.-D. Xu et al., 2012). IRF4 is therefore often considered a "master regulator for autoimmunity" (S. Sundararaj & Casarotto, 2021).

The structure of all members of the IRF4 family is very similar. They consist of a highly conserved tryptophan-rich DNA-binding domain (DBD, see Figure 2, red part) at the *N*-terminus, which recognizes 5'-GAAANNGAAA-3', a part of the IFN-stimulated response element (ISRE), as a core DNA sequence for

binding (Fujii, 1999; P. Li et al., 2012; Wong et al., 2022). A less conserved IRF-associated domain (IAD, see Figure 2, purple part) can be found at the *C*-terminus, which regulates homo- or heteromeric interactions with other IRFs, transcription factors or cofactors and thereby regulates the transcriptional activity of IRFs. The specific protein-protein interactions determine whether the resulting protein complex acts as a transcriptional activator or repressor of gene expression ("context-specific" (Wong et al., 2022) transcription factor) and hence also decides the cellular outcome of a developing cell. In addition to the ISRE, which is bound by a IRF4 homodimer, IRF4 recognizes and binds to Ets-IRF composite elements (EICE, 5'-GGAAnnGAAA-3') in combination with PU.1 or to AP-1-IRF composite elements (AICE, TGAnTCA/GAAA; GAAA is located directly next to or maximum 5 bp distant from the AP-1 motif) when associated with an AP-1 proteins such as BATF (P. Li et al., 2012; J. Lu et al., 2023; Thouenon et al., 2023; Wong et al., 2022). On its own, IRF4 binds only with a low affinity to the 5'-GAAA-3' sequence and therefore needs homo- or heteromerization for efficient binding (see Figure 2B). Additional specificities of IRF4 are that it has an autoinhibitory domain (see Figure 2, light blue part) for DNA binding at the *C*-terminus as well as a nuclear-localization signal sequence in the DBD region (see Figure 2, orange part) (P. S. Biswas, Bhagat, et al., 2010; M. Huber & Lohoff, 2014; Nam & Lim, 2016; Wong et al., 2022; Yanai et al., 2012).

B

DNA recognition site	Binding partner	Relative DNA affinity	Aligned with gene program	Sequence Logo
EICE Ets-IRF4 Composite Element	PU.1 or SpiB	high	B cell GCB	
AICE AP1-IRF Composite Element	BATF/JunB or BATF/cJun	high	B cell GCB / T cell Tfh	
ZICE Ikaros-IRF Composite Element	Ikaros	high	B cell GCB	
ISRE Interferon Stimulated Response Element	IRF4 (homodimer)	low	B cell PC / T cell Teff	

Figure 2: Structure of Interferon Regulatory Factor 4 (IRF4) and overview of IRF4 binding sites. (A) IRF4 consists of a DNA-binding domain (DBD) at the *N*-terminus (shown in red), a IRF-associated domain (IAD) at the *C*-terminus (shown in purple), an autoinhibitory domain (shown in light blue) and a nuclear-localization signal within the DBD (shown in orange). (B) Dependent on the binding partner, IRF4 can recognize and bind characteristic DNA sequences with high or low affinity in different cell subsets. PC: plasma cells; GCB: germinal center B cells; Teff: effector T cells; Tfh: T follicular helper cells (Cook et al., 2020).

IRF4 is described as interacting with many master transcription factors of T cells, such as T-bet in Th1 cells, GATA3 in Th2 cells, RORγT in Th17 cells and FoxP3 in Treg cells. Additionally, members of the AP-1 transcription factor family, e.g. BATF and JUN, are highly expressed in T cells and bind with a high affinity to AICEs while in B cells, IRF4 mainly interacts with PU.1 or SPIB and recognizes EICE motifs (P. Li et al., 2012; J. Lu et al., 2023; Wong et al., 2022).

1.6 Role of IRF4 in Th17 and Treg cells

As detailed in the previous chapter (1.5), the expression of IRF4 in T cells is induced by the stimulation of the T cell receptor. Just a few hours after TCR engagement, high levels of IRF4 are already detectable. The expression levels of IRF4 are also regulated by different proteins e.g. mTOR (mammalian target of rapamycin), ITK (IL-2-inducible T cell kinase), NFAT (nuclear factor of activated T cells), c-Rel, FoxP3, STAT3 and T-bet. While FoxP3 and STAT3 positively regulate the expression of IRF4 in Treg and Th17 cells, T-bet represses the expression of IRF4 in Th17 cells (M. Huber & Lohoff, 2014).

IRF4 plays an important role in the activation, development and function of different $CD4^+$ T cell subtypes (C.-M. Hu et al., 2002; Lohoff et al., 2002; Mittrücker et al., 1997; Nam & Lim, 2016; Rengarajan et al., 2002) as well as in the prevention of disease (Mudter et al., 2008). The relevance of IRF4 to the development of Th17 cells was first described by Brüstle et al., who discovered that naïve $CD4^+$ T cells do not differentiate *in vitro* into Th17 cells when IRF4 is absent (*Irf4*$^{-/-}$). In addition, a lower expression of RORγT and RORα was detected. *In vivo* follow-up studies also demonstrated that animals lacking *Irf4* are resistant to the development of EAE, where the involvement of Th17 cells is described (Brüstle et al., 2007). Results from human IBD biopsies indicated the involvement of IRF4 in active inflammation in a Th17-dependent manner, shown by augmented levels of *Irf4* mRNA as well as a high correlation of IRF4 with Th17-associated cytokines (IL-6, IL-17, IL-22) in inflamed tissue. Data from T cell-dependent colitis mouse models support these findings, as IRF4-deficient animals had reduced levels of Th17-associated cytokines and transcription factors (RORγT and RORα) and showed no chronical inflammation in the gut (Mudter et al., 2008, 2011). It has also been demonstrated that IRF4 directly regulates Th17-characteristic genes, as direct binding of IRF4 was shown in the promoter of *Il17a*, *Il17f*, *Il21* and *Rorc* genes (Q. Chen et al., 2008; Ciofani et al., 2012; M. Huber et al., 2008; Kurebayashi et al., 2013; W.-D. Xu et al., 2012).

In case of Treg cells, IRF4 is described as having more influence on effector function than on the development of this cell type (Cretney et al., 2011; Veldhoen, 2010; Zheng et al., 2007, 2009). The level of FoxP3 expression is unchanged in the absence of IRF4 (Veldhoen, 2010). One study, unravelling the immunosuppressive functions in tumours, revealed that $IRF4^+$ Treg cells play an essential role in the suppressive function in the tumour environment. Different suppressive molecules, e.g. programmed cell death protein 1 (PD1) or T cell immunoreceptor with immunoglobulin and ITIM domain (TIGIT), and multiple exhausted T cell subpopulations were detectable in the presence of $IRF4^+$ Treg cells, in contrast to the $IRF4^-$ counterpart. In general, high levels of $IRF4^+$ intratumoral Treg cells correlated with a poor survival rate and early recurrence of tumour. Murine tumour studies confirmed the important role of IRF4 in Treg cells for suppressive activity, as a deletion of *Irf4* exclusively in these cells resulted

in delayed tumour growth. However, massive cell infiltration causing multi-organ autoimmunity was detected in the absence of IRF4 (Alvisi et al., 2020).

In contrast to Th17 cells where IRF4 is involved upstream in the expression of RORγT, the expression of FoxP3 is independent of IRF4. IRF4 acts downstream of FoxP3 and its expression is directly regulated by FoxP3, which binds to the *Irf4* promoter (Zheng et al., 2009). The interplay of IRF4, FoxP3 and BATF3 is crucial for regulated FoxP3 expression, which in turn is essential for Treg differentiation and effector function (Arnold et al., 2022; J. Lu et al., 2023). Surprisingly, in the absence of IRF4 the number of FoxP3$^+$ Treg cells is increased and the development of spontaneous autoimmune diseases is described as characterized by a high expression of Th2 cytokine. The low activation and suppressor function of Treg cells can be attributed to a low expression of ICOS (inducible T cell co stimulator), IL-10 and/or IL-1 receptor. These molecules are upstream regulated by IRF4, FoxP3 and Blimp-1: IRF4 and FoxP3 cooperatively bind to the *Icos* promoter (Zheng et al., 2009) and the expression of IL-10 in mucosal surfaces is induced by IRF4 and Blimp-1, which itself is regulated by IRF4 (Cretney et al., 2011, 2013).

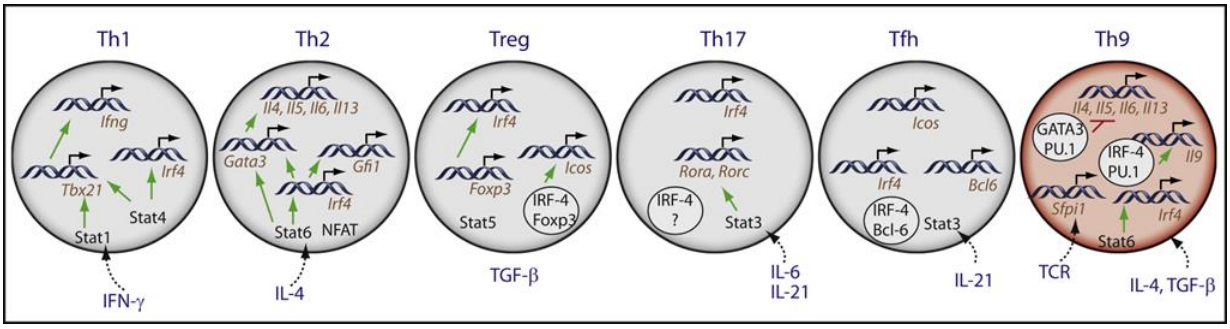

Figure 3: Role of IRF4 in different T cell subsets. IRF4 plays a crucial role for CD4$^+$ T cell functionality including Th1, Th2, Th9 and T follicular helper (Tfh) cells. In Treg cells, FoxP3 induces the expression of IRF4, which in combination with it, is important for the induction of effector molecules. In contrast, in Th17 cells, IRF4 acts upstream of the master transcription factor RORγT (Veldhoen, 2010).

1.7 Protein interaction studies and *in vivo* biotinylation

For the investigation of specific protein-protein or RNA-/DNA-protein interactions, affinity purification is often the method of choice. Affinity purification can be defined as "the capture of biological material via specific enrichment with a ligand coupled to a solid support" (Dunham et al., 2012). Basically a cellular lysate is incubated with an immobilized affinity material (for DNA-protein interactions, a cross-linking step is included before cell lysis), unbound material is washed away and immobilized and captured material gets eluted and further analysed (see Figure 4, A) (Dunham et al., 2012; J. Kim et al., 2009). For protein-protein interactions, western blot can be used to verify supposed protein interactions. Additionally mass spectrometric analysis can be used to detect and identify a target-specific interactome in an unbiased manner, which allowed the identification of novel protein interconnections. In case of DNA-protein interactions, sequencing of eluted DNA fragments reveals the genome-wide binding of a target protein, named chromatin immune precipitation followed by sequencing (ChIP-seq) (J. Kim et al., 2009). Classical affinity purification approaches use an antibody to

directly target the protein of interest or an epitope tag, e.g. FLAG, TAP, Histidine or GFP tag. An affinity purification using an antibody is also referred as an immunopurification (Dunham et al., 2012). However, antibody-based methods are limited by cross-reactivity, restricted availability of a suitable antibody or interference with protein interactions and/or protein localization. An antibody-free alternative is isolation via streptavidin biotin interaction. The streptavidin biotin-based precipitation has some advantages over the classic approach: the high binding affinity ($K_d = 10^{-15}$ M) of streptavidin to biotin (vitamin H) allows efficient and clean – without many contaminating proteins - purification of the target by applying stringent washing conditions. Even extreme pH conditions or detergents do not interfere with the strongest non-covalent binding (Driegen et al., 2005; Dundas et al., 2013; J. Kim et al., 2009). No target-specific antibody has to be generated or used. As there are not many naturally biotinylated proteins present in mammalian cells (up to five endogenous biotinylated proteins, mainly mitochondrial and cytoplasmic proteins), the background derived from cross-reaction with other proteins and/or unspecific binding is low (J. Kim et al., 2009; Rodriguez et al., 2006; Smits & Vermeulen, 2016). A prerequisite for this approach is, of course, the biotinylation of the target protein. In contrast to chemical biotinylation, which non-specifically alters a broad range of similar chemical groups, enzymatic biotinylation modifies proteins with high selectivity. To allow enzymatic biotinylation *in vivo*, a short amino acid long biotin recognition tag, e.g. Avi-tag, has to be fused to the target protein at the *N*- or *C*-terminus and a biotin protein ligase needs to be present. A well-studied enzyme is the *Escherichia coli* biotin ligase BirA. In an ATP-dependent reaction, this enzyme attaches biotin to a lysin (K) residue in the Avi-tag and thereby generates biotinylated target (see Figure 4, B). The artificial modification of proteins with the tag for biotinylation has been reported to have no influence on the interaction with other proteins, DNA-binding capacity or subnuclear distribution (de Boer et al., 2003; Dundas et al., 2013; J. Kim et al., 2009; Rodriguez et al., 2006; Smits & Vermeulen, 2016). However, some limitations have to be considered. Firstly, it should be mentioned that setting up an *in vivo* biotinylation system (cell line or mouse strain) is time consuming. Secondly, the expression level of the target protein has to be checked and considered because overexpression of proteins can result in "non-natural" big protein complexes and unspecific binding to the DNA (J. Kim et al., 2009). The introduction of the $ROSA26^{BirA}$ mouse strain by Driegen and colleagues strongly improved the setup of an *in vivo* biotinylation system. The knock-in of the gene coding for the enzyme at the ROSA26 locus allows an ubiquitous expression of BirA in all types of cells, all tissues and at every stage of cell development (Driegen et al., 2005). Crossing these animals with other transgenic mice that have an Avi-tag fused to the protein of interest allows efficient target biotinylation in a wide range of applications.

Another biotinylation-based approach to studying protein-protein interactions is BioID (Roux et al., 2012; Smits & Vermeulen, 2016; Varnaitė & MacNeill, 2016). This proximity-dependent labelling approach uses a fusion of the target protein with a mutated biotin ligase (promiscuous mutant BirA*) instead of a fusion of the target with the BirA recognition tag. Upon activation of BirA*, it biotinylates all proteins in close proximity (10 nM) to the target. However, this means all nearby proteins get biotinylated, not distinguishing between interacting and non-interacting proteins.

Besides all the obstacles for setting up such systems, (*in vivo*) biotinylation is a very efficient method for studying protein-protein or DNA-protein interactions under physiological conditions and also allows a broad spectrum of experimental read-outs, e.g. microscopy or western blot (Dundas et al., 2013), and thereby fields of application. Various studies have used the biotinylation approach for their investigations. For example, the interaction of 109 human transcription factors in HEK293 cells was performed using the BioID approach (Göös et al., 2022). In another study, Rudensky *et al.* investigated the interactome of FoxP3 after transducing T cell hybridoma TCli cells with AVI-Foxp3 and the BirA enzyme (Rudra et al., 2012), while Soler and colleagues used the Bio-tag in a multi-scale analysis for analysing transcription factor complexes in the development of haematopoietic cells (Soler et al., 2011).

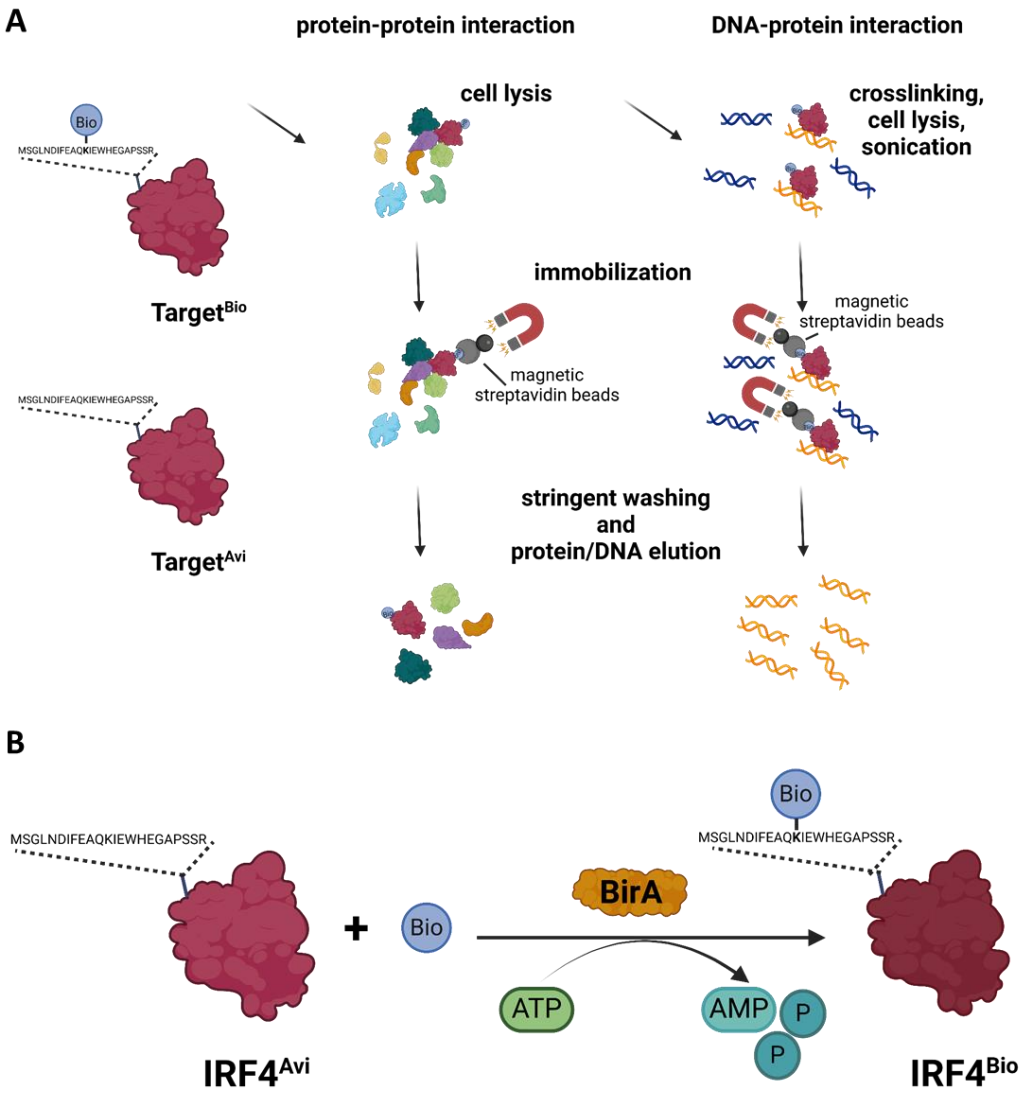

Figure 4: Schematic workflow of protein-protein and DNA-protein interaction analysis using *in vivo* biotinylation. (A) *In vivo* biotinylated proteins (Target^{Bio}) and non-biotinylated control samples (Target) are needed to study protein-protein or DNA-protein interactions using the biotin streptavidin approach. Immobilization, stringent washing and protein/DNA elution are the main steps for affinity purification. (B) For *in vivo* biotinylation, a BirA recognition tag (Avi-tag) has to be fused to the target protein (as exemplified for IRF4) and BirA has to be co-expressed. In an ATP-dependent reaction, biotin is attached to the lysin (K) within the Avi-tag by BirA and results in a biotinylated target protein.

II. AIM OF THIS THESIS

Immune homeostasis is a delicate balance between pro-inflammatory and anti-inflammatory immune responses. Two important members of that interplay are $CD4^+$ T helper 17 (Th17) and regulatory T cells (Treg). Although they exhibit opposing functions in the immune system – Th17 cells induce immune reactions while Treg cells suppress immunological responses and contribute to peripheral tolerance – both $CD4^+$ T cell subsets share distinct elements during their development. Due to their developmental similarities, cell plasticity is reported for both cell types (Taams et al., 2006; Tesmer et al., 2008). The transcription factor interferon regulatory factor 4 (IRF4) is known to be important for the development of fully functional Th17 and Treg cells (Brüstle et al., 2007; Cretney et al., 2011; Veldhoen, 2010; Zheng et al., 2007, 2009) and could therefore, depending on its interaction partners, contribute to the described cell plasticity. Veldhoen and colleagues proposed that the expression levels and especially the IRF4 interactome are even more important in enhancing or suppressing molecular functions than the presence of IRF4 itself (Veldhoen, 2010). However, the molecular mechanisms unravelling the role of IRF4 and its interacting proteins in T cell development and cell plasticity are not fully clear to date.

Therefore one aim of this thesis was to investigate and directly compare in an unbiased approach the protein composition of the IRF4 interactome in Th17 and Treg cells. In contrast to current co-immunoprecipitation studies, the analysis was not performed with isolated effector T cells or at an intermediate-late time point of cell development (48 h after stimulation of naïve $CD4^+$ T cells), but in fully differentiated, 72 h *in vitro* stimulated T cell subtypes. For the experiments of this present thesis, the new $IRF4^{Bio}$ mouse model (Dietzen, 2019) was utilized, where IRF4 was *in vivo* biotinylated by the enzyme BirA. Due to the strong non-covalent interaction of biotin and streptavidin, this *in vivo* biotinylation technique did not require any target-specific antibody, instead magnetic streptavidin-coated beads were used to efficiently isolate IRF4 and its interacting proteins. Those separated proteins were identified by mass spectrometric analysis for which an optimized sample preparation protocol had to be established at first.

In addition to the IRF4 protein interactions, genome-wide IRF4 binding regions in Th17 and Treg cells were investigated performing IRF4-Bio-ChIP-seq analysis. With help of the $IRF4^{Bio}$ mouse model and the *in vivo* biotinylation system, IRF4 binding regions were isolated with magnetic streptavidin-coated beads instead of antibodies, which are used for the classical ChIP-seq approach. Resulting genomic data was integrated with the IRF4 interactome data as well as proteomic analysis of Th17 and Treg cells generated from IRF4 knockout ($Irf4^{-/-}$) and wildtype animals to better understand the molecular mechanisms of IRF4 (and its interacting proteins) in differentiated T cell subsets that might contribute to the balance of the two opposing T cell subtypes, Th17 and Treg cells.

III. MATERIAL AND METHODS

3.1 Material

3.1.1 ANTIBODIES

Table 1: Antibodies

Antibody	Specificity	Source	Company	Application
Anti-β-actin	Monoclonal (clone AC-15)	Mouse	Sigma Life Science	Western blot
Anti-α-tubulin	Monoclonal (clone GT-114)	Mouse	GeneTex	Western blot
Anti-hu/mo IRF4-PE	Monoclonal (clone 3E4)	Rat	Invitrogen	FACS
Anti-Hu/mo RORγT - APC	Monoclonal (clone AFKJS-9)	Rat	Thermo Fisher Scientific	FACS
Anti-IRF4 (F-4)	Monoclonal (clone SC-48338)	Mouse	Santa Cruz Biotechnology	Western blot
Anti-IRF4 (P173)	Polyclonal	Rabbit	Cell Signaling Technology	Western blot
Anti-lamin A/C	Polyclonal	Rabbit	Cell Signaling Technology	Western blot
Anti-mouse IgG, HRP-linked	Polyclonal	Horse	Cell Signaling Technology	Western blot
Anti-rabbit IgG, HRP-linked	Polyclonal	Goat	Cell Signaling Technology	Western blot
IL-17A - PE	Monoclonal (clone eBio 17B7)	Rat	Thermo Fisher Scientific	FACS
CD4 - BV711	Monoclonal (clone GK1.5)	Rat	BD Biosciences	FACS
CD44 - BV605	Monoclonal (clone IM7)	Rat	BioLegend	FACS
CD62L - PE	Monoclonal (clone MEL-14)	Rat	BioLegend	FACS
CD25 - FITC	Monoclonal (clone 3C7)	Rat	Biolegend	FACS
FoxP3 - PE	Monoclonal (clone FJK-16s)	Rat	eBiosciences	FACS
Anti-CD3	Monoclonal (clone 145-2C11)	Mouse	In-house	T cell differentiation
Anti-CD28	Monoclonal (clone 37.51)	Mouse	In-house	T cell differentiation
Anti-IFN-γ	Monoclonal (clone XMG1.2)	Mouse	In-house	Th17 cell differentiation
Anti-IL-4	Monoclonal (clone 11B11)	Mouse	In-house	Th17 cell differentiation

3.1.2 BUFFER AND MEDIA

Table 2: Buffers and media

Buffer/Medium	Composition
10 % NP-40 buffer	10 % (v/v) NP-40 in nuclease-free water
Blocking buffer (for western blot)	5 % (w/v) BSA in TBS-T
Cell fixation for ChIP	1.25 M Glycine in nuclease-free water
ChIP elution buffer	10 mM Tris (pH 7.9) 5 mM EDTA (pH 8.0) 1 % (w/v) SDS 300 mM NaCl in nuclease-free water
ChIP immune precipitation (IP) buffer	30 mM Tris (pH 7.9) 2 mM EDTA (pH 8.0) 165 mM NaCl 0.3 % (w/v) SDS 1 % (v/v) Triton-X in nuclease-free water
ChIP lysis buffer	50 mM Tris (pH 7.9) 10 mM EDTA (pH 8.0) 1 % (w/v) SDS in nuclease-free water
ChIP wash buffer I	2 % (w/v) SDS in nuclease-free water
ChIP wash buffer II	10 mM Tris (pH 7.9) 1 mM EDTA (pH 8.0) 250 mM LiCl 1 % (v/v) NP-40 1 % (w/v) Sodium-deoxycholate in nuclease-free water
ChIP wash buffer III	20 mM Tris (pH 7.9) 1 mM EDTA (pH 8.0) 50 mM NaCl 0.1 % (w/v) SDS in nuclease-free water
Coating buffer	0.1 M Na_2HPO_4 x $2H_2O$ in water, pH 9.3
Elution buffer (for protein immunoprecipitation)	10 mM Tris 10 mM Biotin 1 % (w/v) SDS in LC-MS grade water, pH 7.5
GM buffer	0.5 % (w/v) BSA 5 mM EDTA in PBS
Hypotonic buffer	20 mM Tris-HCl 10 mM NaCl 3 mM $MgCl_2$ in nuclease-free water

Buffer/Medium	Composition
Lysis buffer (for typing)	25 mM NaOH 0.2 mM EDTA in water, pH 12
Neutralization buffer (for typing)	40 mM Tris-HCl in water, pH 5
SDS running buffer	25 mM Tris 190 mM Glycine 0.1 % (w/v) SDS in water
Stripping buffer (for western blot)	0.1 M Glycine 0.1 % (w/v) SDS in aqua dest, pH 2.5
Supplement to ChIP elution buffer	1 M NaCl in nuclease-free water
TBS (20x)	1 mM Tris 9 mM Tris-HCl 150 mM NaCl in water, pH 7.4
TBS-T (20x)	1 mM Tris 9 mM Tris-HCl 150 mM NaCl 1 % (v/v)Tween in aqua dest., pH 7.4
Test medium (TM)-10	10 % (v/v) FCS 1 % (w/v) Glutamine 1 % (w/v) Sodium Pyruvate in IMDM
Th17 cell differentiating medium	1 ng/mL TGF-ß 40 ng/mL IL-6 2.5 µg/mL α-IFNγ 10 µg/mL α-IL4 in TM-10 medium
Treg cell differentiating medium	7.5 ng/mL TGF-ß 250 ng/mL IL-2 in TM-10 medium
Turbo blotting buffer	20 % Transfer buffer 60 % Aqua dest. 20 % Ethanol
Urea buffer (lysis buffer for western blot)	7 M Urea 2 M Thiourea 5 mM DTT 2 % (w/v) Chaps in nuclease-free water
Wash buffer I (adjusted RIPA; for protein immunoprecipitation)	25 mM Tris 150 mM NaCl 1 % (v/v) NP-40 1 % (w/v) DOC 0.35 % (w/v) SDS in LC-MS water, pH 7.5
Wash buffer II (for protein immunoprecipitation)	25 mM Tris in LC-MS grade water, pH 7.5

3.1.3 REAGENTS AND CHEMICALS

Table 3: Reagents and chemicals

Name	Company
1,4-Dithiothreitol (DTT)	Carl Roth
Acetonitrile	Carl Roth
Acrylamide	Carl Roth
Agarose	Biozyme
Bovine Serum Albumin (BSA)	Sigma
Dithiobis(succinimidyl propionate) (DSP)	Thermo Fisher
Dimethyl sulfoxide (DMSO)	Carl Roth
Ethanol (pure)	PanReac AppliChem
Fetal calf serum (FCS)	Life Technologies
Fixation/Permeabilization Concentrate	Invitrogen
Fixation/Permeabilization Diluent	Invitrogen
Fixable Viability Dye eFlour780	ThermoFisher
Formic acid	Carl Roth
Glycogen	Carl Roth
Iodoacetamid (IAA)	Sigma Aldricht
Ionomycin	Sigma Aldricht
Iscove's Modified Bulbecco's Medium (IMDM)	PAN Biotech
Isopropanol (pure)	Carl Roth
N6 Primer	Thermo Scientific
Oligo dT	Thermo Scientific
PageRuler™ Prestained Protein Ladder	Thermo Fisher
Protease inhibitor cocktail (PIC)	Roche
Roti-C/I	Carl Roth
SA-HPO	Roche
Sera-Mag SpeedBeads	GE Healthcare
TRI Reagent	Bio&Sell
Trypsin Gold, Mass Spectrometry Grade	Promega
Dynabeads™ M-280 Streptavidin	Thermo Fisher
NP-40	Sigma Aldricht
Trypan Blue 0.4 %	Carl Roth
Formaldehyde, 16 %, methanol-free	Thermo Fisher Scientific
Phorbol-12-myristat-13.acetat (PMA)	Thermo Fisher Scientific
5x RT Buffer	Thermo Fisher Scientific
DreamTaq DNA Polymerase (5 U/µL)	Thermo Fisher
EvaGreen® (no ROX), 5x	Axon Labortechnik
DNA-loading dye, 6x	Thermo Fisher Scientific
10x DreamTaq Green Buffer (incl. 20 mM $MgCl_2$)	Thermo Fisher
10x Permeabilization Buffer	Invitrogen
dNTPs (10 mM)	Thermo Fisher Scientific
DreamTap Puffer, 10x	Thermo Fisher Scientific
RNaseA (10 mg/mL)	Thermo Fisher Scientific
Proteinase K (20 mg/mL)	Sigma Aldrich
GeneRuler™ 100 bp-DNA ladder	Thermo Fisher Scientific
RevertAid Reverse Transcriptase (200U/µL)	Thermo Fisher Scientific
Pierce 660 nm Protein Assay Reagent	Thermo Fisher Scientific

Name	Company
Monensin 1,000x	Invitrogene/Biolegend
Tris	Carl Roth
Tris-HCl	Carl Roth
Sodium Pyruvate	Carl Roth
Sodium Dodecyl Sulfate (SDS)	Carl Roth
EDTA	Carl Roth
Sodium Chloride (NaCl)	Carl Roth
Biotin	Sigma Aldrich
Magnesium Chloride ($MgCl_2$)	Carl Roth
Triton-X 100	Carl Roth
Urea	Carl Roth
Thiourea	Carl Roth
Chaps	Carl Roth
Sodium deoxycholate (DOC)	Merck
Lithium Chloride (LiCl)	Carl Roth

3.1.4 CYTOKINES

Table 4: Cytokines

Cytokine	Company
TGF-ß	Peprotech
IL-6	Peprotech
IL-2	In-house

3.1.5 PRIMER

Table 5: Oligonucleotides

Name	Sequence (5'-3')	Application	Company
Rosa26BirA fwd-1	GCCAGCCAGAATTTATATGCAG	Typing	Sigma
Rosa26BirA fwd-2	GTGTAACTGTGGACAGAGGAG	Typing	Sigma
Rosa26BirA rev	GAACTTGATGTGTAGACCAGG	Typing	Sigma
$IRF4^{Bio}$ fwd	AGAGATGCAACCTACATCCTCAC	Typing	Sigma
$IRF4^{Bio}$ rev	GTTGATTGATCGAATTGAGGCAC	Typing	Sigma
Internal ctl fwd	GCAGAAGAGGACAGATACATTCAT	Typing	Sigma
Internal ctl rev	CCTACTGAAGAATCTATCCCACAG	Typing	Sigma
IL-17A fwd	TTTAACTCCCTTGGCGCAAAA	qRT-PCR	Sigma
IL-17A rev	CTTTCCCTCCGCATTGACAC	qRT-PCR	Sigma
RORγT fwd	TGAGGCCATTCAGTATGTGG	qRT-PCR	Sigma
RORγT rev	CTTCCATTGCTCCTGCTTTC	qRT-PCR	Sigma
FoxP3 fwd	CCTGGTTGTGAGAAGGTCTTCG	qRT-PCR	Sigma
FoxP3 rev	TGCTCCAGAGACTGCACCACTT	qRT-PCR	Sigma
IRF4 fwd	AGCCTGCCCTCTTCAAGGCTT	qRT-PCR	Sigma
IRF4 rev	TGGCTCCTCTCGACCAATTCC	qRT-PCR	Sigma
HGPRT fwd	GTTGGATACAGGCCAGACTTTGTT	qRT-PCR	Sigma
HGPRT rev	GAGGGTAGGCTGGCCTATAGGCT	qRT-PCR	Sigma
IL-10 intron fwd	AATCCGAGAAACCCACCA	qRT-PCR (ChIP)	Sigma
IL-10 intron rev	TCCATACCAAAACCCCAG	qRT-PCR (ChIP)	Sigma

Primer	Sequence (5'-3')	Application	Company
Ezh2 fwd	CTTCTCAACCCCTTTCCCTAAGA	qRT-PCR (ChIP)	Sigma
Ezh2 rev	CACCTTATTCCCAAAGGCAAGG	qRT-PCR (ChIP)	Sigma

3.1.6 KITS

Table 6: Kits

Name	Company
DNA Clean & Concentrator	Zymo
Naïve $CD4^+$ T Cell Isolation Kit mouse	Miltenyi Biotec
NEBNext Ultra II DNA Library Prep Kit	Illumina
Pierce 660 nm protein Assay Kit	Thermo Fisher Scientific
Qubit® dsDNA HS Assay Kit	Thermo Fisher Scientific
Trans-Blot® Turbo™ RTA Transfer Kit, PVDF	BioRad
Western Bright Chemiluminescence Substrate	Biozym
μMACS FactorFinder Kit	Miltenyi Biotec

3.1.7 CONSUMABLES

Table 7: Consumables

Consumable	Company
24-well plate	Greiner
96-well plate (F-bottom)	Greiner
96-well plate (V-bottom)	Greiner
Cell strainer (40 μm)	Greiner
Eppendorf tubes (0.5 mL, 1.5 mL, 2 mL)	Greiner
Falcon tubes (15 mL, 50 mL)	Greiner
Glass vials	Waters
High sensitivity DNA Chip	Agilent Technologies
HSS-T3 C18 1.8 μm, 75 μm x 250 mm column	Waters analytical
LS columns	Milentyi Biotec
Mini-PROTEAN® TGX™ Precast Gels	BioRad
Needle (0.55x25 mm, 0.8x40 mm)	BD Biosciences
Pasteur pipets	VWR international
PCR microplate	Corning Inc
Pipet tips (10 μL, 100 μL, 1,000 μL)	Starlab
Plastic cover (qPCR plate)	Axon Labortechnik
Protein LoBind falcon tubes (15 mL, 50 mL)	Eppendorf
Protein LoBind tubes (1.5 mL)	Eppendorf
PVDF membran Immobilion®-P, 0.45 μm	Millipore
Serologic pipets (5 mL, 10 mL, 25 mL, 50 mL)	Greiner
Syringe (1 mL)	B. Braun
TPX tubes (1.5 mL)	Diagenode
Whatman paper	Whatman

3.1.8 INSTRUMENTS AND DEVICES

Table 8: Instruments and devices

Instrument/Device	Company
2100 Bioanalyzer	Agilent Technologies
Bioruptor® Plus	Diagenode
Centrifuges	
- Heraeus Megafuge 40R centrifuge	Thermo Scientific
- Heraeus Megafuge 1.0 centrifuge	Thermo Scientific
- Heraeus Fresco 21 centrifuge	Thermo Scientific
- Z216 MK centrifuge	Hermle LaborTechnik
Chemi Doc XR/XRS	BioRad
CO_2 incubator	Sanyo
Exploris 480 Orbitrap	Thermo Fisher Scientific
Heating block	HLC
Mini-PROTEAN Tetra Vertical Electrophoresis Cell	BioRad
Peqstar 2x gradient thermocycler	VWR
Qubit® Flex fluorometer	Invitrogen by Thermo Fisher Scientific
QuickDrop Spectrophotometer	Molecular Devices
Rotating device	IKA
Step One Plus	Thermo Fisher Scientific
T3 Thermocycler	Biometra
TimsTOF Pro 2	Bruker
TransBlot® Turbo™ Transfer System	BioRad
Ultimate 3000 RSLC nano LC system	Thermo Fisher Scientific
Vortexer	VWR
Waterbath	Memmert

3.2 Methods

3.2.1 MOUSE TYPING (PCR)

To identify the genotype of IRF4^{Bio} mice, polymerase-chain reaction (PCR) was performed. To isolate DNA from the ear biopsies 40 µL of lysis buffer was added and the tubes were incubated for 30 min at 95 °C. Afterwards, 40 µL of neutralizations buffer was added to stop the lysis.

To each PCR tube, 22 µL of the following master mix were added and 3 µL of the isolated DNA was transferred into the corresponding reaction tube. For IRF4^{Bio} animals, the genotype of *Irf4* and *BirA* had to be determined.

Table 9: Master mix (1x) for genotyping

Components	***Irf4^{Bio}***	***ROSA26^{BirA}***
10 x DreamTaq Buffer	2.5 µL	2.5 µL
dNTPs (10 mM)	0.5 µL	1 µL
Fwd + rev primer (10 µM)	1 µL	1 µL
Internal ctl primer (10 µM)	1 µL	-
DreamTaq polymerase (5 U/µL)	0.125 µL	0.25 µL
H_2O	16.875 µL	17.25 µL

The following PCR programs were used on a Peqstar 2x gradient or T3 thermocycler.

Table 10: PCR programs for genotyping

	Irf4^{Bio}		***ROSA26^{BirA}***	
Temperature	**Time**	**Number of cycles**	**Time**	**Number of cycles**
94 °C	180 s	1x	300 s	1x
94 °C	30 s	37x	30 s	35x
60 °C	35 s		30 s	
72 °C	35 s		30 s	
72 °C	300 s	1x	300 s	1x

3.2.2 GENERATION OF T HELPER 17 AND REGULATORY T CELLS

Th17 and Treg cell were *in vitro* differentiated from naïve CD4$^+$ T cells. In order to obtain naïve CD4$^+$ T cells, mice were sacrificed by CO_2 asphyxiation. Afterwards, the spleens of IRF4^{Bio} and ROSA26^{BirA} (control) mice were isolated, mechanically disrupted, and filtered of cell debris through a 40-µm cell strainer resulting in splenic single-cell suspensions.

Naïve CD4$^+$ T cells were isolated from splenic single-cell suspensions by negative selection magnetic-activated cell sorting (MACS) using the murine Naïve CD4$^+$ T Cell Isolation Kit according to the manufacturer's protocol. In brief, cells were centrifuged and cell pellets resuspended in GM-buffer. After addition of the biotin-conjugated monoclonal antibody cocktail provided in the Naïve CD4$^+$ T Cell Isolation Kit, cells were incubated at 4 °C for 5 min. Afterwards, cells were further diluted with GM-buffer. Anti-biotin microbeads as well as anti-CD44 microbeads were added to the samples, followed

by incubation for 10 min at 4 °C. Magnetic cell separation was performed using LS columns. After column equilibration, up to 1 x 10^8 cells were loaded per column and columns were washed twice with GM-buffer. The flow-through, containing unlabelled naïve $CD4^+$ cells, was collected and centrifuged at 630 x*g* for 10 min at 4 °C. After centrifugation, naïve $CD4^+$ cells were reconstituted in TM-10 medium and transferred to 24-well cell culture plates, which were coated with anti-CD3 and anti-CD28 antibodies. For Th17 cell differentiation, 4 μg/mL anti-CD3 and anti-CD28 were used. Treg cells were generated with a coat of 4 μg/mL anti-CD3 and 8 μg/mL anti-CD28. Before seeding of the naïve cells, the purity ($CD62L^+$ $CD44^-$) was determined as described in 3.2.3. In total, 1 x 10^6 cells were seeded per well. After the addition of polarizing cytokines, cells were cultured for 72 h at 37 °C in a 5 % CO_2 environment. Th17 cell differentiation was induced by adding 1 ng/mL TGF-ß, 40 ng/mL IL-6, 2.5 μg/mL anti-IFN-γ and 10 μg/mL anti-IL-4 to the medium, while for Treg cells 7.5 ng/mL TGF-ß and 250 ng/mL IL-2 was added. For each experiment, splenocytes of three mice were pooled prior to isolation of naïve $CD4^+$ T cells (to obtain sufficient material for downstream analysis).

3.2.3 FLUORESCENCE-ACTIVATED CELL SEPARATION (FACS)

Fluorescence-activated cell separation (FACS) was used to determine the purity of isolated naïve $CD4^+$ T cells and the percentage of differentiated Th17 and Treg cells. After the isolation of naïve $CD4^+$ T cells or the harvest of differentiated Th17 and Treg cells (on day 3), the cells were transferred into a 96-well (V-bottom) plate and washed twice with GM-buffer (2 min, 1,000 x*g*). Afterwards, dead cells and surface markers (see below) were stained for 15 min at 4 °C. The dye and antibodies were diluted in GM-buffer. For intracellular staining, the cells were fixed and permeabilized after two washing steps with GM-buffer. For the fixation and permeabilization, the fix/perm buffers were used as recommended by the Invitrogen (concentrate/diluent (v/v) 1:4). The fixation was performed for minimum 30 min at 4°C, but could be done overnight, too. The intracellular stain was performed in a fix/perm buffer and lasted for 30 min at 4 °C. After all staining steps, the cells were washed two more times in GM-buffer and finally resuspended in 100 μL GM-buffer for analysis. Flow cytometry data were acquired on a BD FACSCanto flow cytometer and analysed using the FACSDiva (version 6.1.3, BD) and the FlowJo (version 10, BD) software packages.

To determine the purity of naïve, Th17 and Treg cells, different surface or intracellular markers were used: Naïve $CD62L^+$ T cells were separated from activated $CD44^+$ cells. Th17 cells were characterized by the expression of RORγT and IL-17A. To analyse cytokine production, the cells were re-stimulated for 3 hours at 37 °C with ionomycin (0.75 μM), PMA (50 ng/mL) and monensin. Treg cells were identified by their CD25 and FoxP3 expression. Additional to all cell type characteristic markers all cells were stained for CD4 and a dye was used to discriminate live and dead cells.

3.2.4 RNA ISOLATION

For isolating RNA, cells were harvested in 1.5 mL tubes and washed twice with PBS (5 min, 1,520 x*g*, 4 °C). The supernatant was discarded each time and the washed cell pellet was resuspended in 1 mL RNA TRI, followed by vortexing for 5 s and an incubation time of 10 min at room temperature. 200 µL Roti-C/I was added. Samples were vortexed for 10 s before incubating again for 10 min at room temperature. After a centrifugation step at 12,700 x*g*, 4 °C for 15 min, the aqueous phase containing the RNA was transferred into a new tube. The interphase containing the DNA as well as the organic phase with the proteins, lipids, etc. was discarded. To the RNA, 1.5 µL glycogen (as a carrier for the RNA) was added, inverted and incubated for 5 min at room temperature. Afterwards, 500 µL isopropanol was added, mixed and incubated for 5 min at room temperature. The sample was centrifuged for 10 min at 12,700 x*g*, 4 °C and washed twice (5 min, 8,100 x*g*, 4 °C) with ice cold 75 % ethanol in nuclease-free water. The RNA pellet was air-dried, resuspended in 20 µL nuclease-free water and incubated for 5 min at 55 °C. RNA concentration was measured using a QuickDrop spectrophotometer device. Isolated RNA was stored at -80 °C until further use.

3.2.5 GENERATION OF COMPLEMENTARY DNA (CDNA)

To generate complementary DNA (cDNA), RNA was isolated from cells (see chapter 3.2.4) and transcribed into DNA by a reverse transcriptase. Isolated RNA was added to a master mix consisting of reaction buffer, primers, dNTPs and enzyme as follows:

Table 11: Master mix for reverse transcription (1x)

Component	Volume
5 x RT Buffer	4 µL
dNTPs (10 µM)	2 µL
Oligo dT-Primer	1 µL
N6 Primer	1 µL
Reverse transcriptase	1 µL
RNA (200-300 ng)	11 µL

The mixture was briefly centrifuged with a table centrifuge and incubated for 1 h at 42 °C. Afterwards, 80 µL of nuclease-free water was added and the cDNA was stored at -20 °C.

3.2.6 QUANTITATIVE REAL-TIME PCR (QPCR)

To quantify the expression of a particular gene by measuring the amount of RNA in a sample, a quantitative real-time PCR (qPCR) was performed. The specific gene expression levels were normalized to the levels of the house-keeping gene *hypoxanthine-guanin-phosphoribosyl-transferase* (*hgprt*). For each primer that was tested, a master mix for technical triplicates was prepared.

Table 12: Master mix for qPCR (1x)

Component	Volume
Nuclease-free H_2O	40 µL
Primer rev + fwd (10 µM each)	3.2 µL
Eva Green	12.8 µL
cDNA (200-300 ng)	8 µL

In total, 20 µL of the final mix was pipetted into a 96-well plate for qPCR, briefly centrifuged to remove any bubbles and sealed for analysis with the following PCR program:

Table 13: PCR program for qPCR

Temperature	Time	Number of cycles
95 °C	15 min	1x
95 °C	30 s	40x
57 °C	30 s	
72 °C	1 min	
95 °C	10 s	60x
60 °C	1 min	
95 °C	15 min	

As a quality control, the melting curves were analysed, with one single peak indicating good PCR quality. For quantification of the mRNA levels, the $\Delta\Delta C_T$ method was used (Bustin, 2002; Livak & Schmittgen, 2001; Schmittgen & Livak, 2008).

3.2.7 CHROMATIN IMMUNOPRECIPITATION (CHIP-SEQ)

Chromatin immunoprecipitation followed by sequencing (ChIP-seq) was used to determine the specific binding regions of IRF4 genome wide. For this, 10 - 15 x 10^6 differentiated cells were harvested, resuspended in 5 mL TM-5 medium and cross-linked for 7 min at room temperature with 1 % formaldehyde (methanol-free). The cells were inverted during the incubation time. The reaction was quenched by the addition of 125 mM glycine, followed by incubation for 5 min at room temperature. Again, the cells were mixed during that time. Afterwards, the cells were washed twice with cold PBS (630 x*g* for 10 min at 4 °C) and transferred into 1.5 mL TPX tubes. The dry pellet was frozen over-night at -80 °C. The following day the pellet was carefully defrosted on ice and cells were loosened by scratching over an Eppendorf tube rack. To each pellet, 520 µL protease inhibitor cocktail (PIC)-supplemented ChIP lysis buffer was added and vortexed. All cells were quickly spun down and incubated for at least 30 min on ice. Afterwards, the cells were sheered with a 1 mL syringe (21G x 11/2 '' 0.8 x 40 needle) six times on ice, trying to prevent the generation of air bubbles. The lysate was sonicated three times each for 10 cycles (each cycle 30 s/30 s ON/OFF, high) in a Bioruptor Plus. Between each of the three sonication rounds, the lysate was inverted and spun down. After the last round, the lysate was centrifuged for 15 min at 17,000 x*g*, 4 °C. The supernatant was transferred into a new tube and the DNA concentration was determined using a QuickDrop spectrophotometer device. For each condition and matching control, the amount was adjusted so that each sample pair had the

same amount of DNA. 20 µL input material was saved as an input control for the final qPCR. For each sample, 50 µL M-280 magnetic streptavidin beads were washed in ChIP lysis - ChIP IP (20 % - 80 %) buffer. Each tube was split into two samples, each containing 200 µL lysate, and topped up with 800 µL ChIP IP buffer (supplemented with PIC). This sample mix was transferred to the washed beads and incubated, rotating overnight at 4 °C. On the next day, the samples were quickly spun down and washed several times with different ChIP buffers. Each washing step was performed at room temperature, rotating the samples for 30 min. After an initial washing step with the ChIP IP buffer, two washing steps of each ChIP wash buffer (I-III) followed and a last incubation with pure nuclease-free water finished the washing process. Each buffer was supplemented with PIC to prevent the degradation of proteins. To elute the proteins from the beads, 200 µL ChIP elution buffer was added to each sample. The input samples from the previous day were included and filled up with 180 µL ChIP elution buffer to also reach a final volume of 200 µL. To remove RNA, 1 µL RNAseA (10 mg/mL) was added and incubated for 1 hour at 37 °C in a water bath, for which the tubes were sealed with parafilm to prevent any contamination. Proteins were removed by the addition of 1.5 µL proteinase K (20 mg/mL) for 1.5 hours at 42 °C. Afterwards, the samples were incubated at 65 °C overnight, shaking at 700 rpm in the heating block. On the following day, the DNA was purified using the DNA Clean & Concentrator kit from ZYMO according to the manufacturer's instructions. To check for successful precipitation, a qPCR (see chapter 3.2.6) was performed using known IRF4 binding sites as a target region and IRF4 non-binding regions as an off-target. For the target region, the 3' UTR of the *Il10* gene was used, and as an off-target *Ezh2* was used. The fold enrichment was calculated using the $\Delta\Delta C_T$ method (Bustin, 2002; Livak & Schmittgen, 2001; Schmittgen & Livak, 2008). All samples with an at least 4-fold enrichment were used to generate a DNA library. For this, the NEBNext Ultra II DNA Library Prep Kit for Illumina (New England BioLabs) was used according to the manufacturer's recommended protocol for low input material.

3.2.8 CHROMATIN IMMUNOPRECIPITATION (CHIP-SEQ) ANALYSIS

For the analysis of the sequencing data, the software EaSeq (version 1.2, https://easeq.net) (Lerdrup et al., 2016) was used. The GRCm38/mm10 genome (accession ID: GCA_000001305.2, assembly date 12/2011) served as a reference genome. For calling peaks, the following parameters were used:

Table 14: Parameters for IRF4-ChIP-seq peak calling

Cell type	Window size	FDR	p-value	Log2	Merge distance
Th17 cells	100 bp	1×10^{-15}	1×10^{-20}	2.1	0 bp
Treg cells	100 bp	1×10^{-10}	1×10^{-10}	1.5	100 bp

The peaks were annotated to the nearest start or end of a gene (annotation "Start&End"). Additional annotations and visualization were performed using ChIPseeker (Q. Wang et al., 2022; G. Yu et al., 2015).

To search for enrichment in enhancer and silencer regions, SilencerDB (Zeng et al., 2021) and EnhancerAtlas 2.0 (Gao & Qian, 2019) were used to compare the identified peaks with known or

predicted regions. The silencer database was filtered for mouse blood and the EnhancerAtlas 2.0 for $CD4^+$ cells. As the databases were using mm9, USCS LiftOver (UCSC Genome Browser Group, 2023) was used to re-map them to mm10. The search for overlaps with the two databases was performed with ChIPpeakAnno (L. J. Zhu, 2013; L. J. Zhu et al., 2010). To ensure the reported overlap was not random, a random permutation test with 1,100 iterations as implemented in ChIPpeakAnno was performed.
Ab initio motif enrichment analysis of the IRF4-ChIP-Seq peaks derived from Th17 and Treg cells was executed using the MEME suite with default parameters (T. L. Bailey et al., 2009). Identified motifs were annotated using Tomtom (Gupta et al., 2007) with a similarity threshold of 0.05, in conjunction with the position-specific scoring matrices (PSSM) of murine transcription factors from the TRANSFAC database (Matys, 2006). To enhance motif annotation, we additionally employed the MATCH algorithm (Kel, 2003) for annotating known transcription factor binding sites. This process incorporated PSSMs corresponding to Th17 and Treg interactors, as well as the profile of immune-specific transcription factors as defined by TRANSFAC. A stringent cut-off threshold, accepting motif annotations only if they matched both the core sequence and matrix sequence of PSSMs with a similarity score of 0.8 or higher, was established. To further investigate the combinatorial activity of transcription factors, the number of peaks bound by two distinct transcription factor motifs within a spatial proximity of equal or less than 5 bp was investigated. This approach facilitated a detailed exploration into the complex interplay of transcription factors within Th17 and Treg cells.

3.2.9 CELL LYSIS AND BRADFORD ASSAY

The Bradford assay is a standard, colorimetric-based method to determine protein contents. In this thesis, it was used prior to a comparative western blot, which requires the loading of the same amount of protein from each sample. First, cells were lysed in urea buffer and sonicated 1-2 times each for 10 cycles (each cycle 30 s/30 s ON/OFF) in a Bioruptor Plus. Then the samples were centrifuged for 7 min at 12,700 x*g*, 4 °C and the supernatant was transferred into new tubes. For the Bradford assay, 10 µL of each sample were pipetted in duplicates into a 96-well plate (F-bottom). As a reference, a serial dilution of BSA ranging from 0-2 µg/µL was pipetted into the plate. After all samples and a reference dilution at known concentrations were prepared, 150 µL protein assay reagent was added to each well. The absorbance was measured at 660 nm and the corresponding sample concentration was calculated using the BSA standard curve.

3.2.10 SDS-PAGE AND WESTERN BLOT

Western blot is a method for detecting specific proteins on a membrane with an antibody via a chemiluminescent reaction. Prior to western blot analysis, the proteins were separated with SDS-polyacrylamide gel electrophoresis (SDS-PAGE). For that, the samples were supplemented with a loading dye and denatured at 95 °C for 5 min. The samples and a marker were loaded onto a SDS gel and the proteins were separated on the SDS gel using a electrophoresis cell. After that, the proteins were transferred from the gel onto a polyvinylidene fluoride (PVFD) membrane (0.45 µm pore size).

This was done with a semi-dry blotting method: three Whatman papers were soaked in turbo blotting buffer and transferred into a TransBlot Turbo Transfer System for blotting. Next, a methanol-activated PVDC membrane was laid on top of the Whatman papers, followed by the SDS acrylamide gel. On top, another three Whatman papers soaked in turbo blotting buffer were added. Afterwards, any air bubbles were carefully removed by rolling over the stack. The proteins were transferred from the gel to the membrane for 30 min applying 1 A and 25 V (recommended parameters from BioRad). After protein transfer, the membrane was blocked with 5 % BSA in TBS-T buffer for 1 h at room temperature to prevent unspecific binding of the antibodies. To detect IRF4, the primary anti-IRF4 antibody F-4 (1:1,000 diluted in TBS-T) was incubated rolling over night at 4 °C. On the next day, a secondary horseradish peroxidase-conjugated IgG antibody (1:2,000 in TBS-T) was used for the detection. Biotinylated proteins were detected using horseradish peroxidase-conjugated streptavidin (1:1,000 diluted in TBS-T), which was incubated rolling for 1 h at room temperature. A horseradish peroxidase-conjugated β-actin antibody (1:25,000 diluted in TBS-T) was used as a loading control and incubated rolling for 30 min at room temperature. When one western blot was stained with different antibodies, the previous antibody was removed by stripping the blot for 30 min at room temperature. Before a new antibody could be added, the blot was blocked again as described above. Any antibody binding was visualized using the WesternBright Chemiluminescence substrates. The chemiluminescence signal was captured with a BioRad ChemiDoc XRS imager and analysed using the Quantity One software (version 4.4.0, BioRad).

3.2.11 CHEMICAL CROSS-LINKING AND NUCLEI ISOLATION

To preserve also weak and transient protein interactions for mass spectrometric analysis, the cells were incubated directly after the harvest with a cell permeable cross-linker. For each experiment, 20 mM dithiobis(succinimidyl propionate) (DSP) was freshly prepared in DMSO. The final working solution of 0.75 mM DSP was diluted in PBS, pH 8.3. Cells were cross-linked according to the manufacturer's protocol for 30 min at room temperature. The reaction was stopped by adding Tris (pH 7.5) to a final concentration of 10 mM, followed by incubation for 15 min at room temperature. Afterwards, cells were washed twice (630 x*g* for 10 min at 4 °C) with cold PBS to remove any remaining DSP.

The cell nuclei were separated from the cytosolic fraction to reduce the amount of endogenously biotinylated proteins. For that, cells were resuspended in a hypotonic buffer. After incubation for 12 min on ice, NP-40 was added to the samples to obtain a final concentration of 0.5 % (v/v) and cells were vortexed for 10 s to disrupt cell membranes. Nuclei were washed twice with PBS and pelleted by centrifugation at 850 x*g* for 10 min at 4 °C. Isolated nuclei were either stored at -80 °C until further processing or directly subjected to affinity purification.

3.2.12 PROTEIN AFFINITY PURIFICATION (PROTEIN PULLDOWN)

An IRF4 protein pulldown was used to identify IRF4 interacting proteins in fully differentiated Th17 and Treg cells. Isolated nuclei were resuspended in Cell Lysis Buffer from the µMACS FactorFinder Kit, which was supplemented with proteinase inhibitor cocktail according to manufacturer´s instructions. Nuclear lysis and disruption of DNA was promoted by sonication at 4 °C for 10 min using a Bioruptor Plus (30 s/30 s ON/OFF, low). After lysis of cell nuclei, samples were centrifuged for 6 min at 14,850 x*g* at 4 °C and the supernatant containing nuclear proteins was subjected to affinity purification. Streptavidin-coated magnetic beads (Dynabeads™ M-280) were washed with a mixture of Cell Lysis and Binding Buffer (1:3 (v/v)) for 10 min at room temperature. Afterwards, beads were resuspended in Binding Buffer supplemented with Binding Enhancer (both derived from the µMACS FactorFinder Kit) and added to the nuclear lysates. After overnight incubation at 4 °C, samples were incubated for 2 min on a magnetic rack until beads were settled. Supernatant was discarded and samples were washed three times with RIPA buffer for 10 min at room temperature. Afterwards, the samples were washed three times with 25 mM Tris (pH 7.5) for 10 min at room temperature. Proteins were eluted by incubating the streptavidin-coated beads in an SDS/biotin-containing buffer for 5 min at 95 °C. The eluate was either stored at -80 °C or directly subjected to SP3 digestion.

3.2.13 PROTEOLYTIC DIGESTION (SP3 DIGESTION)

To determine the proteomic composition of fully differentiated Th17 and Treg cells and to analyse the IRF4 interactome of these cells, mass spectrometric analysis was performed. Therefore, proteins released from IRF4 pulldown experiments or whole Th17/Treg lysates had to be digested into peptides for analysis. This was done by using the single-pot solid-phase-enhanced sample preparation (SP3) protocol introduced by Hughes et al. (Hughes et al., 2014, 2019) with minor modifications. In the case of IRF4 pulldown experiments, proteins and DSP cross-linker were first reduced with 45 mM dithiothreitol (DTT) for 30 min at 37 °C. Afterwards, temperature was increased to 45 °C and samples were incubated for another 10 min. Whole cellular lysates were incubated with 20 mM DTT for 30 min at 45 °C. In both cases, proteins were alkylated for 30 min at room temperature using iodoacetamide (IAA). Excess IAA was quenched by the addition of DTT. Afterwards, 2 µL of carboxylate-modified paramagnetic beads (Sera-Mag SpeedBeads) were added to the samples. After adding acetonitrile to a final concentration of 70 % (v/v), samples were allowed to settle at room temperature for 20 min. Samples were mixed after 10 min. Subsequently, beads were immobilized by incubation on a magnetic rack for 2 min and washed twice with 70 % (v/v) ethanol in water and once with acetonitrile. Beads were resuspended in 50 mM NH_4HCO_3 supplemented with trypsin at an enzyme-to-protein ratio of 1:25 (w/w) and incubated overnight at 37 °C. After overnight digestion, acetonitrile was added to the samples to reach a final concentration of 95 % (v/v). Subsequently, samples were incubated for 20 min at room temperature (and mixed after 10 min). To increase the yield, supernatants derived from this initial peptide-binding step were additionally subjected to the SP3 peptide purification procedure as described before (Sielaff et al., 2017). Each sample was washed with acetonitrile. To recover bound peptides, paramagnetic beads from the original sample and corresponding supernatants were pooled

in 2 % (v/v) dimethyl sulfoxide (DMSO) in water and sonicated for 1 min. After 2 min of centrifugation at 16,200 x*g* and 4 °C, supernatants containing tryptic peptides were transferred into a glass vial for MS analysis and acidified with 0.1 % (v/v) formic acid.

3.2.14 LIQUID CHROMATOGRAPHY-MASS SPECTROMETRY (LC-MS) ANALYSIS

The generated peptides (see chapter 3.2.13) were analysed by liquid chromatography coupled to mass spectrometry (LC-MS) using an Ultimate 3000 RSLC nano LC system coupled to an Orbitrap Exploris 480 instrument platform. Tryptic peptides were first loaded onto a PEPMAP100 C18 5 µm 0.3 x 5 mm trap column and subsequently separated on an HSS-T3 C18 1.8 µm, 75 µm x 250 mm analytical reversed-phase column. Mobile phase A was water containing 0.1 % (v/v) formic acid and 3 % (v/v) DMSO. Peptides were separated by running a gradient of 2–35 % mobile phase B (0.1 % (v/v) formic acid, 3 % (v/v) DMSO in ACN) over 40 min at a flow rate of 300 nL/min. Total analysis time was 60 min including wash and column re-equilibration steps. Column temperature was set to 55 °C.

The following settings were used for mass spectrometric analysis of eluting peptides on the Orbitrap Exploris 480 instrument platform. Spray voltage was set to 1.8 kV, the funnel RF level to 40, and heated capillary temperature was at 275 °C. Data were acquired in DIA mode. Full MS resolution was set to 120,000 at *m/z* 200 and full MS automated gain control (AGC) target to 300 % with a maximum injection time (IT) of 20 ms. Mass range was set to *m/z* 345 – 1,250. Fragment ion spectra were acquired with an AGC target value of 1,000 %. In total, 20 windows with varying sizes (adjusted to precursor density) were used with an overlap of 0.5 Da. Resolution was set to 30,000 and IT was determined automatically (“auto mode”). Normalized collision energy was fixed at a value of 27 %. All data were acquired in profile mode using positive polarity. All samples were analysed in three technical replicates.

DIA raw data were processed using DIA-NN (version 1.7.13) (Demichev et al., 2020) applying the default parameters for library-free database search. Data were searched using a custom compiled database containing UniProtKB/SwissProt entries of the murine reference proteome (UniProtKB release 2021_04, 17,068 entries) and a list of common contaminants (172 entries). For peptide identification and *in-silico* library generation, trypsin was set as protease allowing one missed cleavage. Carbamidomethylation was set as fixed modification and the maximum number of variable modifications was set to zero. The peptide length ranged from 7–30 amino acids. The precursor *m/z* range was set to 300–1,800, and the product ion *m/z* range to 200–1,800. As quantification strategy, the “any LC (high accuracy)” mode with RT-dependent median-based cross-run normalization was applied for whole-cell proteomic analysis and no normalization was selected for pulldown analyses. The in-build algorithm of DIA-NN to automatically optimize MS2 and MS1 mass accuracies and scan window size was used. Peptide precursor FDRs were controlled below 1 %.

For statistical analysis, the linear model limma was used in R (Ritchie et al., 2015). The data were filtered to only contain proteins that showed more than two (proteome) or three (interactome) peptides and were present in at least eight out of nine runs in at least one condition. To enable limma

to work with the intensities, they were log-transformed. DEP's mixed imputation method was used to impute missing data differently for missing at random (MAR) and missing not at random (MNAR): MNAR values were imputed with the minimum value present in the data, while MAR values were imputed with K-Nearest Neighbor (K-NN) imputation, both as implemented in the DEP package (X. Zhang et al., 2018). The design for limma's linear model was different for the proteome and the interactome analysis respectively: for the proteome analysis, just the cell type - which was the comparison of interest – was given to the model as a factor. For the interactome analysis, in addition to the comparison of interest, which was wildtype against the $IRF4^{Bio}$ mice, the experiments were added as a cofactor. This was done to counteract the bias of an outlier experiment, which had generally lower intensities than its partner experiments. For the IRF4 knockout proteome, the following comparisons were performed: $Irf4^{-/-}$ vs WT in naive cells, as well as in the differentiated Treg and Th17 cells. Proteins with an adjusted p-value of 0.01 or less and a $\log_2$(Th17/Treg)>1 (interactome) and $|\log_2(\text{Th17/Treg})|>0.5$ (proteome) were considered significantly, differentially expressed.

Functional gene enrichment analysis was performed using the gene ontology resource (http://geneontology.org/) (Ashburner et al., 2000; Carbon et al., 2021) powered by PANTHER (v14) (Mi et al., 2013, 2019). Network analysis was conducted using the STRING database (version 11.0) (Szklarczyk et al., 2019) through its web interface as well as the stringApp (Doncheva et al., 2019) in Cytoscape (version 3.8.0) (Shannon et al., 2003). Protein networks in STRING were generated using default settings. Venn diagram data were calculated using the Venny web application (http://bioinfogp.cnb.csic.es/tools/venny/index.html).

IV. RESULTS

4.1 IRF4 expression in Th17 and Treg cells

Before the IRF4 interactome in Th17 and Treg cells was investigated, the IRF4 expression pattern during T cell development was determined to select a time point with high IRF4 expression. Therefore, a kinetic was performed assessing the expression of IRF4 in naïve CD4⁺ T cells (0 h) as well as after 3 h, 8 h, 24 h, 48 h and 72 h (fully differentiated) of T cell receptor stimulation (see Figure 5).

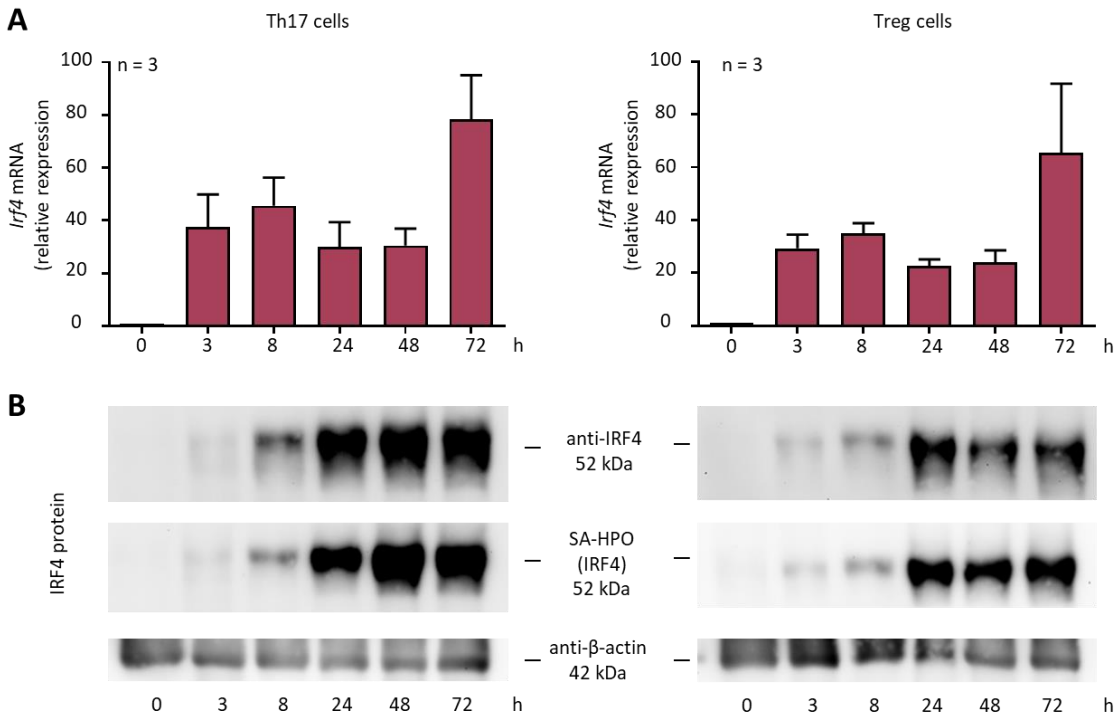

Figure 5: Kinetic of IRF4 expression in differentiating CD4⁺ T cells on mRNA and protein level. The IRF4 expression was analysed during T cell differentiation on mRNA and protein level of Th17/Treg cell. For this, naïve CD4⁺ T cells were isolated and stimulated for 0 h, 3 h, 8 h, 24 h, 48 h or 72 h with Th17-polarizing (1 ng/mL TGF-ß, 40 ng/mL IL-6, 2.5 µg/mL anti-IFN-γ, 10 µg/mL anti-IL-4) or Treg-polarizing (7.5 ng/mL TGF-ß, 250 ng/mL IL-2) cytokines. In naïve CD4⁺ T cells, no IRF4 was expressed at all. Upon TCR stimulation, IRF4 was expressed at different expression levels, shown at mRNA level (A) and protein level (B). The expression levels of IRF4 (monoclonal antibody F-4, clone SC-48338) and biotinylated IRF4 (horseradish-peroxidase conjugated streptavidin, SA-HPO) in full Th17/Treg cells lysates were detected using western blot. A monoclonal antibody against β-actin (clone AC-15) was used as a loading control.

As shown in Figure 5, no IRF4 expression was detected in naïve T cells, at neither mRNA nor protein level. Upon T cell stimulation with anti-CD3 and anti-CD28 antibodies, IRF4 expression was detectable at mRNA level (A) after 3 h. Only low expression is seen at protein level at this timepoint. *Irf4* mRNA levels peak slightly after 8 h before they drop again and show highest *Irf4* mRNA expression at 72 h after T cell stimulation. This can be shown for Th17 as well as for Treg cells. At protein level (B), most IRF4 was expressed after 24 h and a high expression continued until the cells are fully developed into Th17 and Treg cells. In general, it can be seen that IRF4 expression (mRNA and protein) is higher in Th17 cells than in Treg cells.

4.2 Establishment of an IRF4 protein pulldown protocol

For studying the IRF4 protein interactome, an unbiased, robust and highly reproducible protocol had to be established. Fully differentiated cells were well suited as the highest IRF4 expression was after 72 h of T cell stimulation (shown in chapter 4.1). The challenges of a limited number of primary T cells had to be tackled, as well as efficiently reducing unspecific binding, while at the same time preserving weak interaction partners. In addition, the optimal strategy for mass spectrometric analysis of enriched transcription factor complexes had to be investigated.

The first hurdle to getting enough T cells (4 - 5 x 10^6 cells) for interactome studies could be overcome by pooling cells isolated from three animals (per condition and per experiment). To stabilize weak and transient interactions, chemical cross-linkers are described as being a good tool (Smith et al., 2011; Titeca et al., 2019). Therefore, the cell-permeable, reversible cross-linker Dithiobis(succinimidyl propionate) (DSP) was included to preserve all protein-protein interactions directly after harvesting the cells and prior to cell lysis. This cross-linker reacts with primary amines and contains a reducible disulfide bond in the spacer arm, which makes the fixation reversible by the addition of DTT (see Figure 6 A). To include the cross-linker in the final protocol, the optimal concentrations had to be determined: different concentration ranging from 0 mM (not-cross-linked) to 1 mM DSP were tested. A concentration of 0.75 mM DSP was best suited as no non-cross-linked IRF4 was detectable (see Figure 6 B). Therefore this concentration was used for further experiments.

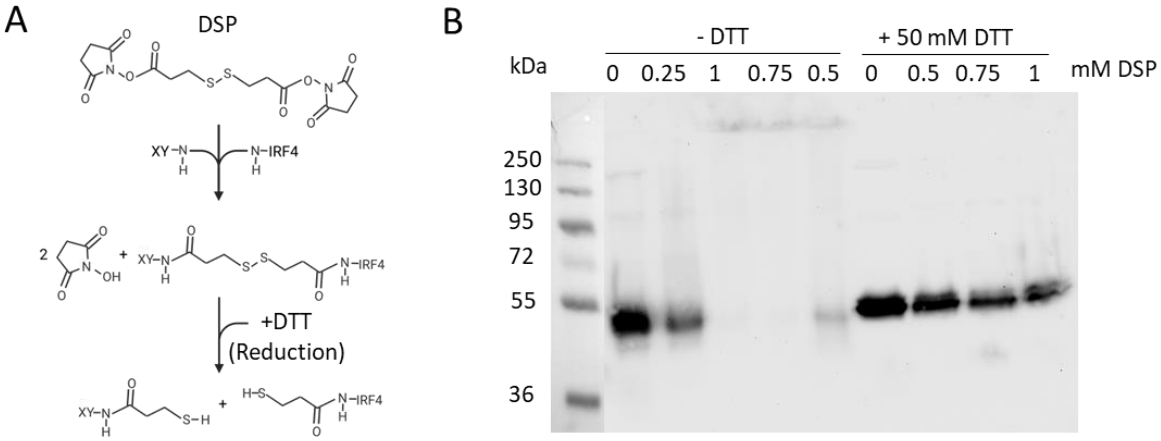

Figure 6: Titration of DSP cross-linker. To stabilize weak and transient IRF4 interactions, a cell-permeable, reversible chemical cross-linker, namely DSP, was used. To investigate the optimal amount of DSP for cross-linking, different concentrations were tested. The efficiency of cross-linking was tested by western blot analysis. (A) Chemical reaction of DSP cross-linking and reversion of cross-linking by the reduction of the disulfide bonds in the spacer arm of the cross-linker using DTT. (B) Western blot analysis of different concentrations (0 – 1 mM DSP) of the DSP cross-linker demonstrated large, cross-linked complexes with increased concentrations of the cross-linker. The addition of DTT (50 mM) reverted the cross-linking. A polyclonal IRF4 antibody (P173) was used to determine the amount of non-cross-linked and cross-linked IRF4 in the cellular lysate of Th17 cells.

In the next step, the optimal washing conditions had to be defined to reduce unspecific background. RIPA buffer – commercially available RIPA buffer is supplemented with 0.1 % (w/v) SDS – was modified with different percentages of SDS (w/v). Buffers complemented with 0.1 %, 0.5 %, 1 %, 2 % and 3 % SDS were tested. Differentiated T cells were used to isolate IRF4 with different washing buffers and the eluates were analysed on western blots. As shown in Figure 7, the commercial RIPA buffer supplemented with 0.1 % (w/v) SDS could not reduce the background as there was still IRF4 in the eluate fraction of the non-biotinylated control sample. Increasing the amount of SDS in the buffer could reduce IRF4 binding in the control (WT). Only very little IRF4 was detectable in the western blot of an eluted fraction where the pulldown was washed with 0.5 % (w/v) SDS in the RIPA buffer (see Figure 7 A). However, concentrations above of 1 % (w/v) of SDS reduced also specific binding of biotinylated IRF4 ($IRF4^{Bio}$). Mass spectrometric analysis of IRF4 pulldown samples showed that in samples that were washed with only 0.35 % (w/v) SDS in the RIPA buffer, more IRF4 peptides could be identified than in samples that were washed with 0.5 % (w/v) SDS in the washing buffer (see Figure 7). In addition, no IRF4 peptides were detected in the WT control when the samples were washed with a RIPA buffer supplemented with 0.35 % (w/v) SDS. Hence a washing buffer containing 0.35 % (w/v) SDS was used for IRF4 pulldown studies. A preliminary study applying the optimized set-up (inclusion of cross-linker and improved washing conditions) for an IRF4 pulldown with isolated splenocytes demonstrates the improvement: 38 IRF4 interaction partners could be identified by LC-MS using these settings. In contrast, only seven interactors could be identified using no cross-linker. In samples using less stringent washing conditions (RIPA buffer containing 0.1 % (w/v) SDS), a higher background could be observed resulting in an overall lower number of IRF4 interacting proteins, even in the sample where the cross-linker was used.

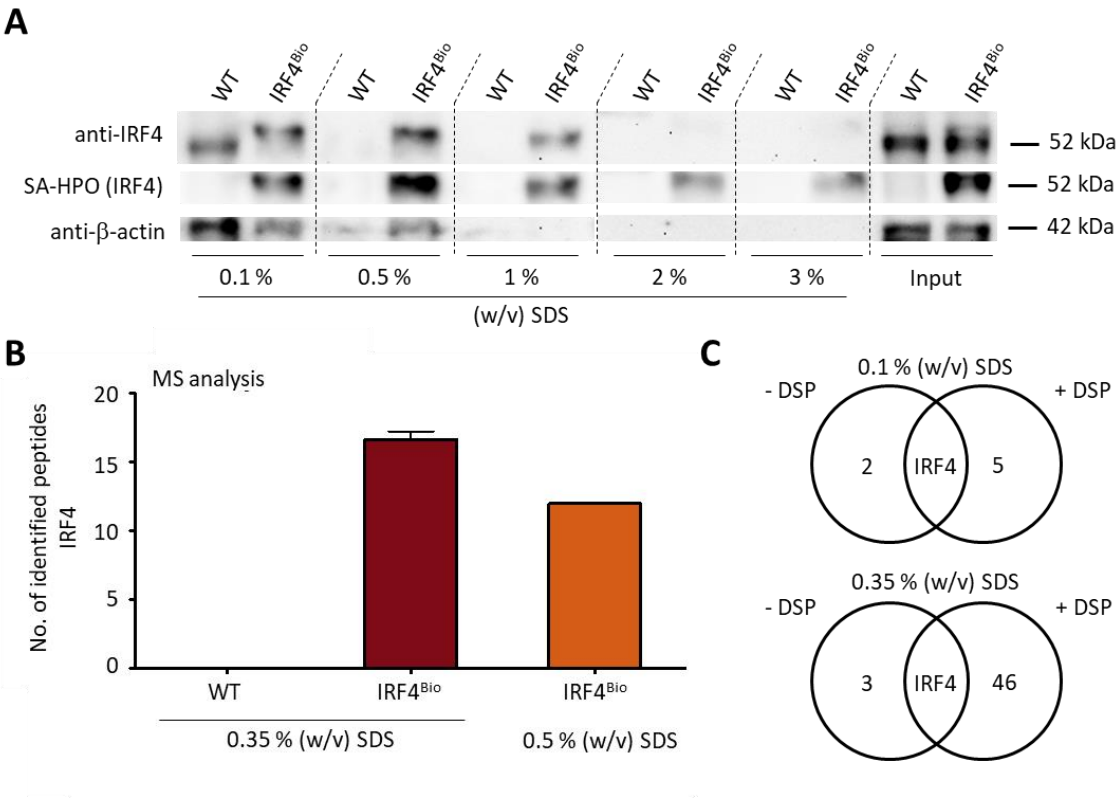

Figure 7: Optimization of washing conditions. To reduce unspecific background, the washing step in the pulldown protocol had to be optimized. For that, different concentrations of SDS (0.1 – 3 % (w/v) in RIPA buffer) were tested and evaluated with western blot analysis (A). Eluates from IRF4 pulldown of fully differentiated T cells were analysed by western blot. IRF4 was detected using a monoclonal (F-4, clone SC-48338) IRF4 antibody. Biotinylated IRF4 was identified with horseradish-peroxidase conjugated streptavidin (SA-HPO). As a loading control, β-actin (clone AC-15) was used. (B) Mass spectrometric analysis of IRF4 pulldown washed with different concentrations of SDS in RIPA buffer. The number of identified peptides of IRF4 by LC-MS in control (WT) and IRF4^{Bio} is shown. (C) Venn diagrams showing IRF4 interaction partners identified under different washing conditions and in the presence or absence of the cross-linker DSP.

Different sample preparation protocols for mass spectrometric analysis were tested to identify the conditions resulting in the best MS data quality. On-bead digestion is an easy and often-used method as the samples can be digested directly on the matrix: in the case of the IRF4 pulldown, on streptavidin beads. As no elution step is required, this also results in high sample recovery. However, streptavidin peptides are digested and released together with peptides from the IRF4 interactome and create a high background signal in the LC-MS analysis (see Figure 8), which negatively affects data quality. Eluting the proteins from the streptavidin beads first and digesting the sample without the matrix by single-pot solid-phase-enhanced sample preparation (SP3), increased the LC-MS data quality as the streptavidin contamination was markedly reduced.

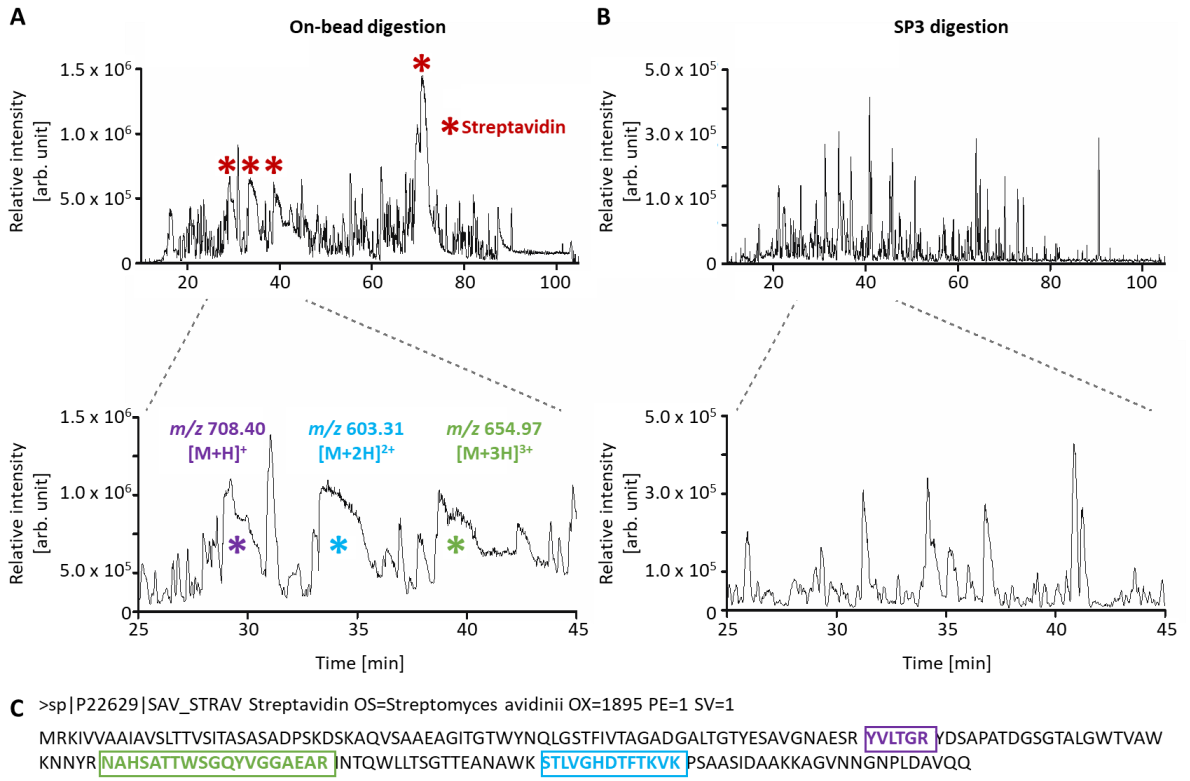

Figure 8: Mass spectrometric analysis of different digestion protocols. Different protein digestion protocols were tested to decrease the amount of contaminating streptavidin peptides during MS analysis. IRF4 was isolated from fully differentiated T cells of IRF4^{Bio} and control animals using magnetic streptavidin-coated beads. For the on-bead digestion (A) the isolated proteins were directly digested on the magnetic beads. This caused broad, tailing peaks which derive from streptavidin (beads). In contrast, for the SP3 digestion (B) the proteins were eluted from the streptavidin beads before digestion and therefore less streptavidin contamination was detectable. The streptavidin peptides that cause bad MS quality are colour-coded in the streptavidin amino acid sequence (C) and in the matching peaks on the chromatogram.

In the final protocol, a sub-cellular fractionation was included which led to the reduction of the background caused by endogenous biotinylated proteins. This was shown by the predecessor to this project, Sarah Dietzen (Dietzen, 2019). Most endogenously biotinylated proteins are mitochondrial proteins. By separating the nuclear fraction from the cytosol, including mitochondria, with a hypotonic buffer, the interfering proteins could be eliminated and in addition led to an enrichment of IRF4, which is mainly expressed in the nucleus.

To summarize the improved protocol for IRF4 pulldown (interactome) studies: Three wildtype and three IRF4^{Bio} animals were pooled to obtain enough T cells, which were cross-linked with 0.75 mM DSP directly after harvest of the cells. Cell nuclei were isolated using a hypotonic buffer. The nuclear lysate, incubated with streptavidin beads, was washed with a RIPA buffer containing 0.35 % (w/v) SDS and eluted from the beads after the pulldown. For mass spectrometric analysis, the samples were digested using a slightly modified SP3-protocol (see Figure 9).

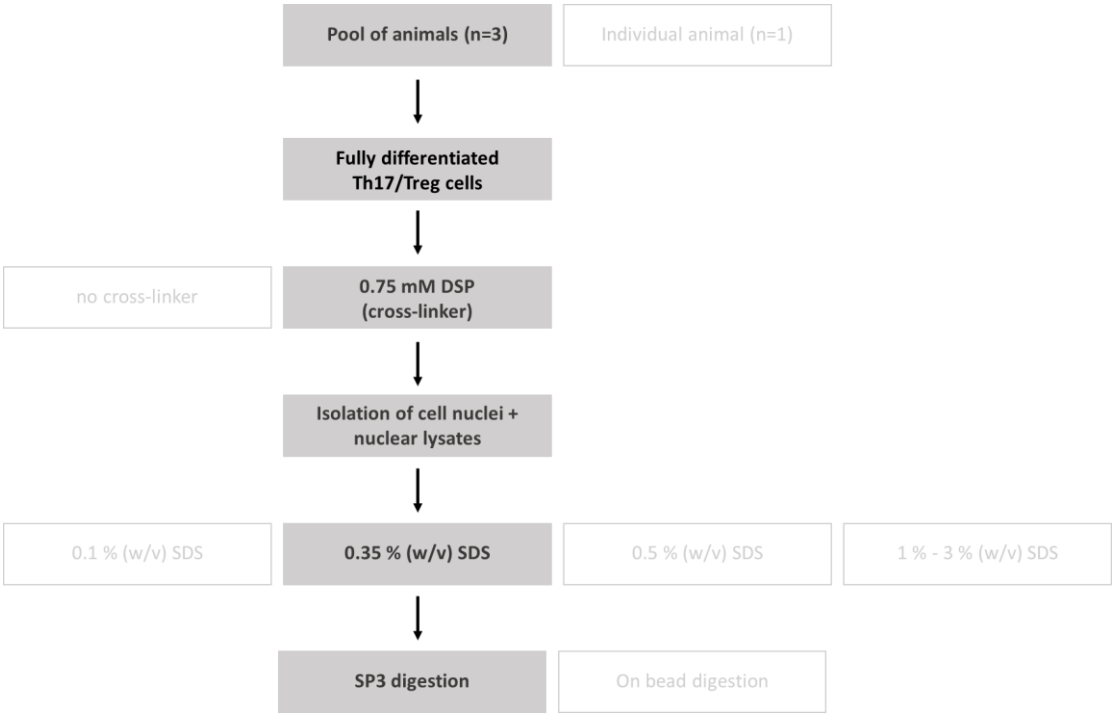

Figure 9: Schematic overview of optimized protein pulldown protocol. Different steps in the protein pulldown protocol were tested and optimized. The selected improvements are highlighted in grey.

4.2 IRF4 interactome analysis (IRF4 pulldown)

With the improved pulldown protocol, the IRF4 interactome of fully differentiated Th17 and Treg cells was characterized. The proteins had to be at least 2-fold enriched in the $IRF4^{Bio}$ sample compared to the WT control, at least three peptides per protein had to be identified and the proteins had to be found in at least eight out of nine runs. Hereby, a total of 440 IRF4 interacting proteins were identified. Overall, 422 proteins (out of 437 proteins that could be matched in the Cytoscape network) were interconnected, whereas 39 proteins were physically or functional directly connected with IRF4 (see Figure 10 A), including the lineage-specific transcription factors FoxP3 and RORγT. Most of these interactors were associated with transcription (see Figure 10 A, grey circle), positive regulation of transcription (DNA-templated, see Figure 10 A, green circle) and/or negative regulation of transcription (RNA polymerase II, see Figure 10 A, yellow circle). Gene enrichment analysis of the direct interactors in the Treg compartment revealed a negative role of these proteins in the development of Th17 cells and positive regulation of IL-4 production. The Th17 enriched direct IRF4 interactors were attributed to T cell differentiation and positive regulation of Th17 immune response (see Figure 10 B). A total of 41 experimentally determined IRF4 interactors of Th17 and Treg cells were already reported as murine or human IRF4 interacting proteins (see S Table 2) in different databases, e.g. STAT3, IRF8, JunB and SATB1 (information derived from PSICQUIC search (EMBL's European Bioinformatics Institute (EMBL-EBI), 2023) and HIPPIE (Human Integrated Protein-Protein Interaction rEference) (Schaefer et al., 2012)). However, it should be mentioned that not all protein interactions were identified by direct protein-protein interaction or physical association; some were only identified by co-localization, proximity, association or were predicted.

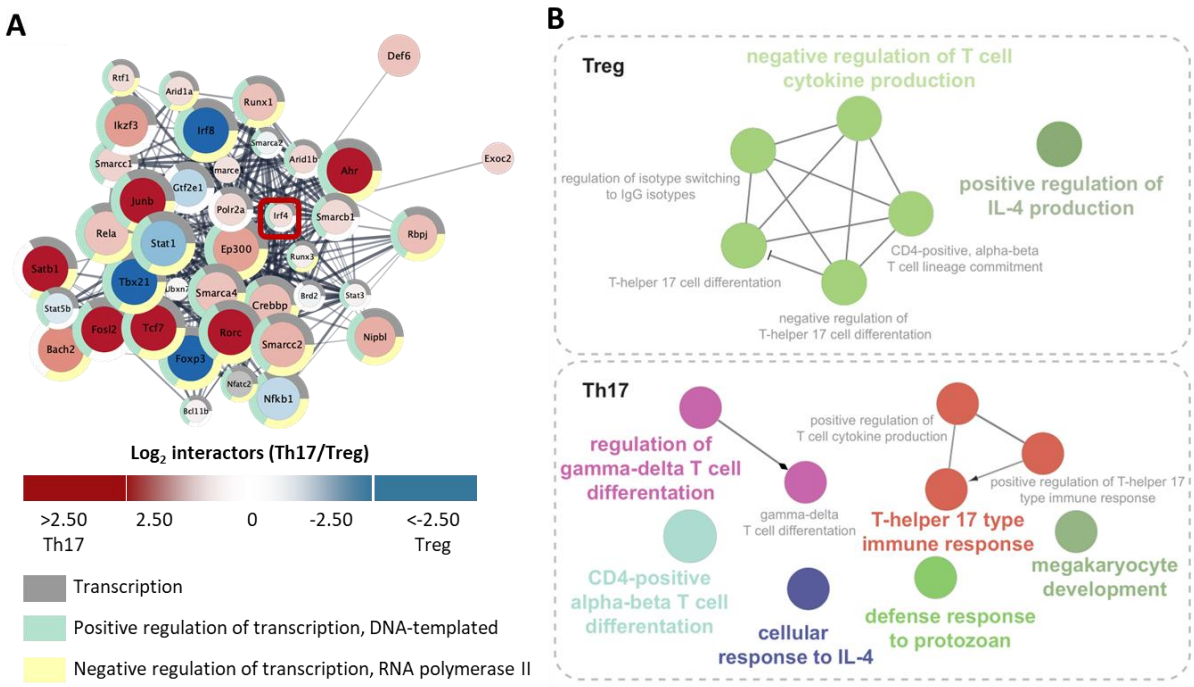

Figure 10: IRF4 interactors in Th17 and Treg cells. IRF4 interactome analysis was performed using fully differentiated (72 h), *in vitro* generated Th17 and Treg cells. After harvesting the cells, they were cross-linked, cell nuclei isolated and IRF4 and its interactors were isolated using magnetic-streptavidin beads. The proteins were eluted from the beads and prepared for mass spectrometric analysis. In total, three independent pulldown experiments per cell types (n=3) were conducted. (A) String-based network of proteins that were physically and/or functionally associated with IRF4 (IRF4 interactors) in Th17 or Treg cells. Interactors that have a higher expression in Th17 cells are shown in different intensities of red; proteins that have a higher expression in Treg cells are depicted in different intensities of blue. Proteins associated with transcription are highlighted with a grey circle. Proteins associated with positive regulation of transcription, DNA-templated are highlighted with a green and proteins associated with negative regulation of transcription, RNA polymerase II are highlighted with a yellow circle. (B) GlueGo analysis (Bindea et al., 2009) of IRF4 interactors that were either significantly enriched in Th17 cells or in Treg cells ($|\log_2(\text{Th17/Treg})|>0.5$, adj.p-value<0.01).

Among all identified IRF4 interactors, a core T cell interactome comprising 286 proteins was identified. Those proteins were identified in both cell types and were not enriched in a particular cell subset. A total of 109 proteins were either only found in the interactome of Th17 cells or Th17-enriched ($\log_2(\text{Th17/Treg})>0.5$, see Figure 11, comment: in the following, these proteins are only referred to as Th17-enriched proteins), among which 41 proteins were also significantly enriched (adj. p-value<0.01) in Th17 cells (see Figure 11, highlighted in red). In Treg cells, 45 proteins were uniquely found or enriched ($\log_2(\text{Th17/Treg})<(-0.5)$, comment: in the following, these proteins are only referred as to Treg-enriched proteins) in this cell type. In addition, 12 proteins were significantly enriched (adj.p-value<0.01) in Treg cells (see Figure 11, highlighted in blue).

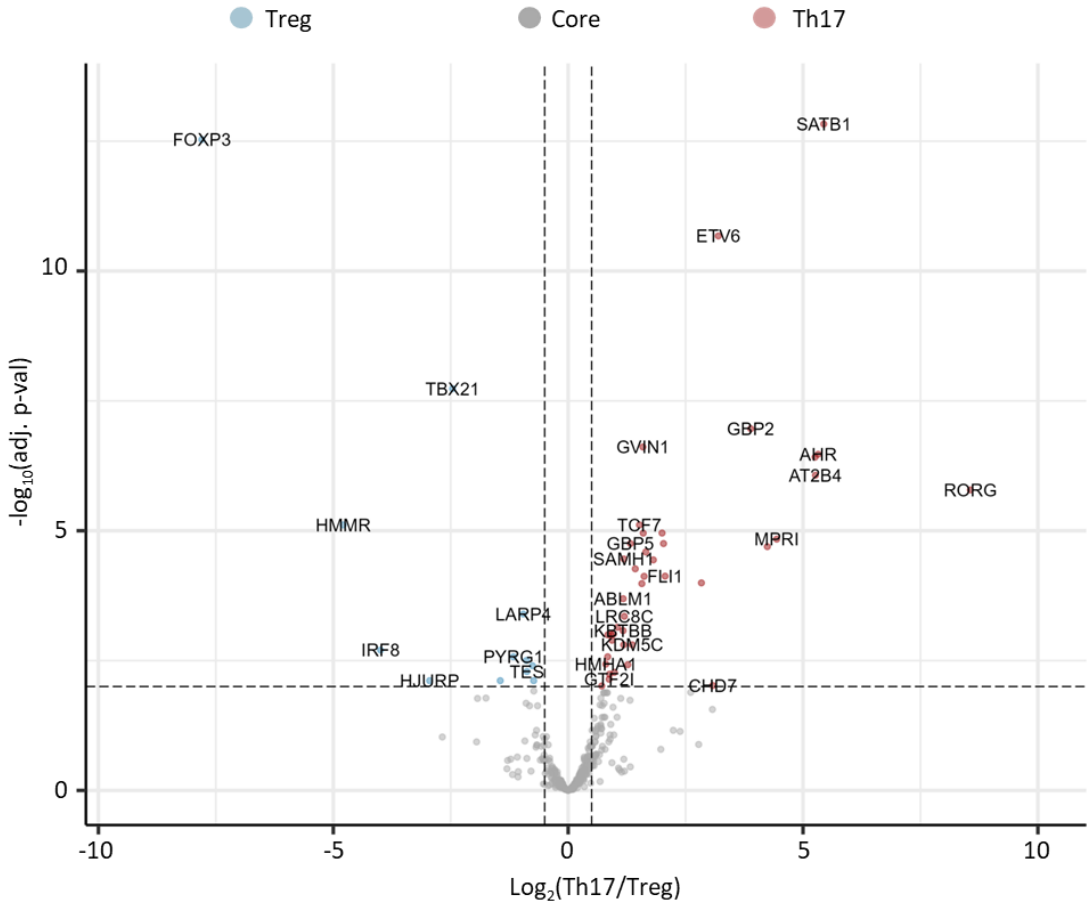

Figure 11: Volcano plot of differentially enriched proteins between Th17 and Treg cells. Volcano plot of IRF4 interactors in Th17 and Treg cells. Three independent pulldown experiments (n=3) of fully differentiated, *in vitro* generated Th17 and Treg cells were performed. For each experiment, naïve $CD4^+$ T cells were pooled prior to cell differentiation. Fully differentiated cells were harvested, cross-linked and cell nuclei isolated. After isolation of IRF4 and its interactors by magnetic streptavidin-coated beads, proteins were analysed by mass spectrometry. Proteins that were exclusively found or significantly enriched in the interactome of Th17 cells are shown in red (log_2(Th17/Treg)>0.5, -log_{10}(adj.p-val)>2) and proteins solely or more highly enriched in Treg cells are depicted in blue (log_2(Th17/Treg)<(-0.5), -log_{10}(adj.p-val)>2). The core T cell interactome, identified in both T cell subsets, is presented in grey. Statistical analysis was performed using the linear model limma. Only proteins that were identified as IRF4 interactors in Th17 and/or Treg cells were used for this volcano plot.

In all three clusters, many nuclear proteins were detected. A high overlap of IRF4 interactors with proteins from the NuRD complex (70.6 %, 12 out of 17 proteins associated with the term identified), the SWI/SNF (superfamily-type) complex (57.1 %, 16 out of 28 proteins associated with the term identified) and from the histone deacetylase complex was found in the core interactome as well as the Th17-enriched interactome (see Figure 12 A). Biological processes of the IRF4 complex from Treg-enriched proteins could be described by positive regulation of protein acetylation or positive regulation of histone acetylation. The Gene ontology (GO) term “binding” united all three fractions of protein in the molecular function, however could only be further distinguished with nuclear acid binding, (m)RNA binding, DNA binding, protein binding, chromatin binding, (DNA-binding) transcription factor binding, sequence-specific DNA binding or histone binding for proteins from the core interactome and Th17-enriched fraction (see Figure 12 A).

RNA metabolism proteins, protein-modifying enzyme, and chromatin/chromatin-binding, or -regulatory proteins represent the three most abundant protein groups of the IRF4 core complex (see Figure 12 B). Latter were also identified among the most abundant protein classes of Th17-enriched proteins. Uniquely identified in the Th17-enriched interactome were gene-specific transcriptional regulators and DNA-binding transcription factors. No enriched protein classes could be determined for proteins enriched in Treg cells (see Figure 12 B).

Similar to the enriched protein classes, enriched reactome pathways could only be identified for the core T cell interactome and proteins enriched in Th17 cells. Here, terms associated with chromatin organization (chromatin-modifying enzymes and chromatin organization) and gene transcription (gene expression (transcription), generic transcription pathways) were determined. Distinct to the proteins of the core interactome was the reactome pathway "metabolism of RNA" (see Figure 12 C).

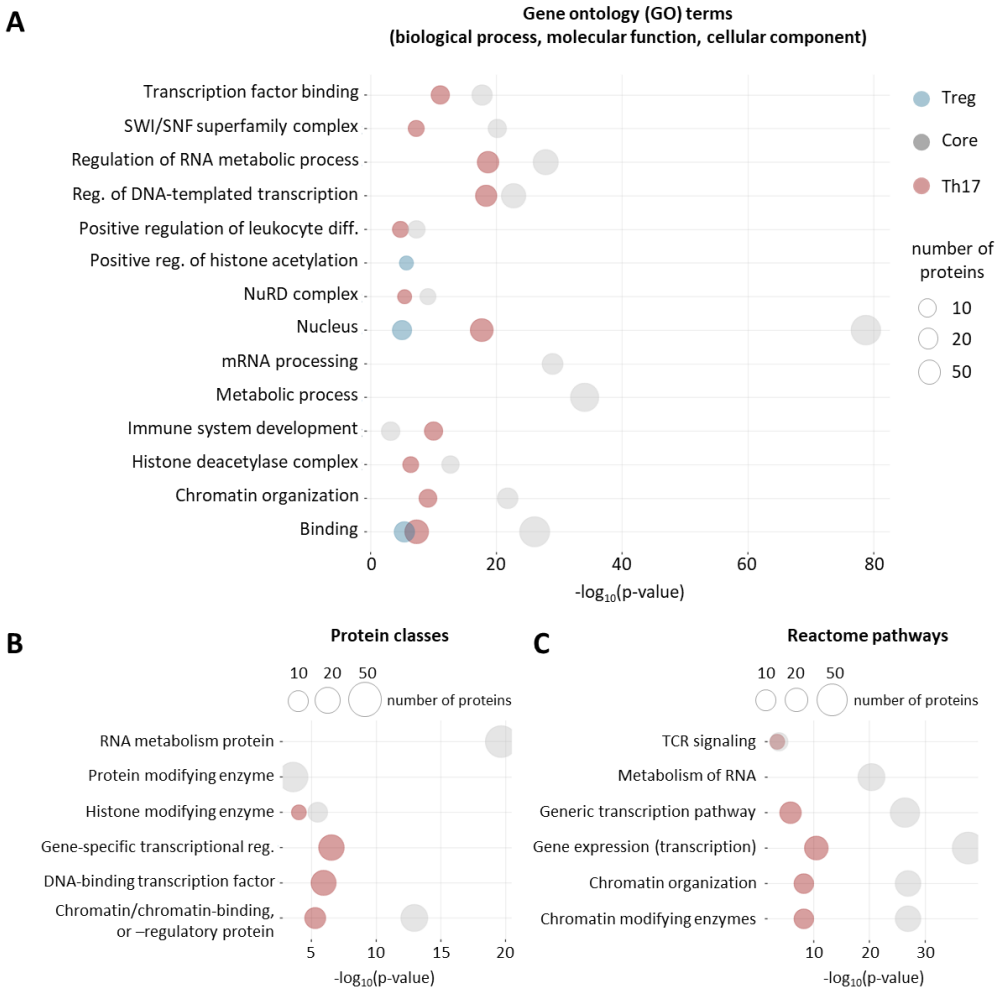

Figure 12: Gene Ontology (GO) enrichment analysis of IRF4 interactors. Enriched (A) GO terms (biological process, molecular function, cellular component), (B) protein classes and (C) reactome pathways from proteins of the IRF4 interactome (n=3 per cell type) of fully differentiated, *in vitro* generated Th17 and Treg cells. Enrichment analysis was performed by gene ontology powered by PANTHER (http://geneontology.org/). GO terms, protein classes and reactome pathways applicable for IRF4 interactors of Th17 cells are depicted in red, applicable for IRF4 interactors of Tregs are depicted in blue and applicable for IRF4 interactors of the core interactome are depicted in grey. The size of the circle represents the number of identified proteins annotated to the respective GO term, protein class and reactome pathway.

4.3 IRF4 chromatin immunoprecipitation followed by sequencing (IRF4-ChIP-seq) analysis

To analyse the genome wide binding sites of IRF4 in Th17 and Treg cells, chromatin immunoprecipitation followed by sequencing (ChIP-seq) was performed. A large peak in the promoter region of the *Irf4* gene revealed that IRF4 regulates its own expression in Th17 and Treg cells. Th17 characteristic genes like *Rorc* or *Il17a* also showed IRF4 binding sites in Th17 cells. However, no peak in or around the *Foxp3* gene was detected in neither of the both cell types (see Figure 13 A).

In total, 21,884 peaks (IRF4 binding regions) that were annotated to 10,918 unique genes were called in differentiated Th17 cells. Most peaks (41.9 %) were found in the promoter region (up to 3 kb downstream of the transcription start site (TSS)), followed by intronic (26.2 %) and distal intergenic binding (26.0 %). In Treg cells, the most abundant binding regions of the 10,189 detected peaks (annotated to 5,789 unique genes) were in intronic (32.9 %), promoter (31.9 %) and distal intergenic (31.0 %) regions (see Figure 13 B). A total of 61.3 % (13,415 peaks) of the identified peaks in the Th17 cells were uniquely found in this cell type and almost half of them (45.7 %) were located in promoter regions. For example, two peaks in the distal intergenic and one peak in the promoter region of *Il17a* (see Figure 13 A, red arrows) and two peaks in the promoter and three peaks in the intron of the *Rorc* gene were only in Th17 cells IRF4 binding regions. In contrast, only 13.7 % of the peaks (1,392 peaks) were unique for Treg cells and these were mainly in intronic gene sections (42.7 % of unique peaks).

To identify the regulatory functions of the binding regions, the peaks were overlapped with the EnhancerAtlas 2.0, which includes predicted enhancer structures (Gao & Qian, 2019), and a Silencer Database, comprising validated silencers (Zeng et al., 2021). In general, a higher overlap with enhancer structures (48.0 % of all enhancers overlapped with Th17 cells and 24.0 % of all enhancers overlayed with Treg cells) could be revealed compared to a low overlay with the SilencerDB (1.4 % of all silencers were detected in Th17 cells and 0.5 % of all silencers overlapped in Treg cells). In sum, 71.9 % of the identified Th17 peaks mapped with predicted enhancer structures (15,738 peaks mapping to 10,990 enhancer structures), while 1,477 peaks (1,707 silencers; 6.7 %) were associated with silencing gene expression (see Figure 13 C). Taking a closer look at the peaks in the enhancer structures, 7,350 peaks were also in the promoter region (≤ 3 kb) of genes. In total, 97 peaks were connected with IRF4 steered gene silencing as these peaks were annotated to silencer and promoter structures.

In Treg cells, slightly more, namely 74.6 % of the peaks overlapped with enhancers (7,589 peaks mapping to 5,484 enhancer structures) and 6.0 % (614 peaks mapping to 666 silencer structures) of the peaks were identified in silencer structures (see Figure 13 C). Among the peaks that were annotated to enhancer structures, 2,656 peaks were also annotated as promoters. IRF4 steered gene silencing was attributed to 25 peaks that have a silencer and promoter characteristic.

Interestingly, Treg cells shared 5,164 (88.7 %) of the matching enhancer structures and 88.4 % (543 silencers) of the silencer structures with Th17 cells (see Figure 13 C).

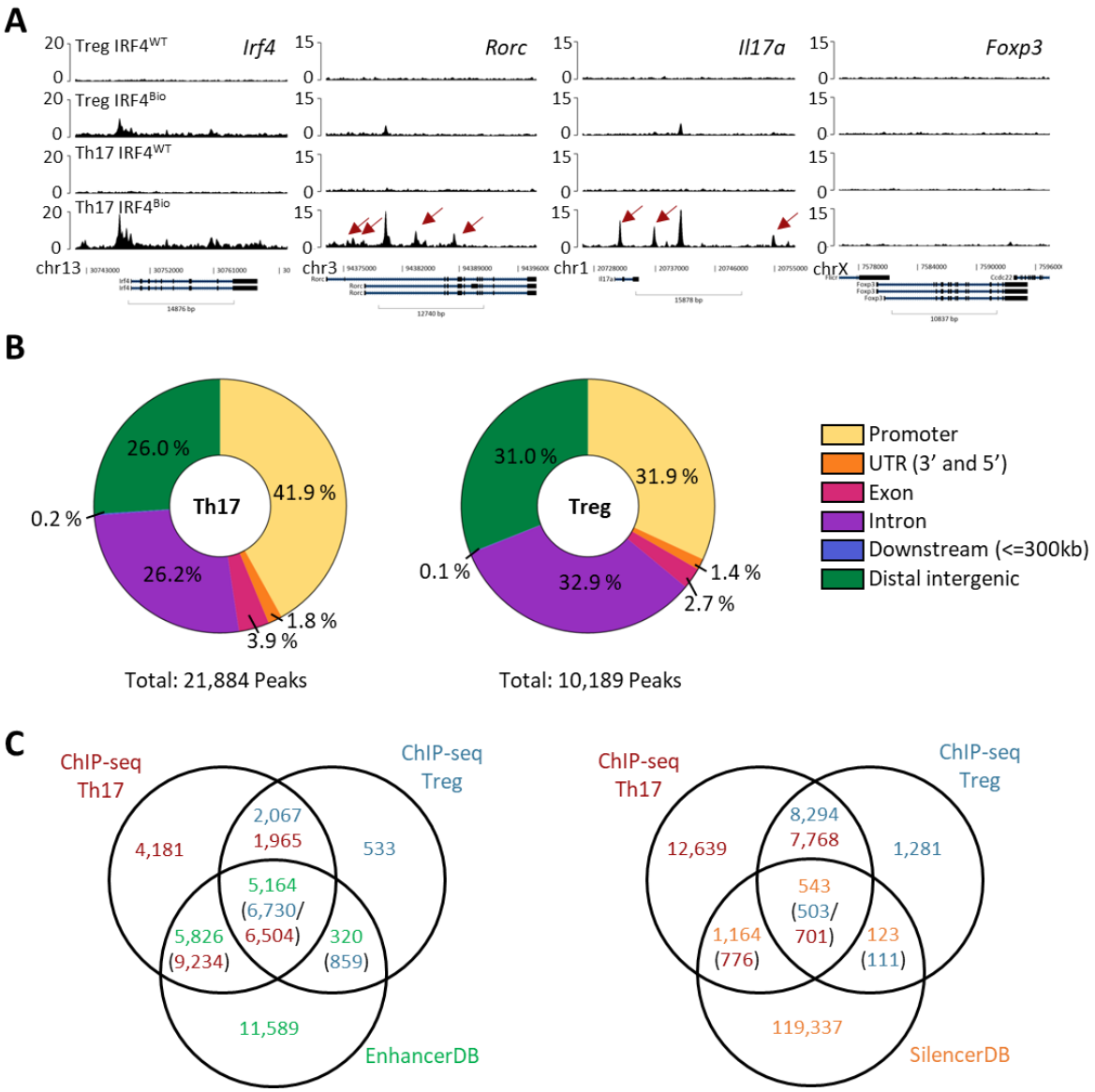

Figure 13: IRF4-ChIP-seq analysis of Th17 and Treg cells. IRF4-ChIP-seq analysis of fully differentiated, *in vitro* generated Th17 and Treg cells. Cells from IRF4^{Bio} and littermate controls were harvested after 72 h of cell differentiation and genome wide IRF4 binding was determined using ChIP-seq analysis. IRF4 DNA binding regions were isolated using magnetic streptavidin-coated beads. At least four technical replicates per cell type were pooled for sequencing. Sequencing results from IRF4-ChIP-seq were analysed using EaSeq (https://easeq.net), version 1.2 (Lerdrup et al., 2016). (A) IRF4-ChIP-seq data for selected genes, characteristic for Th17 or Treg cells. Unique peaks are highlighted with arrows. (B) Percentage distribution of IRF4 binding region in Th17 and Treg cells. The peaks were annotated with ChIPseeker. (C) Overlaps of EaSeq called peaks with the EnhancerDB and SilencerDB. The number of IRF4 peaks in Th17 cells is shown in red, in Treg peaks in blue, enhancer structures are labelled with green and silencers with orange.

Functional enrichment analysis revealed that IRF4 promoted and enhanced (IRF4 binding observed in promoter and enhancer structures) metabolic processes, including RNA, DNA and protein metabolic process, in Th17 and Treg cells. Genes coding for proteins associated with RNA/DNA metabolism were enriched in both cell types. In addition, genes promoting the expression of general transcription factors and histone modifying enzymes, and chromatin/chromatin-binding, or -regulatory proteins were found to be positively regulated by IRF4 (see Figure 14 A). Increased gene expression for gene-specific transcriptional regulator or DNA-binding transcription factors was only seen in Th17 cells. Genes associated with downstream signalling of the TCR were expressed in both cell types. However, genes promoting IL-17 signalling were only expressed in Th17 cells, while in regulatory T cells, IL-2 family signalling as well as IL-4 and IL-13 signalling was enhanced (see Figure 14 A).

Genes that were silenced by IRF4 binding were associated with TLR signalling pathways, MAPK family signalling cascades and Th17 type immune response in Treg cells. In contrast, IRF4 repressed genes that were attributed to transcription regulatory activity, negative regulation of gene expression and regulation of IL-2 production in Th17 cells (see Figure 14 B). Generally, in both cell types, genes associated with signal transduction, regulation of intracellular transduction, GPCR downstream signalling and protein modification processes were negatively regulated by IRF4.

Figure 14: Enriched GO terms of genes that were enhanced or silenced by IRF4. Enriched gene ontology (GO) terms from (A) genes where IRF4 binding was detected in promoter and enhancer structures or (B) silencer structures. Enrichment analysis was performed by gene ontology powered by PANTHER (http://geneontology.org/). GO terms applicable for Th17 cells are depicted in red, applicable for Treg cells are depicted in blue. The size of the circle represents the number of identified genes annotated to the respective GO term.

Motif analysis from the immunoprecipitated DNA fragments using the MATCH algorithm and the murine TRANScription FACtor (TRANSFAC) database revealed motifs from 133 unique proteins (130 motifs identified in Th17 cells, 132 motifs in Treg cells). Most motifs (129 motifs) were found in both cell types, while the motif for the aryl hydrocarbon receptor (AHR) was solely identified in Th17 cells, and FoxP3, IRF8 and NR2C2 motifs were only found in Treg cells (see Figure 15 A). The best matching count matrix for IRF4 was described in 21,846 peaks (99.83 %) of the Th17 IRF4-ChIP-seq and in 10,048 peaks (98.62 %) of Treg cells, representing efficient isolation of IRF4 binding regions and therefore a good quality measure of the IRF4-ChIP-seq analysis.

The MEME-ChIP algorithms were additionally used to search for enriched motifs. In total, 41 motifs were identified in the DNA fragments for Th17 cells and 21 motifs for Treg cells. Comparing and matching them against the murine TRANSFAC database using the Tomtom algorithm revealed 171 corresponding proteins (for 33 motifs) in Th17 cells and 206 unique proteins (for 17 motifs) in Treg cells. Six motifs in the Th17 and four motifs from the Treg IRF4-ChIP-seq were identified as favoured motifs but could not be mapped with any transcription factor from the TRANSFAC database (see Figure 15 B). Enriched motifs mapping with 152 proteins were found in both cell types. In addition, 42 of these motifs were also determined by the MATCH/TRANSFAC algorithm, including BACH2, FLI1, STAT1, STAT3, IRF4 and JunB. Nine motifs were identified in the MATCH/TRANSFAC of both cell types, but only identified as enriched motifs in Treg cells. Similarly, six motifs, including EP300, were found with the MATCH/TRANSFAC algorithm in both cell types but only identified as an enriched motif in Th17 cells. Motifs of IRF8 and NR2C2 were identified as enriched in both cell types but were only found by the MATCH/TRANSFAC algorithm in Treg cells. Interestingly, the motifs for FLI1 and NR2C2 were only detected as reverse complement motifs in Treg cells.

For 18 experimentally determined IRF4 interactors, the matching binding motifs were identified with the MATCH/TRANSFAC and/or the MEME/TOMTOM algorithms (see Figure 15 C), namely FLI1, EP300, STAT3, BACH2, NR2C2, STAT1, JUNB, IRF8, AHR, FoxP3, SATB1, HDAC1, RFX1, NFKB1, CBP, GTF2I and TCF7. Interestingly, the motifs for FLI1 and NR2C2 were exclusively determined as reverse complement in Treg cells.

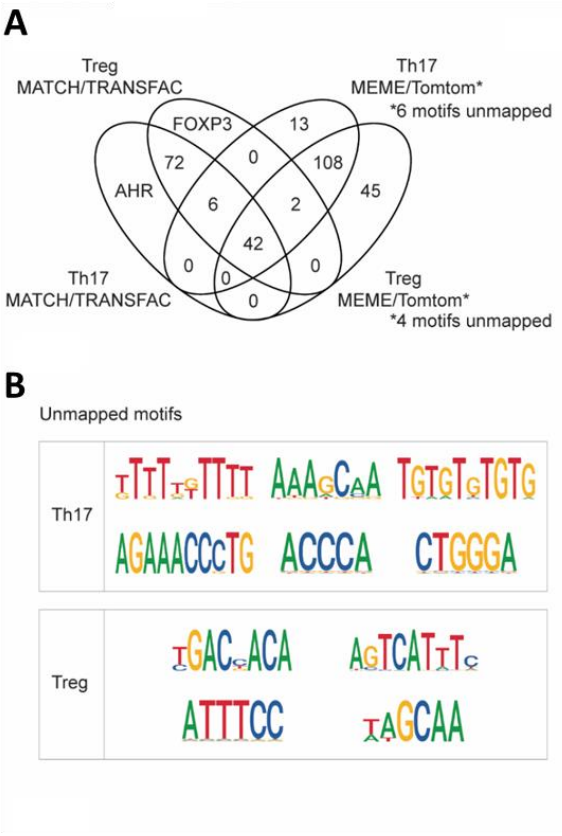

C

	Motif	TRANSFAC Th17	TRANSFAC Treg	MEME/Tomtom Th17	MEME/Tomtom Treg
IRF4		99.83%	98.62%	X	X
FLI1		99.51%	95.74%	X	X*
EP300		99.98%	99.95%	X	-
STAT3		99.84%	98.93%	X	X
BACH2		83.55%	68.84%	X	X
NR2C2		-	98.25%	X	X*
STAT1		98.69%	92.79%	X	X
JUNB		98.67%	94.42%	X	X
IRF8		-	99.35%	X	X
AHR		99.68%	-	-	-
FOXP3		-	98.56%	-	-
SATB1		97.43%	89.33%	-	-
HDAC1		99.93%	99.05%	-	-
RFX1		98.91%	93.11%	-	-
NFKB1		99.61%	96.81%	-	-
CBP		99.99%	99.95%	-	-
GTF2I		97.51%	88.59%	-	-
TCF7		99.29%	95.03%	-	-

*detected exclusively as reverse complement

Figure 15: Binding motifs identified by MATCH/TRANSFAC or MEME/Tomtom algorithm. In fully differentiated, *in vitro* generated Th17 and Treg cells genome wide IRF4 binding was investigated by IRF4-ChIP-seq. Biotinylated IRF4 was isolated from Th17 and Treg cells using magnetic streptavidin-coated beads. Differentiated cells from littermate control animals (WT) served as controls. At least four technical replicates per cell type were pooled for sequencing. Isolated DNA fragments, where IRF4 binding was determined, were investigated for binding motifs of other proteins. (A) Venn diagram of binding motifs identified by the MATCH/TRANSFAC or the MEME/Tomtom algorithm in Th17 and Treg cells. (B) Binding motifs of IRF4 interactors from Th17 and Treg cells that were identified by the MATCH/TRANSFAC or MEME/Tomtom algorithm. (C) Novel unmapped motifs identified in Th17 and Treg cells that were identified by MEME/Tomtom but could not be matched with a known binding motif from the murine TRANSFAC database.

4.4 IRF4 knockout (*Irf4*$^{-/-}$) analysis

To further understand and highlight the importance of IRF4 for the development of T cells, with a focus on Th17 and Treg cells, the proteomes of IRF4 knockout (*Irf4*$^{-/-}$) and IRF4 littermate controls (WT) were analysed. As described previously (Brüstle et al., 2007), an abnormal expression of IL-17A and FoxP3 was detectable upon lack of IRF4 in Th17 and in Treg cells, respectively, as shown by FACS analysis (see Figure 16 A). This could be confirmed by mass spectrometric analysis (see Figure 16 B). In addition, *Irf4*$^{-/-}$ Th17 cells clustered more with Treg cells than with Th17 cells from WT animals, indicating a "Treg-like" phenotype of Th17 cells in the absence of IRF4 (see Figure 16 C).

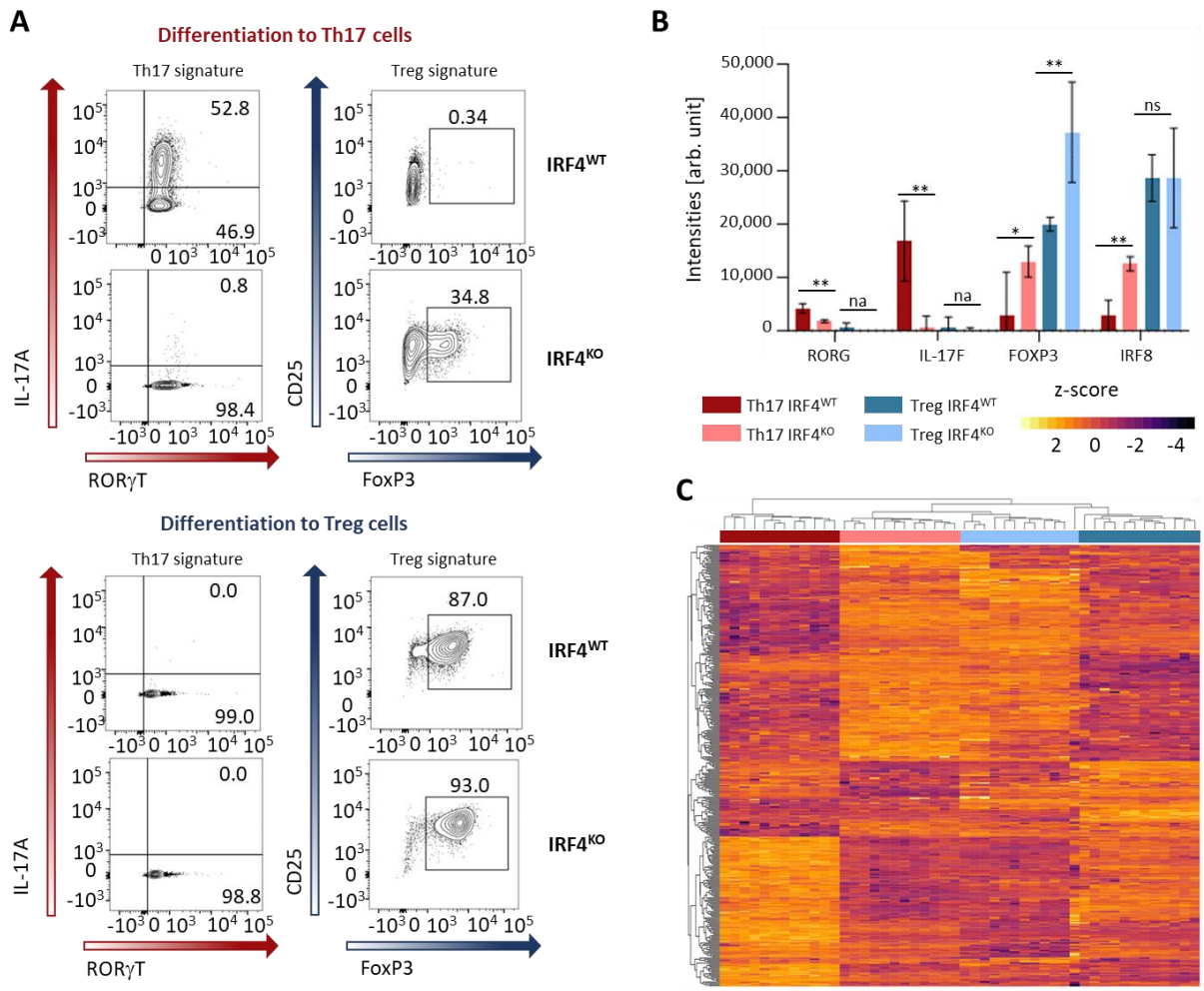

Figure 16: IRF4 knockout (*Irf4*$^{-/-}$) analysis of *in vitro* differentiated Th17 and Treg cells. Naïve CD4$^+$ T cells from *Irf4*$^{-/-}$ and littermate (WT) animals were *in vitro* polarized into Th17 and Treg cells. Fully differentiated (72 h) cells were harvested and further characterized by FACS and mass spectrometric-based proteome analysis. (A) FACS analysis of Th17 (upper panel) and Treg (lower panel) cells. Left column: Th17 cells are characterized by the expression of RORγT (x-axis) and IL-17A (y-axis). Right column: Treg cells express FoxP3 (x-axis) and CD25 (y-axis). The shown FACS plots are representative for four individual cell proliferations per cell type and condition (n=4). (B) LFQ intensity values of RORγT (RORG), IL-17F, FoxP3 and IRF8 from mass spectrometric analysis of Th17 and Treg cells, once in the presence (WT) and once in the absence of IRF4 (*Irf4*$^{-/-}$). Statistical analysis was determined using the linear model limma (** adj.p-value≤0.01, * adj.p-value ≤0.05, ns not significant, na not applicable). (C) Heatmap of differentially expressed proteins (p-value≤0.01 and $|\log_2(\text{Th17/Treg})|>1$) of Th17 and Treg cells from WT and *Irf4*$^{-/-}$ animals.

Proteomic analysis revealed that Th17 cells showed a higher number of differentially expressed proteins between WT and *Irf4*$^{-/-}$ animals as compared to Treg cells (see Figure 17 A). Naïve CD4$^+$ T cells showed a similar protein expression pattern between the WT and *Irf4*$^{-/-}$ conditions in both cell types. Generally, a role of IRF4 in the development (D0 vs D3) of Th17/Treg cells could be seen as well as a role in the differentiated status of the cells (D3, WT vs *Irf4*$^{-/-}$), which can be summarized in four expression patterns that describe the dynamic changes in protein expression (see Figure 17 B). The proteins of cluster I depend on IRF4 only during the development of a particular cell type. The proteins are only up-/down-regulated on day three, but show no differential expression in the differentiated cells. Cluster II comprises proteins that are not only dependent on IRF4 during development but also

in the differentiated status ("WT/*Irf4*$^{-/-}$ axis") as they show a differential (elevated or decreased) expression between D0 and D3 as well as between WT and *Irf4*$^{-/-}$ condition on D3. Cluster III includes all proteins that are up-/down-regulated during the differentiation process, independently of the presence or absence of IRF4, but show a differential expression on D3 between WT and *Irf4*$^{-/-}$ cells. Cluster IV is similar to the previous cluster, except that during the development of the cells, these proteins do not significantly change their expression pattern. As IRF4 is not only important for the up-regulated expression of proteins on D3 but also for a regulated down-regulation of protein expression, clusters I - III can also be found in the opposite direction comparing D0 and D3.

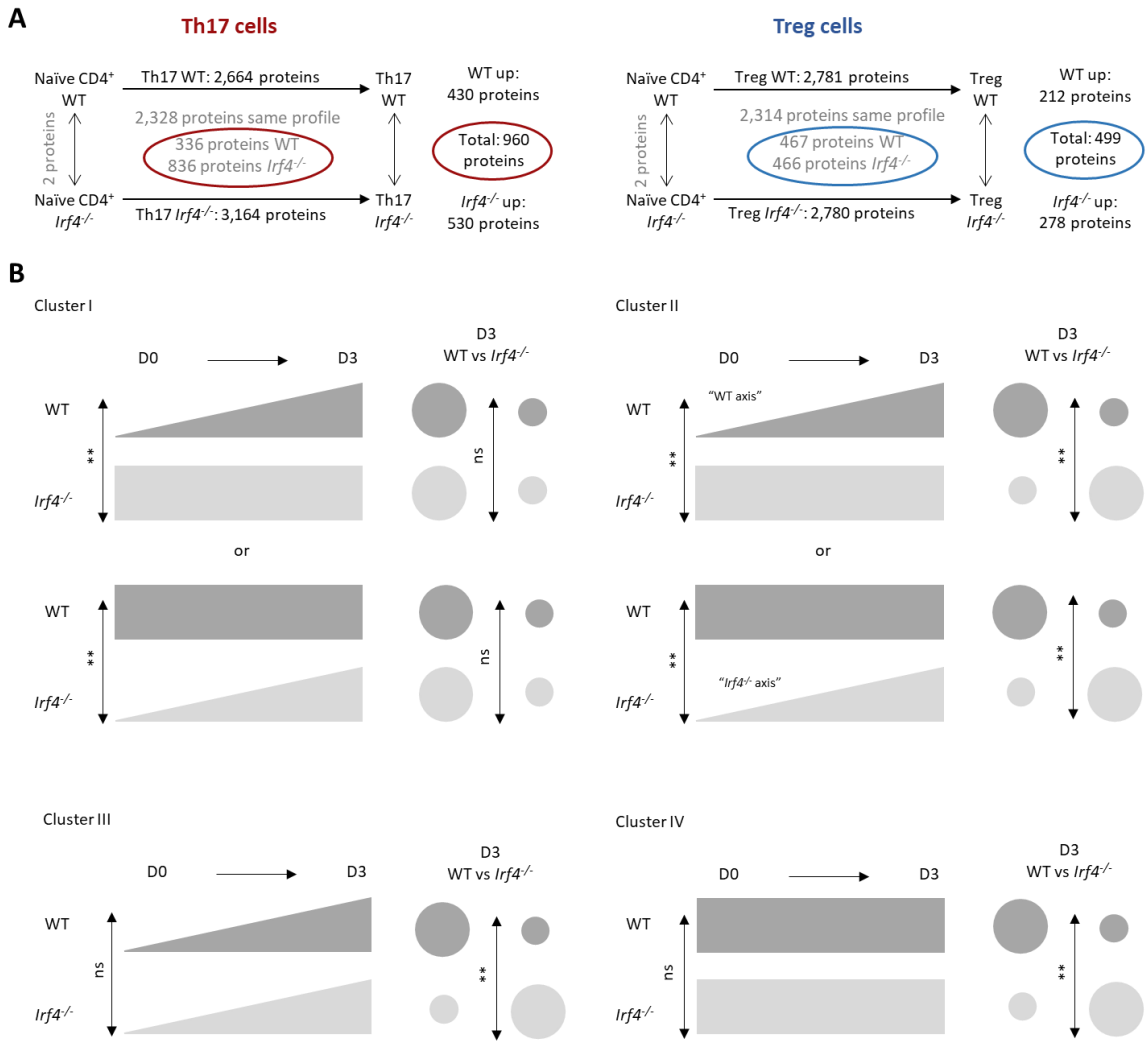

Figure 17: Protein expression patterns of significantly changing proteins during T cell development. To determine IRF4-dependent changing proteins during the development or in fully differentiated T cells, the proteomes of *in vitro* differentiated Th17 and Treg cells from *Irf4*$^{-/-}$ and littermate control animals were analysed by mass spectrometry. An overview of all significantly changing proteins of Th17 or Treg cells is shown in (A). Dynamics in protein expression levels during the development of T cells and/or in differentiated cells can be summarized in four distinct expression patterns (B). Clusters I, II and III could also be seen as a decreasing expression pattern where the expression level was less in the differentiated cells than in naïve CD4^{+} T cells.

Focusing on the up-regulated proteins on D3 first, from the 2,664 proteins that were differentially expressed between naïve and D3 in WT animals, 1,893 proteins were significantly up-regulated in the differentiated status of Th17 cells (cluster I; see Figure 18 A). In *Irf4*$^{-/-}$ animals, a total of 3,164 proteins were differentially expressed between D0 and D3. Among these, 2,203 proteins showed a significantly elevated expression in the differentiated cells. 67.9 % of these differentially expressed proteins (1,657 proteins) were the same in WT and *Irf4*$^{-/-}$ animals, including RORG, STAT3, MYD88, CD166 and CD44. A total of 546 proteins were uniquely elevated in Th17 cells of *Irf4*$^{-/-}$ mice, including IRF8, SMYD3 and FoxP3 (log_2(Th17/Treg)=1.0, adj.p-val=0.0157) and 173 of them were also significantly different on D3 between *Irf4*$^{-/-}$ and WT animals (cluster II), including FoxP3, SMYD3 and IKZF4. In WT animals, 236 proteins were significantly up-regulated three days after initiation of Th17 differentiation compared to naïve CD4$^+$ T cells, including IRF4, IKZF3 and SATB1. Overlapping these proteins with the differentially expressed proteins of Th17 cells on day three between *Irf4*$^{-/-}$ and WT mice resulted in 100 proteins, of which 98 proteins had a significantly higher expression in the WT animals ("WT axis" as these proteins have the same expression pattern as IRF4; see also Figure 17 B, cluster II) compared to *Irf4*$^{-/-}$ mice (see Figure 18 B).

In Treg cells of WT animals, a total of 2,781 proteins were significantly different expressed during the development from naïve CD4$^+$ T cells to differentiated T cells, whereas 1,929 proteins were significantly up-regulated in fully differentiated Treg cells (cluster I; see Figure 18 A). In the absence of IRF4, a total of 2,780 proteins were differentially expressed and 1,994 proteins showed a significantly higher expression in Treg cells of *Irf4*$^{-/-}$ mice. FoxP3 and IRF8, for example, were among the 1,646 proteins that were up-regulated during cell differentiation independently of the presence or absence of IRF4. In the absence of IRF4, 348 proteins were significantly elevated uniquely in Treg cells, e.g. IKZF3, NFATc1, Runx3 and STAT1, while 283 proteins displayed significant higher expression levels when IRF4 was present. A total of 144 proteins showed only a significantly different expression on D3 (cluster II) between *Irf4*$^{-/-}$ and WT animals and was IRF4-independent up-regulated during the development. In sum, 52 proteins followed the expression of the "WT axis" and 92 proteins followed the cluster II expression in *Irf4*$^{-/-}$ animals (see Figure 18 B).

For all proteins with differential expression levels during the development and/or differential expression in the differentiated status under WT or *Irf4*$^{-/-}$ conditions (cluster I - III), enriched reactome pathway analysis was performed. It revealed that proteins of different metabolic pathways were changed in Th17 and Treg cells (see Figure 18 C). The reactome pathway "metabolism of RNA" was only found in Th17 *Irf4*$^{-/-}$ and Treg WT cells while metabolism of proteins was enriched in WT and *Irf4*$^{-/-}$ cells of Tregs as well as in Th17 *Irf4*$^{-/-}$ cells. Glycolysis was only identified as an enriched reactome pathway in the presence of IRF4 in Th17 and Treg cells. Besides metabolism, protein translation was influenced by IRF4 in both cell types. Interestingly, proteins of the cell cycle were only up-regulated in their expression in Treg and "Treg-like" cells (Th17 *Irf4*$^{-/-}$, Treg *Irf4*$^{-/-}$ and WT). Uniquely in Treg cells, IRF4 significantly increased the expression of proteins essential for protein localization while the absence of the transcription factor affected mitochondrial translation (see Figure 18 C). In contrast, different Toll-like receptor (TLR) cascades, e.g. TLR2, gene expression (transcription) and cytokine signalling in immune system were only in *Irf4*$^{-/-}$ Th17 cells significantly elevated, while proteins

associated with signal amplification were only up-regulated in Th17 WT cells (see Figure 18 C). Additional subtype specific differences were seen for protein associated with signal transduction (Th17 cells) and post-translational protein modifications (Treg cells).

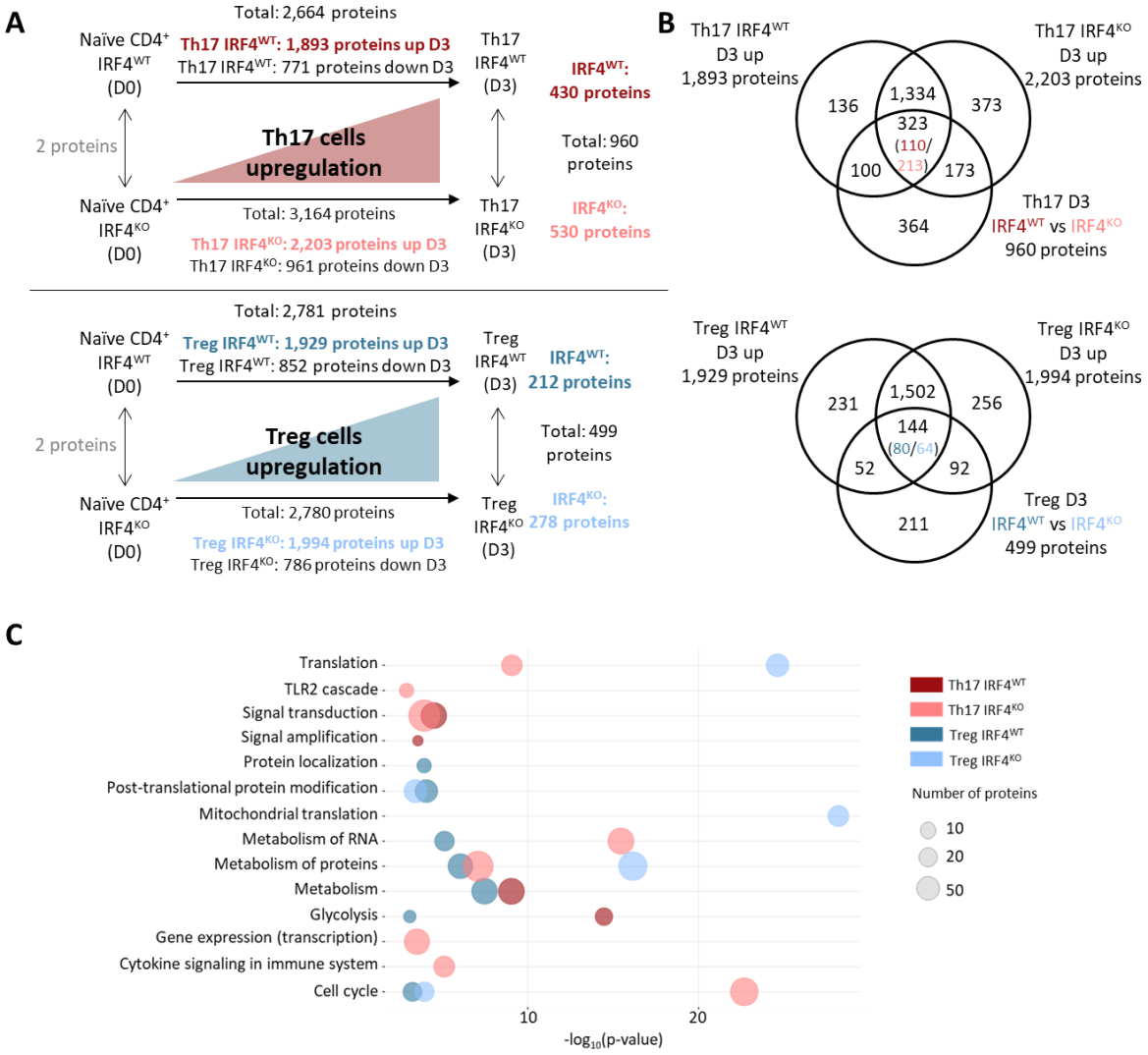

Figure 18: Differentially expressed proteins (up-regulated) in *Irf4*$^{-/-}$ and WT animals and enriched reactome pathways. Naïve CD4$^+$ T cells from *Irf4*$^{-/-}$ and littermate (WT) animals (n=4 per cell type) were *in vitro* differentiated into Th17 and Treg cells. Fully polarized cells were harvested and the whole proteome was further investigated by mass spectrometric analysis. For differentially expressed proteins, reactome pathway analysis was performed. (A) Overview of differentially up-regulated proteins from Th17 (upper part) and Treg (lower part) cells. (B) Overlap of proteins that are differentially expressed between naïve CD4$^+$ T cells and fully differentiated Th17 or Treg cells or between WT and *Irf4*$^{-/-}$. (C) Enriched reactome pathways of proteins that are significantly elevated during T cell development in the absence (*Irf4*$^{-/-}$) or presence (WT) of IRF4. Enrichment analysis was performed by gene ontology powered by PANTHER (http://geneontology.org/). Enriched reactome pathways applicable for Th17 WT cells are depicted in dark red, applicable for Th17 *Irf4*$^{-/-}$ cells are depicted in pink, applicable for Treg WT cells are depicted in dark blue and applicable for Treg *Irf4*$^{-/-}$ cells are depicted in light blue. The size of the circle represents the number of identified proteins annotated to the respective reactome pathway.

On the other hand and as mentioned above, IRF4 is also important for the silencing/down-regulation of proteins during T cell development. Under WT conditions, 771 proteins showed significantly decreased expression levels in fully differentiated Th17 cells whereas in the absence of IRF4, 961 proteins were down-regulated in these pro-inflammatory cells (see Figure 19 A). Many proteins (660 proteins), showed a decreased expression on D3 compared to naïve $CD4^+$ T cells independent of IRF4. Nevertheless from these proteins a total of 100 proteins were significantly different on D3 between WT and *Irf4*$^{-/-}$ animals (cluster III). Among the uniquely regulated proteins, 36 proteins were down-regulated under WT conditions during the development and showed a significantly lower expression on D3, too, compared to Th17 *Irf4*$^{-/-}$ cells on D3 (see Figure 19 B). A total of 87 proteins was only down-regulated on D3 in Th17 *Irf4*$^{-/-}$ cells compared to naïve $CD4^+$ T cells and in addition showed a significantly lower expression level in the differentiated cells compared to Th17 WT (cluster II).

In Treg cells, 852 proteins were significantly decreased on D3 in WT cells while in the absence of IRF4, 786 proteins were down-regulated compared to their naïve progenitor cell (see Figure 19 B). Among the 665 proteins that were down-regulated in both conditions, 48 were significantly different on D3 comparing WT and *Irf4*$^{-/-}$ animals (cluster III). Overall, 45 proteins showed an IRF4-steered down-regulation during development and in the differentiated status under WT conditions, while 24 proteins were significantly decreased during development and in the differentiated status in the absence of IRF4 (cluster II).

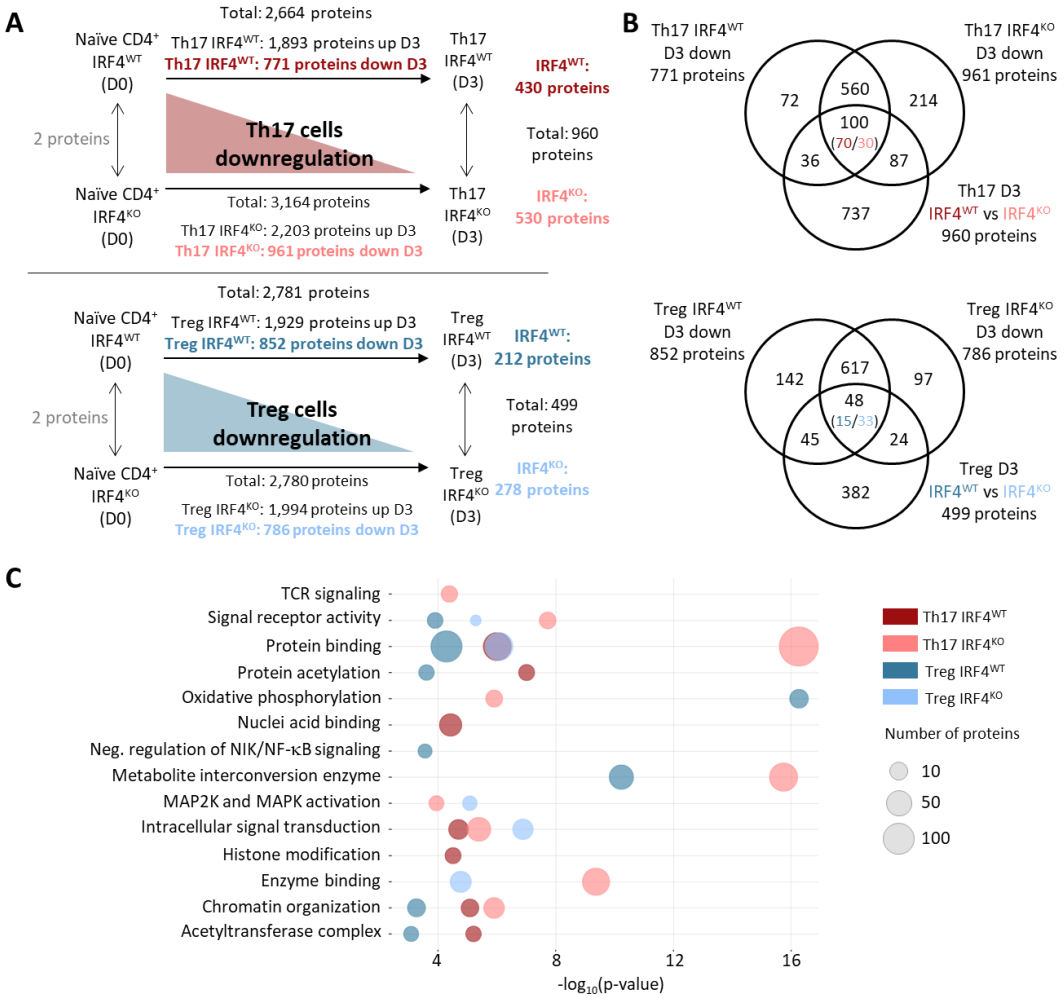

Figure 19: Differentially expressed proteins (down-regulated) in *Irf4*$^{-/-}$ and WT animals and enriched GO terms. Naïve CD4^{+} T cells from *Irf4*$^{-/-}$ and littermate (WT) animals (n=4 per cell type) were *in vitro* differentiated into Th17 and Treg cells. Fully polarized cells were harvested and the whole proteome was further investigated by mass spectrometric analysis. For differentially expressed proteins, GO enrichment analysis was performed. (A) Overview of differentially down-regulated proteins of Th17 (upper panel) and Treg (lower panel) cells. (B) Overlap of proteins that are differentially expressed between naïve CD4^{+} T cells and fully differentiated Th17 or Treg cells or between WT and *Irf4*$^{-/-}$. (C) Enriched GO terms of proteins that are significantly decreased during the T cell development in the absence or presence of IRF4. Enrichment analysis was performed by gene ontology powered by PANTHER (http://geneontology.org/). Enriched GO terms applicable for Th17 WT cells are depicted in dark red, applicable for Th17 *Irf4*$^{-/-}$ cells are depicted in pink, applicable for Treg WT cells are depicted in dark blue and applicable for Treg *Irf4*$^{-/-}$ cells are depicted in light blue. The size of the circle represents the number of identified proteins annotated to the respective GO terms.

GO enrichment analysis of proteins that were down-regulated during the development of Th17 and Treg cells and/or significantly different in differentiated cells revealed that epigenetic, signalling and metabolic pathways were influenced by IRF4 expression. In regard to epigenetics, acetyltransferase complexes were only under WT conditions down-regulated in both cell types, while histone modifications as well as nucleic acid binding was uniquely decreased in Th17 WT cells. Chromatin organization was altered in Th17 cells (WT and *Irf4*$^{-/-}$) and in Treg WT cells (see Figure 19 C). Intracellular signalling was significantly changed in Th17 cells (WT and *Irf4*$^{-/-}$) and in Treg *Irf4*$^{-/-}$ cells, while signal

receptor activity was significantly down-regulated in Treg and "Treg-like" cells (Th17 *Irf4*$^{-/-}$, Treg *Irf4*$^{-/-}$ and WT). Proteins involved in TCR signalling were down-regulated uniquely in Th17 *Irf4*$^{-/-}$ cells. In contrast, the negative regulation of NIK/NF-κB signalling was significantly down-regulated only in Treg WT cells. MAP kinase activation and enzyme binding were changed in the absence of IRF4 in both cell types. The influence of IRF4 on metabolic changes was seen as proteins involved in oxidative phosphorylation and metabolite interconversion enzyme were down-regulated in Treg WT and Th17 *Irf4*$^{-/-}$ conditions (see Figure 19 C).

Cluster IV comprises all proteins that were not significantly altered during development, but showed a different expression pattern in the differentiated cells. In Th17 cells, 60 proteins demonstrated a significantly higher expression under WT conditions while 89 proteins showed a higher expression in Th17 when IRF4 was absent. In Treg cells, 38 proteins were significantly up-regulated in the WT condition while 59 proteins showed a de-regulated expression without IRF4. GO enrichment analysis was able to provide only little information as the number of proteins was too low for a solid enrichment analysis. Nevertheless, the analysis indicated that metabolic proteins, proteins involved in gene expression and RNA processing were affected in their expression by the presence of absence of IRF4. Interestingly, the expression levels of nuclear and cytoplasmatic proteins were influenced by IRF4 in different degrees as for example in Th17 and Treg cells, only proteins from the nucleus showed an altered expression level in the absence of IRF4.

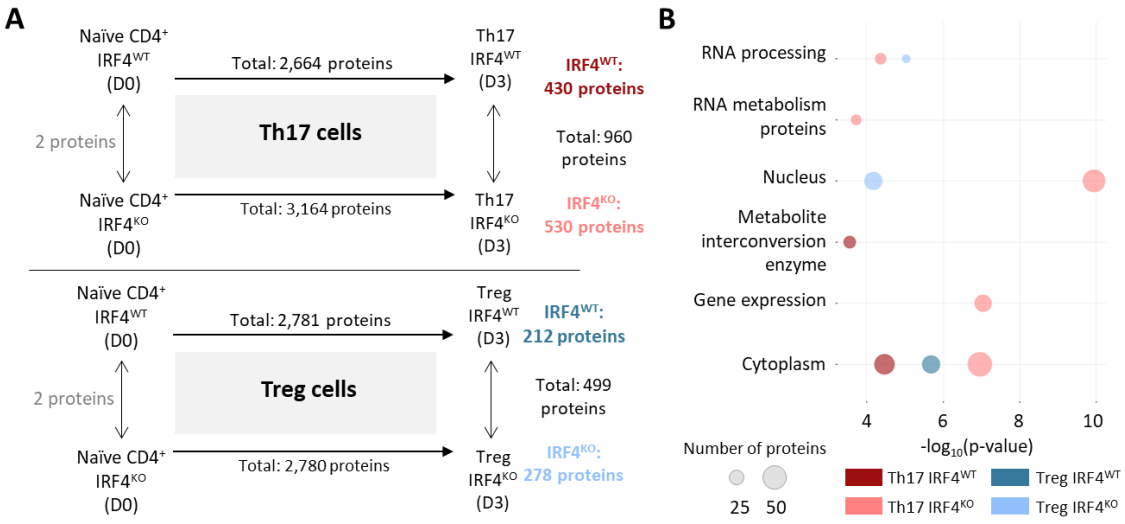

Figure 20: Differentially expressed proteins only on D3 in WT and *Irf4*$^{-/-}$ animals and enriched GO terms. Naïve CD4$^+$ T cells from *Irf4*$^{-/-}$ and littermate (WT) animals (n=4 per cell type) were *in vitro* differentiated into Th17 and Treg cells. Fully polarized cells were harvested and the whole proteome was further investigated by mass spectrometric analysis. For differentially expressed proteins, GO enrichment analysis was performed. (A) Overview of differentially expressed proteins only in fully differentiated Th17 (upper part) and Treg (lower part) cells. (B) Enriched GO terms of proteins that are significantly different between WT and *Irf4*$^{-/-}$ in differentiated Th17 or Treg cells. Enrichment analysis was performed by gene ontology powered by PANTHER (http://geneontology.org/). Enriched GO terms applicable for Th17 WT cells are depicted in dark red, applicable for Th17 *Irf4*$^{-/-}$ cells are depicted in pink, applicable for Treg WT cells are depicted in dark blue and applicable for Treg *Irf4*$^{-/-}$ cells are depicted in light blue. The size of the circle represents the number of identified proteins annotated to the respective GO terms.

4.5 Integrated analysis of IRF4 studies

To investigate IRF4 and its role in the development of Th17 and Treg cells with a focus on IRF4 interacting proteins, all the information from the previous IRF4 interactome, proteome, IRF4-ChIP-seq and *Irf4*$^{-/-}$ analysis was integrated.

Analysis of whole proteomes from Th17 and Treg cells confirmed two distinct populations in a principal component analysis (PCA) and demonstrated 1,130 differentially expressed proteins ($|\log_2(\text{Th17/Treg})|>0.5$, adj.p-value<0.01). In total, 71 of these differentially expressed proteins matched with proteins from the IRF4 interactome (see Figure 21).

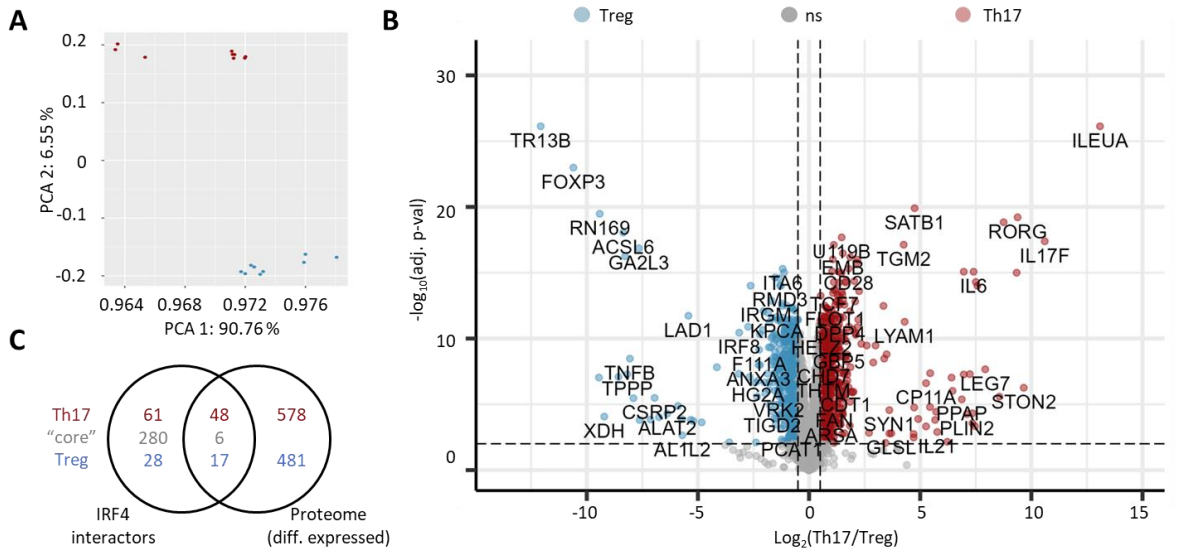

Figure 21: Integration of whole proteome and IRF4 interactome. Naïve CD4$^+$ T cells were *in vitro* polarized into Th17 and Treg cells. Fully differentiated cells were harvested and for 2 x 10^5 cells, the whole proteome was investigated by mass spectrometry. Remaining cells were cross-linked and used for IRF4 interactome analysis. The figure shows results from three independent polarization experiments per cell type (n=3). For each experiment, naïve CD4$^+$ T cells from three animals were pooled prior to cell polarization. (A) Principal component analysis (PCA) from Th17 (red) and Treg (blue) cells showed two distinct populations. (B) Volcano plot presents significantly differentially expressed proteins between Th17 and Treg cells. Statistical analysis was performed using the linear model limma. Proteins with a higher expression level in Th17 cells ($\log_2(\text{Th17/Treg})>0.5$, $-\log_{10}(\text{adj.p-val})>2$) are shown in red. Proteins with a higher expression level in Treg cells ($\log_2(\text{Th17/Treg})<(-0.5)$, $-\log_{10}(\text{adj.p-val})>2$) are shown in blue. (C) Venn diagram of differentially expressed proteins from the proteome and IRF4 interactors of Th17 and Treg cells.

Only six proteins showed a differential expression between Th17 and Treg cells in the proteome, but belonged to the core IRF4 interactome (see Figure 21 C): IRF4 and G3BP2 were elevated in the proteome of Th17 cells while CARM1, ZFR, NFKB1 and TRIPC showed significant higher expression levels in the proteome of Treg cells. The 65 proteins that were differentially expressed in the proteome and the interactome showed similar expression patterns in the respective cell type. In general, IRF4 and its interacting proteins showed a positive correlation between expression on the proteome and the interactome level, as shown by the $\log_2(\text{Th17/Treg})$ correlation plot (see Figure 22). Interestingly, among the 44 proteins (10 % of the interactors) that showed the greatest distance (shown in dotted

line, Figure 22) from the regression line, only three proteins showed a stronger expression difference in the proteome than in the interactome (|log_2(Th17/Treg)) proteome| > |log_2(Th17/Treg)) interactome|), including the two master transcription factors, RORγT (RORG) and FoxP3. Of the remaining 41 proteins, 18 proteins demonstrated higher expression levels in the interactome of Treg cells than in Th17 cells while 23 proteins showed higher expression levels in the IRF4 interactome of Th17 cells compared to the interactome from Treg cells, indicating its strong association with IRF4. These proteins were associated with metabolic processes, especially RNA metabolic processes, cell differentiation, lymphocyte activation and regulation of gene expression/regulation of DNA-templated transcription (data not shown).

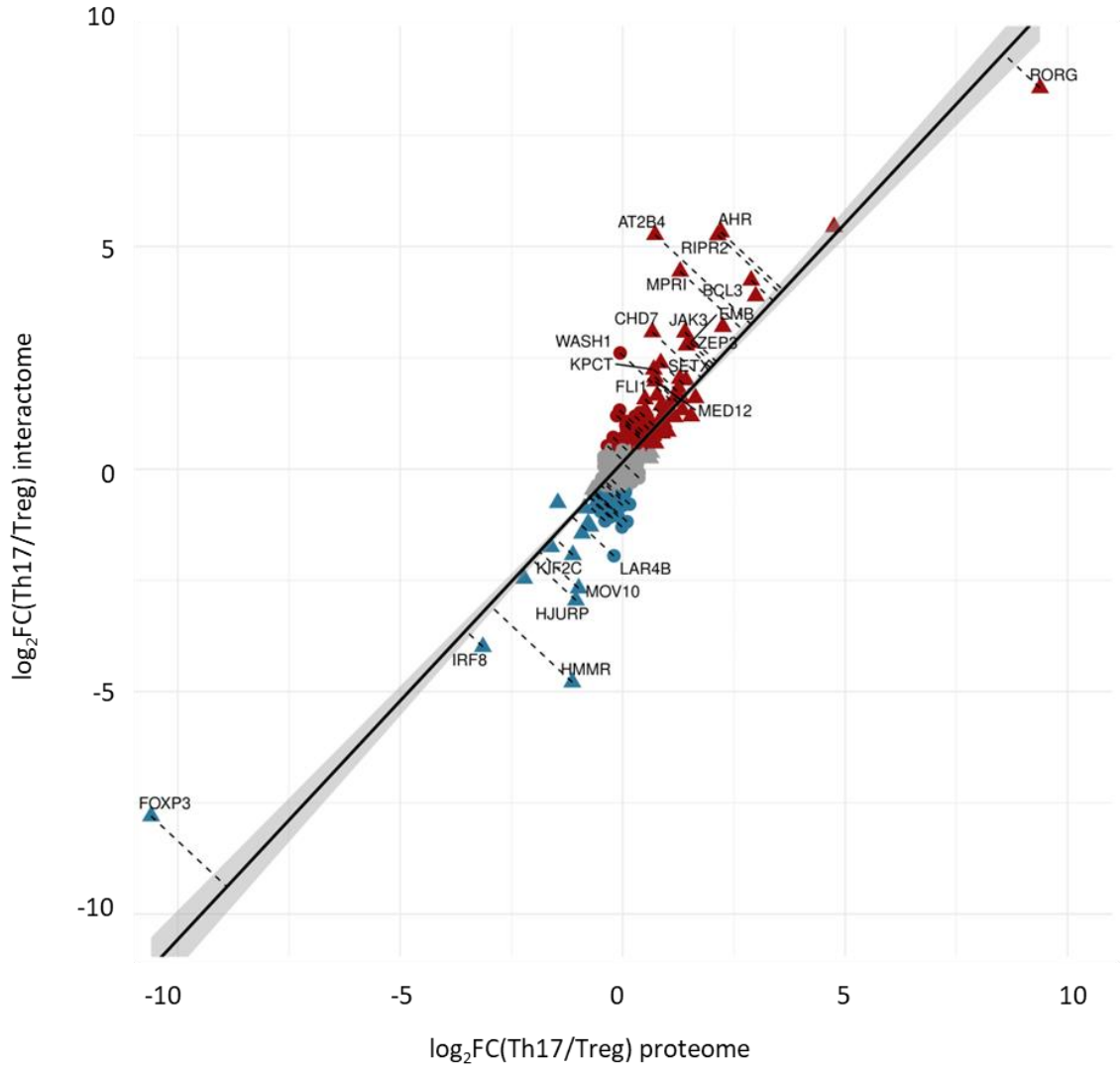

Figure 22: Log_2(Th17/Treg) correlation plot between IRF4 interactome and proteome in Th17 and Treg cells. Log_2 correlation plot between the IRF4 interactome (y-axis) and the proteome (x-axis) of Th17 and Treg cells. Proteins enriched or exclusively found in Treg cells are shown in blue; proteins with a higher expression in Th17 cells are illustrated in red. The core T cell interactome is presented in grey. Proteins that are differentially expressed in proteome and IRF4 interactors are depicted with triangles, while proteins from the interactome that are not differentially expressed in the proteome are shown as dots.

The experimentally determined data from the IRF4 interactome was first validated by the match with known and published proteins (see chapter 4.2). Additional confirmation was retrieved from the IRF4-ChIP-seq data. For 18 IRF4 interactors, the binding motifs were identified with the MATCH/TRANSFAC search. The motifs of nine proteins were also enriched, which could be shown with the MEME/Tomtom examination, namely FLI1, JunB, Bach2, IRF4, STAT3, STAT1, EP300, NR2C2 and IRF8 (see Figure 15 B).

IRF4-ChIP-seq data revealed in addition that IRF4 mainly positively regulated the expression of genes coding for IRF4 interactors – for almost 70 % of the proteins from the IRF4 interactome (306 proteins) IRF4 binding sites were detected less than 1 kb from the TSS in the IRF4-ChIP-seq of Th17 and/or Treg cells, e.g. EP300, SATB1, AHR, ETV6, TCF7 or STAT3 (see Figure 23). For 277 genes coding for IRF4 interactors, IRF4 binding was determined in promoter regions and enhancer structures. Only for two genes IRF4 binding was found in promoter and silencer structures. However, it has to be mentioned that these two peaks were additionally overlapping with coordinates for enhancers.

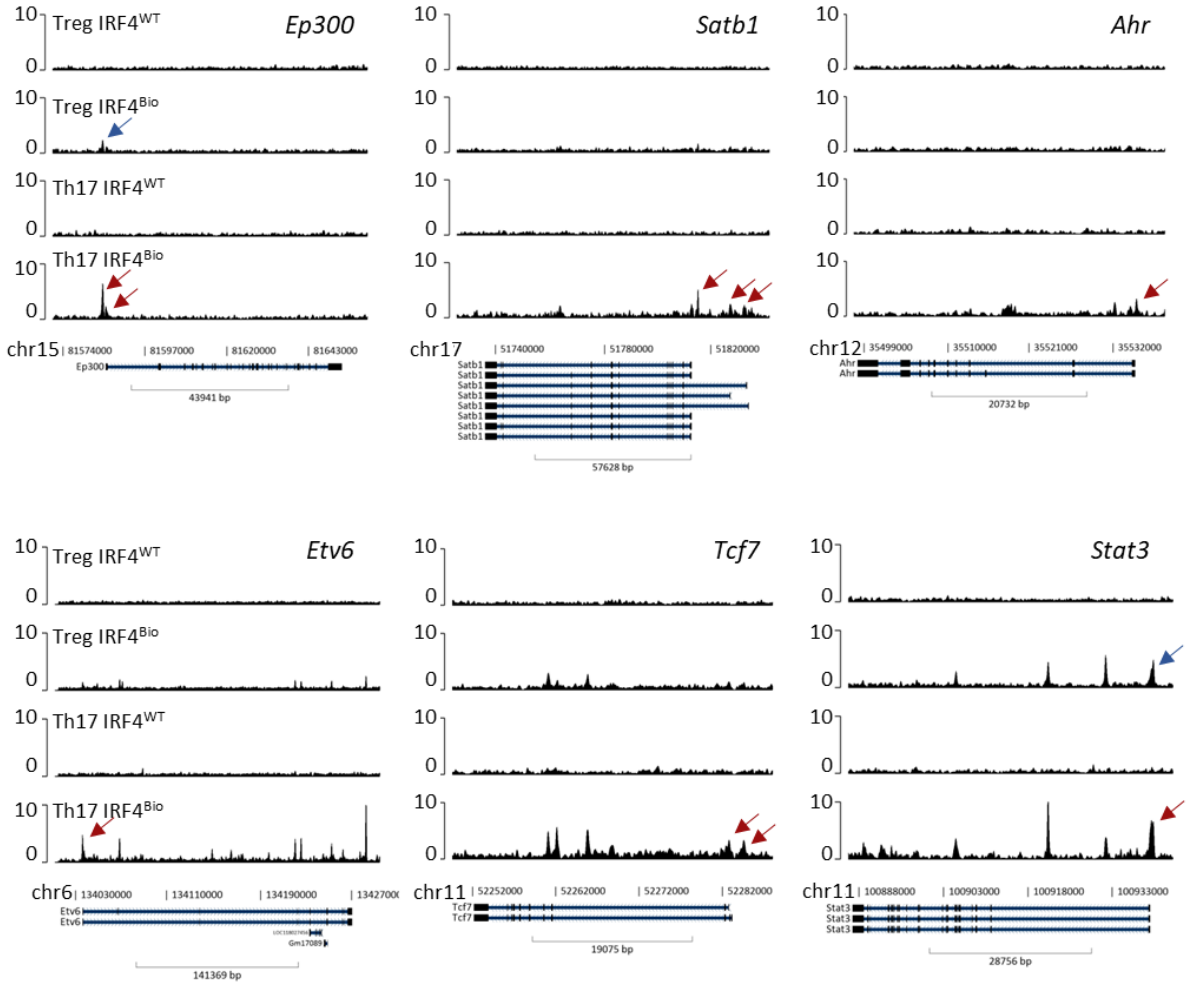

Figure 23: IRF4 regulates the expression of IRF4 interacting proteins. IRF4-ChIP-seq analysis of Th17 and Treg cells revealed that IRF4 regulates the expression of genes coding for IRF4 interacting proteins. IRF4 binding in the promoter region is highlighted with red (for Th17 cells) or blue (for Treg cells) arrows.

Besides an IRF4-steered expression of genes coding for IRF4 interactor, integration of IRF4-ChIP-seq and *Irf4*$^{-/-}$ analysis revealed that IRF4 regulated the expression of a variety of other proteins on DNA and protein level. Comparing these experimental results with a list of Th17 characteristic genes (see S Table 3) from literature, e.g. described by Ciofani et al. (Ciofani et al., 2012), it showed that for many genes IRF4 binding was not only found in the promoter region of Th17 cells but also the respective proteins were significantly different expressed between IRF4 WT and *Irf4*$^{-/-}$ animals. Only one protein, T-bet (TBX21), was differentially expressed at protein level but showed no IRF4 binding in the promoter region of its gene. For Treg cells, the list of signature genes, essential for the differentiation and function of those cells (see S Table 4), were extracted from several publications (Hill et al., 2007; Vasanthakumar et al., 2017; Williams & Rudensky, 2007). Similarly to the Th17 cells, some genes were regulated at DNA level by IRF4 and showed differential expression at protein level in the presence or absence of IRF4, while others were regulated only by IRF4 at DNA or protein level.

As IRF4 binds DNA only weakly as a homodimer and is known to form hetero(di)mers (M. Huber & Lohoff, 2014), the combinatory role of IRF4 and other interacting proteins on gene expression was investigated. To this end, combined motif analysis was performed to identify motifs in close proximity (5 bp distance) to the IRF4 motif (see Figure 24). In the following, the focus is set on the experimentally determined IRF4 interactors. Besides IRF4 motifs, almost all interactors, which motif was found by the MATCH/TRANSFAC algorithm, were identified in combination with the IRF4 motif. In Th17 cells 6,475 genes (annotated to 5,582 proteins) and in Treg cells 2,409 genes (annotated to 2,095 proteins) were regulated by IRF4-complexes. Interestingly, the motifs of IRF4 interactors were also detected in close proximity (up to 5 bp distance) to each other.

The Treg-enriched transcription factors FoxP3 and IRF8 as well as the Th17-enriched transcription factor AHR was identified in combination with IRF4 only in the respective cell type, while Bach2-IRF4, FLI1-IRF4, GTF2I-IRF4, IRF4-EP300, IRF4-TCF7, RFX1-IRF4 and SATB1-IRF4 were found in both cell types (see Figure 24 A). The motif of FoxP3 in close proximity to the IRF4 motif was the most prominent combination in Treg cells (determined 9,601 times), followed by RFX1-IRF4 (7,246 times) and IRF4-EP300 (6,956 times). In Th17 cells the combinatorial regulation of IRF4 with EP300 was found the most (19,405 times). Interestingly, in Th17 cells most combinatorial IRF4-protein bindings were identified in the promoter region whereas in Treg cells, most bindings were revealed in intronic gene structures (see Figure 24 A).

Glycolysis and IL-17 signalling were enriched reactome pathways that were only in Th17 cells regulated by IRF4 and other transcription factors in close proximity, namely AHR, FLI1, EP300, TCF7, RFX1 and SATB1, as shown by combined binding in promoter and enhancer regions of respective genes. Additionally, Toll-like receptor cascade was mainly targeted by IRF4 and co-binding transcription factors in Th17 cells but not in Treg cells. Otherwise, GO analysis showed similar regulatory pattern for IRF4 heterodimers in Th17 and Treg cells. However the number of regulated genes differed strongly between the two cell types (see Figure 24 B).

Figure 24: Combined motif analysis of IRF4 and IRF4 interacting proteins in close proximity (5 bp) to each other. Analysis of isolated DNA fragments from IRF4-ChIP-seq of fully differentiated Th17 and Treg cells identified binding motifs from other IRF4 interactors, which were in close proximity (up to 5 bp distance) to the IRF4 binding motif. (A) Distribution of combined binding motifs across the peaks that were identified by IRF4-ChIP-seq analysis in Th17 and Treg cells. The maximum distance between the two motifs was 5 bp. (B) Reactome analysis of genes that were promoted and enhanced by IRF4 and its interactors in Th17 and Treg cells. Enrichment analysis was performed by gene ontology powered by PANTHER (http://geneontology.org/). Reactome analysis applicable for Th17 cells are depicted in red, applicable for Treg cells are depicted in blue. The different colours of red and blue demonstrate the -$\log_{10}$(p-value) while size of the circle represents the number of identified genes annotated to the respective reactome pathway.

To investigate which proteins are regulated by IRF4-complexes on protein and DNA level, all proteins that showed an IRF4-dependet expression (1,752 differentially expressed proteins in Th17 cells and 1,226 differentially expressed proteins in Treg cells) were integrated with all genes (6,475 genes annotated to 5,582 proteins in Th17 cells and 2,409 genes annotated to 2,095 proteins in Treg cells, see Figure 25 A) that were regulated by IRF4-complexes (IRF4-TF binding in promoter+enhancer or promoter+silencer regions). For this investigation, only the IRF4 heterodimers (IRF4+identified IRF4 interactor of this thesis, see above) described earlier were used. This analysis revealed a total of 1,017 proteins (58.0 %) in Th17 cells and 280 proteins (22.8 %) in Treg cells that showed a regulation by IRF4 on DNA level, too, including proteins from the IRF4 interactome (see Figure 25 A). An IRF4-dependent regulation of nuclear proteins in both cell types on DNA and protein levels was therefore not surprising. Additionally, cytoplasmic proteins, proteins involved in RNA and protein binding, response to cytokines, macromolecule localization as well as establishment of protein localization to

organelle, gene expression and metabolic processes were controlled in both cell types by IRF4 on DNA and protein level. Interestingly, glycolysis and glucose metabolism was only in Th17 cells determined by IRF4 on DNA and protein level. In addition, (DNA-binding) transcription factor binding, transcription coregulator activity, T cell differentiation involved in immune response, including Th17 cell differentiation or cell cycle were only in Th17 cells enriched GO terms or reactome pathways (see Figure 25 B). In contrast, in Treg cells IRF4 regulated the expression of proteins involved in the establishment of RNA localization, protein complex oligomerization, activation of immune response and regulation of DNA-binding/NF-κB transcription factor activity on both levels (see Figure 25 B).

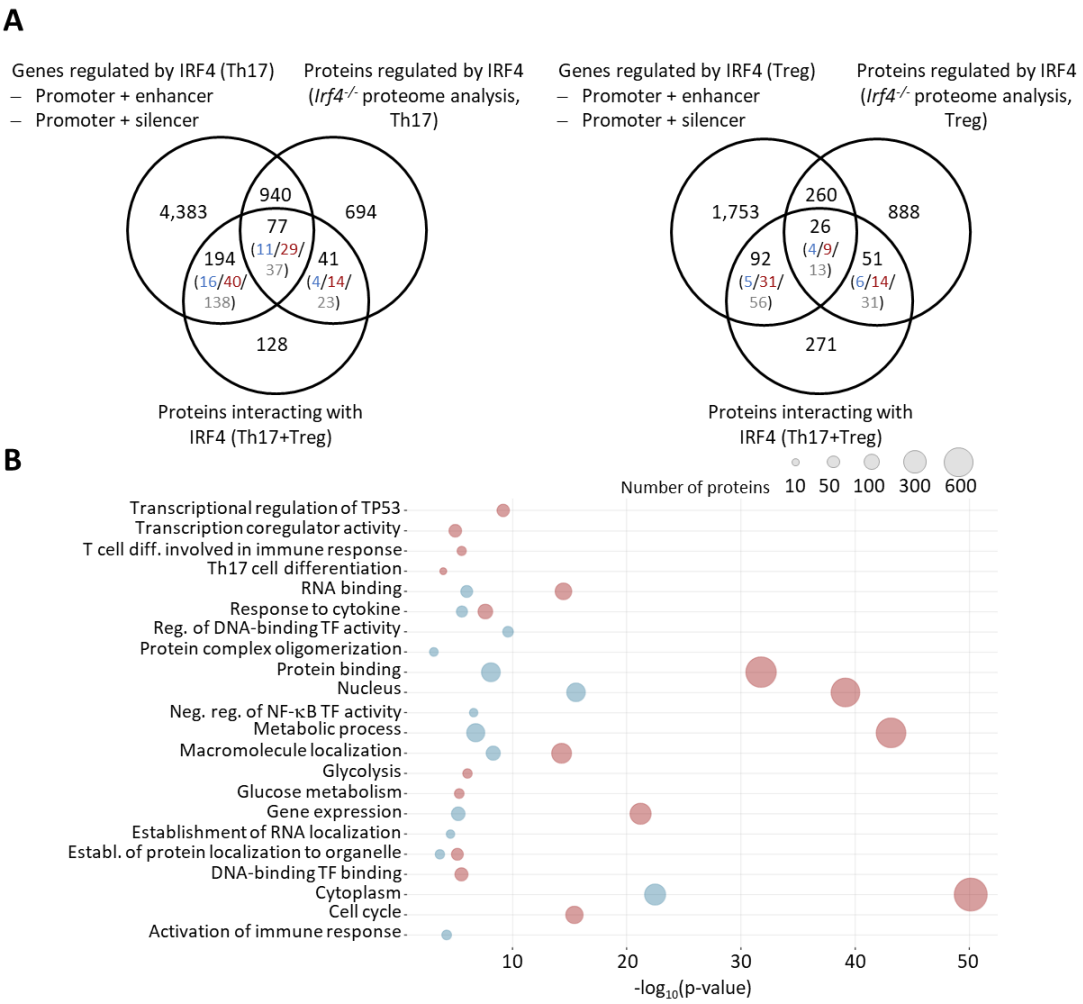

Figure 25: Integration of IRF4-ChIP-seq analysis with *Irf4*$^{-/-}$ study. For IRF4-ChIP-seq analysis, naïve CD4^{+} T cells from IRF4 WT and IRF4^{Bio} animals were differentiated for 72 h into Th17 and Treg cells. Genome wide IRF4-binding regions were investigated by IRF4-ChIP-seq. For the *Irf4*$^{-/-}$ study, naïve CD4^{+} T cells from IRF4 WT and *Irf4*$^{-/-}$ animals were differentiated for 72 h into Th17 and Treg cells and their proteomes were analysed by mass spectrometry. (A) Proteins that showed an IRF4-dependent significantly different expression during the development and/or in differentiated Th17 and Treg cells were overlapped with genes that were regulated by IRF4 (IRF4-transcription factor binding in promoter+enhancer or promoter+silencer regions). IRF4-regulated genes were converted into their respective proteins using the UniProt ID mapping (https://www.uniprot.org/id-mapping). (B) Enriched GO and reactome analysis of proteins that were regulated by IRF4 on DNA and protein level. Enrichment analysis was performed by gene ontology powered by PANTHER (http://geneontology.org/). GO/reactome terms enriched in Th17 cells are shown in red, for Treg cells in blue. The size of the circle represents the number of identified proteins annotated to the respective GO terms.

Further analysis of all proteins that were regulated by IRF4-heterodimers on DNA and protein levels demonstrated that in Th17 cells IRF4 mainly acted in concert with EP300, RFX1, FLI1 and AHR while in Treg cells IRF4-FoxP3 and IRF4-EP300 complexes were predominantly controlling the expression of gene that were also on protein level (translated into its respective protein) regulated by IRF4 (see Figure 26 A). Particular in Th17 cells, IRF4 in complex with other transcription factors demonstrated binding in promoter regions of genes important for glycolysis and transcriptional regulation (see Figure 26 B). Some IRF4 interactors, e.g. AHR, EP300, FLI1, ETV6, RORγT, TCF7, SATB1, MALT1, and SUFU, showed a self-regulating loop as IRF4 and the distinct transcription factor bound in its respective promoter region (see Figure 26 B) and displayed a lower protein expression level in cells that lack IRF4 (see Figure 26 C). Interestingly, IRF4-complexes promoted not only the expression of IRF4 interactors identified in a particular cell type (66 Th17-enriched IRF4 interactors regulated in Th17 cells and 17 Treg-enriched interactors in Treg cells, see Figure 25 A), but also regulated the expression of IRF4 interactors of the opposing cell type: In Th17 cells, the expression of eleven Treg-enriched interactors, such as IRF8, TPX2 or MOV10, was regulated by IRF4 on DNA and protein level and nine Th17-enriched IRF4 interactors, e.g. Def6, Malt1, JAK3 or Runx1, were controlled by IRF4-complexes on DNA and protein level in Treg cells.

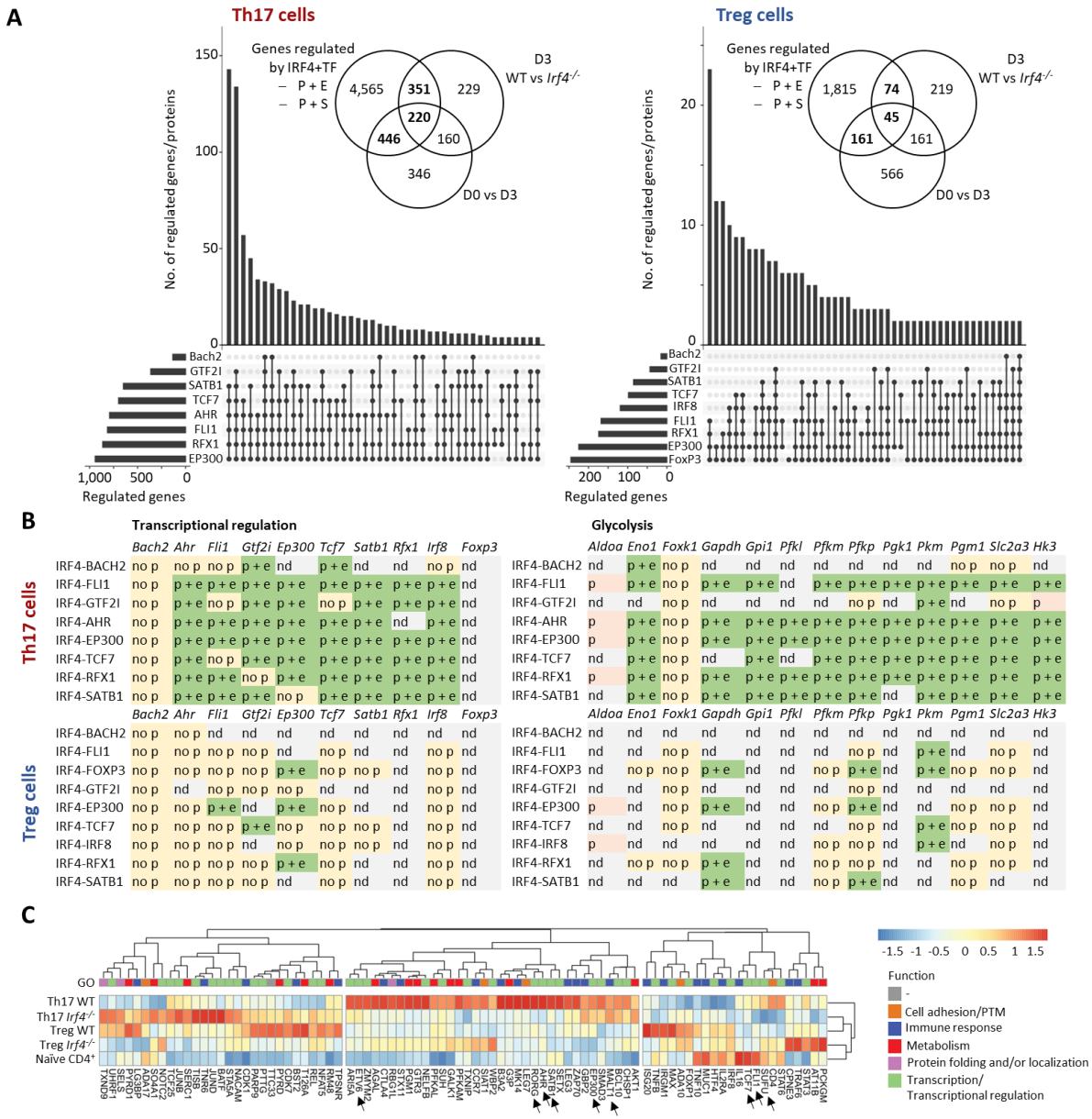

Figure 26: Binding pattern of IRF4 complexes in Th17 and Treg cells. All proteins that were regulated by IRF4 on DNA and protein level during the cell development and/or in differentiated Th17 and Treg cells were selected for further analysis. (A) Number of genes regulated by IRF4+distinct interacting proteins in Th17 and Treg cells. IRF4-regulated genes were converted into their respective proteins using the UniProt ID mapping (https://www.uniprot.org/id-mapping). The insets show the overlap of regulated genes (IRF4-TF combined binding in promoter+enhancer or promoter+silencer region) and IRF4-dependent differentially expressed proteins during the development (D0 vs D3) and in differentiated cells (D3 WT vs *Irf4*$^{-/-}$). The numbers highlighted in bold were used for the analysis. (B) DNA binding pattern of particular IRF4 heterodimers for genes associated with transcriptional regulation and glycolysis. No binding at all in a particular gene is indicated with "nd". Binding in promoter regions is abbreviated with "p", binding in promoter and enhancer regions with "p+e" and binding in other gene regions than the promoter with "no p."(C) Expression pattern of selected proteins regulated by IRF4 complexes that demonstrate a differential expression levels by the lack of IRF4. Arrows indicate the expression pattern of determined IRF4 interactors.

V. DISCUSSION AND OUTLOOK

The development of fully functional immune cells is essential for a balanced immune response. The important role of IRF4 in this context has been described for many different T cell subtypes (Brüstle et al., 2007; Cretney et al., 2011; Lohoff et al., 2002; Mudter et al., 2008; Rengarajan et al., 2002; Staudt et al., 2010; Tominaga, 2003). However, the molecular mechanisms behind IRF4`s role have not been fully uncovered. Therefore, an unbiased interactome study of IRF4 in differentiated Th17 and Treg cells was performed, which was combined with whole proteome, IRF4-ChIP-seq and *Irf4*$^{-/-}$ analysis to elucidate the role of IRF4 in these two opposing cell types.

5.1 Establishment of an IRF4 pulldown protocol

Before the IRF4 interactome in Th17 and Treg cells could be investigated, a robust and highly reproducible IRF4 pulldown protocol had to be established. To this end, different time points during T cell differentiation were investigated to determine a developmental stage with high IRF4 expression. In accordance with literature (M. Huber & Lohoff, 2014), IRF4 expression was detectable already a few hours after T cell stimulation on mRNA and protein level and increased over time with a highest expression after 24-72 h of T cell stimulation. For the establishment of the protocol, fully differentiated Th17 and Treg cells were used as they showed a high expression of IRF4 and an increased number of cells due to cell proliferation. To preserve weak and transient interactions, the cell-permeable, reversible cross-linker DSP was included in the protocol of this thesis. The cross-linking protocol is based on a publication of Smith and colleagues in 2011 (Smith et al., 2011), who combined reversible protein cross-linking with antibody-based immune-precipitation, the so called ReCLIP (Reversible Cross-Link Immuno-Precipitation) protocol. In this publication, the authors investigated the labile interaction of p120-catenin and E-cadherin by mass spectrometric analysis. By including the lysine-reactive, reversible cross-linker DSP in their pulldown protocol, the authors could isolate core components of the cadherin complex as well as several new and unique p120-interacting proteins (Smith et al., 2011). The effectiveness of DSP was also demonstrated in another study, where only DSP cross-linker could stabilize and identify protein complexes and not formaldehyde, another common cross-linker (L. Zhang et al., 2007). In general, amine-reactive, such as lysine-reactive, cross-linkers are the most commonly used cross-linking reagents as proteins have many lysine (K) residues exposed to the surface and therefore reactive groups are easily accessible for the cross-linker (Piersimoni et al., 2022; Smith et al., 2011). As most lysine-reactive cross-linker have an average spacer length of 10-12.5 Å, not only cross-linking within the protein, but also between different proteins is possible, which makes it interesting for studying protein-protein interactions (Piersimoni et al., 2022). In addition to the advantages of cross-linker to preserve labile and transient interactions as well as studying structural dynamics of proteins, some considerations and limits of cross-linking have to be taken into account: First, cross-linkers can alter exposed epitopes, which might limit the use of suitable antibodies for immunoprecipitation. Fortunately, this aspect was not critical for the protocol of this thesis as the immunoprecipitation was performed with magnetic streptavidin-coated beads and was not based on antibodies. Second, after the reduction of the samples, half of the cross-linker is still

attached to the protein, which might alter the proteolytic cleavage. In line with this, an alteration of the peptide mass due to the cross-linker remaining has to be considered during mass spectrometric analysis. This mass-shift might prevent the recognition of peptides and therefore reduce the number of identified peptides per protein. However, as the cross-linked peptides are only a minor fraction in the overall number of generated peptides, these effects do not dramatically affect the data (Piersimoni et al., 2022; Salazar et al., 2009; Smith et al., 2011) and therefore do not overweight the advantages in the gain of biological novelty by including a cross-linker. A further consideration and comment on the usage of a cross-linker is that it not only stabilizes direct and binary protein interactions but also larger protein complexes that include indirect, tertiary protein interactions (Smith et al., 2011).

The usage of a cross-linker does not only preserve labile interaction, but also allows at the same time more stringent washing conditions to reduced non-specific background and the removal of high-abundant contaminants (Smith et al., 2011). After adjusting the washing parameters, an initial pulldown experiment using DSP cross-linked splenocytes from IRF4^{Bio} and littermate controls demonstrated already the advantage of including a cross-linker in the protocol of this study, which was shown by less unspecific background and increased numbers of isolated interactors. These included also already described IRF4 binding partners, such as Ikaros and Aiolos (Ochiai et al., 2018), which set a solid basis for unravelling new and not yet described IRF4 interaction partners.

An additional step included in the new pulldown protocol of this thesis was the sub-cellular fractionation. This separation method not only further reduces contaminating proteins but also enriches the levels of target protein and allows the analysis of low abundant multi-protein complexes (L. A. Huber et al., 2003). In this thesis, IRF4 complexes were isolated by taking advantage of biotinylated IRF4, but therefore other endogenous biotinylated proteins were interfering during affinity purification, creating contaminating background signals. In mammals, a total of four endogenous biotinylated proteins, namely acetyl-CoA-carboxylase (220 kDa), pyruvate-carboxylase (130 kDa), methylcrotonyl-CoA-carboxylase (75 kDa) and propionyl-CoA-carboxylase (72 kDa) exist (Chandler & Ballard, 1986; Kirkeby et al., 1993; Niers et al., 2011), which are located in the mitochondria and/or the cytoplasm (Abu-Elheiga et al., 2000; Chu & Cheng, 2007; Stadler et al., 2005; Wexler et al., 1998). By isolating the nucleus from the cytoplasmatic fraction, which also includes mitochondria, contaminating proteins could be reduced. Further details on the sub-cellular fractionation and endogenous biotinylated proteins can be found in the thesis of Sarah Dietzen (Dietzen, 2019).

As a last step of improvement for a robust pulldown protocol, different digestion protocols of the isolated IRF4-complexes were compared. The digestion of proteins directly on the streptavidin beads resulted not only in a high recovery of peptides derived from IRF4-complexes, but also peptides from the streptavidin matrix, which impeded protein identification by the mass spectrometric analysis. Matrix-derived contamination in mass spectrometric analysis is a topic of discussion and represents a critical drawback of affinity purification of biotinylated proteins (Barshop et al., 2019; Rafiee et al., 2020; St-Germain et al., 2020). Even variations of contamination dependent on the production lots of streptavidin matrices are reported (St-Germain et al., 2020). To overcome these challenges, the

proteins of interest can be eluted from the streptavidin beads prior to protein digestion, which was used in this thesis. A slight modification of the published SP3 protocol (Sielaff et al., 2017) – reduction of the cross-linker – resulted in minimal contamination with streptavidin peptides. To overcome the problem of streptavidin contamination, derivation and chemical modification of streptavidin beads were developed and introduced over the last years (Barshop et al., 2019; Rafiee et al., 2020). In 2019, Barshop and colleagues developed a chemical derivatization of lysine and arginine residues on streptavidin coated beads which made it resistant to tryptic cleavage (Barshop et al., 2019). On year later, in 2020, Rafiee et al. published chemical modified streptavidin beads that were resistant to proteolytic digestion by the enzymes trypsin and LysC and therefore resulted in a 100-1,000-fold reduction of streptavidin contamination as well as improved identification of low abundant proteins (Rafiee et al., 2020). These novel streptavidin beads could be included and add further improvements in protocols of biotin-streptavidin-mediated interaction studies.

5.2 IRF4 interactors

For the investigation of IRF4 interactions, the established, unbiased IRF4 pulldown was performed with fully differentiated Th17 and Treg cells. GO analysis revealed that many proteins are localized in the nucleus, which fits the compartmentalization of a transcription factor and its interacting proteins and additional demonstrated a successful sub-cellular fractionation established in the pulldown protocol. Of the 440 experimentally determined IRF4-interacting proteins, 41 proteins had been described as interacting with IRF4 in other publications (results from PSICQUIC search and HIPPIE). An overlap with literature-curated interactors served as a first quality control. However this overlay did not take into account the species, cell type or type of interaction, where the interaction was reported. Among the literature-curated IRF4 interactors, only ten proteins were described in murine experiments while most interactions were revealed in human cells. The experiments were not only performed in primary $CD4^+$ T cells, but in B cells, macrophages, dendritic cells or cell lines. Some interactions were only predicted (Runx3 (Cao et al., 2010)), others were identified by proximity labelling (ARI1A, ARI1B, ARID2, BRD7, CHD7, EP300, KDM6A, KMT2D, NCOA3, NCOR2, NIPBL, PAXI1, PB1, REQU, SATB1, SMCA2, SMRD1, TCF20, ZN609 (Göös et al., 2022; G. Wu et al., 2010)) or co-localization (STAT3 (Kwon et al., 2009)), and for some a direct interaction or physical association was described (BC11B (Glasmacher et al., 2012), CARM1 (S. Li et al., 2011), DEFI6 (P. S. Biswas et al., 2012; Gupta et al., 2003), FoxP3 (Zheng et al., 2009), HDAC1 (Cao et al., 2010), IKZF1 (Ochiai et al., 2018), IRF4 (Lehtonen et al., 2005; P. Li et al., 2012), IRF8 (Meraro et al., 2002; Rosenbauer et al., 1999), JunB (P. Li et al., 2012), NFAC2 (Rengarajan et al., 2002; Sharma et al., 2002), NF-κB1 (NFKB1_MOUSE) (Grumont & Gerondakis, 2000; Lehtonen et al., 2005; Sharma et al., 2002), STAT1 (Vastrik et al., 2007), STAT3 (P. S. Biswas, Gupta, et al., 2010), SUFU (Benz et al., 2022), TF65 (Lehtonen et al., 2005; Saito et al., 2007; G. Wu et al., 2010), UBP4 (Guo et al., 2017)).

Detailed literature research revealed that some of those interactions, even though they were described as “physical interactions” in the PSICQUIC search and HIPPIE search, were only an IRF4-steered expression of these interactors via binding of IRF4 to the promoter or regulatory regions or

vice versa. Additional details on how a direct interaction has been concluded are missing and inconclusive. Nevertheless, results from the pulldown performed in this thesis demonstrated indeed an interaction of IRF4 and respective proteins and these interactions will be discussed below.

The well-known and described IRF4 interactor BATF, which regulates together with IRF4 chromatin accessibility and is important for the development of Th17 cells (Ciofani et al., 2012; Schraml et al., 2009), was also found in the pulldown data. However, as BATF was only found with two peptides, it did not fulfil the analysis criteria for further analysis (see chapter 4.2). All in all, the overlap with the literature provided confidence in identifying new, undescribed interaction partners of IRF4 in Th17 and Treg cells using the newly established IRF4 pulldown protocol.

Below, proteins that are known from the literature to interact with IRF4 will be briefly described (see chapter 5.2.1). In addition, newly identified proteins, where no partnering with IRF4 has yet been described in literature, but which demonstrated in this thesis in different, independent studies an association with IRF4, will be discussed below (see chapter 5.2.2).

5.2.1 IRF4 INTERACTORS DESCRIBED IN LITERATURE

The PSICQUIC search reported a predicted interaction of IRF4 and Runt-related transcription factor 3 (Runx3) and referred to a publication from Cao et al. (Cao et al., 2010). In this paper, a negative regulation of *Runx3* by IRF4 was described in the thymus during thymocyte development and the authors proposed a similar relationship between these two proteins in the periphery. However, no protein-protein interaction was investigated. Results from the pulldown protocol of this thesis revealed an IRF4-Runx3 interaction, but no regulation of *Runx3* expression was seen by IRF4 in differentiated Th17 or Treg cells. A Runx3-IRF4 interaction has been suggested in another publication where the motifs of both transcription factors overlapped in cytotoxic T lymphocytes (CTLs) (D. Wang et al., 2018). It was shown that Runx3, expressed within 2 h of TCR stimulation, is necessary for normal IRF4 expression and the authors suggested that Runx3 opens chromatin structures, where IRF4 and other important transcription factors in CTL development (e.g. BATF) bind to (D. Wang et al., 2018). In the context of $CD4^+$ T cells, a publication investigated the role of Runx3 in the development of Treg cells and reported defective Treg functions in the absence of Runx3. *Runx3*$^{-/-}$ animals developed tumours and the cells were unable to suppress inflammation (Sugai et al., 2011). Additionally, different publications describe the regulation of FoxP3 expression by Runx3 (and Runx1), a physical interaction of Runx proteins and FoxP3, and in concert the regulation of FoxP3 target gene expression (Bruno et al., 2009; Klunker et al., 2009). As IRF4 and Runx3 are essential for the effector functions of Treg cells as well as for a regulated FoxP3 expression, a physical interaction of IRF4 and Runx3 could be possible in this context and could promote the anti-inflammatory function of Treg cells. For Th17 cells, different results have been shown: in the intestine, high expression of Runx3 was associated with an impairment of Th17 development (Reis et al., 2013; M. Wang et al., 2012). In contrast, in psoriasis patients, elevated levels of Runx3 were detected, which correlated with a higher number of Th17 cells, and inhibition of Runx3 resulted in significantly decreased frequencies of Th17 cells and IL-17 production (FU et al., 2016). It would be interesting to see the effects of Runx3 deletion in *in vitro* differentiated

Th17 cells. A positive association of Runx family members on Th17 cell development was described already described for Runx1 (Dybska et al., 2021). This fact combined with the data from Fu et al. could allow the conclusion that Runx3 together with IRF4 positively promote the development of Th17 cells and expression of Th17 cell characteristics. Even though all the cited publications of $CD4^+$ T cells did not investigate an interaction of IRF4 and Runx3, the results from the pulldown analysis of this thesis revealed an Runx3-IRF4 interaction and that aligns and matches with the context of the mentioned publications. Therefore it can be hypothesized that a Runx3-IRF4 interaction is important for effector functions of Treg cells and the development of pro-inflammatory Th17 cells.

Some studies have suggested an interaction of STAT3 and IRF4, but could not confirm any physical interconnection of the two transcription factors (Brüstle et al., 2007). Biswas et al. speculated that cooperation between IRF4 and STAT3 is very likely to regulate Th17-specific effects (Biswas, Bhagat, et al., 2010), while Brüstle and colleagues additionally proposed that an IRF4-STAT3 interaction specifically enhances the expression of *Rorc* and downregulates FoxP3 levels (Brüstle et al., 2007). Ciofani et al. described the co-localization of STAT3 and IRF4 in Th17 cells at lineage-specific loci, e.g. *Il17a*, *Il17f* and *Rorc*, using ChIP-seq data (Ciofani et al., 2012). Although they investigated the transcription factor binding already 48 h after cell stimulation, high expression of STAT3 and IRF4 was also seen after 72 h using western blot, which would make an interaction at a later time point plausible, too. In another study (Kwon et al., 2009), the co-localization of IRF4 and STAT3 was seen in $CD4^+$ T cells, as demonstrated by overlapping binding profiles of both transcription factors. For IL-21-mediated gene expression, an IRF4-steered STAT3 recruitment was suggested, leading to cooperative gene regulation. Co-precipitation in this study was not able to confirm a physical interaction - only in some experiments a weak interaction could be detected (Kwon et al., 2009). A different study suggested an indirect binding of STAT3 and IRF4 via c-JUN that is mediated through chromatin remodelling (P. Li & Leonard, 2018). Data from the pulldown study in this thesis could for the first time reproducibly demonstrate an IRF4-STAT3 protein complex formation in Th17 cells, which could not be proved in the previously discussed publications.

An interaction of ARI1A, ARI1B, ARID2, BRD7, CHD7, EP300, KDM6A, KMT2D, NCOA3, NCOR2, NIPBL, PAXI1 (=PTIP), PB1 (=BAF180), REQU (=DPF2), SATB1, SMCA2, SMRD1, TCF20 and ZN609 with IRF4 was reported in a recent, large-scale interaction study of human transcription factors in HEK293 cells using BioID and affinity purification coupled with mass spectrometric analysis (Göös et al., 2022). Many of these proteins are chromatin regulators displaying their function directly as a subunit of the SWI/SNF complex (ARI1A, ARI1B, ARID2, SMCA2, SMRD1 (Euskirchen et al., 2012), PB1 (Brownlee et al., 2014), REQU (Cruickshank et al., 2015), BRD7 (Kaeser et al., 2008)), histone acetyltransferase (EP300 (Perissi & Rosenfeld, 2005), NCOA3 (J. Xu et al., 2000)), histone demethylase (KDM6A (Huppertz et al., 2021)), histone methyltransferase (complex) (KMT2D (L.-H. Wang et al., 2021), PAXI1 (Y.-W. Cho et al., 2007)) and by chromatin condensation (NCOR2 (J. Cui et al., 2011)) or other chromosomal regulation mechanisms (SATB1 (Alvarez et al., 2000), CHD7 (Sanosaka et al., 2022)). As IRF4 is known to regulate chromatin accessibility in concert with other proteins (P. Li & Leonard, 2018), e.g. BATF, it is very likely that IRF4 interacts with the aforementioned proteins to regulate gene expression in T cells on an epigenetic level. Alternatively, these proteins could interact indirectly with IRF4, mediated via other

chromatin-remodelling proteins that are already described as interacting with IRF4, e.g. HDAC1 (Cao et al., 2010) or CARM1 (S. Li et al., 2011).

A direct interaction of HDAC1 with IRF4 has been demonstrated in the context of Runx3 repression during thymocyte development. The recruitment of HDAC1 by IRF4 resulted in histone deacetylation at the *Runx3* promoter (Cao et al., 2010). The methyltransferase CARM1 and IRF4 have been identified as high-confident candidate interacting proteins in a human innate immunity interactome for type I interferon using prey and bait analysis (S. Li et al., 2011). Additionally, CARM1 is also listed as (physically) associated with IRF4 in different databases, although it is not transparent and plausible how the authors concluded that as CARM1 was not listed as a validated or known interactor of IRF4 in the supplementary data of this publication (S. Li et al., 2011). Nevertheless, an important role of CARM1 as a transcriptional co-activator in T cell development is described (J. Kim et al., 2004). Interactions of CARM1 with two other IRF4 interactors, TP65 and FLI1, have been reported, which could describe an alternative, indirect interaction of CARM1 with IRF4 (D. Kim et al., 2010). CARM1 is also recruited by the steroid receptor coactivator 1 to Th17 critical loci, e.g. the *Il17a* promoter, making the gene region accessible and thereby enhancing Th17 development (Sen et al., 2018). It remains open if CARM1 and IRF4 interact directly or indirectly via other (chromatin-remodelling) proteins and if both proteins are important for the expression of particular genes in Th17 and Treg cells, e.g. as reported by Sen and colleagues (Sen et al., 2018).

A DNA-based interaction of IRF4 with IKZF1 (Ikaros) could be revealed by immunoprecipitation and subsequent *Irf4*$^{-/-}$ analysis in plasma cells (Ochiai et al., 2018). Interestingly IKZF3 (Aiolos), EP300 and proteins from the NuRD complex (including HDAC1) were also identified in that immunoprecipitation (Ochiai et al., 2018). This indicates once more that IRF4 acts together with other chromatin-remodelling proteins in different immune cells as epigenetic rulers and thereby steer cell type specific transcription. A positive regulation of *Irf4* by IKZF1 has been shown in zebrafish and could additionally be linked with involvement of IKZF1 and IRF4 in the development of T cells (Huang et al., 2019). A reciprocal positive regulation of *Ikzf1* by IRF4 has been described in B cells and in multiple myeloma (Fang et al., 2012; Fionda et al., 2015; G. Lu et al., 2014) and could also be seen in the IRF4-ChIP-seq data of Th17 and Treg cells from this thesis. An IRF4-steered gene expression of *Ikzf3*, which was – as mentioned above – also in the immunoprecipitation described by Ochiai, was not seen in T cells, neither in Th17 nor in Treg cells. Interestingly, results from this thesis revealed that IKZF3 is highly expressed in the presence of IRF4 in Th17 cells and only significantly elevated in *Irf4*$^{-/-}$ Treg cells, which could indicate that IRF4 stabilizes IKZF3 in Th17 cells and suppresses/degrades IKZF3 in Treg cells. Therefore, a Th17-specific function of IKZF3 could be proposed, which is also in line with other experimental data of this thesis: A significant higher expression of IKZF3 was seen in the proteome of Th17 cells compared to Treg and IKZF3 was determined as a Th17-enriched IRF4 interactor. Whether the interaction of IKZF3 and IRF4 is directly or indirectly mediated by IKZF1 (or other proteins) remains open.

In Th2 cells, an interaction of ubiquitin specific peptidase 4 (USP4 = UBP4_MOUSE) and IRF4 has been detected at the IL-4 promoter (Guo et al., 2017). For the enhanced expression of IL-4, cooperation with

the nuclear factor of activated T cell-2 (NFATc2) was necessary. Additionally, it was shown that USP4 acts upstream of IRF4 because knockout of USP4 resulted in decreased levels of IRF4. Mechanistically, a de-ubiquitination and stabilization of IRF4 was demonstrated (Guo et al., 2017). The involvement of NFATc2 in IL-4 expression was not surprising as, in an earlier study, an interaction of IRF4 and NFATc2 at the IL-4 promoter had already been shown (Rengarajan et al., 2002). In other cancer studies, an interaction between both transcription factors was demonstrated as well (Sharma et al., 2002; G. Wu et al., 2010). A regulatory role of different ubiquitin-specific proteases on other (cell type-characteristic) proteins has also been demonstrated in other investigations. For example, the ubiquitin ligase Stub1 promoted the degradation of FoxP3 (Z. Chen et al., 2013) and the de-ubiquitinase USP17 was shown to stabilize RORγT (Han et al., 2014). Therefore, a stabilizing effect of USP4 on IRF4, not only in Th2 but also in Th17 and Treg cells, is plausible. Other ubiquitin protein ligases (UBR4 and UBP5), ubiquitin hydrolases (UBP7 and UBP15) and ubiquitin-associated proteins (UBA6, UBAP2, UBE3A, UBS3A, UBXN7, USP9X) were identified in the core IRF4 interactome, indicating that they might act similarly to UBP4 and stabilize IRF4 or other proteins. In this way, they could additionally contribute to the cell fate decision and the stability or plasticity of Th17 and Treg cells; however, further research is needed.

The role of JunB in the development of Th17 cells and expression of Th17-critical genes was demonstrated in two independent studies (Glasmacher et al., 2012; P. Li et al., 2012). In one publication, a cooperation between BATF, JunB and IRF4 at Th17-critical loci, e.g. *Il17*, *Il21* or *Il22*, was demonstrated *in vitro* and *in vivo*, which highlights the importance of JunB in the differentiation and function of these pro-inflammatory cells (Glasmacher et al., 2012). In the second study, co-localization of BATF, IRF4 and JunB (or JunD) at some selected genes (*Il10*, *Ikzf2, Il17a, Prdm1* and *Ctla4*) was also seen by Li and colleagues (P. Li et al., 2012). Complex formation with all transcription factors was essential for the expression of these genes. The authors could, however, only reproducibly verify the BATF-Jun interaction by co-immunoprecipitation, but not the IRF4-Jun (only in a single experiment) or IRF4-BATF interaction (P. Li et al., 2012). In this thesis, not only a significantly higher expression of JunB was demonstrated in the proteome of Th17 cells compared to Treg cells but also for the first time a reproducible JunB-IRF4 interaction in pro-inflammatory Th17 cells. This highlights the important role of JunB and IRF4 in Th17 cells.

An interplayer in the regulation of IL-17 and IL-21 is Def6 (DEFI6_MOUSE or SWAP-70-like adapter of T cells (SLAT)), which in humans is also known as IRF4-binding protein (Gupta et al., 2003). Interestingly, in the experimental data of this thesis, this protein was only in Th17 cell identified as an IRF4-interacting protein. A first indication that Def6 is involved in regulating the production of pro-inflammatory cytokines was observed by Franzo and colleagues when Def6-deficient animals developed systemic autoimmunity (Fanzo et al., 2006). A few years later, the same working group was able to demonstrate *in vitro* the mechanisms behind this: Def6 regulates IRF4 and thereby (negatively) influences IRF4's capacity to bind its motifs in the *Il17*, *Il21* and *Rorc* loci, so in the absence of Def6 IRF4 was able to bind to these loci and activate their expression. A physical interaction between IRF4 and Def6 in the nucleus of $CD4^+$ T cells was confirmed by co-immunoprecipitation experiments (Q. Chen et al., 2008). Interestingly, increased levels of pro-inflammatory cytokines were only observed when the

cells were stimulated under neutral conditions. No elevated expression of IL-17 and IL-21 was detected under Th17-skewing conditions and no effect on the development and/or function of Treg cells was detected in the absence of Def6. The authors speculated therefore that the function of Def6 may depend on the surrounding cytokine milieu (pro- or anti-inflammatory). The results of this working group are in contrast to others (Canonigo-Balancio et al., 2009; Vistica Barbara P. et al., 2012), which demonstrate a positive role of Def6 in Th17 development. Only in the absence of Def6 cells failed to differentiate into Th17 cells *in vitro. In vivo* studies with *Def6*$^{-/-}$ animals demonstrated less severe EAE symptoms or less ocular inflammation in the experimental autoimmune uveitis model (Canonigo-Balancio et al., 2009; Vistica Barbara P. et al., 2012). Therefore, no clear conclusion can be drawn from these publications as to the positive or negative role of Def6 in the development of Th17 cells.

Beside IRF4 homodimer formation (P. S. Biswas, Bhagat, et al., 2010; P. Li et al., 2012; S. Sundararaj et al., 2021), IRF4 is also known to interact with its homolog IRF8, which expression is also limited to immune cells. The expression of IRF8 is FoxP3 mediated (W. Lee et al., 2016), which proposes IRF8 to be a Treg-characteristic protein. This aligns with the results from this thesis where an IRF4-IRF8 interaction was uniquely demonstrated in Treg cells and the expression levels of IRF8 were significantly higher in the proteome of Treg cells compared to Th17 cells. Additionally, different publications report that IRF8 suppresses the development of Th17 cells (W. Lee et al., 2016; Moorman et al., 2022; Ouyang et al., 2011; Zhong et al., 2017) by preventing the expression of RORγT and subsequent the production of IL-17 (Ivanov et al., 2006; Ouyang et al., 2011; Veldhoen et al., 2006; Zhong et al., 2017). In line with this, a Treg-specific deletion of IRF8 demonstrated a dysregulated expression of pro-inflammatory genes (W. Lee et al., 2016), suggesting that IRF8 might contribute to cell plasticity. In macrophages, cooperative binding of IRF8 and IRF4 was detected at ISRE sites using electrophoretic mobility shift assays. In B cells, both transcription factors additionally associated with IRF2 at such binding sites. Western blot analysis of a co-precipitation confirmed that interaction (Rosenbauer et al., 1999).

The master transcription factor of Treg cells, FoxP3, was shown in several publications to regulate the expression of IRF4 by binding to its promoter (P. S. Biswas, Bhagat, et al., 2010; Zheng et al., 2009). Co-localization of both transcription factors was demonstrated at genes which are essential for the function of this anti-inflammatory T cell subset (up to 20 % of Treg-specific genes), e.g. *Icos, Il10* and *Gzmb*. A direct interaction could be confirmed by co-immunoprecipitation. Additionally, the authors showed that IRF4-FoxP3 suppressed the development of Th2 cells, especially by preventing expression of effector molecules such as IL-4 or IL-5 (P. S. Biswas, Bhagat, et al., 2010; Zheng et al., 2009). A negative effect of FoxP3 on Th17 cell development was demonstrated by a physical interaction of FoxP3 and RORγT, which prevented RORγT-mediated IL-17 expression (Allan, 2005; Ichiyama et al., 2008; Zhou et al., 2008). IRF binding motifs were identified in many genomic regions that are bound by FoxP3, which is known to mainly bind in open chromatin structures and to not contribute on an epigenetic level to opening genomic regions. These findings suggest that IRFs could be crucial in regulating the chromatin accessibility of particular genes and thereby regulate the effector functions of Treg cells (van der Veeken et al., 2020).

As mentioned above, some proteins have been described as physically associating with IRF4, but for TF65 and Bcl11b it remains unclear how this could be concluded from the authors' published data (Glasmacher et al., 2012; Lehtonen et al., 2005; Saito et al., 2007; G. Wu et al., 2010). Nevertheless, an interaction demonstrated in this thesis did indeed support an interaction of the proteins with IRF4. TF65 and Bcl11b will be briefly described and discussed in the next section.

The transcription factor p65 (TF65), also known as RelA, is a part of the nuclear factor kappa B (NF-κB) complex, which is described to influence anti- and pro-inflammatory cell responses. Constitutive activation of the NF-κB pathway is also associated with the development of diseases, e.g. rheumatoid arthritis, cancer, allergy and others (R. Biswas & Bagchi, 2016; Serasanambati & Chilakapati, 2016). Generally, the NF-κB family consists of five members that are involved in different cellular pathways, including inflammatory responses or immune reactions. Upon activation, NF-κB members trans-locate from the cytoplasm into the nucleus where they control transcription (R. Biswas & Bagchi, 2016; Serasanambati & Chilakapati, 2016). The dual function of RelA is something of a rarity as most NF-κB members only elicit pro-inflammatory immune reactions. Combinatorial with another NF-κB protein, e.g. c-Rel, p65 promotes Treg development via the formation of a *Foxp3*-specific enhanceosome (Ruan & Chen, 2012). Additionally, RelA is necessary for the suppressive function of Treg cells and inactivation of it induces inflammatory diseases (Messina et al., 2016). In this thesis, TF65 was identified exclusively in the IRF4 interactome of Th17 cells, which links it to the pro-inflammatory context. Experiments where p65 was inhibited (D. Sun et al., 2018) revealed that it has an important role in Th17 cells as decreased levels of RORγT and IL-17 were detected *in vitro*. Mechanistically, it had been demonstrated that RelA trans-locates into the nucleus and induces *Rorc* expression by binding to its promoter (D. Sun et al., 2018). Another working group confirmed that p65 regulates RORγT expression and demonstrated up to a 70 % reduction in Th17 frequency in animals with a p65 knockout compared with controls (Ruan et al., 2011). Although NF-κB members, including p65, were binding in NF-κB response elements upstream of the IRF4 promoter, a siRNA mediated knockdown of RelA showed no effect on IRF4 expression (Boddicker et al., 2015; Vasanthakumar et al., 2017). The same result was also seen for NF-κB1 (p50), another member of the NF-κB complex, which was identified in the core T cell interactome of IRF4 in this thesis. In a T cell lymphoma cell line, IRF4 was shown to regulate the expression of NF-κB1. In the primary Th17 and Treg cells from this thesis, the *Nfkb1* gene was not regulated by IRF4, only the promoter region (overlapping with an enhancer) of *Rela* was occupied by IRF4, as the IRF4-ChIP-seq data from this thesis revealed. Results from the *Irf4*$^{-/-}$ analysis however demonstrated no significant effect of IRF4 on the expression of the RelA protein.

The C_2H_2 zinc finger domain-containing transcription factor Bcl11b, which binds GC-rich response elements, was identified in this thesis as a core IRF4 interactor. A study revealed that Bcl11b acts as a strong FoxP3 co-factor and is involved in the regulation of suppressive functions of Treg cells, e.g. IL-10, CD103 (*Itgae*), Tigit, Icos and even FoxP3 (Avram & Califano, 2014; Hasan et al., 2019). Interestingly, a large overlap in co-binding between Bcl11b and FoxP3 was found. In gene regions that were FoxP3 independent, Bcl11b acted repressively on translation. In line with the suppressive role of Bcl11b, knockout animals developed severe inflammation (Avram & Califano, 2014). Additionally, elevated

levels of pro-inflammatory cytokine and $CD4^+$ effector T cell phenotypes were seen. Interestingly, IRF4 expression was also negatively affected by the absence of the Bcl11b (Avram & Califano, 2014; Hasan et al., 2019). This could suggest an IRF4-Bcl11b interaction, as shown by the IRF4 pulldown results of this thesis, that regulate Tregs' effector functions either indirectly via FoxP3 or directly at selected gene regions. For Th17 cells, it is known that Bcl11b restricts the plasticity of this subset by blocking Th2 development. In asthma patients, elevated IL-17A and TGF-β1 expression was observed which correlated with decreased levels of Bcl11b. A mouse model for asthma confirmed the human finding and additionally showed that ectopic expression of the transcription factor resulted in reduced Smad2 phosphorylation and decreased IL-17 secretion. The negative effect of Bcl11b on IL-17 expression was also shown in Treg cells where the absence of the transcription factor resulted in elevated levels of pro-inflammatory cytokines, including IL-17, as well as $CD4^+$ effector T cell phenotypes (Avram & Califano, 2014; S. Chen et al., 2018). Further investigations are needed to understand the role of IRF4 and Bcl11b, particular in Th17 cells.

5.2.2 IRF4 INTERACTORS NOT YET DESCRIBED IN LITERATURE

In addition to literature-based IRF4 interactions, the identification of binding motifs from the precipitated DNA fragments (especially those in close proximity to the IRF4 binding motif) by a second method proved the validity of the results from the IRF4 interaction study of this thesis. In total, the motifs of 18 experimentally determined IRF4 interactors were identified and some also enriched in the IRF4-ChIP-seq data of this thesis. From these 18 IRF4 interactors, ten proteins were already described in the literature and discussed above (see chapter 5.2.1), whereas eight proteins (CBP, GTF2I, RFX1, TCF7, AHR, NR2C2, BACH2, FLI1) had not yet been described. Therefore, the following paragraphs will focus on these candidates.

In this thesis, the motifs of the two histone acetyltransferases CBP and EP300 were identified by the MATCH/TRANSFAC algorithm in both cell types and the EP300 motif was additionally determined to be enriched in Th17 cells by MEME/Tomtom. Both proteins, which are often only referred to as CBP/p300 because they have a high sequence homology, functional overlap and cooperation, are frequently described in the context of various tumours. Here they regulate and modulate the expression of different genes via the binding and acetylation of histone modification proteins, transcription factors and transcription co-activators that are recruited to particular genes (Castillo et al., 2019; Q. Chen et al., 2022). Among the EP300-regulated genes is the *Irf4* gene, where EP300 binds the promoter region and also enhances the expression of IRF4 at protein level (W. Wei et al., 2023). Interestingly, *in vitro* treatment of EP300 and CBP in multiple myeloma cell lines revealed that the genes that are most affected by this inhibition are genes regulated by IRF4. Targeted knockout of one of the two histone acetyltransferases by shRNA demonstrated reduced *Irf4* mRNA levels, confirming that CBP/p300 inhibition directly targets the IRF4 expression (Conery et al., 2016). In the context of T cell biology, it has been described that human iTregs have impaired proliferation, as shown by reduced FoxP3 expression and fewer Treg-characteristic markers in the absence of CBP and EP300. This is in accordance with results demonstrating that acetylation of FoxP3 by EP300 is critical to protein stability and function (Malviya et al., 2023; L. Wang et al., 2018). In addition, CBP/p300-deficient Treg

cells were reported to be less suppressive, demonstrating that both transcription factors have an essential role for fully functional Treg cells. Mechanistically, it was determined that CBP and EP300 regulate Treg differentiation via the regulation of expression of the master transcription factor and regulation of its downstream pathways, e.g. production of IL-10 or chemokines (Castillo et al., 2019; Q. Chen et al., 2022; Ghosh et al., 2016). CBP and EP300 have also been reported to play a role in the expression of IL-17A and other pro-inflammatory cytokines in Th17 cells. In murine Th17 cells, direct regulation of the *Il17a* gene has been shown via EP300 binding to the promoter of this pro-inflammatory cytokine. Additionally, the histone acetyltransferase promotes chromatin accessibility. Inhibited IL-17A secretion and reduced *Rorc* expression were detected in human primary cells and patient samples when EP300 and CBP were specifically targeted with inhibitors (Hammitzsch et al., 2015). Co-immunoprecipitation of EP300 and RORγT also demonstrated an interaction of both transcription factors, where EP300 stabilized the RORγT expression by acetylating the protein (Q. Wu et al., 2015). In the treatment of cancer, inhibitors of CBP/p300 are currently in phase I/II clinical trials and such inhibitors are also used to treat Th17-driven autoimmune diseases, e.g. psoriatic arthritis and ankylosing spondylitis (Q. Chen et al., 2022; Hammitzsch et al., 2015). Even though EP300 and CBP are very similar and often considered as one entity, EP300 seems to be the stronger, more important and more sensitive player in the context of disease development and treatment, as well as in the context of IRF4. In a study with two lymphoma cell lines, binding of EP300 but not CBP was observed in DNA fragments that contained the TSS of the *Irf4* gene. In addition, the deletion of EP300, but not the knockout of CBP, had an effect on IRF4 expression (W. Wei et al., 2023). It is also only EP300 that is described as a "Th17-enhancing molecule" (Banuelos et al., 2017) and associated with other Th17-favouring proteins support the activity of STAT3 and RORγT. The results from the different IRF4 studies of this thesis support the important role of EP300 for Th17 cells: EP300 was not only determined as a Th17-enriched IRF4 interactor but also a significantly higher EP300 expression as shown in the proteome of Th17 cells compared to Treg cells. Although the literature suggests that IRF4 is regulated by EP300, IRF4-ChIP-seq data from this thesis reveal a positive regulation of *Ep300* as IRF4 bound in the promoter and enhancer region of the *Ep300* gene in both cell types. At protein level, EP300 was uniquely up-regulated during the development of Th17 cells when IRF4 is present. A recent publication described an interaction of EP300 and IRF4 in HEK293 cells (Göös et al., 2022). No dysregulated expression of CBP at protein level was detected in the *Irf4*$^{-/-}$ analysis of this thesis, although in Th17 cells IRF4 binding was also detected in the promoter and enhancer region of the *Crebbp* gene. Combined motif analysis of IRF4 and EP300/CBP revealed that both motifs were in close proximity (5 bp distance), further supporting the physical interaction identified in the IRF4 pulldown analysis. However, further investigation is needed to better understand the molecular mechanisms of the interaction of IRF4 with both histone acetyltransferases, especially with CBP.

One motif that was in this thesis identified and enriched in both cell types was the motif for the Friend Leukemia Virus Integration 1 (FLI1). Interestingly, the motif was identified in normal and reverse complement direction for Th17 cells while for Tregs it was only found as reverse complement. The protein was identified in the IRF4 interactome of both cell types, but demonstrated higher expression levels in Th17 cells compared to Treg cells. The same expression pattern could be seen on whole

proteome level. Regulation of FLI1 expression by IRF4 could be detected in both cell types where IRF4 bound within the promoter and enhancer region of the *Fli1* gene. *Irf4*$^{-/-}$ analysis revealed also on protein level an IRF4-dependent expression of FLI1 in Th17 cells: FLI1 expression was significantly higher in fully functional Th17 cells than in Th17 cells from *Irf4*$^{-/-}$ animals. Additionally, only in the absence of IRF4, a reduced FLI1 expression was detected in Th17 cells during cell differentiation, indicating that IRF4 is important for high expression levels of FLI1 in Th17 cells. FLI1 is described in the pathogenicity of diseases associated with pro-inflammatory phenotype, e.g. graft-versus-host disease, colitis and lupus, as well as in the context of cancer (Schutt et al., 2019, 2022; K. P. Sundararaj et al., 2015; S. Wang et al., 2020; X. Wang et al., 2021). In general, (over)expression of FLI1 was associated with increased levels of IL-17A, GM-CSF and other pro-inflammatory cytokines. In cancer patients, high FLI1 expression correlated with increased levels of tumour-infiltrating lymphocytes, resulting in a higher anti-tumour response and a longer survival time than in cancers with low expression of FLI1. Differentially expressed genes in FLI1^{high} cancers were also enriched in immune-related pathways including the Th17 cell differentiation or TCR signalling pathway (S. Wang et al., 2020). In contrast, high FLI1 expression was detrimental to transplant recipients or patients with autoimmune diseases. *In vitro* analysis comparing FLI1^{WT} with FLI1^{KO} revealed that levels of pro-inflammatory cytokines were decreased in the absence of FLI1 (K. P. Sundararaj et al., 2015; X. Wang et al., 2021). Direct binding of FLI1 in the promoter of the *Gmcsf* gene was demonstrated by ChIP-seq analysis (X. Wang et al., 2021). In addition, elevated levels of Treg cells and effector molecules were detected in the absence of FLI1. Gene expression analysis demonstrated that genes with anti-inflammatory properties were up-regulated and genes associated with pro-inflammatory states were down-regulated when FLI1 was knocked out. *In vivo* experiments supported the finding from *in vitro* studies, as inhibition of FLI1 showed improved disease outcome in animals with lupus-like disease and reduced clinical scores for graft-versus-host disease, which resulted in an overall increased survival rate (Schutt et al., 2019; K. P. Sundararaj et al., 2015; X. Wang et al., 2021). So far, an interaction of FLI1 and IRF4 can only be assumed from ChIP-seq data of B cells where overlapping DNA binding regions were detected in multiple myeloma cells (Y. Jin et al., 2018). Although a down-regulation of TCR-induced genes is described in T cells from *Fli1*$^{+/-}$ animals, including *Nfkb1* and *Batf* (Schutt et al., 2022), *Irf4* is not mentioned, but it could be affected as its expression is also induced upon TCR stimulation. Data from this thesis demonstrated an interaction of FLI1 and IRF4 in T cells, which could be especially important for the expression of pro-inflammatory molecules in Th17 cells and the inhibition of Treg cells under Th17-skewing conditions. It could be hypothesized that FLI1 is involved in Treg-Th17 plasticity, as decreased glycolytic but increased oxidative phosphorylation gene scores were detected in T cells with a partial or complete *Fli1* knockout (Schutt et al., 2022). These two metabolic pathways in particular are discussed to influence T cell plasticity (see chapter 1.4).

The motif of the testicular receptor 4 (TR4, also known as nuclear receptor subfamily 2, group C, member 2, NR2C2) was enriched in Th17 and Treg cells, but was identified by MATCH/TRANSFAC only in Treg cells (Treg: 98.25 %). TR4 belongs to the superfamily of nuclear receptors that are described as being involved in development, differentiation, homeostasis and reproduction. TR4 was found to also regulate mRNA metabolism, protein translation, ubiquitin cycle, metabolic processes, lipid recruitment

and gluconeogenesis (O'Geen et al., 2010; L. Zhang et al., 2015). It is a ligand-activated transcription factor which trans-locates in the nucleus upon activation and binds AGGTCA repeats in promotors of target genes (L. Hu et al., 2020; R. Jin et al., 2018; Y. Zhang & Dufau, 2004). TR4 has been reported in the progression of cancers such as prostate cancer and non-small cell lung cancer, and its expression correlated with chemotherapy resistance, a marker for metastasis and poor prognosis. The expression of TR4 is higher in tumour tissue than in healthy control tissue. Overexpression of TR4 demonstrated chemo-resistance, increased proliferation, migration and invasion of tumour cells while the knockdown or inhibition of TR4 showed the opposite effects (L. Hu et al., 2020; L. Zhang et al., 2015). Most research on TR4 is performed in the context of cancer because it can be considered a biomarker for some types. No connection between TR4 and IRF4 or Treg cells could be found in the literature. However, an interaction of TR4 with other IRF4 interactors has been determined. For example, an interaction of NR2C2 with IRF8 was described recently by Göös et al in human HEK293 cells (Göös et al., 2022). Interestingly, IRF8 was the second transcription factor that was enriched in both cell types but where the motif could only be determined in Treg cells with the MATCH/TRANSFAC algorithm. The interaction of NR2C2 with another IRF4 interactor (IRF8) could indicate that NR2C2 interacts indirectly with IRF4. The function of NR2C2 in T cells, especially in Treg cells, has to be further elucidated.

In this thesis, the transcription regulator protein BACH2 was identified as an IRF4 interactor uniquely in Th17 cell. Its motif was identified and enriched in both cell types. It is a critical regulator in the immune system as it plays an important role in the balance of immune homeostasis and immunity. Interestingly, BACH2 has been described to play an important role in the development of Treg cells (E. H. Kim et al., 2014). It is essential in the early stages of Treg development programme, as the absence of *Bach2* resulted in increased *Foxp3* methylation, reduced FoxP3 expression (Edwards et al., 2018; E. H. Kim et al., 2014), and led to lethal inflammation in BACH2 deficient animals (Grant et al., 2020; Richer et al., 2016). Roychoudhuri and colleagues described BACH2 also as an essential enhancer of FoxP3 (Roychoudhuri et al., 2016). At a later time point, BACH2 has been shown *in vivo* to play an important role in maintaining the survival of long-term resting Treg cells; however, BACH2 prevented an activated Treg status and limited their effector functions (Grant et al., 2020; Roychoudhuri et al., 2016; Sidwell et al., 2020). Mechanistically, BACH2 negatively regulated IRF4-mediated transcription by diminishing IRF4's DNA-binding capacity as well as reducing chromatin accessibility. In an infection model, *Bach2*$^{-/-}$ animals were mainly protected from colitis, emphasizing the suppressive function of BACH2 on effector functions in Treg cells – only in the absence of BACH2 Treg cells display improved suppressive functions (Sidwell et al., 2020). During cell development, BACH2 represses the expression of genes associated with conventional T cells, e.g. Blimp-1 and GATA3 (Sidwell et al., 2020), and prevents effector cell differentiation (Roychoudhuri et al., 2013). The absence of BACH2 also contributed to the trans-differentiation from anti-inflammatory to pro-inflammatory state, as seen by elevated levels of IL-17A and other cytokines from Th1 and Th2 cells (S. R. Bailey et al., 2014; Edwards et al., 2018). *Ex vivo* Th17 cells derived from diseased mice of an EAE model demonstrated decreased levels of BACH2 and this correlated with an increased disease score in these animals compared to healthy control animals, which showed normal expression of BACH2 (Edwards et al., 2018; Hoppmann et al., 2015). Reduced tumor growth was detected in *Bach2*$^{-/-}$ animals along with an activation of the

adaptive immune system, especially involving IFN-γ secreting $CD8^+$ T cells (Roychoudhuri et al., 2016). In humans, mutations and polymorphisms in the *BACH2* gene or dysregulated BACH2 expression have been associated with different diseases (Edwards et al., 2018; Richer et al., 2016; Roychoudhuri et al., 2013; Sasikala et al., 2018), e.g. chronic myeloid leukaemia (CML) (Y. Zhang et al., 2022), systemic lupus erythematosus (SLE) (Sheng et al., 2021), type 1 diabetes (Cooper et al., 2008; Plagnol et al., 2011), asthma (Ferreira et al., 2011), rheumatoid arthritis (McAllister et al., 2013), Crohn's disease (Christodoulou et al., 2013; Franke et al., 2010), coeliac disease (Dubois et al., 2010) and multiple sclerosis (Sawcer S et al., 2011). GWAS studies postulated *BACH2* as a potential protective gene in the susceptibility of multiple sclerosis (Patsopoulos et al., 2019). In general, a repressive role of BACH2 could be described in Th17 cells – BACH2 probably represses AHR, which is important for Th17 development (Richer et al., 2016; Sasikala et al., 2018). In the context of IRF4 and BACH2, an interaction of both transcription factors has been proposed in T cells from CML patients. This observation resulted however only from co-occurrence, and no further investigation was performed to verify a physical interaction of these transcription factors (Y. Zhang et al., 2022). In a different publication, a negative regulation of IRF4 by BACH2 could be described as overexpression of BACH2 inhibited IRF4 expression (Sheng et al., 2021). A reciprocal regulation of BACH2 by IRF4 was not detected in the IRF4-ChIP-seq data in this thesis as no IRF4 binding was detected in the *Bach2* promoter region, neither in Th17 nor in Treg cells. Although further details on the function of IRF4-BACH2 interaction in Th17 cells could not be revealed in this thesis, a physical interaction of IRF4 and BACH2 was demonstrated in the IRF4 pulldown study and further supported by the IRF4-ChIP-seq data as the motifs of both transcription factors were found in close proximity (5 bp distance).

The motif for the aryl hydrocarbon receptor (AHR) was identified with the MATCH/TRANSFAC search only in Th17 cells (in 99.68 % of identified peaks) of this thesis and was only identified as an IRF4 interactor in the same cell type. In addition, experimental data revealed a higher expression of AHR in Th17 cells compared to Treg cells in the whole proteome analysis, too, indicating an important role of AHR for Th17 cells. Interestingly, a role of AHR in the regulation of adaptive immunity has not only been reported in literature for Th17 cells but also for Treg cells. The ligand-dependent activation of AHR is crucial for the Th17/Treg balance as it can induce anti-inflammatory Treg cells as well as pro-inflammatory, pathogenic Th17 cells. Normally, AHR is located in an inactive form in the cytoplasm of cells, but can trans-locate into the nucleus upon binding. Activated AHR can regulate gene expression not only by binding to a specific consensus motif (5'-TNGCGTG-3') but also by interacting with other transcription factors, e.g. RelA, STAT proteins or members of the SWI/SNF complex (Baricza et al., 2016; Rothhammer & Quintana, 2019). Interestingly, some of these AHR interaction partners were also identified in the experimental data from the IRF4 interactome of this this thesis, which could suggest also an indirect IRF4-AHR interaction. In Th17 cells, AHR expression gets induced by STAT3 and strongly promotes the Th17 cell fate by boosting IL-17A, IL-17F and IL-22 production and by interfering with Treg cell pathways. For example, AHR limits STAT5 and STAT1 signalling and induces the expression of IKZF3 (Aiolos) which silences the expression of IL-2 (Rothhammer & Quintana, 2019). The absence of AHR impaired not only the production of IL-17A and IL-22 *in vitro* and *in vivo* (de Lima et al., 2018; Esser et al., 2009; Quintana et al., 2008; Rothhammer & Quintana, 2019), it also showed

decreased number of IL-17$^+$ CD4$^+$ T cells (Singh et al., 2016) and animals developed less severe EAE *in vivo* (de Lima et al., 2018; Esser et al., 2009; Quintana et al., 2008; Rothhammer & Quintana, 2019). Another study demonstrated that the Th17/Treg balance is mediated via hypo- and hyper-methylation either at the *Foxp3* promoter or at the *Il17* promoter. Ligand-dependent AHR activation was involved in the shift of methylation patterns in CpG islands into either a pro- or an anti-inflammatory state. For example, 2,3,7,8-tetrachlorodibenzo-p-dioxin (TCDD)-induced AHR activation favoured hypomethylation of the *Foxp3* promoter while 6-formylindolo [3,2-b] carbazole (FICZ) favoured *Foxp3* hypermethylation (Singh et al., 2011). Although the important role of AHR in the development of Th17 cells has been confirmed, no interaction of AHR and IRF4 has yet been described. Combined motif analysis of the IRF4-ChIP-seq data from this thesis has shown a close proximity of the AHR and IRF4 binding motifs, suggesting a DNA-based IRF4-AHR interaction in Th17 cells.

The transcription factor 7 (TCF7 or T cell factor 1, TCF1) is a positive regulatory of chromatin accessibility (van der Veeken et al., 2020) and has been described to play an important role in early T cell development in the thymus as well as in the periphery (P. Li & Leonard, 2018; Ma et al., 2011; S. Yu et al., 2012; Y. Zhu et al., 2015). Its motif was identified via MATCH/TRANSFAC in Th17 (99.29 %) and Treg cells (95.03 %) of this thesis. In literature, TCF7 has been described to play an important role especially in the development, survival and expansion of T cells as *Tcf7*$^{-/-}$ mice did not display a normal chromatin landscape (P. Li & Leonard, 2018). For Treg cells, TCF7 is important for a normal Treg pool, for Treg survival and, together with FoxP3 (and other transcription factors), it starts the Treg cell transcriptional programme. Animals with a Treg-specific *Tcf7* deletion developed systemic autoimmunity (B.-H. Yang et al., 2019). A further investigation revealed that TCF7 is important for chromatin accessibility for FoxP3 binding and thereby crucial to the epigenetic identity of Treg cells. Although FoxP3 binds in the *Tcf7* locus and diminished expression of TCF7 is demonstrated at mRNA and protein level, this reduction probably functions as a balanced control for gene accessibility and Treg function. Interestingly, in the contribution of chromatin opening to FoxP3 binding, IRF binding sites have been described alongside Sox binding regions (TCF7 recognition site). Moreover, a co-occupancy of IRF4 and TCF7 for chromatin accessibility has been described (van der Veeken et al., 2020). Therefore, a regulatory function of gene accessibility (for FoxP3 binding) could demonstrate a possible shared feature and mode of interaction between TCF7 and IRF4 in Treg cells, especially as IRF4 is also known to be important for effector functions in this cell type. In Th17 cells, TCF7 has also been proposed to be involved in cell survival and expansion *in vivo* and to be a negative regulator of pro-inflammatory T cell responses. In the absence of TCF7, elevated levels of IL-17A/F and IL-7α (enhancer of Th17 survival) were detectable and animals were sensitive for development of EAE. Yu and colleagues reported the direct binding of TCF7 in the regulatory regions of the *Il17* gene while Ma et al. revealed the epigenetic regulation of the *Il17* gene (Ma et al., 2011; Q. Yu et al., 2011; Y. Zhu et al., 2015). In addition, a role of TCF7 in the plasticity of cells has been described. Interestingly, Th17 cells isolated from IBD patients and stimulated with IL-12 showed trans-differentiation into Th1-like cells. Contrary to the previous studies, a reduction in TCF7 was also accompanied by reduced levels of IL-17A in these cells (Bsat et al., 2019). Little has been reported about any relationship between TCF7 and IRF4 in Th17 cells. The expression of IRF4 seems to not be controlled or affected by TCF7, as the mRNA

expression levels of IRF4 were not different between *Tcf7*$^{-/-}$ and wildtype conditions (Ma et al., 2011; Q. Yu et al., 2011). Interestingly, the results from this thesis indicate that the expression of TCF7 could be regulated by IRF4 as ChIP-seq data demonstrated IRF4 binding in the promoter region of *Tcf7*. Upon stimulation of naïve CD4^{+} T cells, decreased expression of TCF7 were detected, while in differentiated Th17 cells, significantly higher levels of TCF7 were measurable in the presence of IRF4, which is in line with published data (Y. Zhu et al., 2015). Therefore, it can be speculated that IRF4 binds to (a low amount of) TCF7 to repress the repressing effect of TCF7 in IL-17 expression. If this interaction were to occur at DNA level, an interaction in intron 2 of the *Il17f* gene could be proposed, as IRF4 binding was detected there and TCF7 binding has also been described in the second intron of the *Il17* gene (the authors did not distinguish between *Il17a*, *Il17f* and other *Il17* genes) (Q. Yu et al., 2011).

The X-box binding transcription factor RFX1 (Regulatory Factor X 1) is a context-dependent transcription factor, like IRF4, which is associated with inflammatory diseases such as SLE or lupus and with tumorigenesis. This transcription factor was not only identified in the core IRF4 interactome, but its motif was also identified in Th17 and Treg cells (MATCH/TRANSFAC algorithm, 98.91 % in Th17 cells, 93.11 % in Treg cells). RFX1 down-regulation is positively correlated with enhanced Th17 development (Du et al., 2019; Y. Zhang et al., 2013; Zhao et al., 2010, 2018b). Mice with a deletion of RFX1 develop exacerbated EAE disease and pristane-induced lupus-like syndrome. This could be attributed to increased levels of Th17 cells, which was also demonstrated by *in vitro* studies where deficiency of RFX1 led to enhanced levels of pro-inflammatory Th17 cells (more IL-17A, more IL-17F, more RORγT, more CD70, more CD11a) than in *Rfx1* wildtype animals. Mechanistically, RFX1 represses the expression of IL-17A by binding in the promoter of *Il17a*, recruits epigenetic enzymes including HDAC1, and thereby modifies the chromatin conformation to a closed chromatin status shown by decreased H3ac and increased H3K9me3 levels (Zhao et al., 2018a). Interestingly, the RFX1 interacting protein HDAC1 (Zhao et al., 2010) was found in the IRF4 interactome of this thesis and the HDAC1 motif was identified in Th17 and Treg cells, too. As HDAC1 was recruited to the *Il17a* promoter by RFX1, it contributes also to the repressed expression of IL-17A (Zhao et al., 2018a). Independent of RFX1, HDAC1 has been shown to repress IL-17A production and Th17 development by deacetylating and thereby destabilizing RORγT (Q. Wu et al., 2015). In contrast to these studies, which show a negative role of HDAC1 on Th17 differentiation, a positive correlation between HDAC1 expression and pro-inflammatory cell development could be demonstrated in a different publication (Gu et al., 2022). Inhibition of HDAC1 during the differentiation of Th17 cells showed impaired cell development and reduced levels of IL-17A *in vitro*. A colitis mouse model confirmed these results *in vivo* as animals treated with an HDAC1 inhibitor showed improved colitis-associated symptoms, including a lower number of Th17 cells and lower levels of IL-17A compared with the control group without the inhibitor (Gu et al., 2022). Furthermore, resistance to the development of EAE was described in another study by the deletion of *Hdac1* in T cells (Ellmeier & Seiser, 2018). Corroborating these results in Th17 cells, inhibition of HDAC1 resulted in elevated acetylation of FoxP3, which led to up-regulated Treg differentiation as proven by *in vitro* and *in vivo* results (Furusawa et al., 2013; Zhou et al., 2018). Interestingly, an inhibitory function of FoxP3 on HDAC1 expression is described in an infectious model by Holmes (Holmes et al., 2011). In summary, although contrary results are reported for the role of

HDAC1 in the regulation of Th17 cells, a positive role in the development of pro-inflammatory Th17 cells was in accordance with the enhanced proliferation of Treg cells upon HDAC1 inhibition. Therefore, a possible involvement of histone deacetylases in the regulation of Th17/Treg balance can be suggested. The Th17 cell development-enhancing effect of HDAC1 would fit with the data from the IRF4 interactome of this thesis, where the levels of HDAC1 were significantly higher in Th17 cells than in Treg cells. In addition, the published results demonstrate that HDAC1 has a different role in up- or down-regulating gene expression in a context-dependent environment. Regulation of IRF4 transcription by HDAC1-steered histone deacetylation has been described in multiple myeloma cells and during the development of thymic T cells. Inhibition of HDAC1 resulted in decreased *Irf4* transcripts and suppressed growth of MM *in vivo* (Cao et al., 2010; Harada et al., 2018, 2019, 2023). In addition, during the development of T cells in the thymus, Cao and colleagues described a direct interaction of HDAC1 and IRF4 which thereby regulated the expression of *Runx3* by deacetylating H3 and H4 (Cao et al., 2010). As RFX1 interacts with HDAC1, an indirect interaction of RFX1 with IRF4 via HDAC1 could be proposed. The usage of a cross-linker not only stabilizes direct interaction partners, but also indirect, weak or transient interacting proteins.

Elevated protein levels and single nucleotide polymorphisms (SNPs) in the gene coding for the general transcription factor II-I (GTF2I or TFII-I) – another motif that was identified with the MATCH/TRANSFAC algorithm in this thesis – have been associated with different autoimmune diseases, e.g. Sjögren's syndrome, systemic lupus erythematosus and systemic sclerosis (Shimoyama et al., 2021; L. Zhang et al., 2022). From the experimental data in this thesis, an association and interaction of GTF2I with IRF4 can be shown at different levels: The motif of GTF2I was identified and the transcription factor was among the IRF4-interacting proteins in the pulldown results of Th17 and Treg cells. On a whole cell level, the expression of GTF2I was significantly elevated in Th17 cells and showed the same expression pattern as IRF4 in the knockout study ($IRF4^{WT}$ axis). This suggests a special role of GTF2I in Th17 cells. In addition to the GWAS studies that demonstrate a correlation of GTFII-I with (Th17-driven) autoimmune diseases, a further study reported increased levels of IL-6, IL-17A and other pro-inflammatory cytokines in Sjögren's disease as well as enhanced NF-κB and STAT3 activation (Shimoyama et al., 2021). However, these results were only shown for non-immune cells and could not be reproduced in immune cells (Shimoyama et al., 2021). Therefore, to date, not much is known about the role of GTF2I in immune cells. Investigation of the genes regulated by TFII-I has revealed its involvement in immune response, transcriptional regulation, gene expression, chromatin remodelling, cell cycle, glycolysis and gluconeogenesis, regulation of the TGF-β signalling pathway, muscle development and neurogenesis (Chimge et al., 2007, 2008; Segura-Puimedon et al., 2013). Involvement of TFII-I in the regulation of IL-17A production was shown in a study by Bafrani and colleagues: In the promoter region of the *Il17a* gene, a SNP (A to G) was found in 65.35 % of knee osteoarthritis patients. This SNP could create a new binding site for the TFII-I as predicted by *in silico* analysis (Bafrani et al., 2019), indicating that GTF2I binding in the promoter of the *Il17a* gene could enhance the secretion of this pro-inflammatory cytokine. This is in line with the data from the $Irf4^{-/-}$ study in this thesis, showing that GTF2I has the same expression pattern as IRF4 and which is known to be involved in the regulation of IL-17 secretion. Additionally, this locus could predict a potential

IRF4-GTF2I interaction site. Alternatively, an indirect IRF4-GTF2I interaction could be proposed, too, as it is known that TFII-I interacts with other proteins that are known or shown in the experimental data to interact with IRF4, e.g. STAT1, STAT3, NFKB and HDAC (Chimge et al., 2007).

In summary, different publications confirmed experimental determined IRF4 interactions of this thesis, which represented a solid basis for the identification of new, yet unknown IRF4 interactors, particular in Th17 and Treg cells. In addition, for newly identified IRF4 interacting proteins, literature researched aligned the experimental data with reported findings in the pro- or anti-inflammatory context or described a particular role of an IRF4 interactor in the development and/or function of Th17 and Treg cells, fitting the information into the experimental context.

Additionally, literature research revealed a strong involvement of IRF4 with chromatin-remodelling enzymes and other transcription factors that either enhance or repress IRF4-steered gene expression, which was also demonstrated by GO analysis of the experimental determined IRF4 interactors. Chromatin organization, histone deacetylase complex, the regulation of histone acetylation, protein modifying enzymes, NuRD complex and the SWI/SNF superfamily complex were especially found in the core and Th17 interactome. Interestingly, the NuRD complex is described as a chromosomal regulator that dampens and fine-tunes gene expression by modulating enhancers and promoters. In contrast, the SWI/SNF complex, another ATP-dependent chromatin-remodelling complex, is generally known to antagonize chromatin-mediated gene repression; however, it can context-dependently (depending on the transcription factor for recruitment) activate or repress gene expression (Z. Wang et al., 2021). An interaction between IRF4 and SWI/SNF remodelling complex has also been determined by RIME analysis (Centore et al., 2020). This shows that IRF4 modulates gene expression not only by direct binding to (open) enhancers, promoters or other regulatory structures but also acts as an epigenetic regulator via the opening or closing of chromatin. It is already known that IRF4, together with BATF, opens chromatin at an early stage of Th17 differentiation to allow other Th17-specific transcription factors to bind and initiate Th17 development (M. Huber & Lohoff, 2014). In line with the literature, regulation of gene expression and transcription as well as transcription factor binding were GO terms and reactome pathways that were expected for the analysis of a transcription factor and its interactors. Göös et al. performed GO analysis of the identified interactome for their studied transcription factors and demonstrated that GO terms associated with transcription or the regulation of transcription were significantly enriched, e.g. “Negative/positive regulation of transcription” (p-value $<2.17 \times 10^{-31}$) or “Transcription, DNA-templated” (p-value = 9.15×10^{-97}) as the most significantly enriched GO term (Göös et al., 2022). The regulation of transcription is not only mediated by the binding or non-binding of a transcription factor at the promoter of a particular gene but also by a complex interplay of transcription factors, chromatin-remodelling proteins, RNA polymerases, transcription factor binding proteins, modulating enzymes and other cofactors (Brivanlou & Darnell, 2002; Duguet et al., 2017; Fontaine et al., 2015; Rivera-Reyes et al., 2018). The enriched GO terms “DNA-binding transcription factors”, “transcription factor binding”, “regulation of DNA-templated transcription” and “gene-specific transcriptional regulators” identified from the experimentally determined IRF4 interactors in this thesis reflect this involved interplay nicely.

Gene expression and the subsequent translation into proteins is a complex process that can be interfered with and controlled in many ways, including chromatin structure and epigenetic modification, binding of transcription factors to regulatory elements, protein-protein interactions and mRNA processing. Additionally, post-translational modification at the translated protein, e.g. phosphorylation, acetylation or methylation, influences the stability and function of these proteins (Buccitelli & Selbach, 2020; Göös et al., 2022; J. M. Lee et al., 2023). Protein phosphorylation or dephosphorylation for example is important for regulating metabolism, cell division or development (LILLO et al., 2014). Context-dependent transcription factors such as IRF4, can enhance (positive regulation) or silence (negative regulation) gene expression, depending on the molecular interactions. To investigate the role of IRF4 on the regulation of genes and proteins, IRF4-ChIP-seq and *Irf4*$^{-/-}$ analysis were investigated. The results are discussed in the following sections.

5.3 IRF4 chromatin immunoprecipitation followed by sequencing (IRF4-ChIP-seq)

The IRF4-ChIP-seq data revealed that more genes are regulated by IRF4 in Th17 cells (21,884 peaks) than in Tregs (10,189 peaks), although much more stringent parameters were applied for the Th17 cells compared with the Treg cells. Nevertheless, the high number of peaks in Th17 cells is consistent with the literature; for example, Li and colleagues identified 21,775 IRF4 binding sites in Th17 cells (P. Li et al., 2012). The large number of genes in Th17 cells being dependent on IRF4 for their expression is in line with the important role of IRF4 for the development of these pro-inflammatory cells. The number of IRF4 binding peaks in iTreg cells ranges from 1,526 peaks reported by Vasanthakumar and colleagues (Vasanthakumar et al., 2017) up to 22,915 peaks detected by Arnold and colleagues (Arnold et al., 2022). Alvisi et al. described 7,154 IRF4 binding site in isolated Treg cells (Alvisi et al., 2020). The differences in peak numbers described in the literature could be attributed to differences in the selected parameters in the software for peak-calling, as this is a critical parameter for the analysis of ChIP-seq data. Additional discrepancies in the numbers of peaks between the literature and this thesis could be influenced by the time point of the analysis: in the referenced publications, the IRF4 binding was analysed 48 h after cell stimulation, while the cells in this thesis were stimulated for 72 h.

Many of the IRF4 binding sites described in the literature were also identified in this thesis although, as described above, the peaks demonstrated in the referenced publications were found 48 h after T cell stimulation and not in fully differentiated cells. Li et al. reported IRF4 binding in Th17-crucial genes, including *Il17a*, *Il17f*, *Il12rb1*, *Il1r1* and *Rorc* (P. Li et al., 2012). Those IRF4 binding sites were identified in fully differentiated Th17 cells in this thesis as well, demonstrating that IRF4 is important for the regulated expression of those Th17 characteristics. Many Treg-characteristics, e.g. *Prdm1*, *Tigit*, *Il10, Icos* and *Ctla4*, which have been described by Vasanthakumar (Vasanthakumar et al., 2017), Sidwell (Sidwell et al., 2020) or Arnold and colleagues (Arnold et al., 2022) to be bound by IRF4, were also detected in the Treg IRF4-ChIP-seq data of this thesis. That the expression of the master transcription factor of Treg cells, FoxP3, is not regulated by IRF4 is in line with data from Arnold (Arnold et al., 2022) who found IRF4 binding neither within the gene body nor in known *Foxp3* enhancers.

Interestingly, the authors described IRF4 binding in a cis-regulatory element (super enhancer) 14 kb downstream of the TSS from the *Foxp3* gene. This could not be demonstrated in the data of the fully differentiated Treg cells. However, the IRF4 binding in this super enhancer was BATF3 driven and BATF3 was not identified in the proteome of Treg cells, which could explain the "missing" IRF4 binding in the IRF4-ChIP-seq data presented in this thesis.

Published ChIP-seq analyses of IRF4 interacting proteins report transcription factor binding sites that were also occupied by IRF4 in the experimental data of this thesis. RORγT-ChIP-seq data demonstrated its binding at Th17-critical loci, including *Il17*, *Il23r*, *Rorc* and *Ccr6* (He et al., 2017), which were found to be also bound by IRF4, too, as data from this thesis showed. Fos-related antigen 2 (Fosl2), a STAT3 downstream target, negatively regulated Th17 cells at early time points by suppressing Th17-enhancing genes (*Il17a/f*, *Il23r*, *Ccr6, Batf*) and enhancing Th17-antagonizing genes (*Il7r*, *Stat4*, *Prdm1*) from distal regulatory elements in human cells. Interestingly, in the murine context, Ciofani indicated that in mice Fosl2 represses only Th17 effector responses, but not genes important for maintaining lineage identity, such as *Il6ra*, *Il23r* or *Il21* (Ciofani et al., 2012). At the latter gene location, IRF4 binding was detected in Th17 cells of this thesis as well, which could demonstrate that IRF4 in concert with Fosl2 (and other transcription factors) regulates maintenance of cell identity. The negative role on effector molecules could be explained by Fosl2 (maybe in combination with IRF4) critically controlling and down-regulating Th17 responses by inducing a negative feedback-loop from intergenic regions. Such a regulation of Th17 responses is described for STAT3 as limiting Th17-induced tissue damage in humans, for example (Ciofani et al., 2012; Purvis et al., 2014; Shetty et al., 2022). Ciofani also described the co-localization of transcription factors, such as RORγT, BATF, STAT3, IRF4 and EP300, at Th17-important sites by ChIP-seq (Ciofani et al., 2012), which additionally indicated a physical interaction between these proteins that enhanced the development of pro-inflammatory Th17 cells. STAT1-ChIP-seq data revealed that the transcription factor not only bound to IFN-γ activation site (GAS) elements, but also to interferon-stimulated response elements. STAT1, a Treg-enriched IRF4 interactor, is known to control Th17 and Treg development: it negatively influences Th17 cell development, but is crucial for Treg differentiation and suppressive function. STAT1-deficient animals had a lower number of Treg cells and were susceptible to developing autoimmune diseases. As it is a transcriptional regulator, the effects of STAT1 on transcription depend strongly on interaction partners (Nishibori et al., 2004; Robertson et al., 2007; Satoh & Tabunoki, 2013; B. Wei et al., 2010). In Treg cells, a physical interaction between IRF4 and STAT1 could be mediated via co-binding to ISRE sites, which could further contribute to an enhanced suppressive function in Treg cells as well as the control and repression of Th17-associated genes. Additionally, the majority of STAT1 binding was detected in intronic regions (Satoh & Tabunoki, 2013), which is consistent with the distribution of IRF4 binding sites in Treg cells.

The best-characterized gene regulation includes binding of a transcription factor in the promoter region of a gene. In the IRF4-ChIP-seq of Th17 cells, most binding of IRF4 was seen in such gene regions, which implies proximal regulation of the genes. In addition, binding in intronic structures, particularly in introns close to the TSS (less than 1 kb), can also promote gene expression (Rose, 2004, 2019). In Treg cells, binding of IRF4 was more often seen in introns than in promoter regions. In line with the findings of the IRF4-ChIP-seq analysis in this thesis, Alvisi et al. described only a small fraction of IRF4

binding in the promoter region. The majority was found 10-100 kb from the TSS (Alvisi et al., 2020). The different IRF4 binding distribution could indicate a different mode of regulation by IRF4 in the two cell types. In Th17 cells, IRF4 seems to be directly involved in the initiation of translation, while in Treg cells, IRF4 could instead regulate gene expression from distal regions, e.g. enhancer or silencer.

A high overlap with enhancer structures retrieved from the enhancer database in both cell types suggests that IRF4 mainly promotes the expression of genes. Proximal regulation by IRF4 binding in promoter and enhancer structures was found for genes coding for histone modifying enzymes, general transcription factors, gene-specific transcriptional regulators and DNA-binding transcription factors as well as chromatin/chromatin-binding, or -regulatory proteins. This suggests that IRF4 boosts the expression of other gene/chromatin-regulating proteins that contribute to the opening/closing as well as the modulation of genes and thereby define the particular cell fate. Metabolic processes of DNA, RNA or proteins were also enhanced by IRF4 binding, indicating that such pathways are also important for the development and function of both cell types. Only a few IRF4 binding regions were detected in silencers, especially in promoter regions (97 peaks in Th17 cells, 25 peaks in Treg cells). The genes where IRF4 was binding in silencer structures were involved in signalling cascades, negative regulation of gene expression in Th17 cells and genes that contribute to the opposing cell type (Th17-type immune response silenced in Treg cells), implying that IRF4 not only promotes a specific cell type but also interferes with other subsets. In Treg cells, for example, IRF4 was only binding in a silencer region within the *Rorc* gene while in Th17 cells, IRF4 was also binding in enhancer structures.

5.4 IRF4 knockout (*Irf4*$^{-/-}$) in Th17 and Treg cells

Although many proteins showed elevated expression in the differentiated cells compared with the naïve CD4^{+} T cells, interestingly, in Th17 cells, more proteins showed an enhanced expression in the absence of IRF4. As already observed and described at DNA level, also at protein level IRF4 not only promoted the expression of “needed” proteins, but also repressed “interfering” proteins. In general, as described with the four clusters in chapter 4.4, IRF4 can regulate the expression levels of other proteins during the development of cells (cluster I), development and function (cluster II), or function alone (clusters III and IV). It can influence other proteins by down-regulating or suppressing their expression levels and therefore their function during the development and/or in the differentiated cells or, in the opposite direction, IRF4 can enhance or prevent the down-regulation of other proteins. A major effect of IRF4 on other proteins was seen during the development of cells (cluster I), whereas most proteins had an elevated expression in the differentiated cells only when IRF4 was absent (e.g. for Th17 cells: 546 proteins uniquely elevated on D3 in the absence of IRF4 vs 236 proteins only elevated on D3 in the presence of IRF4), indicating that IRF4 normally negatively affects their expression levels. Treg-characteristics, e.g. IRF8, CD25 (IL-2RA) and FoxP3, were only up-regulated in Th17 cells when IRF4 was absent. In Treg cells, IRF4 has been reported to have a regulatory role on the expression levels of its master transcription factor, as described in the literature (in cooperation with BATF3). Mechanistically, the authors demonstrated that AMPKα and TET enzymes demethylate CNS2 enhancer, which consequently enhances FoxP3 expression (Alvisi et al., 2020).

GO analysis of differentially expressed (up-regulated) proteins showed that IRF4 seems to have a role in cell cycle, protein localization and post-translational protein modifications particularly in Treg cells, whereas terms assigned to signal transduction or amplification as well as gene expression (transcription) were only enriched in Th17 cells. Proteins associated with protein acetylation, acetyltransferase complex, chromatin organization or histone modifications were only down-regulated in the presence of IRF4. This could suggest that epigenetic regulation, such as post-translational modifications or chromatin remodelling mediated by acetylation of methylation (Ma et al., 2011), steered by IRF4 takes place at an early time point of cell polarization rather than in fully differentiated cells. Interestingly, protein acetylation not only influences protein folding or stability, but also protein-protein interactions (Drazic et al., 2016). The phosphorylation status of a protein is also an important switch in controlling a protein's activity or interaction with other proteins (LILLO et al., 2014). In the absence of IRF4, enzyme binding, TCR signalling and MAP kinase activation were dysregulated. Moreover, glycolysis, oxidative phosphorylation and the metabolism of RNA and proteins was influenced by the presence or absence of IRF4. In line with this observation, it has been described that glycolysis, which is regulated by BATF3 and IRF4 in Treg cells, influences the expression and stability of FoxP3 (Arnold et al., 2022).

5.5 Integrated IRF4 studies

Integration of IRF4 interactome, IRF4-ChIP-seq and *Irf4*$^{-/-}$ analysis revealed that the expression of many proteins, including IRF4 interactors, were regulated by IRF4 itself. The finding that transcription factors regulate the expression of its own partnering proteins was also described in a study by the Rudensky lab (Rudra et al., 2012). This publication revealed that 50 % of FoxP3's associated proteins were also transcriptionally controlled by FoxP3 as interactome and FoxP3-ChIP-seq analysis demonstrated.

Enriched GO analysis of genes and proteins that were controlled by IRF4 revealed that IRF4 was involved in steering metabolic processes in Th17 and Treg cells. Both subsets rely, of course, on metabolism to fuel their metabolic needs, but Th17 and Treg cells are described to use different metabolic pathways for it: While Th17 cells mainly use glycolysis, glutaminolysis and pentose-phosphate anabolic pathways, Treg cells largely rely on fatty acid oxidation and oxidative phosphorylation (OXPHOS) (Beier et al., 2015; Papadopoulou & Xanthou, 2022; Shin et al., 2020). Interestingly, it is reported that metabolites are involved in immune signalling and the regulation of immune cell differentiation. Therefore, targeting the metabolism of cells could be used as a therapeutic intervention to influence the generation and function of particular cell types (Beier et al., 2015). Aerobic glycolysis is important for shaping Th17 cell fate, including cell plasticity. Additionally, secretion of pro-inflammatory cytokines as well as other effector functions or needs for proliferating cells is regulated by this metabolic pathway (Chang et al., 2013; Papadopoulou & Xanthou, 2022). Upon activation of Th17 cells, a mTORC1-induced activation of different transcription factor, e.g. c-Myc or HIF-1α, regulates the expression of glycolytic genes, such as the glucose transporter *Glut1*, hexokinase 2 *Hk2*, pyruvate kinase *Pkm* or L-lactate dehydrogenase A *Ldha* (Papadopoulou & Xanthou, 2022; Shin et al., 2020). Myc and HIF-1α not only induce glycolysis but also inhibit FoxP3 transcription

(Pollizzi & Powell, 2014; Shin et al., 2020). Elevated levels of GLUT1 were detected in Th17 cells from patients suffering from the primary Sjögren's syndrome and genes associated with Myc targets, mTORC1 signalling and glycolysis were enriched (Xiao et al., 2022). In line with these findings, the absence of a mTORC1 activator or the inhibition of glycolytic enzymes prevented the differentiation of Th17 cells and secretion of pro-inflammatory cytokines (Papadopoulou & Xanthou, 2022). Different publications reported that Th17-mediated diseases were prevented when glycolysis or glucose metabolism were interrupted (Araujo et al., 2017; Gerriets et al., 2015; T. Xu et al., 2017). An IRF4-dependent regulation of proteins and genes associated with glycolysis and glucose metabolism, e.g. the expression of the glucose transporter GLUT3 (*Slc2a3*), alpha-enolase (*Eno1*), ATP-dependent 6-phosphofructokinases (*Pfkm*, *Pfkl*, *Pfkp*), hexokinase 3 (*Hk3*) or the pyruvate kinase PKM (*Pkm*) was seen in Th17 cells in this thesis, too. A link between glycolysis and IRF4 was also described in different publications, which aligns the experimental data with literature: Angiari and colleagues described that the inhibition of the glycolytic enzyme pyruvate kinase muscle isozyme 2, short PKM2, resulted in a reduced expression of the *Irf4* gene (Angiari et al., 2020) while Xio et al. reported a decrease of key glycolytic genes, including *Slc2a1*, and a reduced uptake of glucose due to a lower expression of GLUT1 transporters in the absence of IRF4 (Xiao et al., 2022). Also for other T cell subsets, an involvement of IRF4 in metabolic programming was described. Arnold et al. described for example a IRF4-BATF3-mediated glycolytic reprogramming of activated Treg cells (Arnold et al., 2022), while Man et al. reported an IRF4-regulated expression of key molecules of aerobic glycolysis in $CD8^+$ T cells (Man et al., 2013) and Mahnke and colleagues published an involvement of IRF4 in the metabolism of Th1 cells, shown by a diminished uptake of glucose, limited oxidative phosphorylation and reduced aerobic glycolysis in the absence of IRF4 (Mahnke et al., 2016).

In addition to glycolytic genes and proteins which expression is IRF4-steered, experimental data from this thesis demonstrated that particular in Th17 cells IRF4 influenced also the expression of OXPHOS-associated proteins. The mitochondrial transcription elongation factor TEFM for example is not only important for general mitochondrial functions but also specifically for OXPHOS (Jiang et al., 2019). TEFM was significantly up-regulated in the experimental data from *Irf4*$^{-/-}$ Th17 cells of this thesis compared to the littermate control. An IRF4-steered expression of OXPHOS genes was reported in B cells although in this context, IRF4 promoted the expression of OXPHOS (Patterson et al., 2021). A positive effect on oxidative metabolism by IRF4 was seen in Th1 cells, too (Kratchmarov et al., 2017). In Th17 cells, Shin et al. reported significantly higher *Irf4* mRNA level when the cells were treated with a OXPHOS inhibitor and demonstrated a BATF-mediated essential role of OXPHOS "for early molecular events associated with Th17 development" (Shin et al., 2020). No reciprocal regulation of IRF4 on OXPHOS is reported so far in any immune cells. Combination of experimental data with the finding from literature could therefore allow the hypothesis that the expression levels of IRF4 either induce a metabolic switch from OXPHOS at early time points to glycolysis in fully differentiated Th17 cells or IRF4 fine-tunes expression pattern for optimal metabolic needs.

In addition to metabolic pathways, experimental data from this thesis demonstrated that in Th17 cells IRF4 regulated cell cycle on DNA and protein level, e.g. the cyclin-dependent kinase 1, CDK1, or the G2/mitotic-specific cyclin-B1. In literature, a close relationship between metabolism and cell cycle

could be found: The publication by Shin and colleagues reported that upon OXPHOS inhibition, Th17 cells showed an reduced proliferation and cell-cycle-associated events were among the most regulated pathways when the metabolic pathway was disturbed (Shin et al., 2020). In B cells, a direct link between IRF4 and cell cycle was described, too, where IRF4-deficient B cells had an aberrant cell cycle (Patterson et al., 2021). In myeloma cells with IRF4 overexpression, a targeted inhibition of IRF4 resulted in cell cycle arrest, a reduced survival of myeloma cells and improved survival rates in a pre-clinical xenograft model (Mondala et al., 2021).

As mentioned above, experimental data of this thesis demonstrated that IRF4 regulated also the expression of its own interactors on DNA and protein level, e.g. SATB1, RORγT or ETV6 in Th17 cells or STAT1 or TCEA1 in Treg cells.

The DNA-binding protein special AT-rich sequence binding protein 1 (SABT1) was, as mentioned earlier, reported in a recent, large-scale interaction study of HEK293 cells as an IRF4 interaction partner shown by BioID and affinity purification coupled with mass spectrometric analysis (Göös et al., 2022). However, no IRF4-SATB1 interaction has yet been reported in primary cells or *in vivo* studies. SATB1 is known to bind to matrix attachment DNA regions (MAR), which are involved in rearrangement of chromatin structure and gene regulation, additionally, by recruiting and interacting with other chromatin-remodelling complexes at genomic region. It is therefore also referred to as the "landing platform for chromatin-remodelling factors" (S. Cai et al., 2003). Its expression is mainly restricted to the T cell lineage and crucial in the early stages of thymocyte development as well as development of nTreg cells in the thymus (Alvarez et al., 2000; S. Cai et al., 2003; Krangel, 2007; Yasuda et al., 2019). Although SATB1 was originally thought to predominantly act as a transcriptional repressor, it could be shown that in Th2 cells, SATB1 is important in inducing the characteristic Th2 cytokines IL-4, IL-5 and IL-13 (S. Cai et al., 2006). Also for Th17 cells, SATB1 has been described to have a crucial role in development and function, which was critically influenced by environmental cues. *In vitro* differentiated Th17 cells showed reduced levels of IL-17 in the absence of SATB1 (Ciofani et al., 2012). Another study demonstrated that in $SATB1^+$ cell lines, genes that induce and enhance Th17 differentiation, e.g. *Il6*, *Stat3*, *Irf4*, *Rorc*, *Il17a/f* and *Il22*, were elevated compared to $SATB1^-$ cell lines (J. Sun et al., 2018). Additionally, genes that would antagonize Th17 cell development were negatively regulated by SATB1. In the same publication, human skin samples from $SATB1^+$ $CD30^+$ lymphoproliferative disorder patients confirmed the observation of SATB1's influence on Th17 characteristics (J. Sun et al., 2018). Köhne and colleagues reported a positive effect of SATB1 on the proliferation of Th17 while its absence promoted the development of iTreg cells. Furthermore, the author demonstrated that *Satb1*$^{-/-}$ animals were protected from developing EAE or colitis (Köhne, 2021). In line with these findings, Duguet and colleagues reported also that a down-regulation of SATB1 was important for the Treg phenotype (Duguet et al., 2017), indicating that SATB1 is involved in Th17-Treg balance. A previous study reported an involvement in the pathogenic effector function in EAE, as shown by elevated levels of IL-17 and GM-CSF in inflamed tissue (Yasuda et al., 2019). In Th2 cells, ChIP-seq data revealed co-binding of SATB1 and IRF4 at Th2 cytokine loci and co-immunoprecipitation additionally demonstrated a physical association (Hwang et al., 2017; Jang & Lee, 2018). A similar mode of interaction for SATB1 and IRF4 at Th17-critical gene loci could be proposed in

Th17 cells, especially as IRF4-ChIP-seq data from this thesis revealed a close proximity of SATB1 and IRF4 binding motifs, also in genes involved in IL-17 signalling.

Experimental data in this thesis demonstrated that the expression of RORγT is regulated by IRF4. This is in line with publications by Brüstel at al. and Mudter et al., where reduced levels of Th17's master transcription factor were detected in *Irf4*$^{-/-}$ studies (Brüstle et al., 2007; Mudter et al., 2008, 2011). Interestingly, studies with a conditional knockout of the *Rorc* gene have shown that RORγT is important for maintaining Th17 cell fate, but not for inducing Th17-mediated diseases (Brucklacher-Waldert et al., 2016; Hall et al., 2022). Inhibition or deletion of RORγT suppressed the production of IL-17 and delayed onset and severity of EAE (Awasthi & Kuchroo, 2009; Huh & Littman, 2012; Kumar et al., 2012). As mentioned above (see chapter 5.3), RORγT-ChIP-seq data revealed RORγT binding at Th17 critical loci (He et al., 2017), where IRF4 binding could also be detected in the IRF4-ChIP-seq data from this thesis. In addition, Ciofani et al. reported a co-localization of IRF4 and RORγT at gene regions important for Th17 cells (Ciofani et al., 2012). These publications align and corroborate the experimental determined IRF4-RORγT interaction.

The transcription factor ETV6, which was identified as an Th17-enriched IRF4 interactor, was demonstrated to be on DNA and protein level regulated by IRF4. Although ETV6 is described as a "strong transcriptional repressor" (De Braekeleer et al., 2012), for Th17 cells a positive role has been reported in different publications: Forced overexpression led to elevated levels of IL-17^{+} cells, which was in line with siRNA-mediated knockdown that resulted in reduced levels of RORγT, IL-23R, IL-17 and IL-22 in the absence of ETV6 (Ciofani et al., 2012; De Braekeleer et al., 2012; M. Liu et al., 2016). A recent study with HEK293T cells demonstrated that ETV6 influences IRF4's binding capacity at ISRE sites and consequently changes the transcriptional programme mediated by IRF4 (Thouenon et al., 2023). The positive influence of ETV6 for the Th17 lineage aligns and brings the reported findings together with the experimental data of IRF4. Interactome data of this thesis reported additionally an interaction of the two transcription factors. Further details on the interaction have to be investigated, but a concerted role in the expression of effector molecules can be speculated as both transcription factor are involved in the expression of Th17-associated cytokines for example.

Interestingly, experimental data of this thesis demonstrated that IRF4 not only positively regulates the expression of particular IRF4 interactors supporting a particular cell fate, as described above, but also negatively influences the expression of IRF4 interactors of other, opposing cell types. An example is the Treg-enriched IRF4 interactor IRF8, which was negatively regulated by IRF4 in Th17 cells. As stated already above, IRF8 is described to have a critical role in antagonizing Th17 cell development by interacting with RORγT at an enhancer structure downstream of the *Il17* gene (CNS2), which in the end inhibits IL-17 production (Kurebayashi et al., 2013; Ouyang et al., 2011). *In vitro* polarized Th17 cells showed higher expression of IL-17 and IL-22 in the absence of IRF8 compared with wildtype controls and *Rag*-deficient animals reconstituted with *Irf8*$^{-/-}$ T cells developed severe symptoms in an experimental colitis model (Ouyang et al., 2011). In a study by Ouyang and colleagues, it was shown that IRF8 was induced by TGF-β and TCR signalling, which aligns and matches with IRF8 in the Treg

context (Ouyang et al., 2011). A role of IRF4 in the expression of IRF8 has not yet been reported by literature, but was revealed by the data from this thesis.

Another Treg-enriched IRF4 interactor, which expression was negatively regulated by IRF4 in Th17 cells was the serine/threonine-protein phosphatase 6 regulatory subunit 1 (PP6R1). The protein phosphatase 6 (PP6) is known to regulate FoxP3 expression and Treg cell differentiation as well as stability (W. Cai et al., 2022). A conditional knockout of the enzyme in Treg cells resulted in decreased FoxP3 levels, impaired suppressive function and development of spontaneous auto-inflammation, which was mediated by increased methylation of CpG motifs in the FoxP3 locus and in the end resulted in decreased levels of *Foxp3* mRNA and protein. Data from flow cytometry and ELISA demonstrated that the inflammation was mainly driven by Th17 cells as shown by more Th17 cells in the spleen of *Ppp6r1*$^{-/-}$ animals and elevated IL-17A levels in the plasma of *Ppp6r1*$^{-/-}$ animals (W. Cai et al., 2022). In the study, the authors did not specify the different subunits of protein phosphatase 6, e.g. whether only the catalytic subunit was involved or whether a regulatory subunit had to be assembled and a whole holoenzyme was needed for those observations (Ziembik et al., 2017). However as in humans PP6 is always associated with a regulatory subunit, PP6R1-PP6R3 (LILLO et al., 2014), an involvement of the regulatory subunit could be plausible. As a Treg-promoting protein, it would be consistent that PP6R1 is negatively regulated in Th17 cells, which, as the data from this thesis demonstrated, could be IRF4 mediated. No IRF4-PP6R1 connection or interaction has yet been described in literature and therefore further research is required to understand details on that.

The Th17-enriched IRF4 interactor Runt-related transcription factor 1, short Runx1, was IRF4-mediated downregulated in Treg cells from WT animals as shown in the proteome analysis from *Irf4*$^{-/-}$ and littermate animals in this thesis. Runx proteins play a role in diverse biological processes, such as cell proliferation, apoptosis, differentiation and lineage determination, and Runx1 is particularly important for the differentiation of hematopoietic cells (Lin, 2022). A positive effect of Runx1 on RORγT expression and subsequent Th17 proliferation is described in literature by Lazarevic and colleagues. The expression of Runx1 is induced by TCR stimulation in the presence of TGF-β and IL-6. Runx1 binds 2 kb upstream of *Rorc* exon 1, transactivates its transcription and, in complex with RORγT, induces the expression of *Il17a* and *Il17f* (Lazarevic et al., 2011; H. Liu et al., 2015; Zhou & Littman, 2009). Interestingly, the Runx motif was the most enriched non-AP1 motif bound by IRF4 in Treg cells (Arnold et al., 2022), which could indicate that in Treg cells, IRF4 prevents the binding of Runx1 at the genome level and consequently the induction of the Th17 cell fate.

Interestingly, in the data of this thesis the mucosa-associated lymphoid tissue lymphoma translocation protein 1 (MALT1) was on DNA and protein level IRF4-dependent significantly elevated in fully differentiated Treg cells, although it is well known to be important for the differentiation and the encephalitogenic potential of Th17 cells, shown by *Malt1*$^{-/-}$ animals that were resistant to EAE (Brüstle et al., 2012; J. J. Cho et al., 2019). Experimental data of this thesis support this important role for Th17 cell as a higher expression of MALT1 was determined in Th17 cells compared to Treg cells and IRF4-ChIP-seq data revealed an IRF4-dependent enhanced expression of *Malt1* in Th17 cells. Nevertheless, a significant but dual role of MALT1 for Treg cells has been described in literature, too (Brüstle et al.,

2017; Demeyer et al., 2019; Jaworski & Thome, 2016): In the thymus, MALT1 promotes the generation of nTreg cells while in the periphery MALT1 suppressed the generation of iTreg cells and controls the threshold for Treg induction. Therefore the authors termed MALT1 a "gatekeeper for iTreg induction" (Brüstle et al., 2017). Another publication agreed on the MALT1-dependent generation of nTreg cells, however described the differentiation of naïve $CD4^+$ T cells to iTreg cells to be MALT1 independent (Jaworski & Thome, 2016). Although the role of MALT1 on formation of iTreg cells may not be fully understood, several studies reported that the enzymatic activity of the paracaspase MALT1 is crucial for the effector functions of Treg cells. Protease deficient animals developed spontaneous multiorgan inflammation arising not only from decreased numbers of Treg cells but also from reduced immunosuppressive functions (Bornancin et al., 2015; Jaworski et al., 2014). In line with this, Demeyer and colleagues demonstrated that *Malt1*$^{-/-}$ animals expressed less CTLA-4, a surface marker critical to Treg's inhibitory function, compared to their controls (Demeyer et al., 2019). As IRF4 contributes to the effector functions in Treg cells as well (Cretney et al., 2011; Veldhoen, 2010; Zheng et al., 2007, 2009), it can be hypothesized that IRF4 induces the expression of MALT1 to support Treg's effector functions. A publication by Brüstle et al. implied that MALT1 had rather an effect on the effector functions of Th17 cells than on its development as *Malt1*$^{-/-}$ animals had no reduced *Irf4, Rorc* or *Rora* expression compared to their wildtype control (Brüstle et al., 2012). In line with this, Jeltsch and colleagues reported that MALT1 stabilizes mRNA transcripts of Th17-promoting factors including IL-6, ICOS and IRF4 by cleaving the E3 ubiquitin ligase Roquin-1, which promotes mRNA degradation (Jeltsch et al., 2014). Data from this thesis further demonstrated that IRF4 and MALT1 form complexes that might regulate Th17 effector functions and/or the development of pro-inflammatory T cells.

In summary, the combined analysis of the IRF4 interactome with *Irf4*$^{-/-}$ analysis and IRF4-ChIP-seq revealed that IRF4 regulated cell type specific important cellular processes, such as metabolism or cell cycle, and also the expression of its own interacting proteins. In addition, IRF4 not only enhances the expression of subset-characteristic genes as well as stabilizes or recruits cell fate-favouring proteins, but also represses the expression of genes that negatively influence the development of a particular cell type.

5.6 Summary and outlook

In this thesis, an improved IRF4 pulldown protocol was established in fully differentiated Th17 and Treg cells, which could not only reproduce and confirm previously published IRF4 interactions but also revealed new, previously undescribed IRF4 interacting proteins. Beside transcription factor, many histone modifying and chromatin/chromatin-binding, or -regulatory proteins were detected in the interactome. This highlights that IRF4 not only acts as a transcriptional regulator by binding directly to open chromatin structures but also acts as an epigenetic ruler by remodelling chromatin structures to open or close gene loci. Protein modifying enzymes as interacting protein imply that IRF4 has a role in post-translational modifications as well. Additionally, the involvement of IRF4 in metabolism was demonstrated. These findings were demonstrated at different levels (IRF4 interactome, proteome, IRF4-ChIP-seq and I*rf4*$^{-/-}$ analysis). In addition, data from this thesis revealed that IRF4 regulated also

the expression of its own interactors. IRF4-ChIP-seq analysis unravelled IRF4 binding in the promoter and enhancer regions of genes coding for IRF4 interacting proteins. *Irf4*$^{-/-}$ analysis demonstrated on protein level the influence of IRF4 on the expression of other proteins, of which some were also at DNA level steered by IRF4. Motif analysis of the immunoprecipitated DNA fragments matched with proteins identified by pulldown analysis. Combined motif analysis demonstrated a close proximity of motifs mapping with interactors, which further confirms and supports the results from the IRF4 interactome analysis.

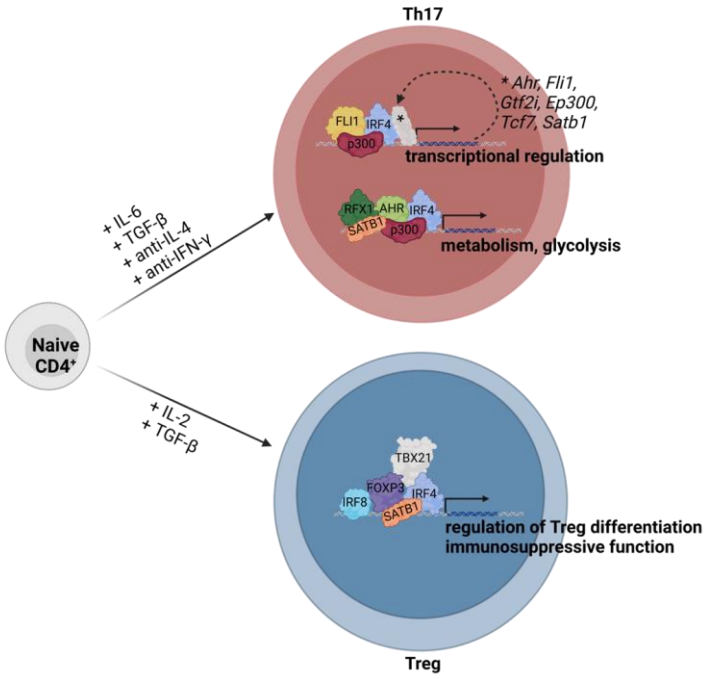

Figure 27: Graphical summary. In this thesis pro-inflammatory Th17 cells and anti-inflammatory Treg cells were generated from naïve CD4$^+$ T cells by the addition of polarizing cytokines. IRF4 interactome analysis revealed not only previously described, but also newly identified interacting proteins, of which some were subtype specific. In Th17 cells, IRF4 and its interactors were involved in the transcription of genes coding for transcriptional regulators, but also for genes involved in metabolism and glycolysis. Interestingly, some IRF4 interactors demonstrated a self-regulatory feedback loop. In Treg cells, IRF4 complexes mainly steered the expression of genes participating in the regulation of Treg differentiation and its immunosuppressive function.

The direct comparison of pro-inflammatory Th17 and anti-inflammatory Treg cells revealed some interplayers that are specifically important for one or the other cell subset. Especially in Th17 cells, many IRF4 partners were detected, highlighting an important role of IRF4 in the pro-inflammatory cell type. Additionally, a core T cell interactome was determined, which was identified in both cell types. Not all 440 IRF4 partners could be addressed and discussed here, but nevertheless many examples demonstrated a matching cellular context and/or could link IRF4 to a particular molecular setting. The *Irf4*$^{-/-}$ analysis demonstrated that in the absence of this transcription factor, Th17 cells gained the expression of Treg characteristics, which supports a critical role of IRF4 in Th17/Treg plasticity. Some IRF4 interactors have also been described to be involved in Th17/Treg balance or, in its absence, contributed to the development of the opposing cell type, which links them to the role of IRF4 in these two cell types.

To further validate IRF4 interaction partners and mechanistically understand the association between them, additional experiments are needed. Inhibition or siRNA-mediated knockout of IRF4 interactors can reveal *in vitro* its influence and important influence in the development of Th17 or Treg cells and particularly demonstrate a potential role in the balance of T cell subsets. FACS analysis would be an easy and fast read-out technique for investigating that question. Western blot analysis for example can verify the inhibition/knockout of a particular protein. The global downstream effects of an inhibition or knockout can be further elucidated by transcriptome analysis on mRNA level or mass-spectrometric analysis of the proteome on protein level. Selected key cellular targets could also be investigated by FACS (protein level) or qPCR (mRNA level).

In this study, immunoprecipitation was used as an unbiased method for determining protein interactions. Motif analysis from IRF4-ChIP-seq analysis, especially those in close proximity to each other, further supported and validated the experimental data for DNA-binding transcription factors. Electrophoretic mobility-shift assays (EMSA) or mutagenesis studies can provide further information on protein-DNA interactions and DNA-binding motifs. Additionally, publicly available ChIP-seq datasets from IRF4 interactors could be used to check for co-binding of these proteins at particular gene locations and therefore corroborate and validate the experimental findings of this thesis.

As IRF4 is involved in the effector function of Treg cells, the knockout/inhibition of IRF4 partners and a subsequent suppression assay would be one way to investigate its role in this regard. To validate and translate *in vitro*-gained knowledge in the biological system, *in vivo* studies using for example EAE or other inflammatory models could be used. Such experiments would be especially interesting for proteins detected in the Th17-enriched IRF4 interactome.

Although this study unravelled the influence of IRF4 in fully differentiated Th17 and Treg cells at different levels, kinetics of T cell polarization or the investigation at an earlier time point during cell development, e.g. 12 h or 24 h after T cell induction, could give more details on which proteins are the driver for a particular cell type and contribute in complex with IRF4 to the development of pro- or anti-inflammatory cell programmes.

VI. ABSTRACT

T helper 17 cells (Th17) are pro-inflammatory cells that induce immune responses to fight invading pathogens, but are also involved in the development of autoimmune diseases. On the other hand, regulatory T cells (Tregs) are anti-inflammatory cells that down-regulate/prevent effector functions and contribute to peripheral tolerance. In recent years, it has become evident that Th17 and Treg cells are dependent on interferon regulatory factor 4 (IRF4) for their development and/or effector functions: in the absence of IRF4, cells fail to differentiate into IL-17-producing Th17 cells and Treg cells have impaired effector functions. However, the molecular mechanisms in IRF4-steered T cell determination are not fully understood.

To investigate the role of IRF4 in the development of these two opposing cell types, an unbiased approach was used to directly compare both subsets on DNA and protein level. Genome-wide binding of IRF4 was elucidated by chromatin immunoprecipitation followed by deep sequencing (ChIP-seq). To unravel the effects of IRF4 on protein level, the proteome of *Irf4*$^{-/-}$ animals was compared to littermate controls. The cell type specific IRF4 interactome was analysed by mass-spectrometry to determine which proteins act together with IRF4 to promote Th17 or Treg phenotype. By integrating aforementioned studies, further information on the molecular mechanisms was gained. A total of 440 IRF4-interacting proteins were identified in the interactome analysis of Th17 and Treg cells, including proteins that were found in both subsets ('core' interactome) as well as cell type-specific interactors. Among the IRF4 interactors, chromatin/chromatin-binding, or -regulatory proteins including members of the NuRD and SWI/SNF complex, protein modifying enzymes, metabolic proteins and DNA-binding transcription factors were found. Some IRF4 interactors were already described in literature to interact with IRF4, but also novel, not yet described IRF4 partners in general or particular in the Th17/Treg context were identified. IRF4-ChIP-seq analysis demonstrated that many IRF4 partners, particularly in Th17 cells, were also positively regulated by IRF4 on DNA level as IRF4 binding was determined in the promoter regions of the respective genes. On the other hand, genes involved in the development of the opposing cell type were silenced by IRF4. Furthermore, in immunoprecipitated DNA fragments, the motifs of 18 IRF4 partners, including IRF4, were identified, e.g. BACH2, JunB, STAT3 and EP300. Combined motif analysis revealed that many motifs were found in proximity to each other, corroborating a physical interaction. Data from *Irf4*$^{-/-}$ analysis confirmed published findings that Th17 cells fail to differentiate into IL-17-producing T cells in the absence of IRF4 while Treg cells develop into FoxP3^{+} CD25^{+} T cells. Experimental data from this thesis revealed even significantly higher levels of FoxP3 in Treg cells derived from *Irf4*$^{-/-}$ animals. Additionally, Th17 cells form *Irf4*$^{-/-}$ animals display a Treg-like phenotype by expressing markers of Treg cells such as FoxP3, IRF8 and CTLA4.

The results from the IRF4 interactome reveal not only novel IRF4 interactors but also provide in combination with IRF4-ChIP-seq and *Irf4*$^{-/-}$ analysis new insights into subtype-specific, IRF4-mediated molecular mechanisms of Th17 and Treg cells. Additionally, this data serves as a rich source for further investigations, which can in the future also be translated in therapeutic approaches.

VII. ZUSAMMENFASSUNG

T Helfer 17-Zellen (Th17) sind pro-inflammatorische Zellen, die Immunreaktionen auslösen, aber auch an der Entstehung von Autoimmunerkrankungen beteiligt sind. Regulatorische T-Zellen (Treg) hingegen sind anti-inflammatorische Zellen, die Effektor Funktionen herunterregulieren bzw. verhindern und zur peripheren Toleranz beitragen. In den letzten Jahren wurde deutlich, dass Th17- und Treg-Zellen für ihre Entwicklung und/oder Effektor-Funktionen *Interferon Regulatory Factor 4* (IRF4) benötigen: In Abwesenheit von IRF4 differenzieren Zellen nicht in IL-17$^+$ Th17-Zellen und Treg-Zellen haben eingeschränkte Effektor Funktionen. Die molekularen Mechanismen, die zu IRF4-gesteuerten T-Zellentwicklung beitragen, sind jedoch noch nicht vollständig geklärt.

Um die Rolle von IRF4 für die Th17- und Treg-Entwicklung zu untersuchen, wurde ein unvoreingenommener Ansatz gewählt, der beide Zelltypen auf DNA- und Proteinebene vergleicht. Die genomweite Bindung von IRF4 wurde mittels Chromatin-Immunpräzipitation (ChIP-seq) untersucht. Zur Bestimmung des Einflusses von IRF4 auf Proteinebene, wurde das Proteom von *Irf4*$^{-/-}$ und WT-Tieren verglichen. Um herauszufinden welche Proteine mit IRF4 zusammenwirken, um einen Th17- oder Treg-Phänotyp hervorzurufen, wurde das zelltypspezifische IRF4 Interaktom mittels Massenspektrometrie analysiert. Durch die Integration eben genannter Analysen konnten weitere Informationen über molekulare Mechanismen gewonnen werden. Die Interaktomanalyse ergab insgesamt 440 IRF4-interagierende Proteine, von denen einige in beiden Zelltypen ("Kern"-Interaktom) gefunden wurden, andere nur in einem Zelltypen. Unter den Interaktoren befanden sich Chromatin/Chromatin-bindende oder -regulierende Proteine, u.a. Mitglieder des NuRD- und SWI/SNF-Komplexes, proteinmodifizierende Enzyme, Stoffwechselproteine sowie DNA-bindende Transkriptionsfaktoren. Ein paar Proteine waren bereits als IRF4 interagierende Proteine beschrieben, aber auch neue, bisher noch nicht beschriebene IRF4 Interaktoren im Allgemeinen oder speziell im Th17 bzw. Treg Kontext wurden identifiziert. Die IRF4-ChIP-seq Analyse zeigte, dass viele IRF4-Partner, insbesondere in Th17 Zellen, ebenfalls positiv von IRF4 reguliert wurden, da IRF4 in der Promotorregion des entsprechenden Gens band. Andererseits wurden Gene, die an der Entwicklung des gegensätzlichen Zelltyps beteiligt sind, durch IRF4 unterdrückt. In den immunpräzipitierten DNA-Fragmenten wurden Motive von 18 IRF4-Partnern, einschließlich IRF4, identifiziert, bspw. von BACH2, JunB, STAT3 oder EP300. Eine kombinierte Motivanalyse ergab, dass viele Motive in unmittelbarer Nähe zueinander lagen, was eine physikalische Interaktion bekräftigt. Daten der *Irf4*$^{-/-}$ Analyse bestätigten die bereits veröffentlichten Ergebnisse, dass Th17 in Abwesenheit von IRF4 nicht in IL-17-produzierende Th17-Zellen differenzieren, während Treg-Zellen in FoxP3$^+$ CD25$^+$ T-Zellen polarisieren. Experimentelle Daten dieser Arbeit zeigten sogar eine signifikant höhere FoxP3 Expression. Des Weiteren bildeten Th17-Zellen aus *Irf4*$^{-/-}$ Tieren einen Treg-ähnlichen Phänotyp aus, indem sie Marker, die für regulatorische T-Zellen charakteristisch sind, z.B. FoxP3, IRF8 oder CTLA4, exprimierten.

Ergebnisse des IRF4 Interaktoms offenbarten nicht nur neue IRF4 Interaktoren, sondern lieferten in Kombination mit IRF4-ChIP-seq und *Irf4*$^{-/-}$ Analyse neue Erkenntnisse über spezifische, IRF4-vermittelte molekulare Mechanismen in Th17 und Treg Zellen. Zudem dienen die Daten als reichhaltige Quelle für weitere Untersuchungen, die in Zukunft auch für therapeutische Ansätze genutzt werden können.

VIII. LITERATURE

Abu-Elheiga, L., Brinkley, W. R., Zhong, L., Chirala, S. S., Woldegiorgis, G., & Wakil, S. J. (2000). The subcellular localization of acetyl-CoA carboxylase 2. *Proceedings of the National Academy of Sciences*, *97*(4), 1444–1449. https://doi.org/10.1073/pnas.97.4.1444

Allan, S. E. (2005). The role of 2 FOXP3 isoforms in the generation of human CD4+ Tregs. *Journal of Clinical Investigation*, *115*(11), 3276–3284. https://doi.org/10.1172/JCI24685

Alvarez, J. D., Yasui, D. H., Niida, H., Joh, T., Loh, D. Y., & Kohwi-Shigematsu, T. (2000). The MAR-binding protein SATB1 orchestrates temporal and spatial expression of multiple genes during T-cell development. *Genes & Development*, *14*(5), 521–535. https://doi.org/10.1101/gad.14.5.521

Alvisi, G., Brummelman, J., Puccio, S., Mazza, E. M. C., Tomada, E. P., Losurdo, A., Zanon, V., Peano, C., Colombo, F. S., Scarpa, A., Alloisio, M., Vasanthakumar, A., Roychoudhuri, R., Kallikourdis, M., Pagani, M., Lopci, E., Novellis, P., Blume, J., Kallies, A., … Lugli, E. (2020). IRF4 instructs effector Treg differentiation and immune suppression in human cancer. *Journal of Clinical Investigation*, *130*(6), 3137–3150. https://doi.org/10.1172/JCI130426

Angiari, S., Runtsch, M. C., Sutton, C. E., Palsson-McDermott, E. M., Kelly, B., Rana, N., Kane, H., Papadopoulou, G., Pearce, E. L., Mills, K. H. G., & O'Neill, L. A. J. (2020). Pharmacological Activation of Pyruvate Kinase M2 Inhibits CD4+ T Cell Pathogenicity and Suppresses Autoimmunity. *Cell Metabolism*, *31*(2), 391-405.e8. https://doi.org/10.1016/j.cmet.2019.10.015

Araujo, L., Khim, P., Mkhikian, H., Mortales, C.-L., & Demetriou, M. (2017). Glycolysis and glutaminolysis cooperatively control T cell function by limiting metabolite supply to N-glycosylation. *ELife*, *6*. https://doi.org/10.7554/eLife.21330

Arnold, P. R., Wen, M., Zhang, L., Ying, Y., Xiao, X., Chu, X., Wang, G., Zhang, X., Mao, Z., Zhang, A., Hamilton, D. J., Chen, W., & Li, X. C. (2022). Suppression of FOXP3 expression by the AP-1 family transcription factor BATF3 requires partnering with IRF4. *Frontiers in Immunology*, *13*. https://doi.org/10.3389/fimmu.2022.966364

Ashburner, M., Ball, C. A., Blake, J. A., Botstein, D., Butler, H., Cherry, J. M., Davis, A. P., Dolinski, K., Dwight, S. S., Eppig, J. T., Harris, M. A., Hill, D. P., Issel-Tarver, L., Kasarskis, A., Lewis, S., Matese, J. C., Richardson, J. E., Ringwald, M., Rubin, G. M., & Sherlock, G. (2000). Gene Ontology: tool for the unification of biology. *Nature Genetics*, *25*(1), 25–29. https://doi.org/10.1038/75556

Avram, D., & Califano, D. (2014). The Multifaceted Roles of Bcl11b in Thymic and Peripheral T Cells: Impact on Immune Diseases. *The Journal of Immunology*, *193*(5), 2059–2065. https://doi.org/10.4049/jimmunol.1400930

Awasthi, A., & Kuchroo, V. K. (2009). Th17 cells: from precursors to players in inflammation and infection. *International Immunology*, *21*(5), 489–498. https://doi.org/10.1093/intimm/dxp021

Bafrani, H. H., Ahmadi, M., Jahantigh, D., & Karimian, M. (2019). Association analysis of the common varieties of *IL17A* and *IL17F* genes with the risk of knee osteoarthritis. *Journal of Cellular Biochemistry*, *120*(10), 18020–18030. https://doi.org/10.1002/jcb.29105

Bailey, S. R., Nelson, M. H., Himes, R. A., Li, Z., Mehrotra, S., & Paulos, C. M. (2014). Th17 Cells in Cancer: The Ultimate Identity Crisis. *Frontiers in Immunology*, *5*. https://doi.org/10.3389/fimmu.2014.00276

Bailey, T. L., Boden, M., Buske, F. A., Frith, M., Grant, C. E., Clementi, L., Ren, J., Li, W. W., & Noble, W. S. (2009). MEME SUITE: tools for motif discovery and searching. *Nucleic Acids Research*, *37*(Web Server), W202–W208. https://doi.org/10.1093/nar/gkp335

Bandini, C., Pupuleku, A., Spaccarotella, E., Pellegrino, E., Wang, R., Vitale, N., Duval, C., Cantarella, D., Rinaldi, A., Provero, P., Di Cunto, F., Medico, E., Bertoni, F., Inghirami, G., & Piva, R. (2018). IRF4 Mediates the Oncogenic Effects of STAT3 in Anaplastic Large Cell Lymphomas. *Cancers*, *10*(1), 21. https://doi.org/10.3390/cancers10010021

Banuelos, J., Cao, Y., Shin, S. C., & Lu, N. Z. (2017). Immunopathology alters Th17 cell glucocorticoid sensitivity. *Allergy*, *72*(3), 331–341. https://doi.org/10.1111/all.13051

Barbi, J., Pardoll, D., & Pan, F. (2013). Metabolic control of the Treg/Th17 axis. *Immunological Reviews*, *252*(1), 52–77. https://doi.org/10.1111/imr.12029

Baricza, E., Tamási, V., Marton, N., Buzás, E. I., & Nagy, G. (2016). The emerging role of aryl hydrocarbon receptor in the activation and differentiation of Th17 cells. *Cellular and Molecular Life Sciences*, *73*(1), 95–117. https://doi.org/10.1007/s00018-015-2056-2

Barshop, W. D., Kim, H. J., Fan, X., Sha, J., Rayatpisheh, S., & Wohlschlegel, J. A. (2019). Chemical Derivatization of Affinity Matrices Provides Protection from Tryptic Proteolysis. *Journal of Proteome Research*, *18*(10), 3586–3596. https://doi.org/10.1021/acs.jproteome.9b00254

Beier, U. H., Angelin, A., Akimova, T., Wang, L., Liu, Y., Xiao, H., Koike, M. A., Hancock, S. A., Bhatti, T. R., Han, R., Jiao, J., Veasey, S. C., Sims, C. A., Baur, J. A., Wallace, D. C., & Hancock, W. W. (2015). Essential role of mitochondrial energy metabolism in Foxp3 $^{+}$ T-regulatory cell function and allograft survival. *The FASEB Journal*, *29*(6), 2315–2326. https://doi.org/10.1096/fj.14-268409

Benz, C., Ali, M., Krystkowiak, I., Simonetti, L., Sayadi, A., Mihalic, F., Kliche, J., Andersson, E., Jemth, P., Davey, N. E., & Ivarsson, Y. (2022). Proteome-scale mapping of binding sites in the unstructured regions of the human proteome. *Molecular Systems Biology*, *18*(1). https://doi.org/10.15252/msb.202110584

Bindea, G., Mlecnik, B., Hackl, H., Charoentong, P., Tosolini, M., Kirilovsky, A., Fridman, W.-H., Pagès, F., Trajanoski, Z., & Galon, J. (2009). ClueGO: a Cytoscape plug-in to decipher functionally grouped gene ontology and pathway annotation networks. *Bioinformatics*, *25*(8), 1091–1093. https://doi.org/10.1093/bioinformatics/btp101

Biswas, P. S., Bhagat, G., & Pernis, A. B. (2010). IRF4 and its regulators: evolving insights into the pathogenesis of inflammatory arthritis? *Immunological Reviews*, *233*(1), 79–96. https://doi.org/10.1111/j.0105-2896.2009.00864.x

Biswas, P. S., Gupta, S., Chang, E., Song, L., Stirzaker, R. A., Liao, J. K., Bhagat, G., & Pernis, A. B. (2010). Phosphorylation of IRF4 by ROCK2 regulates IL-17 and IL-21 production and the development of autoimmunity in mice. *Journal of Clinical Investigation*, *120*(9), 3280–3295. https://doi.org/10.1172/JCI42856

Biswas, P. S., Gupta, S., Stirzaker, R. A., Kumar, V., Jessberger, R., Lu, T. T., Bhagat, G., & Pernis, A. B. (2012). Dual regulation of IRF4 function in T and B cells is required for the coordination of T–B cell interactions and the prevention of autoimmunity. *Journal of Experimental Medicine*, *209*(3), 581–596. https://doi.org/10.1084/jem.20111195

Biswas, R., & Bagchi, A. (2016). NFkB pathway and inhibition: an overview. *Computational Molecular Biology*. https://doi.org/10.5376/cmb.2016.06.0001

Boddicker, R. L., Kip, N. S., Xing, X., Zeng, Y., Yang, Z.-Z., Lee, J.-H., Almada, L. L., Elsawa, S. F., Knudson, R. A., Law, M. E., Ketterling, R. P., Cunningham, J. M., Wu, Y., Maurer, M. J., O'Byrne, M. M., Cerhan, J. R., Slager, S. L., Link, B. K., Porcher, J. C., … Feldman, A. L. (2015). The oncogenic transcription factor IRF4 is regulated by a novel CD30/NF-κB positive feedback loop in peripheral T-cell lymphoma. *Blood*, *125*(20), 3118–3127. https://doi.org/10.1182/blood-2014-05-578575

Bornancin, F., Renner, F., Touil, R., Sic, H., Kolb, Y., Touil-Allaoui, I., Rush, J. S., Smith, P. A., Bigaud, M., Junker-Walker, U., Burkhart, C., Dawson, J., Niwa, S., Katopodis, A., Nuesslein-Hildesheim, B., Weckbecker, G., Zenke, G., Kinzel, B., Traggiai, E., … Calzascia, T. (2015). Deficiency of MALT1 Paracaspase Activity Results in Unbalanced Regulatory and Effector T and B Cell Responses Leading to Multiorgan Inflammation. *The Journal of Immunology*, *194*(8), 3723–3734. https://doi.org/10.4049/jimmunol.1402254

Brivanlou, A. H., & Darnell, J. E. (2002). Signal Transduction and the Control of Gene Expression. *Science*, *295*(5556), 813–818. https://doi.org/10.1126/science.1066355

Brownlee, P. M., Chambers, A. L., Cloney, R., Bianchi, A., & Downs, J. A. (2014). BAF180 Promotes Cohesion and Prevents Genome Instability and Aneuploidy. *Cell Reports*, *6*(6), 973–981. https://doi.org/10.1016/j.celrep.2014.02.012

Brucklacher-Waldert, V., Ferreira, C., Innocentin, S., Kamdar, S., Withers, D. R., Kullberg, M. C., & Veldhoen, M. (2016). Tbet or Continued RORγt Expression Is Not Required for Th17-Associated Immunopathology. *The Journal of Immunology*, *196*(12), 4893–4904. https://doi.org/10.4049/jimmunol.1600137

Bruno, L., Mazzarella, L., Hoogenkamp, M., Hertweck, A., Cobb, B. S., Sauer, S., Hadjur, S., Leleu, M., Naoe, Y., Telfer, J. C., Bonifer, C., Taniuchi, I., Fisher, A. G., & Merkenschlager, M. (2009). Runx proteins regulate Foxp3 expression. *Journal of Experimental Medicine*, *206*(11), 2329–2337. https://doi.org/10.1084/jem.20090226

Brüstle, A., Brenner, D., Knobbe-Thomsen, C. B., Cox, M., Lang, P. A., Lang, K. S., & Mak, T. W. (2017). MALT1 is an intrinsic regulator of regulatory T cells. *Cell Death & Differentiation*, *24*(7), 1214–1223. https://doi.org/10.1038/cdd.2015.104

Brüstle, A., Brenner, D., Knobbe, C. B., Lang, P. A., Virtanen, C., Hershenfield, B. M., Reardon, C., Lacher, S. M., Ruland, J., Ohashi, P. S., & Mak, T. W. (2012). The NF-κB regulator MALT1 determines the encephalitogenic potential of Th17 cells. *Journal of Clinical Investigation*, *122*(12), 4698–4709. https://doi.org/10.1172/JCI63528

Brüstle, A., Heink, S., Huber, M., Rosenplänter, C., Stadelmann, C., Yu, P., Arpaia, E., Mak, T. W., Kamradt, T., & Lohoff, M. (2007). The development of inflammatory TH-17 cells requires interferon-regulatory factor 4. *Nature Immunology*, *8*(9), 958–966. https://doi.org/10.1038/ni1500

Bsat, M., Chapuy, L., Rubio, M., Wassef, R., Richard, C., Schwenter, F., Loungnarath, R., Soucy, G., Mehta, H., & Sarfati, M. (2019). Differential Pathogenic Th17 Profile in Mesenteric Lymph Nodes of Crohn's Disease and Ulcerative Colitis Patients. *Frontiers in Immunology*, *10*. https://doi.org/10.3389/fimmu.2019.01177

Buccitelli, C., & Selbach, M. (2020). mRNAs, proteins and the emerging principles of gene expression control. *Nature Reviews Genetics*, *21*(10), 630–644. https://doi.org/10.1038/s41576-020-0258-4

Bustin, S. (2002). Quantification of mRNA using real-time reverse transcription PCR (RT-PCR): trends and problems. *Journal of Molecular Endocrinology*, *29*(1), 23–39. https://doi.org/10.1677/jme.0.0290023

Cai, S., Han, H.-J., & Kohwi-Shigematsu, T. (2003). Tissue-specific nuclear architecture and gene expession regulated by SATB1. *Nature Genetics*, *34*(1), 42–51. https://doi.org/10.1038/ng1146

Cai, S., Lee, C. C., & Kohwi-Shigematsu, T. (2006). SATB1 packages densely looped, transcriptionally active chromatin for coordinated expression of cytokine genes. *Nature Genetics*, *38*(11), 1278–1288. https://doi.org/10.1038/ng1913

Cai, W., Zhang, J., Zhou, H., Li, X., Lou, F., Sun, Y., Xu, Z., Bai, J., Yin, Q., Wang, Z., Sun, L., Cai, X., Tang,

S., Wu, Y., Fan, L., Wang, H., Wang, H., & Li, Q. (2022). Protein phosphatase 6 (Pp6) is crucial for regulatory T cell function and stability in autoimmunity. *Genes & Diseases*, *9*(2), 562–575. https://doi.org/10.1016/j.gendis.2021.07.005

Canonigo-Balancio, A. J., Fos, C., Prod'homme, T., Bécart, S., & Altman, A. (2009). SLAT/Def6 Plays a Critical Role in the Development of Th17 Cell-Mediated Experimental Autoimmune Encephalomyelitis. *The Journal of Immunology*, *183*(11), 7259–7267. https://doi.org/10.4049/jimmunol.0902573

Cao, Y., Li, H., Sun, Y., Chen, X., Liu, H., Gao, X., & Liu, X. (2010). Interferon regulatory factor 4 regulates thymocyte differentiation by repressing Runx3 expression. *European Journal of Immunology*, *40*(11), 3198–3209. https://doi.org/10.1002/eji.201040570

Carbon, S., Douglass, E., Good, B. M., Unni, D. R., Harris, N. L., Mungall, C. J., Basu, S., Chisholm, R. L., Dodson, R. J., Hartline, E., Fey, P., Thomas, P. D., Albou, L.-P., Ebert, D., Kesling, M. J., Mi, H., Muruganujan, A., Huang, X., Mushayahama, T., … Elser, J. (2021). The Gene Ontology resource: enriching a GOld mine. *Nucleic Acids Research*, *49*(D1), D325–D334. https://doi.org/10.1093/nar/gkaa1113

Castillo, J., Wu, E., Lowe, C., Srinivasan, S., McCord, R., Wagle, M.-C., Jayakar, S., Edick, M. G., Eastham-Anderson, J., Liu, B., Hutchinson, K. E., Jones, W., Stokes, M. P., Tarighat, S. S., Holcomb, T., Glibicky, A., Romero, F. A., Magnuson, S., Huang, S.-M. A., … Mounir, Z. (2019). CBP/p300 Drives the Differentiation of Regulatory T Cells through Transcriptional and Non-Transcriptional Mechanisms. *Cancer Research*, *79*(15), 3916–3927. https://doi.org/10.1158/0008-5472.CAN-18-3622

Centore, R. C., Sandoval, G. J., Soares, L. M. M., Kadoch, C., & Chan, H. M. (2020). Mammalian SWI/SNF Chromatin Remodeling Complexes: Emerging Mechanisms and Therapeutic Strategies. *Trends in Genetics*, *36*(12), 936–950. https://doi.org/10.1016/j.tig.2020.07.011

Chandler, C. S., & Ballard, F. J. (1986). Multiple biotin-containing proteins in 3T3-L1 cells. *Biochemical Journal*, *237*(1), 123–130. https://doi.org/10.1042/bj2370123

Chang, C.-H., Curtis, J. D., Maggi, L. B., Faubert, B., Villarino, A. V., O'Sullivan, D., Huang, S. C.-C., van der Windt, G. J. W., Blagih, J., Qiu, J., Weber, J. D., Pearce, E. J., Jones, R. G., & Pearce, E. L. (2013). Posttranscriptional Control of T Cell Effector Function by Aerobic Glycolysis. *Cell*, *153*(6), 1239–1251. https://doi.org/10.1016/j.cell.2013.05.016

Chaplin, D. D. (2010). Overview of the immune response. *Journal of Allergy and Clinical Immunology*, *125*(2), S3–S23. https://doi.org/10.1016/j.jaci.2009.12.980

Chen, Q., Yang, B., Liu, X., Zhang, X. D., Zhang, L., & Liu, T. (2022). Histone acetyltransferases CBP/p300 in tumorigenesis and CBP/p300 inhibitors as promising novel anticancer agents. *Theranostics*, *12*(11), 4935–4948. https://doi.org/10.7150/thno.73223

Chen, Q., Yang, W., Gupta, S., Biswas, P., Smith, P., Bhagat, G., & Pernis, A. B. (2008). IRF-4-Binding Protein Inhibits Interleukin-17 and Interleukin-21 Production by Controlling the Activity of IRF-4 Transcription Factor. *Immunity*, *29*(6), 899–911. https://doi.org/10.1016/j.immuni.2008.10.011

Chen, S., Han, Y., Chen, H., Wu, J., & Zhang, M. (2018). Bcl11b Regulates IL-17 Through the TGF-β/Smad Pathway in HDM-Induced Asthma. *Allergy, Asthma & Immunology Research*, *10*(5), 543. https://doi.org/10.4168/aair.2018.10.5.543

Chen, Z., Barbi, J., Bu, S., Yang, H.-Y., Li, Z., Gao, Y., Jinasena, D., Fu, J., Lin, F., Chen, C., Zhang, J., Yu, N., Li, X., Shan, Z., Nie, J., Gao, Z., Tian, H., Li, Y., Yao, Z., … Li, B. (2013). The Ubiquitin Ligase Stub1 Negatively Modulates Regulatory T Cell Suppressive Activity by Promoting Degradation of the Transcription Factor Foxp3. *Immunity*, *39*(2), 272–285. https://doi.org/10.1016/j.immuni.2013.08.006

Chimge, N.-O., Makeyev, A. V., Ruddle, F. H., & Bayarsaihan, D. (2008). Identification of the TFII-I family target genes in the vertebrate genome. *Proceedings of the National Academy of Sciences*, *105*(26), 9006–9010. https://doi.org/10.1073/pnas.0803051105

Chimge, N.-O., Mungunsukh, O., Ruddle, F., & Bayarsaihan, D. (2007). Gene expression analysis of TFII-I modulated genes in mouse embryonic fibroblasts. *Journal of Experimental Zoology Part B: Molecular and Developmental Evolution*, *308B*(3), 225–235. https://doi.org/10.1002/jez.b.21134

Cho, J. J., Xu, Z., Parthasarathy, U., Drashansky, T. T., Helm, E. Y., Zuniga, A. N., Lorentsen, K. J., Mansouri, S., Cho, J. Y., Edelmann, M. J., Duong, D. M., Gehring, T., Seeholzer, T., Krappmann, D., Uddin, M. N., Califano, D., Wang, R. L., Jin, L., Li, H., … Avram, D. (2019). Hectd3 promotes pathogenic Th17 lineage through Stat3 activation and Malt1 signaling in neuroinflammation. *Nature Communications*, *10*(1), 701. https://doi.org/10.1038/s41467-019-08605-3

Cho, Y.-W., Hong, T., Hong, S., Guo, H., Yu, H., Kim, D., Guszczynski, T., Dressler, G. R., Copeland, T. D., Kalkum, M., & Ge, K. (2007). PTIP Associates with MLL3- and MLL4-containing Histone H3 Lysine 4 Methyltransferase Complex. *Journal of Biological Chemistry*, *282*(28), 20395–20406. https://doi.org/10.1074/jbc.M701574200

Christodoulou, K., Wiskin, A. E., Gibson, J., Tapper, W., Willis, C., Afzal, N. A., Upstill-Goddard, R., Holloway, J. W., Simpson, M. A., Beattie, R. M., Collins, A., & Ennis, S. (2013). Next generation exome sequencing of paediatric inflammatory bowel disease patients identifies rare and novel variants in candidate genes. *Gut*, *62*(7), 977–984. https://doi.org/10.1136/gutjnl-2011-301833

Chu, C.-H., & Cheng, D. (2007). Expression, purification, characterization of human 3-methylcrotonyl-CoA carboxylase (MCCC). *Protein Expression and Purification*, *53*(2), 421–427. https://doi.org/10.1016/j.pep.2007.01.012

Ciofani, M., Madar, A., Galan, C., Sellars, M., Mace, K., Pauli, F., Agarwal, A., Huang, W., Parkurst, C. N., Muratet, M., Newberry, K. M., Meadows, S., Greenfield, A., Yang, Y., Jain, P., Kirigin, F. K., Birchmeier, C., Wagner, E. F., Murphy, K. M., … Littman, D. R. (2012). A Validated Regulatory Network for Th17 Cell Specification. *Cell*, *151*(2), 289–303. https://doi.org/10.1016/j.cell.2012.09.016

Conery, A. R., Centore, R. C., Neiss, A., Keller, P. J., Joshi, S., Spillane, K. L., Sandy, P., Hatton, C., Pardo, E., Zawadzke, L., Bommi-Reddy, A., Gascoigne, K. E., Bryant, B. M., Mertz, J. A., & Sims, R. J. (2016). Bromodomain inhibition of the transcriptional coactivators CBP/EP300 as a therapeutic strategy to target the IRF4 network in multiple myeloma. *ELife*, *5*. https://doi.org/10.7554/eLife.10483

Cook, S. L., Franke, M. C., Sievert, E. P., & Sciammas, R. (2020). A Synchronous IRF4-Dependent Gene Regulatory Network in B and Helper T Cells Orchestrating the Antibody Response. *Trends in Immunology*, *41*(7), 614–628. https://doi.org/10.1016/j.it.2020.05.001

Cooper, J. D., Smyth, D. J., Smiles, A. M., Plagnol, V., Walker, N. M., Allen, J. E., Downes, K., Barrett, J. C., Healy, B. C., Mychaleckyj, J. C., Warram, J. H., & Todd, J. A. (2008). Meta-analysis of genome-wide association study data identifies additional type 1 diabetes risk loci. *Nature Genetics*, *40*(12), 1399–1401. https://doi.org/10.1038/ng.249

Corcoran, S. E., & O'Neill, L. A. J. (2016). HIF1α and metabolic reprogramming in inflammation. *Journal of Clinical Investigation*, *126*(10), 3699–3707. https://doi.org/10.1172/JCI84431

Cretney, E., Kallies, A., & Nutt, S. L. (2013). Differentiation and function of Foxp3+ effector regulatory T cells. *Trends in Immunology*, *34*(2), 74–80. https://doi.org/10.1016/j.it.2012.11.002

Cretney, E., Xin, A., Shi, W., Minnich, M., Masson, F., Miasari, M., Belz, G. T., Smyth, G. K., Busslinger, M., Nutt, S. L., & Kallies, A. (2011). The transcription factors Blimp-1 and IRF4 jointly control the

differentiation and function of effector regulatory T cells. *Nature Immunology*, *12*(4), 304–311. https://doi.org/10.1038/ni.2006

Cruickshank, V. A., Sroczynska, P., Sankar, A., Miyagi, S., Rundsten, C. F., Johansen, J. V., & Helin, K. (2015). SWI/SNF Subunits SMARCA4, SMARCD2 and DPF2 Collaborate in MLL-Rearranged Leukaemia Maintenance. *PLOS ONE*, *10*(11), e0142806. https://doi.org/10.1371/journal.pone.0142806

Cui, G. (2019). TH9, TH17, and TH22 Cell Subsets and Their Main Cytokine Products in the Pathogenesis of Colorectal Cancer. *Frontiers in Oncology*, *9*. https://doi.org/10.3389/fonc.2019.01002

Cui, J., Yang, Y., Zhang, C., Hu, P., Kan, W., Bai, X., Liu, X., & Song, H. (2011). FBI-1 functions as a novel AR co-repressor in prostate cancer cells. *Cellular and Molecular Life Sciences*, *68*(6), 1091–1103. https://doi.org/10.1007/s00018-010-0511-7

de Boer, E., Rodriguez, P., Bonte, E., Krijgsveld, J., Katsantoni, E., Heck, A., Grosveld, F., & Strouboulis, J. (2003). Efficient biotinylation and single-step purification of tagged transcription factors in mammalian cells and transgenic mice. *Proceedings of the National Academy of Sciences*, *100*(13), 7480–7485. https://doi.org/10.1073/pnas.1332608100

De Braekeleer, E., Douet-Guilbert, N., Morel, F., Le Bris, M.-J., Basinko, A., & De Braekeleer, M. (2012). ETV6 fusion genes in hematological malignancies: A review. *Leukemia Research*, *36*(8), 945–961. https://doi.org/10.1016/j.leukres.2012.04.010

de Lima, K. A., Donate, P. B., Talbot, J., Davoli-Ferreira, M., Peres, R. S., Cunha, T. M., Alves-Filho, J. C., & Cunha, F. Q. (2018). TGFβ1 signaling sustains aryl hydrocarbon receptor (AHR) expression and restrains the pathogenic potential of TH17 cells by an AHR-independent mechanism. *Cell Death & Disease*, *9*(11), 1130. https://doi.org/10.1038/s41419-018-1107-7

Demeyer, A., Skordos, I., Driege, Y., Kreike, M., Hochepied, T., Baens, M., Staal, J., & Beyaert, R. (2019). MALT1 Proteolytic Activity Suppresses Autoimmunity in a T Cell Intrinsic Manner. *Frontiers in Immunology*, *10*. https://doi.org/10.3389/fimmu.2019.01898

Demichev, V., Messner, C. B., Vernardis, S. I., Lilley, K. S., & Ralser, M. (2020). DIA-NN: neural networks and interference correction enable deep proteome coverage in high throughput. *Nature Methods*, *17*(1), 41–44. https://doi.org/10.1038/s41592-019-0638-x

Dietzen, S. (2019). *Funktionelle Charakterisierung IRF4-gesteuerter Transkriptionsfaktorkomplexe in Th9-Zellen* [Institute for Immunology]. https://doi.org/http://doi.org/10.25358/openscience-2371

Doncheva, N. T., Morris, J. H., Gorodkin, J., & Jensen, L. J. (2019). Cytoscape StringApp: Network Analysis and Visualization of Proteomics Data. *Journal of Proteome Research*, *18*(2), 623–632. https://doi.org/10.1021/acs.jproteome.8b00702

Drazic, A., Myklebust, L. M., Ree, R., & Arnesen, T. (2016). The world of protein acetylation. *Biochimica et Biophysica Acta (BBA) - Proteins and Proteomics*, *1864*(10), 1372–1401. https://doi.org/10.1016/j.bbapap.2016.06.007

Driegen, S., Ferreira, R., van Zon, A., Strouboulis, J., Jaegle, M., Grosveld, F., Philipsen, S., & Meijer, D. (2005). A generic tool for biotinylation of tagged proteins in transgenic mice. *Transgenic Research*, *14*(4), 477–482. https://doi.org/10.1007/s11248-005-7220-2

Du, P., Gao, K., Cao, Y., Yang, S., Wang, Y., Guo, R., Zhao, M., & Jia, S. (2019). RFX1 downregulation contributes to TLR4 overexpression in CD14+ monocytes via epigenetic mechanisms in coronary artery disease. *Clinical Epigenetics*, *11*(1), 44. https://doi.org/10.1186/s13148-019-0646-9

Dubois, P. C. A., Trynka, G., Franke, L., Hunt, K. A., Romanos, J., Curtotti, A., Zhernakova, A., Heap, G. A. R., Ádány, R., Aromaa, A., Bardella, M. T., van den Berg, L. H., Bockett, N. A., de la Concha, E. G., Dema, B., Fehrmann, R. S. N., Fernández-Arquero, M., Fiatal, S., Grandone, E., … van Heel, D. A. (2010). Multiple common variants for celiac disease influencing immune gene expression. *Nature Genetics*, *42*(4), 295–302. https://doi.org/10.1038/ng.543

Duguet, F., Locard-Paulet, M., Marcellin, M., Chaoui, K., Bernard, I., Andreoletti, O., Lesourne, R., Burlet-Schiltz, O., Gonzalez de Peredo, A., & Saoudi, A. (2017). Proteomic Analysis of Regulatory T Cells Reveals the Importance of Themis1 in the Control of Their Suppressive Function. *Molecular & Cellular Proteomics*, *16*(8), 1416–1432. https://doi.org/10.1074/mcp.M116.062745

Dundas, C. M., Demonte, D., & Park, S. (2013). Streptavidin–biotin technology: improvements and innovations in chemical and biological applications. *Applied Microbiology and Biotechnology*, *97*(21), 9343–9353. https://doi.org/10.1007/s00253-013-5232-z

Dunham, W. H., Mullin, M., & Gingras, A.-C. (2012). Affinity-purification coupled to mass spectrometry: Basic principles and strategies. *PROTEOMICS*, *12*(10), 1576–1590. https://doi.org/10.1002/pmic.201100523

Dybska, E., Adams, A. T., Duclaux-Loras, R., Walkowiak, J., & Nowak, J. K. (2021). Waiting in the wings: *RUNX3* reveals hidden depths of immune regulation with potential implications for inflammatory bowel disease. *Scandinavian Journal of Immunology*, *93*(5). https://doi.org/10.1111/sji.13025

Edwards, C. L., de Oca, M. M., de Labastida Rivera, F., Kumar, R., Ng, S. S., Wang, Y., Amante, F. H., Kometani, K., Kurosaki, T., Sidwell, T., Kallies, A., & Engwerda, C. R. (2018). The Role of BACH2 in T Cells in Experimental Malaria Caused by Plasmodium chabaudi chabaudi AS. *Frontiers in Immunology*, *9*. https://doi.org/10.3389/fimmu.2018.02578

Ellmeier, W., & Seiser, C. (2018). Histone deacetylase function in CD4+ T cells. *Nature Reviews Immunology*, *18*(10), 617–634. https://doi.org/10.1038/s41577-018-0037-z

EMBL's European Bioinformatics Institute (EMBL-EBI). (2023). *PSICQUIC View*. http://www.ebi.ac.uk/Tools/webservices/psicquic/view/main.xhtml

Esser, C., Rannug, A., & Stockinger, B. (2009). The aryl hydrocarbon receptor in immunity. *Trends in Immunology*, *30*(9), 447–454. https://doi.org/10.1016/j.it.2009.06.005

Euskirchen, G., Auerbach, R. K., & Snyder, M. (2012). SWI/SNF chromatin-remodeling factors: Multiscale analyses and diverse functions. *Journal of Biological Chemistry*, *287*(37), 30897–30905. https://doi.org/10.1074/jbc.R111.309302

Fang, C.-M., Roy, S., Nielsen, E., Paul, M., Maul, R., Paun, A., Koentgen, F., Raval, F. M., Szomolanyi-Tsuda, E., & Pitha, P. M. (2012). Unique contribution of IRF-5-Ikaros axis to the B-cell IgG2a response. *Genes & Immunity*, *13*(5), 421–430. https://doi.org/10.1038/gene.2012.10

Fanzo, J. C., Yang, W., Jang, S. Y., Gupta, S., Chen, Q., Siddiq, A., Greenberg, , teven, & Pernis, A. B. (2006). Loss of IRF-4–binding protein leads to the spontaneous development of systemic autoimmunity. *Journal of Clinical Investigation*, *116*(3), 703–714. https://doi.org/10.1172/JCI24096

Ferreira, M. A., Matheson, M. C., Duffy, D. L., Marks, G. B., Hui, J., Le Souëf, P., Danoy, P., Baltic, S., Nyholt, D. R., Jenkins, M., Hayden, C., Willemsen, G., Ang, W., Kuokkanen, M., Beilby, J., Cheah, F., de Geus, E. J., Ramasamy, A., Vedantam, S., … Thompson, P. J. (2011). Identification of IL6R and chromosome 11q13.5 as risk loci for asthma. *The Lancet*, *378*(9795), 1006–1014. https://doi.org/10.1016/S0140-6736(11)60874-X

Fionda, C., Abruzzese, M. P., Zingoni, A., Cecere, F., Vulpis, E., Peruzzi, G., Soriani, A., Molfetta, R.,

Paolini, R., Ricciardi, M. R., Petrucci, M. T., Santoni, A., & Cippitelli, M. (2015). The IMiDs targets IKZF-1/3 and IRF4 as novel negative regulators of NK cell-activating ligands expression in multiple myeloma. *Oncotarget*, *6*(27), 23609–23630. https://doi.org/10.18632/oncotarget.4603

Fontaine, F., Overman, J., & François, M. (2015). Pharmacological manipulation of transcription factor protein-protein interactions: opportunities and obstacles. *Cell Regeneration*, *4*(1), 4:2. https://doi.org/10.1186/s13619-015-0015-x

Franke, A., McGovern, D. P. B., Barrett, J. C., Wang, K., Radford-Smith, G. L., Ahmad, T., Lees, C. W., Balschun, T., Lee, J., Roberts, R., Anderson, C. A., Bis, J. C., Bumpstead, S., Ellinghaus, D., Festen, E. M., Georges, M., Green, T., Haritunians, T., Jostins, L., … Parkes, M. (2010). Genome-wide meta-analysis increases to 71 the number of confirmed Crohn's disease susceptibility loci. *Nature Genetics*, *42*(12), 1118–1125. https://doi.org/10.1038/ng.717

FU, D., SONG, X., HU, H., SUN, M., LI, Z., & TIAN, Z. (2016). Downregulation of RUNX3 moderates the frequency of Th17 and Th22 cells in patients with psoriasis. *Molecular Medicine Reports*, *13*(6), 4606–4612. https://doi.org/10.3892/mmr.2016.5108

Fujii, Y. (1999). Crystal structure of an IRF-DNA complex reveals novel DNA recognition and cooperative binding to a tandem repeat of core sequences. *The EMBO Journal*, *18*(18), 5028–5041. https://doi.org/10.1093/emboj/18.18.5028

Furusawa, Y., Obata, Y., Fukuda, S., Endo, T. A., Nakato, G., Takahashi, D., Nakanishi, Y., Uetake, C., Kato, K., Kato, T., Takahashi, M., Fukuda, N. N., Murakami, S., Miyauchi, E., Hino, S., Atarashi, K., Onawa, S., Fujimura, Y., Lockett, T., … Ohno, H. (2013). Commensal microbe-derived butyrate induces the differentiation of colonic regulatory T cells. *Nature*, *504*(7480), 446–450. https://doi.org/10.1038/nature12721

Gao, T., & Qian, J. (2019). EnhancerAtlas 2.0: an updated resource with enhancer annotation in 586 tissue/cell types across nine species. *Nucleic Acids Research*. https://doi.org/10.1093/nar/gkz980

Gerriets, V. A., Kishton, R. J., Nichols, A. G., Macintyre, A. N., Inoue, M., Ilkayeva, O., Winter, P. S., Liu, X., Priyadharshini, B., Slawinska, M. E., Haeberli, L., Huck, C., Turka, L. A., Wood, K. C., Hale, L. P., Smith, P. A., Schneider, M. A., MacIver, N. J., Locasale, J. W., … Rathmell, J. C. (2015). Metabolic programming and PDHK1 control CD4+ T cell subsets and inflammation. *Journal of Clinical Investigation*, *125*(1), 194–207. https://doi.org/10.1172/JCI76012

Ghosh, S., Taylor, A., Chin, M., Huang, H.-R., Conery, A. R., Mertz, J. A., Salmeron, A., Dakle, P. J., Mele, D., Cote, A., Jayaram, H., Setser, J. W., Poy, F., Hatzivassiliou, G., DeAlmeida-Nagata, D., Sandy, P., Hatton, C., Romero, F. A., Chiang, E., … Lora, J. M. (2016). Regulatory T Cell Modulation by CBP/EP300 Bromodomain Inhibition. *Journal of Biological Chemistry*, *291*(25), 13014–13027. https://doi.org/10.1074/jbc.M115.708560

Glasmacher, E., Agrawal, S., Chang, A. B., Murphy, T. L., Zeng, W., Vander Lugt, B., Khan, A. A., Ciofani, M., Spooner, C. J., Rutz, S., Hackney, J., Nurieva, R., Escalante, C. R., Ouyang, W., Littman, D. R., Murphy, K. M., & Singh, H. (2012). A Genomic Regulatory Element That Directs Assembly and Function of Immune-Specific AP-1–IRF Complexes. *Science*, *338*(6109), 975–980. https://doi.org/10.1126/science.1228309

Goldsmith, C. D., Donovan, T., Vlahovich, N., & Pyne, D. B. (2021). Unlocking the Role of Exercise on CD4+ T Cell Plasticity. *Frontiers in Immunology*, *12*. https://doi.org/10.3389/fimmu.2021.729366

Göös, H., Kinnunen, M., Salokas, K., Tan, Z., Liu, X., Yadav, L., Zhang, Q., Wei, G.-H., & Varjosalo, M. (2022). Human transcription factor protein interaction networks. *Nature Communications*, *13*(1), 766. https://doi.org/10.1038/s41467-022-28341-5

Grant, F. M., Yang, J., Nasrallah, R., Clarke, J., Sadiyah, F., Whiteside, S. K., Imianowski, C. J., Kuo, P., Vardaka, P., Todorov, T., Zandhuis, N., Patrascan, I., Tough, D. F., Kometani, K., Eil, R., Kurosaki, T., Okkenhaug, K., & Roychoudhuri, R. (2020). BACH2 drives quiescence and maintenance of resting Treg cells to promote homeostasis and cancer immunosuppression. *Journal of Experimental Medicine*, *217*(9). https://doi.org/10.1084/jem.20190711

Grumont, R. J., & Gerondakis, S. (2000). Rel Induces Interferon Regulatory Factor 4 (IRF-4) Expression in Lymphocytes. *Journal of Experimental Medicine*, *191*(8), 1281–1292. https://doi.org/10.1084/jem.191.8.1281

Gu, Z., Chen, X., Zhu, D., Wu, S., & Yu, C. (2022). Histone deacetylase 1 and 3 inhibitors alleviate colon inflammation by inhibiting Th17 cell differentiation. *Journal of Clinical Laboratory Analysis*, *36*(10). https://doi.org/10.1002/jcla.24699

Guo, Z., Xu, P., Ge, S., Zhang, C., Zheng, X., Xu, J., Liu, Z., Li, B., & Ge, S. (2017). Ubiquitin specific peptidase 4 stabilizes interferon regulatory factor protein and promotes its function to facilitate interleukin-4 expression in T helper type 2 cells. *International Journal of Molecular Medicine*, *40*(4), 979–986. https://doi.org/10.3892/ijmm.2017.3087

Gupta, S., Lee, A., Hu, C., Fanzo, J., Goldberg, I., Cattoretti, G., & Pernis, A. B. (2003). Molecular cloning of IBP, a SWAP-70 homologous GEF, which is highly expressed in the immune system. *Human Immunology*, *64*(4), 389–401. https://doi.org/10.1016/S0198-8859(03)00024-7

Gupta, S., Stamatoyannopoulos, J. A., Bailey, T. L., & Noble, W. (2007). Quantifying similarity between motifs. *Genome Biology*, *8*(2), R24. https://doi.org/10.1186/gb-2007-8-2-r24

Hall, J. A., Pokrovskii, M., Kroehling, L., Kim, B.-R., Kim, S. Y., Wu, L., Lee, J.-Y., & Littman, D. R. (2022). Transcription factor RORα enforces stability of the Th17 cell effector program by binding to a Rorc cis-regulatory element. *Immunity*, *55*(11), 2027-2043.e9. https://doi.org/10.1016/j.immuni.2022.09.013

Hammitzsch, A., Tallant, C., Fedorov, O., O'Mahony, A., Brennan, P. E., Hay, D. A., Martinez, F. O., Al-Mossawi, M. H., de Wit, J., Vecellio, M., Wells, C., Wordsworth, P., Müller, S., Knapp, S., & Bowness, P. (2015). CBP30, a selective CBP/p300 bromodomain inhibitor, suppresses human Th17 responses. *Proceedings of the National Academy of Sciences*, *112*(34), 10768–10773. https://doi.org/10.1073/pnas.1501956112

Han, L., Yang, J., Wang, X., Wu, Q., Yin, S., Li, Z., Zhang, J., Xing, Y., Chen, Z., Tsun, A., Li, D., Piccioni, M., Zhang, Y., Guo, Q., Jiang, L., Bao, L., Lv, L., & Li, B. (2014). The E3 Deubiquitinase USP17 Is a Positive Regulator of Retinoic Acid-related Orphan Nuclear Receptor γt (RORγt) in Th17 Cells. *Journal of Biological Chemistry*, *289*(37), 25546–25555. https://doi.org/10.1074/jbc.M114.565291

Harada, T., Oda, A., Grondin, Y., Teramachi, J., Bat-Erdene, A., Iwasa, M., Oura, M., Nakamura, S., Kagawa, K., Okamoto, Y., Sogabe, K., Fujii, S., Miki, H., Ozaki, S., Hideshima, T., Anderson, K. C., & Abe, M. (2018). The Critical Role of HDAC1-IRF4-Pim-2 Axis in Myeloma Cell Growth and Survival: Therapeutic Impacts of Targeting the HDAC1-IRF4-Pim-2 Axis. *Blood*, *132*(Supplement 1), 1939–1939. https://doi.org/10.1182/blood-2018-99-114086

Harada, T., Oda, A., Ohguchi, H., Grondin, Y., Tenshin, H., Hiasa, M., Teramachi, J., Oura, M., Sogabe, K., Fujii, S., Nakamura, S., Miki, H., Kagawa, K., Ozaki, S., Hideshima, T., Anderson, K. C., & Abe, M. (2019). Novel Therapeutic Rationale for Targeting HDAC1 and PIM2 in Multiple Myeloma. *Blood*, *134*(Supplement_1), 3111–3111. https://doi.org/10.1182/blood-2019-127679

Harada, T., Ohguchi, H., Oda, A., Nakao, M., Teramachi, J., Hiasa, M., Sumitani, R., Oura, M., Sogabe, K., Maruhashi, T., Takahashi, M., Fujii, S., Nakamura, S., Miki, H., Kagawa, K., Ozaki, S., Sano, S., Hideshima, T., & Abe, M. (2023). Novel antimyeloma therapeutic option with inhibition of the

HDAC1-IRF4 axis and PIM kinase. *Blood Advances*, *7*(6), 1019–1032. https://doi.org/10.1182/bloodadvances.2022007155

Hasan, S. N., Sharma, A., Ghosh, S., Hong, S.-W., Roy-Chowdhuri, S., Im, S.-H., Kang, K., & Rudra, D. (2019). Bcl11b prevents catastrophic autoimmunity by controlling multiple aspects of a regulatory T cell gene expression program. *Science Advances*, *5*(8). https://doi.org/10.1126/sciadv.aaw0706

He, Z., Ma, J., Wang, R., Zhang, J., Huang, Z., Wang, F., Sen, S., Rothenberg, E. V, & Sun, Z. (2017). A two-amino-acid substitution in the transcription factor RORγt disrupts its function in TH17 differentiation but not in thymocyte development. *Nature Immunology*, *18*(10), 1128–1138. https://doi.org/10.1038/ni.3832

Hill, J. A., Feuerer, M., Tash, K., Haxhinasto, S., Perez, J., Melamed, R., Mathis, D., & Benoist, C. (2007). Foxp3 Transcription-Factor-Dependent and -Independent Regulation of the Regulatory T Cell Transcriptional Signature. *Immunity*, *27*(5), 786–800. https://doi.org/10.1016/j.immuni.2007.09.010

Holmes, D., Gao, J., & Su, L. (2011). Foxp3 inhibits HDAC1 activity to modulate gene expression in human T cells. *Virology*, *421*(1), 12–18. https://doi.org/10.1016/j.virol.2011.09.002

Hoppmann, N., Graetz, C., Paterka, M., Poisa-Beiro, L., Larochelle, C., Hasan, M., Lill, C. M., Zipp, F., & Siffrin, V. (2015). New candidates for CD4 T cell pathogenicity in experimental neuroinflammation and multiple sclerosis. *Brain*, *138*(4), 902–917. https://doi.org/10.1093/brain/awu408

Hu, C.-M., Jang, S. Y., Fanzo, J. C., & Pernis, A. B. (2002). Modulation of T Cell Cytokine Production by Interferon Regulatory Factor-4. *Journal of Biological Chemistry*, *277*(51), 49238–49246. https://doi.org/10.1074/jbc.M205895200

Hu, L., Sun, Y., Luo, J., He, X., Ye, M., Li, G., Zhang, Y., Bai, J., Zhang, D., & Chang, C. (2020). Targeting TR4 nuclear receptor with antagonist bexarotene increases docetaxel sensitivity to better suppress the metastatic castration-resistant prostate cancer progression. *Oncogene*, *39*(9), 1891–1903. https://doi.org/10.1038/s41388-019-1070-5

Huang, Y., Lu, Y., He, Y., Feng, Z., Zhan, Y., Huang, X., Liu, Q., Zhang, J., Li, H., Huang, H., Ma, M., Luo, L., & Li, L. (2019). Ikzf1 regulates embryonic T lymphopoiesis via Ccr9 and Irf4 in zebrafish. *Journal of Biological Chemistry*, *294*(44), 16152–16163. https://doi.org/10.1074/jbc.RA119.009883

Huber, L. A., Pfaller, K., & Vietor, I. (2003). Organelle Proteomics. *Circulation Research*, *92*(9), 962–968. https://doi.org/10.1161/01.RES.0000071748.48338.25

Huber, M., Brüstle, A., Reinhard, K., Guralnik, A., Walter, G., Mahiny, A., von Löw, E., & Lohoff, M. (2008). IRF4 is essential for IL-21-mediated induction, amplification, and stabilization of the Th17 phenotype. *Proceedings of the National Academy of Sciences*, *105*(52), 20846–20851. https://doi.org/10.1073/pnas.0809077106

Huber, M., & Lohoff, M. (2014). IRF4 at the crossroads of effector T-cell fate decision. *European Journal of Immunology*, *44*(7), 1886–1895. https://doi.org/10.1002/eji.201344279

Hughes, C. S., Foehr, S., Garfield, D. A., Furlong, E. E., Steinmetz, L. M., & Krijgsveld, J. (2014). Ultrasensitive proteome analysis using paramagnetic bead technology. *Molecular Systems Biology*, *10*(10), 757. https://doi.org/10.15252/msb.20145625

Hughes, C. S., Moggridge, S., Müller, T., Sorensen, P. H., Morin, G. B., & Krijgsveld, J. (2019). Single-pot, solid-phase-enhanced sample preparation for proteomics experiments. *Nature Protocols*, *14*(1), 68–85. https://doi.org/10.1038/s41596-018-0082-x

Huh, J. R., & Littman, D. R. (2012). Small molecule inhibitors of RORγt: Targeting Th17 cells and other applications. *European Journal of Immunology*, *42*(9), 2232–2237. https://doi.org/10.1002/eji.201242740

Huppertz, S., Senger, K., Brown, A., Leins, H., Eiwen, K., Mulaw, M. A., Geiger, H., & Becker, M. (2021). KDM6A, a histone demethylase, regulates stress hematopoiesis and early B-cell differentiation. *Experimental Hematology*, *99*, 32-43.e13. https://doi.org/10.1016/j.exphem.2021.06.001

Hwang, S. S., Jang, S. W., Lee, K. O., Kim, H. S., & Lee, G. R. (2017). RHS6 coordinately regulates the Th2 cytokine genes by recruiting GATA3, SATB1, and IRF4. *Allergy*, *72*(5), 772–782. https://doi.org/10.1111/all.13078

Ichiyama, K., Yoshida, H., Wakabayashi, Y., Chinen, T., Saeki, K., Nakaya, M., Takaesu, G., Hori, S., Yoshimura, A., & Kobayashi, T. (2008). Foxp3 Inhibits RORγt-mediated IL-17A mRNA Transcription through Direct Interaction with RORγt*. *Journal of Biological Chemistry*, *283*(25), 17003–17008. https://doi.org/10.1074/jbc.M801286200

Ivanov, I. I., McKenzie, B. S., Zhou, L., Tadokoro, C. E., Lepelley, A., Lafaille, J. J., Cua, D. J., & Littman, D. R. (2006). The Orphan Nuclear Receptor RORγt Directs the Differentiation Program of Proinflammatory IL-17+ T Helper Cells. *Cell*, *126*(6), 1121–1133. https://doi.org/10.1016/j.cell.2006.07.035

Jang, S. W., & Lee, G. R. (2018). GATA3, SATB1, IRF4 complex binds to the Th2 cytokine locus through *cis* -acting element RHS6, regulating allergic airway inflammation. *The Journal of Immunology*, *200*(1_Supplement), 44.35-44.35. https://doi.org/10.4049/jimmunol.200.Supp.44.35

Jaworski, M., Marsland, B. J., Gehrig, J., Held, W., Favre, S., Luther, S. A., Perroud, M., Golshayan, D., Gaide, O., & Thome, M. (2014). Malt1 protease inactivation efficiently dampens immune responses but causes spontaneous autoimmunity. *The EMBO Journal*, *33*(23), 2765–2781. https://doi.org/10.15252/embj.201488987

Jaworski, M., & Thome, M. (2016). The paracaspase MALT1: biological function and potential for therapeutic inhibition. *Cellular and Molecular Life Sciences*, *73*(3), 459–473. https://doi.org/10.1007/s00018-015-2059-z

Jefferies, C. A. (2019). Regulating IRFs in IFN Driven Disease. *Frontiers in Immunology*, *10*. https://doi.org/10.3389/fimmu.2019.00325

Jeltsch, K. M., Hu, D., Brenner, S., Zöller, J., Heinz, G. A., Nagel, D., Vogel, K. U., Rehage, N., Warth, S. C., Edelmann, S. L., Gloury, R., Martin, N., Lohs, C., Lech, M., Stehklein, J. E., Geerlof, A., Kremmer, E., Weber, A., Anders, H.-J., … Heissmeyer, V. (2014). Cleavage of roquin and regnase-1 by the paracaspase MALT1 releases their cooperatively repressed targets to promote TH17 differentiation. *Nature Immunology*, *15*(11), 1079–1089. https://doi.org/10.1038/ni.3008

Jiang, S., Koolmeister, C., Misic, J., Siira, S., Kühl, I., Silva Ramos, E., Miranda, M., Jiang, M., Posse, V., Lytovchenko, O., Atanassov, I., Schober, F. A., Wibom, R., Hultenby, K., Milenkovic, D., Gustafsson, C. M., Filipovska, A., & Larsson, N. (2019). <scp>TEFM</scp> regulates both transcription elongation and <scp>RNA</scp> processing in mitochondria. *EMBO Reports*, *20*(6). https://doi.org/10.15252/embr.201948101

Jin, R., Lin, H., Li, G., Xu, J., Shi, L., Chang, C., & Cai, X. (2018). TR4 nuclear receptor suppresses HCC cell invasion via downregulating the EphA2 expression. *Cell Death & Disease*, *9*(3), 283. https://doi.org/10.1038/s41419-018-0287-5

Jin, Y., Chen, K., De Paepe, A., Hellqvist, E., Krstic, A. D., Metang, L., Gustafsson, C., Davis, R. E., Levy, Y. M., Surapaneni, R., Wallblom, A., Nahi, H., Mansson, R., & Lin, Y. C. (2018). Active enhancer and chromatin accessibility landscapes chart the regulatory network of primary multiple

myeloma. *Blood*, *131*(19), 2138–2150. https://doi.org/10.1182/blood-2017-09-808063

Kaeser, M. D., Aslanian, A., Dong, M.-Q., Yates, J. R., & Emerson, B. M. (2008). BRD7, a Novel PBAF-specific SWI/SNF Subunit, Is Required for Target Gene Activation and Repression in Embryonic Stem Cells. *Journal of Biological Chemistry*, *283*(47), 32254–32263. https://doi.org/10.1074/jbc.M806061200

Kel, A. E. (2003). MATCHTM: a tool for searching transcription factor binding sites in DNA sequences. *Nucleic Acids Research*, *31*(13), 3576–3579. https://doi.org/10.1093/nar/gkg585

Kim, D., Lee, J., Cheng, D., Li, J., Carter, C., Richie, E., & Bedford, M. T. (2010). Enzymatic Activity Is Required for the in Vivo Functions of CARM1. *Journal of Biological Chemistry*, *285*(2), 1147–1152. https://doi.org/10.1074/jbc.M109.035865

Kim, E. H., Gasper, D. J., Lee, S. H., Plisch, E. H., Svaren, J., & Suresh, M. (2014). Bach2 Regulates Homeostasis of Foxp3+ Regulatory T Cells and Protects against Fatal Lung Disease in Mice. *The Journal of Immunology*, *192*(3), 985–995. https://doi.org/10.4049/jimmunol.1302378

Kim, J., Cantor, A. B., Orkin, S. H., & Wang, J. (2009). Use of in vivo biotinylation to study protein–protein and protein–DNA interactions in mouse embryonic stem cells. *Nature Protocols*, *4*(4), 506–517. https://doi.org/10.1038/nprot.2009.23

Kim, J., Lee, J., Yadav, N., Wu, Q., Carter, C., Richard, S., Richie, E., & Bedford, M. T. (2004). Loss of CARM1 Results in Hypomethylation of Thymocyte Cyclic AMP-regulated Phosphoprotein and Deregulated Early T Cell Development. *Journal of Biological Chemistry*, *279*(24), 25339–25344. https://doi.org/10.1074/jbc.M402544200

Kirkeby, S., Moe, D., Bøg-Hansen, T. C., & van Noorden, C. J. F. (1993). Biotin carboxylases in mitochondria and the cytosol from skeletal and cardiac muscle as detected by avidin binding. *Histochemistry*, *100*(6), 415–421. https://doi.org/10.1007/BF00267821

Klunker, S., Chong, M. M. W., Mantel, P.-Y., Palomares, O., Bassin, C., Ziegler, M., Rückert, B., Meiler, F., Akdis, M., Littman, D. R., & Akdis, C. A. (2009). Transcription factors RUNX1 and RUNX3 in the induction and suppressive function of Foxp3+ inducible regulatory T cells. *Journal of Experimental Medicine*, *206*(12), 2701–2715. https://doi.org/10.1084/jem.20090596

Köhne, M. C. (2021). *The chromatin organizer Satb1 regulates the differentiation into CD4+ TH subsets and is essential for the development of TH17 cells* [Rheinische Friedrich-Wilhelms-Universität Bonn]. https://nbn-resolving.org/urn:nbn:de:hbz:5-62543

Krangel, M. S. (2007). T cell development: better living through chromatin. *Nature Immunology*, *8*(7), 687–694. https://doi.org/10.1038/ni1484

Kratchmarov, R., Nish, S. A., Lin, W.-H. W., Adams, W. C., Chen, Y.-H., Yen, B., Rothman, N. J., Klein, U., & Reiner, S. L. (2017). IRF4 Couples Anabolic Metabolism to Th1 Cell Fate Determination. *ImmunoHorizons*, *1*(7), 156–161. https://doi.org/10.4049/immunohorizons.1700012

Kumar, N., Lyda, B., Chang, M. R., Lauer, J. L., Solt, L. A., Burris, T. P., Kamenecka, T. M., & Griffin, P. R. (2012). Identification of SR2211: A Potent Synthetic RORγ-Selective Modulator. *ACS Chemical Biology*, *7*(4), 672–677. https://doi.org/10.1021/cb200496y

Kurebayashi, Y., Nagai, S., Ikejiri, A., & Koyasu, S. (2013). Recent advances in understanding the molecular mechanisms of the development and function of <scp>T</scp> h17 cells. *Genes to Cells*, *18*(4), 247–265. https://doi.org/10.1111/gtc.12039

Kwon, H., Thierry-Mieg, D., Thierry-Mieg, J., Kim, H.-P., Oh, J., Tunyaplin, C., Carotta, S., Donovan, C. E., Goldman, M. L., Tailor, P., Ozato, K., Levy, D. E., Nutt, S. L., Calame, K., & Leonard, W. J. (2009). Analysis of Interleukin-21-Induced Prdm1 Gene Regulation Reveals Functional

Cooperation of STAT3 and IRF4 Transcription Factors. *Immunity*, *31*(6), 941–952. https://doi.org/10.1016/j.immuni.2009.10.008

Lazarevic, V., Chen, X., Shim, J.-H., Hwang, E.-S., Jang, E., Bolm, A. N., Oukka, M., Kuchroo, V. K., & Glimcher, L. H. (2011). T-bet represses TH17 differentiation by preventing Runx1-mediated activation of the gene encoding RORγt. *Nature Immunology*, *12*(1), 96–104. https://doi.org/10.1038/ni.1969

Lee, J. M., Hammarén, H. M., Savitski, M. M., & Baek, S. H. (2023). Control of protein stability by post-translational modifications. *Nature Communications*, *14*(1), 201. https://doi.org/10.1038/s41467-023-35795-8

Lee, W., Kim, H. S., Baek, S. Y., & Lee, G. R. (2016). Transcription factor IRF8 controls Th1-like regulatory T-cell function. *Cellular & Molecular Immunology*, *13*(6), 785–794. https://doi.org/10.1038/cmi.2015.72

Lehtonen, A., Veckman, V., Nikula, T., Lahesmaa, R., Kinnunen, L., Matikainen, S., & Julkunen, I. (2005). Differential Expression of IFN Regulatory Factor 4 Gene in Human Monocyte-Derived Dendritic Cells and Macrophages. *The Journal of Immunology*, *175*(10), 6570–6579. https://doi.org/10.4049/jimmunol.175.10.6570

Lerdrup, M., Johansen, J. V., Agrawal-Singh, S., & Hansen, K. (2016). An interactive environment for agile analysis and visualization of ChIP-sequencing data. *Nature Structural & Molecular Biology*, *23*(4), 349–357. https://doi.org/10.1038/nsmb.3180

Li, P., & Leonard, W. J. (2018). Chromatin Accessibility and Interactions in the Transcriptional Regulation of T Cells. *Frontiers in Immunology*, *9*. https://doi.org/10.3389/fimmu.2018.02738

Li, P., Spolski, R., Liao, W., Wang, L., Murphy, T. L., Murphy, K. M., & Leonard, W. J. (2012). BATF–JUN is critical for IRF4-mediated transcription in T cells. *Nature*, *490*(7421), 543–546. https://doi.org/10.1038/nature11530

Li, S., Wang, L., Berman, M., Kong, Y.-Y., & Dorf, M. E. (2011). Mapping a Dynamic Innate Immunity Protein Interaction Network Regulating Type I Interferon Production. *Immunity*, *35*(3), 426–440. https://doi.org/10.1016/j.immuni.2011.06.014

Li, X., & Zheng, Y. (2015). Regulatory T cell identity: formation and maintenance. *Trends in Immunology*, *36*(6), 344–353. https://doi.org/10.1016/j.it.2015.04.006

Liljevald, M., Rehnberg, M., Söderberg, M., Ramnegård, M., Börjesson, J., Luciani, D., Krutrök, N., Brändén, L., Johansson, C., Xu, X., Bjursell, M., Sjögren, A.-K., Hornberg, J., Andersson, U., Keeling, D., & Jirholt, J. (2016). Retinoid-related orphan receptor γ (RORγ) adult induced knockout mice develop lymphoblastic lymphoma. *Autoimmunity Reviews*, *15*(11), 1062–1070. https://doi.org/10.1016/j.autrev.2016.07.036

LILLO, C., KATAYA, A. R. A., HEIDARI, B., CREIGHTON, M. T., NEMIE-FEYISSA, D., GINBOT, Z., & JONASSEN, E. M. (2014). Protein phosphatases <scp>PP</scp> 2A, <scp>PP</scp> 4 and <scp>PP</scp> 6: mediators and regulators in development and responses to environmental cues. *Plant, Cell & Environment*, *37*(12), 2631–2648. https://doi.org/10.1111/pce.12364

Lin, T.-C. (2022). RUNX1 and cancer. *Biochimica et Biophysica Acta (BBA) - Reviews on Cancer*, *1877*(3), 188715. https://doi.org/10.1016/j.bbcan.2022.188715

Liu, H., Cao, A. T., Feng, T., Li, Q., Zhang, W., Yao, S., Dann, S. M., Elson, C. O., & Cong, Y. (2015). TGF-β converts Th1 cells into Th17 cells through stimulation of Runx1 expression. *European Journal of Immunology*, *45*(4), 1010–1018. https://doi.org/10.1002/eji.201444726

Liu, M., Gao, W., van Velkinburgh, J. C., Wu, Y., Ni, B., & Tian, Y. (2016). Role of Ets Proteins in

Development, Differentiation, and Function of T-Cell Subsets. *Medicinal Research Reviews*, *36*(2), 193–220. https://doi.org/10.1002/med.21361

Livak, K. J., & Schmittgen, T. D. (2001). Analysis of Relative Gene Expression Data Using Real-Time Quantitative PCR and the 2−ΔΔCT Method. *Methods*, *25*(4), 402–408. https://doi.org/10.1006/meth.2001.1262

Lohoff, M., Mittrücker, H.-W., Prechtl, S., Bischof, S., Sommer, F., Kock, S., Ferrick, D. A., Duncan, G. S., Gessner, A., & Mak, T. W. (2002). Dysregulated T helper cell differentiation in the absence of interferon regulatory factor 4. *Proceedings of the National Academy of Sciences*, *99*(18), 11808–11812. https://doi.org/10.1073/pnas.182425099

Lu, G., Middleton, R. E., Sun, H., Naniong, M., Ott, C. J., Mitsiades, C. S., Wong, K.-K., Bradner, J. E., & Kaelin, W. G. (2014). The Myeloma Drug Lenalidomide Promotes the Cereblon-Dependent Destruction of Ikaros Proteins. *Science*, *343*(6168), 305–309. https://doi.org/10.1126/science.1244917

Lu, J., Liang, T., Li, P., & Yin, Q. (2023). Regulatory effects of IRF4 on immune cells in the tumor microenvironment. *Frontiers in Immunology*, *14*. https://doi.org/10.3389/fimmu.2023.1086803

Luckheeram, R. V., Zhou, R., Verma, A. D., & Xia, B. (2012). CD4 $^{+}$ T Cells: Differentiation and Functions. *Clinical and Developmental Immunology*, *2012*, 1–12. https://doi.org/10.1155/2012/925135

Ma, J., Wang, R., Fang, X., Ding, Y., & Sun, Z. (2011). Critical Role of TCF-1 in Repression of the IL-17 Gene. *PLoS ONE*, *6*(9), e24768. https://doi.org/10.1371/journal.pone.0024768

Mahnke, J., Schumacher, V., Ahrens, S., Käding, N., Feldhoff, L. M., Huber, M., Rupp, J., Raczkowski, F., & Mittrücker, H.-W. (2016). Interferon Regulatory Factor 4 controls TH1 cell effector function and metabolism. *Scientific Reports*, *6*(1), 35521. https://doi.org/10.1038/srep35521

Malviya, V., Yshii, L., Junius, S., Garg, A. D., Humblet-Baron, S., & Schlenner, S. M. (2023). Regulatory T-cell stability and functional plasticity in health and disease. *Immunology & Cell Biology*, *101*(2), 112–129. https://doi.org/10.1111/imcb.12613

Man, K., Miasari, M., Shi, W., Xin, A., Henstridge, D. C., Preston, S., Pellegrini, M., Belz, G. T., Smyth, G. K., Febbraio, M. A., Nutt, S. L., & Kallies, A. (2013). The transcription factor IRF4 is essential for TCR affinity–mediated metabolic programming and clonal expansion of T cells. *Nature Immunology*, *14*(11), 1155–1165. https://doi.org/10.1038/ni.2710

Matys, V. (2006). TRANSFAC(R) and its module TRANSCompel(R): transcriptional gene regulation in eukaryotes. *Nucleic Acids Research*, *34*(90001), D108–D110. https://doi.org/10.1093/nar/gkj143

McAllister, K., Yarwood, A., Bowes, J., Orozco, G., Viatte, S., Diogo, D., Hocking, L. J., Steer, S., Wordsworth, P., Wilson, A. G., Morgan, A. W., Kremer, J. M., Pappas, D., Gregersen, P., Klareskog, L., Plenge, R., Barton, A., Greenberg, J., Worthington, J., & Eyre, S. (2013). Brief Report: Identification of *BACH2* and *RAD51B* as Rheumatoid Arthritis Susceptibility Loci in a Meta-Analysis of Genome-Wide Data. *Arthritis & Rheumatism*, *65*(12), 3058–3062. https://doi.org/10.1002/art.38183

Meraro, D., Gleit-Kielmanowicz, M., Hauser, H., & Levi, B.-Z. (2002). IFN-Stimulated Gene 15 Is Synergistically Activated Through Interactions Between the Myelocyte/Lymphocyte-Specific Transcription Factors, PU.1, IFN Regulatory Factor-8/IFN Consensus Sequence Binding Protein, and IFN Regulatory Factor-4: Characterization of a New Subtype of IFN-Stimulated Response Element. *The Journal of Immunology*, *168*(12), 6224–6231. https://doi.org/10.4049/jimmunol.168.12.6224

Messina, N., Fulford, T., O'Reilly, L., Loh, W. X., Motyer, J. M., Ellis, D., McLean, C., Naeem, H., Lin, A., Gugasyan, R., Slattery, R. M., Grumont, R. J., & Gerondakis, S. (2016). The NF-κB transcription factor RelA is required for the tolerogenic function of Foxp3+ regulatory T cells. *Journal of Autoimmunity*, *70*, 52–62. https://doi.org/10.1016/j.jaut.2016.03.017

Mi, H., Muruganujan, A., Casagrande, J. T., & Thomas, P. D. (2013). Large-scale gene function analysis with the PANTHER classification system. *Nature Protocols*, *8*(8), 1551–1566. https://doi.org/10.1038/nprot.2013.092

Mi, H., Muruganujan, A., Ebert, D., Huang, X., & Thomas, P. D. (2019). PANTHER version 14: more genomes, a new PANTHER GO-slim and improvements in enrichment analysis tools. *Nucleic Acids Research*, *47*(D1), D419–D426. https://doi.org/10.1093/nar/gky1038

Mittrücker, H.-W., Matsuyama, T., Grossman, A., Kündig, T. M., Potter, J., Shahinian, A., Wakeham, A., Patterson, B., Ohashi, P. S., & Mak, T. W. (1997). Requirement for the Transcription Factor LSIRF/IRF4 for Mature B and T Lymphocyte Function. *Science*, *275*(5299), 540–543. https://doi.org/10.1126/science.275.5299.540

Mondala, P. K., Vora, A. A., Zhou, T., Lazzari, E., Ladel, L., Luo, X., Kim, Y., Costello, C., MacLeod, A. R., Jamieson, C. H. M., & Crews, L. A. (2021). Selective antisense oligonucleotide inhibition of human IRF4 prevents malignant myeloma regeneration via cell cycle disruption. *Cell Stem Cell*, *28*(4), 623-636.e9. https://doi.org/10.1016/j.stem.2020.12.017

Moorman, H. R., Reategui, Y., Poschel, D. B., & Liu, K. (2022). IRF8: Mechanism of Action and Health Implications. *Cells*, *11*(17), 2630. https://doi.org/10.3390/cells11172630

Mudter, J., Amoussina, L., Schenk, M., Yu, J., Brüstle, A., Weigmann, B., Atreya, R., Wirtz, S., Becker, C., Hoffman, A., Atreya, I., Biesterfeld, S., Galle, P. R., Lehr, H. A., Rose-John, S., Mueller, C., Lohoff, M., & Neurath, M. F. (2008). The transcription factor IFN regulatory factor–4 controls experimental colitis in mice via T cell–derived IL-6. *Journal of Clinical Investigation*. https://doi.org/10.1172/JCI33227

Mudter, J., Yu, J., Zufferey, C., Brüstle, A., Wirtz, S., Weigmann, B., Hoffman, A., Schenk, M., Galle, P. R., Lehr, H. A., Mueller, C., Lohoff, M., & Neurath, M. F. (2011). IRF4 regulates IL-17A promoter activity and controls RORγt-dependent Th17 colitis in vivo. *Inflammatory Bowel Diseases*, *17*(6), 1343–1358. https://doi.org/10.1002/ibd.21476

Murphy, K. (Kenneth M. ., Weaver, C., & Janeway, C. (n.d.). *Janeway's immunobiology* (9th, 2016th ed.).

Nam, S., & Lim, J.-S. (2016). Essential role of interferon regulatory factor 4 (IRF4) in immune cell development. *Archives of Pharmacal Research*, *39*(11), 1548–1555. https://doi.org/10.1007/s12272-016-0854-1

Niers, J. M., Chen, J. W., Weissleder, R., & Tannous, B. A. (2011). Enhanced in Vivo Imaging of Metabolically Biotinylated Cell Surface Reporters. *Analytical Chemistry*, *83*(3), 994–999. https://doi.org/10.1021/ac102758m

Nishibori, T., Tanabe, Y., Su, L., & David, M. (2004). Impaired Development of CD4+ CD25+ Regulatory T Cells in the Absence of STAT1. *Journal of Experimental Medicine*, *199*(1), 25–34. https://doi.org/10.1084/jem.20020509

O'Geen, H., Lin, Y.-H., Xu, X., Echipare, L., Komashko, V. M., He, D., Frietze, S., Tanabe, O., Shi, L., Sartor, M. A., Engel, J. D., & Farnham, P. J. (2010). Genome-wide binding of the orphan nuclear receptor TR4 suggests its general role in fundamental biological processes. *BMC Genomics*, *11*(1), 689. https://doi.org/10.1186/1471-2164-11-689

Ochiai, K., Kondo, H., Okamura, Y., Shima, H., Kurokochi, Y., Kimura, K., Funayama, R., Nagashima, T.,

Nakayama, K., Yui, K., Kinoshita, K., & Igarashi, K. (2018). Zinc finger–IRF composite elements bound by Ikaros/IRF4 complexes function as gene repression in plasma cell. *Blood Advances*, *2*(8), 883–894. https://doi.org/10.1182/bloodadvances.2017010413

Ouyang, X., Zhang, R., Yang, J., Li, Q., Qin, L., Zhu, C., Liu, J., Ning, H., Shin, M. S., Gupta, M., Qi, C.-F., He, J. C., Lira, S. A., Morse, H. C., Ozato, K., Mayer, L., & Xiong, H. (2011). Transcription factor IRF8 directs a silencing programme for TH17 cell differentiation. *Nature Communications*, *2*(1), 314. https://doi.org/10.1038/ncomms1311

Papadopoulou, G., & Xanthou, G. (2022). Metabolic rewiring: a new master of Th17 cell plasticity and heterogeneity. *The FEBS Journal*, *289*(9), 2448–2466. https://doi.org/10.1111/febs.15853

Patsopoulos, N. A., Baranzini, S. E., Santaniello, A., Shoostari, P., Cotsapas, C., Wong, G., Beecham, A. H., James, T., Replogle, J., Vlachos, I. S., McCabe, C., Pers, T. H., Brandes, A., White, C., Keenan, B., Cimpean, M., Winn, P., Panteliadis, I.-P., Robbins, A., … De Jager, P. L. (2019). Multiple sclerosis genomic map implicates peripheral immune cells and microglia in susceptibility. *Science*, *365*(6460). https://doi.org/10.1126/science.aav7188

Patterson, D. G., Kania, A. K., Price, M. J., Rose, J. R., Scharer, C. D., & Boss, J. M. (2021). An IRF4–MYC–mTORC1 Integrated Pathway Controls Cell Growth and the Proliferative Capacity of Activated B Cells during B Cell Differentiation In Vivo. *The Journal of Immunology*, *207*(7), 1798–1811. https://doi.org/10.4049/jimmunol.2100440

Perissi, V., & Rosenfeld, M. G. (2005). Controlling nuclear receptors: the circular logic of cofactor cycles. *Nature Reviews Molecular Cell Biology*, *6*(7), 542–554. https://doi.org/10.1038/nrm1680

Piersimoni, L., Kastritis, P. L., Arlt, C., & Sinz, A. (2022). Cross-Linking Mass Spectrometry for Investigating Protein Conformations and Protein–Protein Interactions–A Method for All Seasons. *Chemical Reviews*, *122*(8), 7500–7531. https://doi.org/10.1021/acs.chemrev.1c00786

Plagnol, V., Howson, J. M. M., Smyth, D. J., Walker, N., Hafler, J. P., Wallace, C., Stevens, H., Jackson, L., Simmonds, M. J., Bingley, P. J., Gough, S. C., & Todd, J. A. (2011). Genome-Wide Association Analysis of Autoantibody Positivity in Type 1 Diabetes Cases. *PLoS Genetics*, *7*(8), e1002216. https://doi.org/10.1371/journal.pgen.1002216

Pollizzi, K. N., & Powell, J. D. (2014). Integrating canonical and metabolic signalling programmes in the regulation of T cell responses. *Nature Reviews Immunology*, *14*(7), 435–446. https://doi.org/10.1038/nri3701

Purvis, H. A., Anderson, A. E., Young, D. A., Isaacs, J. D., & Hilkens, C. M. U. (2014). A Negative Feedback Loop Mediated by STAT3 Limits Human Th17 Responses. *The Journal of Immunology*, *193*(3), 1142–1150. https://doi.org/10.4049/jimmunol.1302467

Quintana, F. J., Basso, A. S., Iglesias, A. H., Korn, T., Farez, M. F., Bettelli, E., Caccamo, M., Oukka, M., & Weiner, H. L. (2008). Control of Treg and TH17 cell differentiation by the aryl hydrocarbon receptor. *Nature*, *453*(7191), 65–71. https://doi.org/10.1038/nature06880

Rafiee, M., Sigismondo, G., Kalxdorf, M., Förster, L., Brügger, B., Béthune, J., & Krijgsveld, J. (2020). Protease-resistant streptavidin for interaction proteomics. *Molecular Systems Biology*, *16*(5). https://doi.org/10.15252/msb.20199370

Reis, B. S., Rogoz, A., Costa-Pinto, F. A., Taniuchi, I., & Mucida, D. (2013). Mutual expression of the transcription factors Runx3 and ThPOK regulates intestinal CD4+ T cell immunity. *Nature Immunology*, *14*(3), 271–280. https://doi.org/10.1038/ni.2518

Rengarajan, J., Mowen, K. A., McBride, K. D., Smith, E. D., Singh, H., & Glimcher, L. H. (2002). Interferon Regulatory Factor 4 (IRF4) Interacts with NFATc2 to Modulate Interleukin 4 Gene Expression. *Journal of Experimental Medicine*, *195*(8), 1003–1012.

https://doi.org/10.1084/jem.20011128

Richer, M. J., Lang, M. L., & Butler, N. S. (2016). T Cell Fates Zipped Up: How the Bach2 Basic Leucine Zipper Transcriptional Repressor Directs T Cell Differentiation and Function. *The Journal of Immunology*, *197*(4), 1009–1015. https://doi.org/10.4049/jimmunol.1600847

Ritchie, M. E., Phipson, B., Wu, D., Hu, Y., Law, C. W., Shi, W., & Smyth, G. K. (2015). limma powers differential expression analyses for RNA-sequencing and microarray studies. *Nucleic Acids Research*, *43*(7), e47–e47. https://doi.org/10.1093/nar/gkv007

Rivera-Reyes, R., Kleppa, M.-J., & Kispert, A. (2018). Proteomic analysis identifies transcriptional cofactors and homeobox transcription factors as TBX18 binding proteins. *PLOS ONE*, *13*(8), e0200964. https://doi.org/10.1371/journal.pone.0200964

Robertson, G., Hirst, M., Bainbridge, M., Bilenky, M., Zhao, Y., Zeng, T., Euskirchen, G., Bernier, B., Varhol, R., Delaney, A., Thiessen, N., Griffith, O. L., He, A., Marra, M., Snyder, M., & Jones, S. (2007). Genome-wide profiles of STAT1 DNA association using chromatin immunoprecipitation and massively parallel sequencing. *Nature Methods*, *4*(8), 651–657. https://doi.org/10.1038/nmeth1068

Rodriguez, P., Braun, H., Kolodziej, K. E., Boer, E. de, Campbell, J., Bonte, E., Grosveld, F., Philipsen, S., & Strouboulis, J. (2006). Isolation of Transcription Factor Complexes by In Vivo Biotinylation Tagging and Direct Binding to Streptavidin Beads. In *Gene Mapping, Discovery, and Expression* (pp. 305–323). Humana Press. https://doi.org/10.1385/1-59745-097-9:305

Rose, A. B. (2004). The effect of intron location on intron-mediated enhancement of gene expression in Arabidopsis. *The Plant Journal*, *40*(5), 744–751. https://doi.org/10.1111/j.1365-313X.2004.02247.x

Rose, A. B. (2019). Introns as Gene Regulators: A Brick on the Accelerator. *Frontiers in Genetics*, *9*. https://doi.org/10.3389/fgene.2018.00672

Rosenbauer, F., Waring, J. F., Foerster, J., Wietstruk, M., Philipp, D., & Horak, I. (1999). Interferon consensus sequence binding protein and interferon regulatory factor-4/Pip form a complex that represses the expression of the interferon-stimulated gene-15 in macrophages. *Blood*, *94*(12), 4274–4281.

Rothhammer, V., & Quintana, F. J. (2019). The aryl hydrocarbon receptor: an environmental sensor integrating immune responses in health and disease. *Nature Reviews Immunology*, *19*(3), 184–197. https://doi.org/10.1038/s41577-019-0125-8

Roux, K. J., Kim, D. I., Raida, M., & Burke, B. (2012). A promiscuous biotin ligase fusion protein identifies proximal and interacting proteins in mammalian cells. *Journal of Cell Biology*, *196*(6), 801–810. https://doi.org/10.1083/jcb.201112098

Roychoudhuri, R., Eil, R. L., Clever, D., Klebanoff, C. A., Sukumar, M., Grant, F. M., Yu, Z., Mehta, G., Liu, H., Jin, P., Ji, Y., Palmer, D. C., Pan, J. H., Chichura, A., Crompton, J. G., Patel, S. J., Stroncek, D., Wang, E., Marincola, F. M., … Restifo, N. P. (2016). The transcription factor BACH2 promotes tumor immunosuppression. *Journal of Clinical Investigation*, *126*(2), 599–604. https://doi.org/10.1172/JCI82884

Roychoudhuri, R., Hirahara, K., Mousavi, K., Clever, D., Klebanoff, C. A., Bonelli, M., Sciumè, G., Zare, H., Vahedi, G., Dema, B., Yu, Z., Liu, H., Takahashi, H., Rao, M., Muranski, P., Crompton, J. G., Punkosdy, G., Bedognetti, D., Wang, E., … Restifo, N. P. (2013). BACH2 represses effector programs to stabilize Treg-mediated immune homeostasis. *Nature*, *498*(7455), 506–510. https://doi.org/10.1038/nature12199

Ruan, Q., & Chen, Y. H. (2012). *Nuclear Factor-κB in Immunity and Inflammation: The Treg and Th17*

Connection (pp. 207–221). https://doi.org/10.1007/978-1-4614-0106-3_12

Ruan, Q., Kameswaran, V., Zhang, Y., Zheng, S., Sun, J., Wang, J., DeVirgiliis, J., Liou, H.-C., Beg, A. A., & Chen, Y. H. (2011). The Th17 immune response is controlled by the Rel–RORγ–RORγT transcriptional axis. *Journal of Experimental Medicine*, *208*(11), 2321–2333. https://doi.org/10.1084/jem.20110462

Rudra, D., deRoos, P., Chaudhry, A., Niec, R. E., Arvey, A., Samstein, R. M., Leslie, C., Shaffer, S. A., Goodlett, D. R., & Rudensky, A. Y. (2012). Transcription factor Foxp3 and its protein partners form a complex regulatory network. *Nature Immunology*, *13*(10), 1010–1019. https://doi.org/10.1038/ni.2402

Saito, M., Gao, J., Basso, K., Kitagawa, Y., Smith, P. M., Bhagat, G., Pernis, A., Pasqualucci, L., & Dalla-Favera, R. (2007). A Signaling Pathway Mediating Downregulation of BCL6 in Germinal Center B Cells Is Blocked by BCL6 Gene Alterations in B Cell Lymphoma. *Cancer Cell*, *12*(3), 280–292. https://doi.org/10.1016/j.ccr.2007.08.011

Sakaguchi, S., Sakaguchi, N., Asano, M., Itoh, M., & Toda, M. (1995). Immunologic self-tolerance maintained by activated T cells expressing IL-2 receptor alpha-chains (CD25). Breakdown of a single mechanism of self-tolerance causes various autoimmune diseases. *Journal of Immunology (Baltimore, Md. : 1950)*, *155*(3), 1151–1164.

Salazar, G., Zlatic, S., Craige, B., Peden, A. A., Pohl, J., & Faundez, V. (2009). Hermansky-Pudlak Syndrome Protein Complexes Associate with Phosphatidylinositol 4-Kinase Type II α in Neuronal and Non-neuronal Cells. *Journal of Biological Chemistry*, *284*(3), 1790–1802. https://doi.org/10.1074/jbc.M805991200

Sanosaka, T., Okuno, H., Mizota, N., Andoh-Noda, T., Sato, M., Tomooka, R., Banno, S., Kohyama, J., & Okano, H. (2022). Chromatin remodeler CHD7 targets active enhancer region to regulate cell type-specific gene expression in human neural crest cells. *Scientific Reports*, *12*(1), 22648. https://doi.org/10.1038/s41598-022-27293-6

Sasikala, M., Ravikanth, V., Murali Manohar, K., Deshpande, N., Singh, S., Pavan Kumar, P., Talukdar, R., Ghosh, S., Aslam, M., Rao, G., Pradeep, R., & Reddy, D. N. (2018). Bach2 repression mediates Th17 cell induced inflammation and associates with clinical features of advanced disease in chronic pancreatitis. *United European Gastroenterology Journal*, *6*(2), 272–282. https://doi.org/10.1177/2050640617716596

Satoh, J., & Tabunoki, H. (2013). A Comprehensive Profile of ChIP-Seq-Based STAT1 Target Genes Suggests the Complexity of STAT1-Mediated Gene Regulatory Mechanisms. *Gene Regulation and Systems Biology*, *7*, GRSB.S11433. https://doi.org/10.4137/GRSB.S11433

Sawcer S, Hellenthal G, Pirinen M, Spencer CC, Patsopoulos NA, & Moutsianas L. (2011). Genetic risk and a primary role for cell-mediated immune mechanisms in multiple sclerosis. *Nature*, *476*(7359), 214–219. https://doi.org/10.1038/nature10251

Schaefer, M. H., Fontaine, J.-F., Vinayagam, A., Porras, P., Wanker, E. E., & Andrade-Navarro, M. A. (2012). HIPPIE: Integrating Protein Interaction Networks with Experiment Based Quality Scores. *PLoS ONE*, *7*(2), e31826. https://doi.org/10.1371/journal.pone.0031826

Schmittgen, T. D., & Livak, K. J. (2008). Analyzing real-time PCR data by the comparative CT method. *Nature Protocols*, *3*(6), 1101–1108. https://doi.org/10.1038/nprot.2008.73

Schraml, B. U., Hildner, K., Ise, W., Lee, W.-L., Smith, W. A.-E., Solomon, B., Sahota, G., Sim, J., Mukasa, R., Cemerski, S., Hatton, R. D., Stormo, G. D., Weaver, C. T., Russell, J. H., Murphy, T. L., & Murphy, K. M. (2009). The AP-1 transcription factor Batf controls TH17 differentiation. *Nature*, *460*(7253), 405–409. https://doi.org/10.1038/nature08114

Schutt, S. D., Bastian, D., Choi, H.-J., Wu, Y., Sofi, M. H., Nguyen, H., Zhang, X., & Yu, X.-Z. (2019). Fli-1 Regulates Multiple T-Cell Subsets during Inflammatory Responses and Experimental Graft-Versus-Host Disease. *Blood*, *134*(Supplement_1), 3201–3201. https://doi.org/10.1182/blood-2019-127577

Schutt, S. D., Wu, Y., Kharel, A., Bastian, D., Choi, H.-J., Hanief Sofi, M., Mealer, C., McDaniel Mims, B., Nguyen, H., Liu, C., Helke, K., Cui, W., Zhang, X., Ben-David, Y., & Yu, X.-Z. (2022). The druggable transcription factor Fli-1 regulates T cell immunity and tolerance in graft-versus-host disease. *Journal of Clinical Investigation*, *132*(21). https://doi.org/10.1172/JCI143950

Segura-Puimedon, M., Borralleras, C., Pérez-Jurado, L. A., & Campuzano, V. (2013). TFII-I regulates target genes in the PI-3K and TGF-β signaling pathways through a novel DNA binding motif. *Gene*, *527*(2), 529–536. https://doi.org/10.1016/j.gene.2013.06.050

Sen, S., Wang, F., Zhang, J., He, Z., Ma, J., Gwack, Y., Xu, J., & Sun, Z. (2018). SRC1 promotes Th17 differentiation by overriding Foxp3 suppression to stimulate RORγt activity in a PKC-θ–dependent manner. *Proceedings of the National Academy of Sciences*, *115*(3). https://doi.org/10.1073/pnas.1717789115

Serasanambati, M., & Chilakapati, S. R. (2016). Function of Nuclear Factor kappa B (NF-kB) in human diseases-A Review. *South Indian Journal Of Biological Sciences*.

Shannon, P., Markiel, A., Ozier, O., Baliga, N. S., Wang, J. T., Ramage, D., Amin, N., Schwikowski, B., & Ideker, T. (2003). Cytoscape: A Software Environment for Integrated Models of Biomolecular Interaction Networks. *Genome Research*, *13*(11), 2498–2504. https://doi.org/10.1101/gr.1239303

Sharma, S., Grandvaux, N., Mamane, Y., Genin, P., Azimi, N., Waldmann, T., & Hiscott, J. (2002). Regulation of IFN Regulatory Factor 4 Expression in Human T Cell Leukemia Virus-I-Transformed T Cells. *The Journal of Immunology*, *169*(6), 3120–3130. https://doi.org/10.4049/jimmunol.169.6.3120

Sheng, Y., Zhang, J., Li, K., Wang, H., Wang, W., Wen, L., Gao, J., Tang, X., Tang, H., Huang, H., Cai, M., Yuan, T., Liu, L., Zheng, X., Zhu, Z., & Cui, Y. (2021). Bach2 overexpression represses Th9 cell differentiation by suppressing IRF4 expression in systemic lupus erythematosus. *FEBS Open Bio*, *11*(2), 395–403. https://doi.org/10.1002/2211-5463.13050

Shetty, A., Tripathi, S. K., Junttila, S., Buchacher, T., Biradar, R., Bhosale, S. D., Envall, T., Laiho, A., Moulder, R., Rasool, O., Galande, S., Elo, L. L., & Lahesmaa, R. (2022). A systematic comparison of FOSL1, FOSL2 and BATF-mediated transcriptional regulation during early human Th17 differentiation. *Nucleic Acids Research*, *50*(9), 4938–4958. https://doi.org/10.1093/nar/gkac256

Shi, L. Z., Wang, R., Huang, G., Vogel, P., Neale, G., Green, D. R., & Chi, H. (2011). HIF1α–dependent glycolytic pathway orchestrates a metabolic checkpoint for the differentiation of TH17 and Treg cells. *Journal of Experimental Medicine*, *208*(7), 1367–1376. https://doi.org/10.1084/jem.20110278

Shimoyama, S., Nakagawa, I., Jiang, J.-J., Matsumoto, I., Chiorini, J. A., Hasegawa, Y., Ohara, O., Hasebe, R., Ota, M., Uchida, M., Kamimura, D., Hojyo, S., Tanaka, Y., Atsumi, T., & Murakami, M. (2021). Sjögren's syndrome-associated SNPs increase GTF2I expression in salivary gland cells to enhance inflammation development. *International Immunology*, *33*(8), 423–434. https://doi.org/10.1093/intimm/dxab025

Shin, B., Benavides, G. A., Geng, J., Koralov, S. B., Hu, H., Darley-Usmar, V. M., & Harrington, L. E. (2020). Mitochondrial Oxidative Phosphorylation Regulates the Fate Decision between Pathogenic Th17 and Regulatory T Cells. *Cell Reports*, *30*(6), 1898-1909.e4. https://doi.org/10.1016/j.celrep.2020.01.022

Sidwell, T., Liao, Y., Garnham, A. L., Vasanthakumar, A., Gloury, R., Blume, J., Teh, P. P., Chisanga, D., Thelemann, C., de Labastida Rivera, F., Engwerda, C. R., Corcoran, L., Kometani, K., Kurosaki, T., Smyth, G. K., Shi, W., & Kallies, A. (2020). Attenuation of TCR-induced transcription by Bach2 controls regulatory T cell differentiation and homeostasis. *Nature Communications*, *11*(1), 252. https://doi.org/10.1038/s41467-019-14112-2

Sielaff, M., Kuharev, J., Bohn, T., Hahlbrock, J., Bopp, T., Tenzer, S., & Distler, U. (2017). Evaluation of FASP, SP3, and iST Protocols for Proteomic Sample Preparation in the Low Microgram Range. *Journal of Proteome Research*, *16*(11), 4060–4072. https://doi.org/10.1021/acs.jproteome.7b00433

Singh, N. P., Singh, U. P., Rouse, M., Zhang, J., Chatterjee, S., Nagarkatti, P. S., & Nagarkatti, M. (2016). Dietary Indoles Suppress Delayed-Type Hypersensitivity by Inducing a Switch from Proinflammatory Th17 Cells to Anti-Inflammatory Regulatory T Cells through Regulation of MicroRNA. *The Journal of Immunology*, *196*(3), 1108–1122. https://doi.org/10.4049/jimmunol.1501727

Singh, N. P., Singh, U. P., Singh, B., Price, R. L., Nagarkatti, M., & Nagarkatti, P. S. (2011). Activation of Aryl Hydrocarbon Receptor (AhR) Leads to Reciprocal Epigenetic Regulation of FoxP3 and IL-17 Expression and Amelioration of Experimental Colitis. *PLoS ONE*, *6*(8), e23522. https://doi.org/10.1371/journal.pone.0023522

Smith, A. L., Friedman, D. B., Yu, H., Carnahan, R. H., & Reynolds, A. B. (2011). ReCLIP (Reversible Cross-Link Immuno-Precipitation): An Efficient Method for Interrogation of Labile Protein Complexes. *PLoS ONE*, *6*(1), e16206. https://doi.org/10.1371/journal.pone.0016206

Smits, A. H., & Vermeulen, M. (2016). Characterizing Protein–Protein Interactions Using Mass Spectrometry: Challenges and Opportunities. *Trends in Biotechnology*, *34*(10), 825–834. https://doi.org/10.1016/j.tibtech.2016.02.014

Soler, E., Andrieu-Soler, C., Boer, E. de, Bryne, J. C., Thongjuea, S., Rijkers, E., Demmers, J., van IJcken, W., & Grosveld, F. (2011). A systems approach to analyze transcription factors in mammalian cells. *Methods*, *53*(2), 151–162. https://doi.org/10.1016/j.ymeth.2010.08.002

St-Germain, J. R., Samavarchi Tehrani, P., Wong, C., Larsen, B., Gingras, A. C., & Raught, B. (2020). Variability in Streptavidin-Sepharose Matrix Quality Can Significantly Affect Proximity-Dependent Biotinylation (BioID) Data. *Journal of Proteome Research*, *19*(8), 3554–3561. https://doi.org/10.1021/acs.jproteome.0c00117

Stadler, S. C., Polanetz, R., Meier, S., Mayerhofer, P. U., Herrmann, J. M., Anslinger, K., Roscher, A. A., Röschinger, W., & Holzinger, A. (2005). Mitochondrial targeting signals and mature peptides of 3-methylcrotonyl-CoA carboxylase. *Biochemical and Biophysical Research Communications*, *334*(3), 939–946. https://doi.org/10.1016/j.bbrc.2005.06.190

Staudt, V., Bothur, E., Klein, M., Lingnau, K., Reuter, S., Grebe, N., Gerlitzki, B., Hoffmann, M., Ulges, A., Taube, C., Dehzad, N., Becker, M., Stassen, M., Steinborn, A., Lohoff, M., Schild, H., Schmitt, E., & Bopp, T. (2010). Interferon-Regulatory Factor 4 Is Essential for the Developmental Program of T Helper 9 Cells. *Immunity*, *33*(2), 192–202. https://doi.org/10.1016/j.immuni.2010.07.014

Stockinger, B., & Omenetti, S. (2017). The dichotomous nature of T helper 17 cells. *Nature Reviews Immunology*, *17*(9), 535–544. https://doi.org/10.1038/nri.2017.50

Sugai, M., Aoki, K., Osato, M., Nambu, Y., Ito, K., Taketo, M. M., & Shimizu, A. (2011). Runx3 Is Required for Full Activation of Regulatory T Cells To Prevent Colitis-Associated Tumor Formation. *The Journal of Immunology*, *186*(11), 6515–6520. https://doi.org/10.4049/jimmunol.1001671

Sun, D., Luo, F., Xing, J., Zhang, F., Xu, J., & Zhang, Z. (2018). 1,25(<scp>OH</scp>) $_2$ D $_3$ inhibited

Th17 cells differentiation via regulating the <scp>NF</scp> -κB activity and expression of <scp>IL</scp> -17. *Cell Proliferation*, *51*(5). https://doi.org/10.1111/cpr.12461

Sun, J., Yi, S., Qiu, L., Fu, W., Wang, A., Liu, F., Wang, L., Wang, T., Chen, H., Wang, L., Kadin, M. E., Tu, P., & Wang, Y. (2018). SATB1 Defines a Subtype of Cutaneous CD30+ Lymphoproliferative Disorders Associated with a T-Helper 17 Cytokine Profile. *Journal of Investigative Dermatology*, *138*(8), 1795–1804. https://doi.org/10.1016/j.jid.2018.02.028

Sun, L., Fu, J., & Zhou, Y. (2017). Metabolism Controls the Balance of Th17/T-Regulatory Cells. *Frontiers in Immunology*, *8*. https://doi.org/10.3389/fimmu.2017.01632

Sundararaj, K. P., Thiyagarajan, T., Molano, I., Basher, F., Powers, T. W., Drake, R. R., & Nowling, T. K. (2015). FLI1 Levels Impact CXCR3 Expression and Renal Infiltration of T Cells and Renal Glycosphingolipid Metabolism in the MRL/lpr Lupus Mouse Strain. *The Journal of Immunology*, *195*(12), 5551–5560. https://doi.org/10.4049/jimmunol.1500961

Sundararaj, S., & Casarotto, M. G. (2021). Molecular interactions of IRF4 in B cell development and malignancies. *Biophysical Reviews*, *13*(6), 1219–1227. https://doi.org/10.1007/s12551-021-00825-6

Sundararaj, S., Seneviratne, S., Williams, S. J., Enders, A., & Casarotto, M. G. (2021). Structural determinants of the IRF4/DNA homodimeric complex. *Nucleic Acids Research*, *49*(4), 2255–2265. https://doi.org/10.1093/nar/gkaa1287

Szklarczyk, D., Gable, A. L., Lyon, D., Junge, A., Wyder, S., Huerta-Cepas, J., Simonovic, M., Doncheva, N. T., Morris, J. H., Bork, P., Jensen, L. J., & Mering, C. von. (2019). STRING v11: protein–protein association networks with increased coverage, supporting functional discovery in genome-wide experimental datasets. *Nucleic Acids Research*, *47*(D1), D607–D613. https://doi.org/10.1093/nar/gky1131

Taams, L. S., Palmer, D. B., Akbar, A. N., Robinson, D. S., Brown, Z., & Hawrylowicz, C. M. (2006). Regulatory T cells in human disease and their potential for therapeutic manipulation. *Immunology*, *118*(1), 1–9. https://doi.org/10.1111/j.1365-2567.2006.02348.x

Tesmer, L. A., Lundy, S. K., Sarkar, S., & Fox, D. A. (2008). Th17 cells in human disease. *Immunological Reviews*, *223*(1), 87–113. https://doi.org/10.1111/j.1600-065X.2008.00628.x

Thouenon, R., Chentout, L., Moreno-Corona, N., Poggi, L., Lombardi, E. P., Hoareau, B., Schmitt, Y., Lagresle-Peyrou, C., Bustamante, J., André, I., Cavazzana, M., Durandy, A., Casanova, J.-L., Galicier, L., Fadlallah, J., Fischer, A., & Kracker, S. (2023). A neomorphic mutation in the interferon activation domain of IRF4 causes a dominant primary immunodeficiency. *Journal of Experimental Medicine*, *220*(6). https://doi.org/10.1084/jem.20221292

Titeca, K., Lemmens, I., Tavernier, J., & Eyckerman, S. (2019). Discovering cellular protein-protein interactions: Technological strategies and opportunities. *Mass Spectrometry Reviews*, *38*(1), 79–111. https://doi.org/10.1002/mas.21574

Tominaga, N. (2003). Development of Th1 and not Th2 immune responses in mice lacking IFN-regulatory factor-4. *International Immunology*, *15*(1), 1–10. https://doi.org/10.1093/intimm/dxg001

UCSC Genome Browser Group. (2023). *Lift Genome Annotations* . https://genome.ucsc.edu/cgi-bin/hgLiftOver

van der Veeken, J., Glasner, A., Zhong, Y., Hu, W., Wang, Z.-M., Bou-Puerto, R., Charbonnier, L.-M., Chatila, T. A., Leslie, C. S., & Rudensky, A. Y. (2020). The Transcription Factor Foxp3 Shapes Regulatory T Cell Identity by Tuning the Activity of trans-Acting Intermediaries. *Immunity*, *53*(5), 971-984.e5. https://doi.org/10.1016/j.immuni.2020.10.010

Vanderbilt University Medical Center. (2023). *My cancer genome*. https://www.mycancergenome.org/content/gene/irf4/

Varnaitė, R., & MacNeill, S. A. (2016). Meet the neighbors: Mapping local protein interactomes by proximity-dependent labeling with BioID. *PROTEOMICS*, *16*(19), 2503–2518. https://doi.org/10.1002/pmic.201600123

Vasanthakumar, A., Liao, Y., Teh, P., Pascutti, M. F., Oja, A. E., Garnham, A. L., Gloury, R., Tempany, J. C., Sidwell, T., Cuadrado, E., Tuijnenburg, P., Kuijpers, T. W., Lalaoui, N., Mielke, L. A., Bryant, V. L., Hodgkin, P. D., Silke, J., Smyth, G. K., Nolte, M. A., … Kallies, A. (2017). The TNF Receptor Superfamily-NF-κB Axis Is Critical to Maintain Effector Regulatory T Cells in Lymphoid and Non-lymphoid Tissues. *Cell Reports*, *20*(12), 2906–2920. https://doi.org/10.1016/j.celrep.2017.08.068

Vastrik, I., D'Eustachio, P., Schmidt, E., Joshi-Tope, G., Gopinath, G., Croft, D., de Bono, B., Gillespie, M., Jassal, B., Lewis, S., Matthews, L., Wu, G., Birney, E., & Stein, L. (2007). Reactome: a knowledge base of biologic pathways and processes. *Genome Biology*, *8*(3), R39. https://doi.org/10.1186/gb-2007-8-3-r39

Veldhoen, M. (2010). Interferon Regulatory Factor 4: Combinational Control of Lymphocyte Differentiation. *Immunity*, *33*(2), 141–143. https://doi.org/10.1016/j.immuni.2010.08.007

Veldhoen, M., Hocking, R. J., Atkins, C. J., Locksley, R. M., & Stockinger, B. (2006). TGFβ in the Context of an Inflammatory Cytokine Milieu Supports De Novo Differentiation of IL-17-Producing T Cells. *Immunity*, *24*(2), 179–189. https://doi.org/10.1016/j.immuni.2006.01.001

Vistica Barbara P., Shi Guangpu, Nugent Lindsey, Tan Cuiyan, Altman Amnon, & Gery Igal. (2012). SLAT/Def6 plays a critical role in the pathogenic process of experimental autoimmune uveitis (EAU). *Molecular Vision*. http://www.molvis.org/molvis/v18/a192

Wang, D., Diao, H., Getzler, A. J., Rogal, W., Frederick, M. A., Milner, J., Yu, B., Crotty, S., Goldrath, A. W., & Pipkin, M. E. (2018). The Transcription Factor Runx3 Establishes Chromatin Accessibility of cis-Regulatory Landscapes that Drive Memory Cytotoxic T Lymphocyte Formation. *Immunity*, *48*(4), 659-674.e6. https://doi.org/10.1016/j.immuni.2018.03.028

Wang, L.-H., Aberin, M. A. E., Wu, S., & Wang, S.-P. (2021). The MLL3/4 H3K4 methyltransferase complex in establishing an active enhancer landscape. *Biochemical Society Transactions*, *49*(3), 1041–1054. https://doi.org/10.1042/BST20191164

Wang, L., Beier, U. H., Akimova, T., Dahiya, S., Han, R., Samanta, A., Levine, M. H., & Hancock, W. W. (2018). Histone/protein deacetylase inhibitor therapy for enhancement of Foxp3+ T-regulatory cell function posttransplantation. *American Journal of Transplantation*, *18*(7), 1596–1603. https://doi.org/10.1111/ajt.14749

Wang, M., Okamoto, M., Domenico, J., Han, J., Ashino, S., Shin, Y. S., & Gelfand, E. W. (2012). Inhibition of Pim1 kinase prevents peanut allergy by enhancing Runx3 expression and suppressing TH2 and TH17 T-cell differentiation. *Journal of Allergy and Clinical Immunology*, *130*(4), 932-944.e12. https://doi.org/10.1016/j.jaci.2012.07.032

Wang, Q., Li, M., Wu, T., Zhan, L., Li, L., Chen, M., Xie, W., Xie, Z., Hu, E., Xu, S., & Yu, G. (2022). Exploring Epigenomic Datasets by ChIPseeker. *Current Protocols*, *2*(10). https://doi.org/10.1002/cpz1.585

Wang, S., Wang, Y., Yu, C., Cao, Y., Yu, Y., Pan, Y., Su, D., Lu, Q., Yang, W., Zuo, Y., & Yang, L. (2020). Characterization of the relationship between FLI1 and immune infiltrate level in tumour immune microenvironment for breast cancer. *Journal of Cellular and Molecular Medicine*, *24*(10), 5501–5514. https://doi.org/10.1111/jcmm.15205

Wang, X., Lennard Richard, M., Li, P., Henry, B., Schutt, S., Yu, X.-Z., Fan, H., Zhang, W., Gilkeson, G., & Zhang, X. K. (2021). Expression of GM-CSF Is Regulated by Fli-1 Transcription Factor, a Potential Drug Target. *The Journal of Immunology*, *206*(1), 59–66. https://doi.org/10.4049/jimmunol.2000664

Wang, Z., Wang, P., Li, Y., Peng, H., Zhu, Y., Mohandas, N., & Liu, J. (2021). Interplay between cofactors and transcription factors in hematopoiesis and hematological malignancies. *Signal Transduction and Targeted Therapy*, *6*(1), 24. https://doi.org/10.1038/s41392-020-00422-1

Wei, B., Baker, S., Wieckiewicz, J., & Wood, K. J. (2010). IFN-γ Triggered STAT1-PKB/AKT Signalling Pathway Influences the Function of Alloantigen Reactive Regulatory T Cells. *American Journal of Transplantation*, *10*(1), 69–80. https://doi.org/10.1111/j.1600-6143.2009.02858.x

Wei, W., Song, Z., Chiba, M., Wu, W., Jeong, S., Zhang, J.-P., Kadin, M. E., Nakagawa, M., & Yang, Y. (2023). Analysis and therapeutic targeting of the EP300 and CREBBP acetyltransferases in anaplastic large cell lymphoma and Hodgkin lymphoma. *Leukemia*, *37*(2), 396–407. https://doi.org/10.1038/s41375-022-01774-z

Wexler, I. D., Kerr, D. S., Du, Y., Kaung, M. M., Stephenson, W., Lusk, M. M., Wappner, R. S., & Higgins, J. J. (1998). Molecular Characterization of Pyruvate Carboxylase Deficiency in Two Consanguineous Families. *Pediatric Research*, *43*(5), 579–584. https://doi.org/10.1203/00006450-199805000-00004

Williams, L. M., & Rudensky, A. Y. (2007). Maintenance of the Foxp3-dependent developmental program in mature regulatory T cells requires continued expression of Foxp3. *Nature Immunology*, *8*(3), 277–284. https://doi.org/10.1038/ni1437

Wong, R. W. J., Ong, J. Z. L., Theardy, M. S., & Sanda, T. (2022). IRF4 as an Oncogenic Master Transcription Factor. *Cancers*, *14*(17), 4314. https://doi.org/10.3390/cancers14174314

Wu, G., Feng, X., & Stein, L. (2010). A human functional protein interaction network and its application to cancer data analysis. *Genome Biology*, *11*(5), R53. https://doi.org/10.1186/gb-2010-11-5-r53

Wu, Q., Nie, J., Gao, Y., Xu, P., Sun, Q., Yang, J., Han, L., Chen, Z., Wang, X., Lv, L., Tsun, A., Shen, J., & Li, B. (2015). Reciprocal regulation of RORγt acetylation and function by p300 and HDAC1. *Scientific Reports*, *5*(1), 16355. https://doi.org/10.1038/srep16355

Xiao, F., Rui, K., Han, M., Zou, L., Huang, E., Tian, J., Zhang, L., Jiang, Q., Wu, Y., & Lu, L. (2022). Artesunate suppresses Th17 response via inhibiting IRF4-mediated glycolysis and ameliorates Sjoğren's syndrome. *Signal Transduction and Targeted Therapy*, *7*(1), 274. https://doi.org/10.1038/s41392-022-01103-x

Xu, J., Liao, L., Ning, G., Yoshida-Komiya, H., Deng, C., & O'Malley, B. W. (2000). The steroid receptor coactivator SRC-3 (p/CIP/RAC3/AIB1/ACTR/TRAM-1) is required for normal growth, puberty, female reproductive function, and mammary gland development. *Proceedings of the National Academy of Sciences*, *97*(12), 6379–6384. https://doi.org/10.1073/pnas.120166297

Xu, L., Kitani, A., Fuss, I., & Strober, W. (2007). Cutting Edge: Regulatory T Cells Induce $CD4^+$ $CD25^-$ $Foxp3^-$ T Cells or Are Self-Induced to Become Th17 Cells in the Absence of Exogenous TGF-β. *The Journal of Immunology*, *178*(11), 6725–6729. https://doi.org/10.4049/jimmunol.178.11.6725

Xu, T., Stewart, K. M., Wang, X., Liu, K., Xie, M., Ryu, J. K., Li, K., Ma, T., Wang, H., Ni, L., Zhu, S., Cao, N., Zhu, D., Zhang, Y., Akassoglou, K., Dong, C., Driggers, E. M., & Ding, S. (2017). Metabolic control of TH17 and induced Treg cell balance by an epigenetic mechanism. *Nature*, *548*(7666), 228–233. https://doi.org/10.1038/nature23475

Xu, W.-D., Pan, H.-F., Ye, D.-Q., & Xu, Y. (2012). Targeting IRF4 in autoimmune diseases. *Autoimmunity Reviews*, *11*(12), 918–924. https://doi.org/10.1016/j.autrev.2012.08.011

Yanai, H., Negishi, H., & Taniguchi, T. (2012). The IRF family of transcription factors inception, impact and implications in oncogenesis. *OncoImmunology*, *1*(8), 1376–1386. https://doi.org/10.4161/onci.22475

Yang, B.-H., Wang, K., Wan, S., Liang, Y., Yuan, X., Dong, Y., Cho, S., Xu, W., Jepsen, K., Feng, G.-S., Lu, L.-F., Xue, H.-H., & Fu, W. (2019). TCF1 and LEF1 Control Treg Competitive Survival and Tfr Development to Prevent Autoimmune Diseases. *Cell Reports*, *27*(12), 3629-3645.e6. https://doi.org/10.1016/j.celrep.2019.05.061

Yang, X. O., Nurieva, R., Martinez, G. J., Kang, H. S., Chung, Y., Pappu, B. P., Shah, B., Chang, S. H., Schluns, K. S., Watowich, S. S., Feng, X.-H., Jetten, A. M., & Dong, C. (2008a). Molecular Antagonism and Plasticity of Regulatory and Inflammatory T Cell Programs. *Immunity*, *29*(1), 44–56. https://doi.org/10.1016/j.immuni.2008.05.007

Yang, X. O., Nurieva, R., Martinez, G. J., Kang, H. S., Chung, Y., Pappu, B. P., Shah, B., Chang, S. H., Schluns, K. S., Watowich, S. S., Feng, X.-H., Jetten, A. M., & Dong, C. (2008b). Molecular antagonism and plasticity of regulatory and inflammatory T cell programs. *Immunity*, *29*(1), 44–56. https://doi.org/10.1016/j.immuni.2008.05.007

Yasuda, K., Kitagawa, Y., Kawakami, R., Isaka, Y., Watanabe, H., Kondoh, G., Kohwi-Shigematsu, T., Sakaguchi, S., & Hirota, K. (2019). Satb1 regulates the effector program of encephalitogenic tissue Th17 cells in chronic inflammation. *Nature Communications*, *10*(1), 549. https://doi.org/10.1038/s41467-019-08404-w

Yu, G., Wang, L.-G., & He, Q.-Y. (2015). ChIPseeker: an R/Bioconductor package for ChIP peak annotation, comparison and visualization. *Bioinformatics*, *31*(14), 2382–2383. https://doi.org/10.1093/bioinformatics/btv145

Yu, Q., Sharma, A., Ghosh, A., & Sen, J. M. (2011). T Cell Factor-1 Negatively Regulates Expression of IL-17 Family of Cytokines and Protects Mice from Experimental Autoimmune Encephalomyelitis. *The Journal of Immunology*, *186*(7), 3946–3952. https://doi.org/10.4049/jimmunol.1003497

Yu, S., Zhou, X., Steinke, F. C., Liu, C., Chen, S.-C., Zagorodna, O., Jing, X., Yokota, Y., Meyerholz, D. K., Mullighan, C. G., Knudson, C. M., Zhao, D.-M., & Xue, H.-H. (2012). The TCF-1 and LEF-1 Transcription Factors Have Cooperative and Opposing Roles in T Cell Development and Malignancy. *Immunity*, *37*(5), 813–826. https://doi.org/10.1016/j.immuni.2012.08.009

Zeng, W., Chen, S., Cui, X., Chen, X., Gao, Z., & Jiang, R. (2021). SilencerDB: a comprehensive database of silencers. *Nucleic Acids Research*, *49*(D1), D221–D228. https://doi.org/10.1093/nar/gkaa839

Zhang, L., Rayner, S., Katoku-Kikyo, N., Romanova, L., & Kikyo, N. (2007). Successful co-immunoprecipitation of Oct4 and Nanog using cross-linking. *Biochemical and Biophysical Research Communications*, *361*(3), 611–614. https://doi.org/10.1016/j.bbrc.2007.07.089

Zhang, L., Wax, J., Huang, R., Petersen, F., & Yu, X. (2022). Meta-Analysis and Systematic Review of the Association between a Hypoactive NCF1 Variant and Various Autoimmune Diseases. *Antioxidants*, *11*(8), 1589. https://doi.org/10.3390/antiox11081589

Zhang, L., Zhang, J., Ma, Y., Chen, J., Dong, B., Zhao, W., Wang, X., Zheng, Q., Fang, F., & Yang, Y. (2015). Testicular orphan receptor 4 (TR4) is a marker for metastasis and poor prognosis in non-small cell lung cancer that drives the EMT phenotype. *Lung Cancer*, *89*(3), 320–328. https://doi.org/10.1016/j.lungcan.2015.06.007

Zhang, X., Smits, A. H., van Tilburg, G. B., Ovaa, H., Huber, W., & Vermeulen, M. (2018). Proteome-

wide identification of ubiquitin interactions using UbIA-MS. *Nature Protocols*, *13*(3), 530–550. https://doi.org/10.1038/nprot.2017.147

Zhang, Y., & Dufau, M. L. (2004). *Gene Silencing by Nuclear Orphan Receptors* (pp. 1–48). https://doi.org/10.1016/S0083-6729(04)68001-0

Zhang, Y., Zeng, X., Zha, X., Lai, J., Tan, G., Chen, S., Yu, X., Li, Y., & Xu, L. (2022). Correlation of the transcription factors *IRF4* and *BACH2* with the abnormal *NFATC1* expression in T cells from chronic myeloid leukemia patients. *Hematology*, *27*(1), 523–529. https://doi.org/10.1080/16078454.2022.2066245

Zhang, Y., Zhao, M., Sawalha, A. H., Richardson, B., & Lu, Q. (2013). Impaired DNA methylation and its mechanisms in CD4+T cells of systemic lupus erythematosus. *Journal of Autoimmunity*, *41*, 92–99. https://doi.org/10.1016/j.jaut.2013.01.005

Zhao, M., Sun, Y., Gao, F., Wu, X., Tang, J., Yin, H., Luo, Y., Richardson, B., & Lu, Q. (2010). Epigenetics and SLE: RFX1 downregulation causes CD11a and CD70 overexpression by altering epigenetic modifications in lupus CD4+ T cells. *Journal of Autoimmunity*, *35*(1), 58–69. https://doi.org/10.1016/j.jaut.2010.02.002

Zhao, M., Tan, Y., Peng, Q., Huang, C., Guo, Y., Liang, G., Zhu, B., Huang, Y., Liu, A., Wang, Z., Li, M., Gao, X., Wu, R., Wu, H., Long, H., & Lu, Q. (2018a). IL-6/STAT3 pathway induced deficiency of RFX1 contributes to Th17-dependent autoimmune diseases via epigenetic regulation. *Nature Communications*, *9*(1), 1–14. https://doi.org/10.1038/s41467-018-02890-0

Zhao, M., Tan, Y., Peng, Q., Huang, C., Guo, Y., Liang, G., Zhu, B., Huang, Y., Liu, A., Wang, Z., Li, M., Gao, X., Wu, R., Wu, H., Long, H., & Lu, Q. (2018b). IL-6/STAT3 pathway induced deficiency of RFX1 contributes to Th17-dependent autoimmune diseases via epigenetic regulation. *Nature Communications*, *9*(1), 583. https://doi.org/10.1038/s41467-018-02890-0

Zheng, Y., Chaudhry, A., Kas, A., deRoos, P., Kim, J. M., Chu, T.-T., Corcoran, L., Treuting, P., Klein, U., & Rudensky, A. Y. (2009). Regulatory T-cell suppressor program co-opts transcription factor IRF4 to control TH2 responses. *Nature*, *458*(7236), 351–356. https://doi.org/10.1038/nature07674

Zheng, Y., Josefowicz, S. Z., Kas, A., Chu, T.-T., Gavin, M. A., & Rudensky, A. Y. (2007). Genome-wide analysis of Foxp3 target genes in developing and mature regulatory T cells. *Nature*, *445*(7130), 936–940. https://doi.org/10.1038/nature05563

Zhong, W.-J., Xu, X., Zhu, Z.-G., Du, Q.-H., Du, H., Yang, L., Ling, Y.-Y., Xiong, H.-B., & Li, Q.-S. (2017). Increased expression of IRF8 in tumor cells inhibits the generation of Th17 cells and predicts unfavorable survival of diffuse large B cell lymphoma patients. *Oncotarget*, *8*(30), 49757–49772. https://doi.org/10.18632/oncotarget.17693

Zhou, L., Chong, M. M. W., & Littman, D. R. (2009). Plasticity of CD4+ T Cell Lineage Differentiation. *Immunity*, *30*(5), 646–655. https://doi.org/10.1016/j.immuni.2009.05.001

Zhou, L., & Littman, D. R. (2009). Transcriptional regulatory networks in Th17 cell differentiation. *Current Opinion in Immunology*, *21*(2), 146–152. https://doi.org/10.1016/j.coi.2009.03.001

Zhou, L., Lopes, J. E., Chong, M. M. W., Ivanov, I. I., Min, R., Victora, G. D., Shen, Y., Du, J., Rubtsov, Y. P., Rudensky, A. Y., Ziegler, S. F., & Littman, D. R. (2008). TGF-β-induced Foxp3 inhibits TH17 cell differentiation by antagonizing RORγt function. *Nature*, *453*(7192), 236–240. https://doi.org/10.1038/nature06878

Zhou, L., Zhang, M., Wang, Y., Dorfman, R. G., Liu, H., Yu, T., Chen, X., Tang, D., Xu, L., Yin, Y., Pan, Y., Zhou, Q., Zhou, Y., & Yu, C. (2018). Faecalibacterium prausnitzii Produces Butyrate to Maintain Th17/Treg Balance and to Ameliorate Colorectal Colitis by Inhibiting Histone Deacetylase 1. *Inflammatory Bowel Diseases*, *24*(9), 1926–1940. https://doi.org/10.1093/ibd/izy182

Zhu, J., & Paul, W. E. (2010). Heterogeneity and plasticity of T helper cells. *Cell Research*, *20*(1), 4–12. https://doi.org/10.1038/cr.2009.138

Zhu, L. J. (2013). *Integrative Analysis of ChIP-Chip and ChIP-Seq Dataset* (pp. 105–124). https://doi.org/10.1007/978-1-62703-607-8_8

Zhu, L. J., Gazin, C., Lawson, N. D., Pagès, H., Lin, S. M., Lapointe, D. S., & Green, M. R. (2010). ChIPpeakAnno: a Bioconductor package to annotate ChIP-seq and ChIP-chip data. *BMC Bioinformatics*, *11*(1), 237. https://doi.org/10.1186/1471-2105-11-237

Zhu, X., & Zhu, J. (2020). CD4 T Helper Cell Subsets and Related Human Immunological Disorders. *International Journal of Molecular Sciences*, *21*(21), 8011. https://doi.org/10.3390/ijms21218011

Zhu, Y., Wang, W., & Wang, X. (2015). Roles of transcriptional factor 7 in production of inflammatory factors for lung diseases. *Journal of Translational Medicine*, *13*(1), 273. https://doi.org/10.1186/s12967-015-0617-7

Ziembik, M. A., Bender, T. P., Larner, J. M., & Brautigan, D. L. (2017). Functions of protein phosphatase-6 in NF-κB signaling and in lymphocytes. *Biochemical Society Transactions*, *45*(3), 693–701. https://doi.org/10.1042/BST201601

IX. APPENDIX

S Table 1: List of IRF4 interactors in Th17 and Treg cells with additional information from other (IRF4) studies (proteome, IRF4 ChIP-seq, *Irf4*$^{-/-}$)

Protein name	Gene name	Interactome	Proteome	ChIP-seq (Promoter)	ChIP-seq (Motif)	*Irf4*$^{-/-}$ analysis (*Irf4*$^{-/-}$ vs WT D3)	*Irf4*$^{-/-}$ analysis (D0 vs D3)
1433T	*Ywhaq*	Core (log_2=-0.15)	ns (log_2=-0.40)	-	-	ns	ns
2AAA	*Ppp2r1a*	Core (log_2=0.47)	ns (log_2=0.03)	Th17	-	ns	ns
3BP1	*Sh3bp1*	Core (log_2=-0.11)	ns (log_2=0.30)	Th17	-	ns	naïve cells: Th17 WT/*Irf4*$^{-/-}$, Treg WT/*Irf4*$^{-/-}$
ABLM1	*Ablim1*	Th17 enriched** (log_2=1.17)	Th17 enriched (log_2=0.88)	-	-	Th17 WT	naïve cells: Th17 WT/*Irf4*$^{-/-}$, Treg WT/*Irf4*$^{-/-}$
ACAP1	*Acap1*	Th17 enriched** (log_2=0.96)	ns (log_2=0.33)	Th17	-	ns	ns
ACL6A	*Actl6a*	Core (log_2=0.09)	ns (log_2=-0.02)	Th17, Treg	-	ns	ns
ADNP	*Adnp*	Core (log_2=0.25)	ns (log_2=0.11)	Th17	-	ns	differentiated cells: Th17 WT/*Irf4*$^{-/-}$, Treg WT/*Irf4*$^{-/-}$
ADPRH	*Adprh*	Core (log_2=-0.44)	ns (log_2=-0.30)	Th17	-	ns	differentiated cells: Th17 WT/*Irf4*$^{-/-}$, Treg WT/*Irf4*$^{-/-}$
AGO2	*Ago2*	Core (log_2=-0.13)	ns (log_2=-0.06)	Th17		ns	naïve cells: Treg WT/ *Irf4*$^{-/-}$
AHR	*Ahr*	Th17 enriched** (log_2=5.32)	Th17 enriched (log_2=2.21)	Th17	TRANSFAC: Th17	Th17 WT	differentiated cells: Th17 WT/*Irf4*$^{-/-}$
AIP	*Aip*	Core (log_2=-0.08)	ns (log_2=0.37)	Th17	-	ns	ns
AKAP8	*Akap8*	Core (log_2=0.38)	ns (log_2=0.01)	-	-	ns	ns
AKP13	*Akap13*	Core (log_2=0.49)	ns (log_2=-0.20)	Th17	-	Th17 *Irf4*$^{-/-}$, Treg *Irf4*$^{-/-}$	naïve cells: Th17 WT
AMRA1	*Ambra1*	Core (log_2=0.29)	ns (log_2=0.07)	Th17, Treg	-	ns	ns
AN32B	*Anp32b*	Core (log_2=0.36)	ns (log_2=0.20)	Th17	-	ns	ns
ANM1	*Prmt1*	Core (log_2=0.28)	ns (log_2=0.29)	-	-	ns	ns
APC1	*Anapc1*	Th17 enriched (log_2=1.07)	ns (log_2=0.08)	-	-	ns	differentiated cells: Th17 WT, Treg *Irf4*$^{-/-}$
APC4	*Anapc4*	Core (log_2=0.39)	ns (log_2=0.14)	Th17	-	ns	differentiated cells: Th17 *Irf4*$^{-/-}$, Treg *Irf4*$^{-/-}$
ARBK1	*Grk2*	Treg enriched (log_2=-0.67)	ns (log_2=-0.05)	Th17, Treg	-	Th17 WT, Treg WT	naïve cells: Th17 *Irf4*$^{-/-}$, Treg *Irf4*$^{-/-}$
ARFG2	*Arfgap2*	Core (log_2=0.37)	ns (log_2=0.08)	-	-	ns	differentiated cells: Th17 WT/*Irf4*$^{-/-}$, Treg WT/*Irf4*$^{-/-}$
ARHG2	*Arhgef2*	Core (log_2=-0.23)	ns (log_2=-0.19)	Th17	-	ns	differentiated cells: Th17 WT/*Irf4*$^{-/-}$, Treg WT/*Irf4*$^{-/-}$
ARHG6	*Arhgef6*	Core (log_2=0.24)	ns (log_2=0.29)	-	-	ns	naïve cells: Th17 *Irf4*$^{-/-}$, Treg WT/ *Irf4*$^{-/-}$
ARI1A	*Arid1a*	Core (log_2=0.26)	ns (log_2=-0.02)	Th17	-	ns	ns
ARI1B	*Arid1b*	Core (log_2=0.32)	ns (0.13)	Th17, Treg	-	ns	ns
ARI5A	*Arid5a*	Th17 enriched** (log_2=1.65)	Th17 enriched (log_2=0.77)	Th17, Treg	-	Th17 WT	naïve cells: Th17 *Irf4*$^{-/-}$
ARID2	*Arid2*	Th17 enriched (log_2=0.91)	ns (log_2=0.09)	Th17	-	ns	differentiated cells: Th17 WT, Treg WT
ASH2L	*Ash2l*	Core (log_2=0.02)	ns (log_2=-0.03)	Th17	-	ns	ns

Protein name	Gene name	Interactome	Proteome	ChIP-seq (Promoter)	ChIP-seq (Motif)	*Irf4*$^{-/-}$ analysis (*Irf4*$^{-/-}$ vs WT D3)	*Irf4*$^{-/-}$ analysis (D0 vs D3)
AT2B4	*Atp2b4*	Th17 enriched** (log_2=5.26)	Th17 enriched (log_2=0.73)	-	-	Th17 WT, Treg WT	differentiated cells: Th17 WT/*Irf4*$^{-/-}$, Treg WT/*Irf4*$^{-/-}$
ATN1	*Atn1*	Core (log_2=-0.28)	ns (log_2=-0.22)	Th17	-	ns	ns
ATX2	*Atxn2*	Treg enriched (log_2=-0.92)	ns (log_2=-0.40)		-	ns	differentiated cells: Treg WT
ATX2L	*Atxn2l*	Core (log_2=-0.42)	ns (log_2=-0.22)	Th17, Treg	-	ns	differentiated cells: Th17 WT/*Irf4*$^{-/-}$, Treg WT/*Irf4*$^{-/-}$
BACH2	*Bach2*	Th17 enriched** (log_2=1.05)	Th17 enriched (log_2=0.92)	-	TRANSFAC: Th17,Treg MEME: Th17/Treg	Th17 WT	differentiated cells: Th17 WT/*Irf4*$^{-/-}$, Treg WT/*Irf4*$^{-/-}$
BAG6	*Bag6*	Core (log_2=0.13)	ns (log_2=0.06)	Th17	-	ns	differentiated cells: Th17 WT/*Irf4*$^{-/-}$, Treg WT/*Irf4*$^{-/-}$
BAZ1A	*Baz1a*	Core (log_2=0.28)	ns (log_2=-0.42)	Th17	-	ns	differentiated cells: Th17 WT/*Irf4*$^{-/-}$, Treg WT/*Irf4*$^{-/-}$
BC11B	*Bcl11b*	Core (log_2=0.06)	ns (log_2=-0.18)	Th17	-	ns	naïve cells: Th17 WT, Treg *Irf4*$^{-/-}$
BCL3	*Bcl3*	Th17 enriched** (log_2=4.24)	Th17 enriched (log_2=2.89)	Th17	-	Treg WT	differentiated cells: Th17 WT/*Irf4*$^{-/-}$, Treg WT
BCL7C	*Bcl7c*	Core (log_2=-0.09)	ns (log_2=-0.24)		-	ns	differentiated cells: Treg WT
BD1L1	*Bod1l*	Core (log_2=0.47)	ns (log_2=-0.06)	Th17, Treg	-	ns	ns
BIG2	*Arfgef2*	Core (log_2=-0.27)	ns (log_2=-0.08)	Th17	-	ns	ns
BIN2	*Bin2*	Th17 enriched (log_2=0.75)	Th17 enriched (log_2=0.69)	Th17, Treg	-	ns	naïve cells: Th17 WT/*Irf4*$^{-/-}$, Treg WT/*Irf4*$^{-/-}$
BIRC6	*Birc6*	Core (log_2=-0.35)	ns (log_2=-0.01)	Th17, Treg	-	ns	differentiated cells: Th17 WT/*Irf4*$^{-/-}$, Treg WT/*Irf4*$^{-/-}$
BRCA1	*Brca1*	Treg enriched (log_2=-1.29)	Treg enriched (log_2=-0.73)	Th17, Treg	-	Th17 *Irf4*$^{-/-}$	differentiated cells: Th17 WT/*Irf4*$^{-/-}$, Treg WT/*Irf4*$^{-/-}$
BRD2	*Brd2*	Core (log_2=-0.05)	ns (log_2=-0.12)	-	-	ns	ns
BRD7	*Brd7*	Treg enriched (log_2=-1.18)	ns (log_2=0.10)	-	-	ns	differentiated cells: Th17 WT/*Irf4*$^{-/-}$, Treg WT/*Irf4*$^{-/-}$
BRE1A	*Rnf20*	Core (log_2=0.42)	ns (log_2=0.30)	-	-	ns	differentiated cells: Th17 *Irf4*$^{-/-}$
BRE1B	*Rnf40*	Core (log_2=0.28)	ns (log_2=0.26)	Th17	-	ns	differentiated cells: Th17 WT/*Irf4*$^{-/-}$, Treg WT/*Irf4*$^{-/-}$
C19L1	*Cwf19l1*	Core (log_2=0.08)	ns (log_2=0.15)	-	-	ns	naïve cells: TregWT
CARF	*Cdkn2aip*	Core (log_2=-0.03)	ns (log_2=-0.20)	Th17, Treg	-	ns	ns
CARM1	*Carm1*	Core (log_2=-0.28)	Treg enriched (log_2=-0.50)	Th17, Treg	-	ns	differentiated cells: Th17 WT/*Irf4*$^{-/-}$, Treg WT/*Irf4*$^{-/-}$
CBLB	*Cblb*	Th17 enriched** (log_2=1.43)	Th17 enriched (log_2=0.87)	Th17	-	Th17 WT	differentiated cells: Th17 WT/*Irf4*$^{-/-}$
CBP	*Crebbp*	Th17 enriched (log_2=0.57)	ns (log_2=0.35)	Th17	TRANSFAC: Th17/Treg	ns	ns
CCAR1	*Ccar1*	Core (log_2=0.07)	ns (log_2=0.16)	Th17, Treg	-	ns	ns
CCAR2	*Ccar2*	Core (log_2=0.46)	ns (log_2=0.37)		-	ns	naïve cells: Treg *Irf4*$^{-/-}$
CD2B2	*Cd2bp2*	Core (log_2=0.38)	ns (log_2=0.36)	Th17, Treg	-	ns	differentiated cells: Th17 WT/*Irf4*$^{-/-}$, Treg WT/*Irf4*$^{-/-}$
CDC16	*Cdc16*	Core (log_2=0.16)	ns (log_2=-0.03)	-	-	ns	differentiated cells: Th17 WT/*Irf4*$^{-/-}$, Treg WT/*Irf4*$^{-/-}$

Protein name	Gene name	Interactome	Proteome	ChIP-seq (Promoter)	ChIP-seq (Motif)	*Irf4*$^{-/-}$ analysis (*Irf4*$^{-/-}$ vs WT D3)	*Irf4*$^{-/-}$ analysis (D0 vs D3)
CDC37	*Cdc37*	Core (log_2=-0.23)	ns (log_2=-0.19)	Th17, Treg	-	ns	ns
CDC73	*Cdc73*	Core (log_2=-0.10)	ns (log_2=-0.27)	-	-	ns	ns
CDK1	*Cdk1*	Core (log_2=-0.12)	ns (log_2=0.12)	Th17	-	Th17 *Irf4*$^{-/-}$	differentiated cells: Th17 WT/*Irf4*$^{-/-}$, Treg WT/*Irf4*$^{-/-}$
CDK2	*Cdk2*	Core (log_2=0.03)	ns (log_2=0.01)	Th17	-	ns	differentiated cells: Th17 WT/*Irf4*$^{-/-}$, Treg WT/*Irf4*$^{-/-}$
CDK7	*Cdk7*	Core (log_2=0.04)	ns (log_2=-0.16)	Th17, Treg	-	Th17 *Irf4*$^{-/-}$	differentiated cells: Th17 *Irf4*$^{-/-}$, Treg *Irf4*$^{-/-}$
CDK9	*Cdk9*	Core (log_2=-0.12)	ns (log_2=-0.21)	Th17	-	ns	ns
CDN1B	*Cdkn1b*	Th17 enriched** (log_2=1.62)	Th17 enriched (log_2=1.21)	Th17	-	Th17 WT	naïve cells: Th17 *Irf4*$^{-/-}$, Treg WT/*Irf4*$^{-/-}$
CE170	*Cep170*	Th17 enriched (log_2=0.73)	ns (log_2=0.30)	-	-	Th17 WT, Treg WT	differentiated cells: Th17 WT/*Irf4*$^{-/-}$, Treg WT/*Irf4*$^{-/-}$
CHD4	*Chd4*	Core (log_2=0.49)	ns (log_2=0.03)	Th17	-	ns	differentiated cells: Th17 WT/*Irf4*$^{-/-}$, Treg *Irf4*$^{-/-}$
CHD7	*Chd7*	Th17 enriched** (log_2=3.08)	Th17 enriched (log_2=0.67)	-	-	ns	differentiated cells: Th17 WT/*Irf4*$^{-/-}$, Treg WT/*Irf4*$^{-/-}$
CHD8	*Chd8*	Th17 enriched (log_2=0.77)	ns (log_2=0.12)	Th17	-	ns	ns
CHERP	*Cherp*	Core (log_2=-0.23)	ns (log_2=-0.07)	Th17	-	ns	differentiated cells: Th17 WT/*Irf4*$^{-/-}$, Treg WT/*Irf4*$^{-/-}$
CLIP1	*Clip1*	Treg enriched (log_2=-1.30)	ns (log_2=-0.02)	Th17	-	ns	naïve cells: Treg WT/*Irf4*$^{-/-}$
CMTR1	*Cmtr1*	Core (log_2=-0.29)	ns (log_2=-0.17)	Th17	-	ns	ns
CND1	*Ncapd2*	Core (log_2=0.34)	ns (log_2=0.17)	-	-	ns	differentiated cells: Th17 WT/*Irf4*$^{-/-}$, Treg WT/*Irf4*$^{-/-}$
CNDG2	*Ncapg2*	Treg enriched (log_2=-0.50)	ns (log_2=-0.07)	Treg	-	ns	differentiated cells: Th17 WT/*Irf4*$^{-/-}$, Treg WT/*Irf4*$^{-/-}$
CNN3	*Cnn3*	Treg enriched** (log_2=-1.45)	Treg enriched (log_2=-0.91)	Th17	-	Th17 WT, Treg WT	differentiated cells: Th17 WT/*Irf4*$^{-/-}$, Treg WT/*Irf4*$^{-/-}$
CNOT1	*Cnot1*	Core (log_2=-0.27)	ns (log_2=0.06)	Th17, Treg	-	ns	differentiated cells: Th17 WT/*Irf4*$^{-/-}$, Treg WT/*Irf4*$^{-/-}$
COG2	*Cog2*	Th17 enriched (log_2=1.32)	ns (log_2=-0.07)	Treg	-	ns	differentiated cells: Th17 *Irf4*$^{-/-}$
COPG2	*Copg2*	Core (log_2=0.08)	ns (log_2=-0.20)	-	-	Treg WT	differentiated cells: Treg WT
CPSF1	*Cpsf1*	Core (log_2=0.12)	ns (log_2=0.13)	Th17	-	ns	ns
CSK21	*Csnk2a1*	Core (log_2=0.04)	ns (log_2=-0.04)	Th17	-	ns	differentiated cells: Th17 WT/*Irf4*$^{-/-}$, Treg WT/*Irf4*$^{-/-}$
CSN6	*Cops6*	Core (log_2=-0.11)	ns (log_2=-0.09)	Th17	-	ns	ns
CSN8	*Cops8*	Core (log_2=-0.17)	ns (log_2=-0.09)	Th17, Treg	-	ns	differentiated cells: Th17 *Irf4*$^{-/-}$, Treg WT/*Irf4*$^{-/-}$
CSTF3	*Cstf3*	Core (log_2=0.11)	ns (log_2=0.17)	Th17, Treg	-	ns	ns
CTBP1	*Ctbp1*	Core (log_2=0.28)	ns (log_2=-0.02)	Th17	-	ns	naïve cells: Th17 *Irf4*$^{-/-}$, Treg *Irf4*$^{-/-}$
CTDP1	*Ctdp1*	Core (log_2=0.45)	ns (log_2=0.21)	Th17	-	ns	ns
CUL3	*Cul3*	Core (log_2=0.02)	ns (log_2=-0.16)	Th17, Treg	-	ns	ns

Protein name	Gene name	Interactome log_2(Th17/Treg)	Proteome	ChIP-seq (Promoter)	ChIP-seq (Motif)	*Irf4*$^{-/-}$ analysis (*Irf4*$^{-/-}$ vs WT D3)	*Irf4*$^{-/-}$ analysis (D0 vs D3)
CWC27	*Cwc27*	Core (log_2=0.00)	ns (log_2=-0.02)	Th17	-	ns	differentiated cells: Th17 WT, Treg WT
CXXC1	*Cxxc1*	Core (log_2=0.40)	ns (log_2=0.14)	Th17	-	ns	ns
DCAF5	*Dcaf5*	Th17 enriched (log_2=0.93)	ns (log_2=0.26)	Th17	-	ns	ns
DCAF7	*Dcaf7*	Core (log_2=-0.33)	ns (log_2=-0.28)	Th17, Treg	-	ns	ns
DCPS	*Dcps*	Core (log_2=-0.07)	ns (log_2=0.16)	Th17, Treg	-	ns	naïve cells: Th17 WT/*Irf4*$^{-/-}$, Treg WT/*Irf4*$^{-/-}$
DDI2	*Ddi2*	Core (log_2=0.20)	ns (log_2=0.29)	-	-	ns	ns
DDX20	*Ddx20*	Core (log_2=-0.04)	ns (log_2=-0.26)	Th17, Treg	-	Th17 *Irf4*$^{-/-}$	differentiated cells: Th17 WT/*Irf4*$^{-/-}$, Treg WT/*Irf4*$^{-/-}$
DDX41	*Ddx41*	Core (log_2=0.09)	ns (log_2=0.11)	Th17, Treg	-	ns	ns
DDX42	*Ddx42*	Core (log_2=0.04)	ns (log_2=0.01)	-	-	ns	ns
DEFI6	*Def6*	Th17 enriched (log_2=0.51)	ns (log_2=-0.10)	Th17, Treg	-	Treg WT	naïve cells: Treg WT
DHPR	*Qdpr*	Core (log_2=-0.27)	ns (log_2=-0.25)	Th17	-	ns	naïve cells: Th17 WT
DHX15	*Dhx15*	Core (log_2=-0.09)	ns (log_2=-0.10)	-	-	ns	ns
DIAP1	*Diaph1*	Core (log_2=-0.01)	ns (log_2=0.04)	-	-	ns	naïve cells: Th17 *Irf4*$^{-/-}$, Treg WT/*Irf4*$^{-/-}$
DIDO1	*Dido1*	Th17 enriched (log_2=0.59)	ns (log_2=0.21)	Th17	-	ns	ns
DNJA1	*Dnaja1*	Th17 enriched (log_2=0.71)	ns (log_2=0.33)	Treg	-	ns	differentiated cells: Th17 WT/*Irf4*$^{-/-}$, Treg *Irf4*$^{-/-}$
DNJA2	*Dnaja2*	Core (log_2=0.18)	ns (log_2=-0.11)	Th17, Treg	-	ns	differentiated cells: Treg *Irf4*$^{-/-}$
DNLI1	*Lig1*	Core (log_2=-0.29)	ns (log_2=-0.04)	Th17	-	ns	differentiated cells: Th17 WT/*Irf4*$^{-/-}$, Treg WT/*Irf4*$^{-/-}$
DOC11	*Dock11*	Th17 enriched (log_2=0.70)	ns (log_2=-0.01)	Th17	-	ns	naïve cells: Th17 WT/*Irf4*$^{-/-}$, Treg WT/*Irf4*$^{-/-}$
DPOA2	*Pola2*	Core (log_2=-0.10)	ns (log_2=0.10)	Th17	-	ns	differentiated cells: Th17 WT/*Irf4*$^{-/-}$, Treg WT/*Irf4*$^{-/-}$
DPOD1	*Pold1*	Core (log_2=-0.11)	ns (log_2=-0.18)	Treg	-	Th17 WT, Treg WT	differentiated cells: Th17 WT/*Irf4*$^{-/-}$, Treg WT/*Irf4*$^{-/-}$
DPOD2	*Pold2*	Core (log_2=-0.27)	ns (log_2=-0.06)	Th17	-	Treg WT	differentiated cells: Th17 WT/*Irf4*$^{-/-}$, Treg WT/*Irf4*$^{-/-}$
DPOD3	*Pold3*	Core (log_2=-0.22)	ns (log_2=-0.23)	Th17, Treg	-	ns	differentiated cells: Th17 WT/*Irf4*$^{-/-}$, Treg WT/*Irf4*$^{-/-}$
DPOLA	*Pola1*	Core (log_2=0.09)	ns (log_2=-0.09)	-	-	ns	differentiated cells: Th17 WT/*Irf4*$^{-/-}$, Treg WT/*Irf4*$^{-/-}$
ECM29	*Ecpas*	Core (log_2=-0.28)	ns (log_2=-0.04)	-	-	ns	differentiated cells: Th17 WT/*Irf4*$^{-/-}$, Treg WT/*Irf4*$^{-/-}$
EEA1	*Eea1*	Th17 enriched (log_2=0.79)	ns (log_2=0.24)	-	-	ns	differentiated cells: Th17 WT/*Irf4*$^{-/-}$
EHMT2	*Ehmt2*	Core (log_2=0.34)	ns (log_2=-0.08)	-	-	ns	differentiated cells: Th17 WT/*Irf4*$^{-/-}$, Treg WT/*Irf4*$^{-/-}$
EMAL4	*Eml4*	Treg enriched (log_2=-0.82)	ns (log_2=0.00)	-	-	ns	ns
EMB	*Emb*	Th17 enriched** (log_2=2.84)	Th17 enriched (log_2=1.52)	Th17	-	Th17 WT	differentiated cells: Th17 WT/*Irf4*$^{-/-}$, Treg WT/*Irf4*$^{-/-}$

Protein name	Gene name	Interactome log_2(Th17/Treg)	Proteome	ChIP-seq (Promoter)	ChIP-seq (Motif)	*Irf4*$^{-/-}$ analysis (*Irf4*$^{-/-}$ vs WT D3)	*Irf4*$^{-/-}$ analysis (D0 vs D3)
EP300	*Ep300*	Th17 enriched** (log_2=0.84)	Th17 enriched (log_2=1.01)	Th17, Treg	TRANSFAC: Th17/Treg MEME: Th17	ns	differentiated cells: Th17 WT
EP400	*Ep400*	Core (log_2=0.23)	ns (log_2=0.05)	Th17, Treg	-	ns	naïve cells: Th17 WT, Treg WT
ERF3A	*Gspt1*	Treg enriched (log_2=-0.51)	ns (log_2=-0.01)	Treg	-	ns	differentiated cells: Th17 WT/*Irf4*$^{-/-}$, Treg WT/*Irf4*$^{-/-}$
ESYT2	*Esyt2*	Th17 enriched** (log_2=0.98)	ns (log_2=0.07)	Th17, Treg	-	ns	naïve cells: Th17 WT/*Irf4*$^{-/-}$, Treg WT/*Irf4*$^{-/-}$
ETV6	*Etv6*	Th17 enriched** (log_2=3.20)	Th17 enriched (log_2=2.25)	Th17, Treg	-	Th17 WT	differentiated cells: Th17 WT/*Irf4*$^{-/-}$, Treg WT/*Irf4*$^{-/-}$
EXOC2	*Exoc2*	Core (log_2=0.36)	ns (log_2=0.01)	Th17, Treg	-	ns	differentiated cells: Th17 WT
FA98B	*Fam98b*	Core (log_2=-0.34)	ns (log_2=-0.29)	Th17	-	ns	differentiated cells: Treg WT
FAK2	*Ptk2b*	Th17 enriched (log_2=0.77)	ns (log_2=0.45)	Th17	-	Th17 WT	ns
FIP1	*Fip1l1*	Core (log_2=-0.12)	ns (log_2=-0.11)	Th17	-	ns	ns
FLI1	*Fli1*	Th17 enriched** (log_2=2.06)	Th17 enriched (log_2=0.73)	Th17, Treg	TRANSFAC: Th17,Treg MEME: Th17/Treg	Th17 WT	naïve cells: Th17 *Irf4*$^{-/-}$, Treg WT/*Irf4*$^{-/-}$
FNBP1	*Fnbp1*	Core (log_2=-0.49)	ns (log_2=-0.26)	Th17	-	ns	naïve cells: Th17 WT/*Irf4*$^{-/-}$
FNBP4	*Fnbp4*	Th17 enriched (0.73)	ns (log_2=0.38)	Th17, Treg	-	ns	naïve cells: Th17 WT/*Irf4*$^{-/-}$
FOSL2	*Fosl2*	Th17 enriched** (log_2=2.00)	Th17 enriched (log_2=1.42)	Th17, Treg	-	ns	differentiated cells: Th17 WT/*Irf4*$^{-/-}$, Treg WT/*Irf4*$^{-/-}$
FOXP3	*Foxp3*	Treg enriched** (log_2=-7.80)	Treg enriched (log_2=-10.60)	-	-	Treg *Irf4*$^{-/-}$	differentiated cells: Treg WT/*Irf4*$^{-/-}$
FRG1	*Frg1*	Core (log_2=0.13)	ns (log_2=0.00)	Th17, Treg	-	ns	ns
FUBP2	*Khsrp*	Core (log_2=0.25)	ns (log_2=0.11)	Th17	-	ns	ns
G3BP2	*G3bp2*	Core (log_2=0.37)	Th17 enriched (log_2=0.64)	Th17, Treg	-	Th17 *Irf4*$^{-/-}$, Treg *Irf4*$^{-/-}$	differentiated cells: Th17 *Irf4*$^{-/-}$
GALK1	*Galk1*	Core (log_2=0.03)	ns (log_2=0.23)	Th17	-	Th17 WT, Treg WT	differentiated cells: Th17 WT/*Irf4*$^{-/-}$, Treg WT/*Irf4*$^{-/-}$
GBP2	*Gbp2*	Th17 enriched** (log_2=3.89)	Th17 enriched (log_2=2.99)	Treg	-	Treg *Irf4*$^{-/-}$	differentiated cells: Th17 WT/*Irf4*$^{-/-}$, Treg *Irf4*$^{-/-}$ naïve cells: Treg WT
GBP5	*Gbp5*	Th17 enriched** (log_2=1.33)	Th17 enriched (log_2=1.34)	Th17, Treg	-	Th17 WT	differentiated cells: Th17 WT/*Irf4*$^{-/-}$, Treg WT/*Irf4*$^{-/-}$
GCN1	*Gcn1*	Core (log_2=-0.33)	ns (log_2=-0.30)	-	-	ns	differentiated cells: Th17 WT/*Irf4*$^{-/-}$, Treg WT/*Irf4*$^{-/-}$
GEMI5	*Gemin5*	Core (log_2=-0.32)	ns (log_2=-0.16)	Th17	-	Th17 *Irf4*$^{-/-}$	differentiated cells: Th17 *Irf4*$^{-/-}$, Treg WT/*Irf4*$^{-/-}$
GEPH	*Gphn*	Treg enriched** (log_2=-0.73)	Treg enriched (log_2=-0.59)	Th17	-	Th17 *Irf4*$^{-/-}$	differentiated cells: Th17 WT/*Irf4*$^{-/-}$, Treg WT/*Irf4*$^{-/-}$
GLRX3	*Glrx3*	Treg enriched (log_2=-0.53)	ns (log_2=-0.36)	Th17	-	ns	differentiated cells: Th17 WT/*Irf4*$^{-/-}$, Treg WT/*Irf4*$^{-/-}$
GMIP	*Gmip*	Core (log_2=0.26)	ns (log_2=0.14)	Th17	-	ns	ns
GOGA5	*Golga5*	Core (log_2=0.03)	ns (log_2=-0.03)	-	-	ns	differentiated cells: Th17 WT/*Irf4*$^{-/-}$, Treg *Irf4*$^{-/-}$

Protein name	Gene name	Interactome log_2(Th17/Treg)	Proteome	ChIP-seq (Promoter)	ChIP-seq (Motif)	*Irf4*$^{-/-}$ analysis (*Irf4*$^{-/-}$ vs WT D3)	*Irf4*$^{-/-}$ analysis (D0 vs D3)
GRAP2	*Grap2*	Core (log_2=-0.13)	ns (log_2=-0.20)	Th17, Treg	-	ns	naïve cells: Th17 WT/*Irf4*$^{-/-}$, Treg WT
GSK3B	*Gsk3b*	Core (log_2=0.44)	ns (log_2=0.30)	Treg	-	ns	ns
GTF2I	*Gtf2i*	Th17 enriched** (log_2=0.87)	Th17 enriched (log_2=0.74)	Th17, Treg	TRANSFAC: Th17/Treg	Th17 WT	differentiated cells: Th17 WT
GUAA	*Gmps*	Core (log_2=0.04)	ns (log_2=0.03)	-	-	ns	differentiated cells: Th17 WT/*Irf4*$^{-/-}$, Treg WT/*Irf4*$^{-/-}$
GVIN1	*Gvin1*	Th17 enriched** (log_2=1.59)	Th17 enriched (log_2=1.32)	-	-	Treg *Irf4*$^{-/-}$	differentiated cells: Th17 WT/*Irf4*$^{-/-}$, Treg *Irf4*$^{-/-}$
HAT1	*Hat1*	Core (log_2=-0.16)	ns (log_2=-0.04)	Th17, Treg	-	ns	differentiated cells: Th17 WT/*Irf4*$^{-/-}$, Treg WT/*Irf4*$^{-/-}$
HDAC1	*Hdac1*	Th17 enriched (log_2=0.71)	ns (log_2=0.30)	Th17, Treg	TRANSFAC: Th17/Treg	ns	ns
HERC4	*Herc4*	Core (log_2=0.43)	ns (log_2=0.10)	Th17	-	ns	ns
HEXI1	*Hexim1*	Th17 enriched (log_2=0.86)	Th17 enriched (log_2=0.52)	Th17, Treg	-	ns	ns
HJURP	*Hjurp*	Treg enriched** (log_2=-2.95)	Treg enriched (log_2=-1.05)	Th17	-	Th17 *Irf4*$^{-/-}$	differentiated cells: Th17 WT/*Irf4*$^{-/-}$, Treg WT/*Irf4*$^{-/-}$
HMHA1	*Arhgap45*	Th17 enriched** (log_2=0.80)	Th17 enriched (log_2=0.88)	Th17	-	ns	naïve cells: Th17 WT/*Irf4*$^{-/-}$, Treg WT/*Irf4*$^{-/-}$
HMMR	*Hmmr*	Treg enriched** (log_2=-4.79)	Treg enriched (log_2=-1.13)	-	-	Th17 *Irf4*$^{-/-}$	differentiated cells: Th17 WT/*Irf4*$^{-/-}$, Treg WT/*Irf4*$^{-/-}$
HNRL1	*Hnrnpul1*	Core (log_2=0.01)	ns (log_2=-0.04)	-	-	ns	naïve cells: Th17 *Irf4*$^{-/-}$
HNRLL	*Hnrnpll*	Core (log_2=-0.03)	ns (log_2=-0.21)	Th17	-	ns	differentiated cells: Th17 WT, Treg WT/*Irf4*$^{-/-}$
HSP7E	*Hspa14*	Treg enriched (log_2=-0.90)	ns (log_2=-0.23)	-	-	ns	differentiated cells: Th17 WT/*Irf4*$^{-/-}$, Treg WT/*Irf4*$^{-/-}$
HUWE1	*Huwe1*	Treg enriched (log_2=-1.06)	ns (log_2=-0.10)	Th17	-	ns	differentiated cells: Th17 WT/*Irf4*$^{-/-}$, Treg WT
I2BP1	*Irf2bp1*	Core (log_2=0.49)	ns (log_2=0.11)	Treg	-	ns	ns
I2BP2	*Irf2bp2*	Core (log_2=0.46)	ns (log_2=0.26)	Th17, Treg	-	ns	differentiated cells: Th17 WT/*Irf4*$^{-/-}$, Treg WT/*Irf4*$^{-/-}$
I2BPL	*Irf2bpl*	Th17 enriched (log_2=1.32)	Th17 enriched (log_2=0.50)	Th17, Treg	-	ns	ns
IKKB	*Ikbkb*	Core (log_2=0.33)	ns (log_2=0.09)	-	-	ns	naïve cells: Th17 WT/*Irf4*$^{-/-}$, Treg WT/*Irf4*$^{-/-}$
IKZF1	*Ikzf1*	Th17 enriched (log_2=0.69)	ns (log_2=0.37)	Th17, Treg	-	ns	ns
IKZF3	*Ikzf3*	Th17 enriched (log_2=0.89)	Th17 enriched (log_2=0.55)	-	-	ns	differentiated cells: Th17 WT, Treg *Irf4*$^{-/-}$
INT1	*Ints1*	Th17 enriched (0.60)	ns (log_2=0.03)	Th17	-	ns	differentiated cells: Th17 WT/*Irf4*$^{-/-}$
INT10	*Ints10*	Th17 enriched** (log_2=0.88)	ns (log_2=0.24)	Th17, Treg	-	ns	ns
INT13	*IntS13*	Core (log_2=0.37)	ns (log_2=0.11)	Th17, Treg	-	ns	ns
INT2	*Ints2*	Th17 enriched (log_2=0.57)	ns (log_2=0.02)	Th17	-	ns	differentiated cells: Th17 WT
INT3	*Ints3*	Th17 enriched (log_2=0.97)	ns (log_2=0.28)	Th17, Treg	-	ns	ns
INT4	*Ints4*	Th17 enriched (log_2=0.82)	ns (log_2=0.14)	Th17	-	ns	differentiated cells: Th17 WT/*Irf4*$^{-/-}$, Treg WT/*Irf4*$^{-/-}$
INT5	*Ints5*	Th17 enriched (log_2=0.51)	ns (log_2=0.09)	Th17	-	ns	ns

Protein name	Gene name	Interactome log_2(Th17/Treg)	Proteome	ChIP-seq (Promoter)	ChIP-seq (Motif)	*Irf4*$^{-/-}$ analysis (*Irf4*$^{-/-}$ vs WT D3)	*Irf4*$^{-/-}$ analysis (D0 vs D3)
INT8	Ints8	Th17 enriched (log_2=0.72)	ns (log_2=0.13)	Th17	-	ns	ns
IPO4	Ipo4	Treg enriched (log_2=-0.51)	ns (log_2=-0.08)	-	-	ns	differentiated cells: Th17 WT/*Irf4*$^{-/-}$, Treg WT/*Irf4*$^{-/-}$
IPO9	Ipo9	Treg enriched (log_2=-0.67)	ns (log_2=-0.13)	Th17	-	ns	differentiated cells: Th17 *Irf4*$^{-/-}$, Treg WT/*Irf4*$^{-/-}$
IRF4	Irf4	Core (log_2=0.24)	Th17 enriched (log_2=0.62)	Th17, Treg	TRANSFAC: Th17, Treg MEME: Th17, Treg	Th17 WT, Treg WT	differentiated cells: Th17 WT, Treg WT
IRF8	Irf8	Treg enriched** (log_2=-3.99)	Treg enriched (log_2=-3.14)	Th17	TRANSFAC: Th17, Treg MEME: Treg	Th17 *Irf4*$^{-/-}$	differentiated cells: Treg WT/*Irf4*$^{-/-}$
ITSN2	Itsn2	Core (log_2=0.04)	ns (log_2=0.00)	-	-	ns	ns
IWS1	*Iws1*	Core (log_2=0.48)	ns (log_2=0.01)	Th17	-	ns	ns
JAK3	*Jak3*	Th17 enriched (log_2=3.07)	Th17 enriched (log_2=1.40)	Th17, Treg	-	Treg *Irf4*$^{-/-}$	differentiated cells: Th17 WT/*Irf4*$^{-/-}$
JHD2C	*Jmjd1c*	Core (log_2=-0.27)	ns (log_2=-0.23)	Th17, Treg	-	ns	ns
JUNB	*Junb*	Th17 enriched** (log_2=1.81)	Th17 enriched (log_2=1.26)	Th17, Treg	TRANSFAC: Th17, Treg MEME: Th17, Treg	Th17 *Irf4*$^{-/-}$	differentiated cells: Th17 WT/*Irf4*$^{-/-}$, Treg WT/*Irf4*$^{-/-}$
KBTBB	*Kbtbd11*	Th17 enriched** (log_2=1.17)	Th17 enriched (log_2=1.17)	Th17, Treg	-	ns	differentiated cells: Th17 WT/*Irf4*$^{-/-}$, Treg WT/*Irf4*$^{-/-}$
KC1A	*Csnk1a1*	Core (log_2=0.12)	ns (log_2=0.12)	Th17, Treg	-	ns	ns
KDM1A	*Kdm1a*	Core (log_2=0.47)	ns (log_2=0.16)	Th17	-	ns	differentiated cells: Th17 WT, Treg WT
KDM3A	*Kdm3a*	Core (log_2=0.25)	ns (log_2=-0.17)	Th17, Treg	-	ns	differentiated cells: Th17 WT/*Irf4*$^{-/-}$, Treg WT/*Irf4*$^{-/-}$
KDM3B	*Kdm3b*	Core (log_2=-0.03)	ns (log_2=-0.15)	Th17	-	ns	differentiated cells: Treg WT
KDM4B	*Kdm4b*	Core (log_2=0.11)	ns (log_2=0.12)	Th17	-	Th17 WT	differentiated cells: Th17 WT/*Irf4*$^{-/-}$, Treg WT/*Irf4*$^{-/-}$
KDM5C	*Kdm5c*	Th17 enriched** (log_2=1.36)	Th17 enriched (log_2=1.00)	Treg	-	ns	differentiated cells: Th17 WT/*Irf4*$^{-/-}$, Treg WT/*Irf4*$^{-/-}$
KDM6A	*Kdm6a*	Core (log_2=-0.14)	ns (log_2=-0.07)	-	-	ns	ns
KI20B	*Kif20b*	Core (log_2=0.19)	ns (log_2=-0.42)	Th17, Treg	-	Th17 *Irf4*$^{-/-}$	differentiated cells: Th17 WT/*Irf4*$^{-/-}$, Treg WT/*Irf4*$^{-/-}$
KIF2C	*Kif2c*	Treg enriched (log_2=-1.93)	Th17 enriched (log_2=-1.12)	Th17	-	ns	differentiated cells: Th17 WT/*Irf4*$^{-/-}$, Treg WT/*Irf4*$^{-/-}$
KIF4	*Kif4*	Core (log_2=-0.37)	ns (log_2=-0.38)	-	-	Th17 *Irf4*$^{-/-}$	differentiated cells: Th17 *Irf4*$^{-/-}$, Treg *Irf4*$^{-/-}$
KMT2D	*Kmt2d*	Core (log_2=-0.08)	ns (log_2=-0.12)Th17	Th17	-	ns	ns
KNTC1	*Kntc1*	Core (log_2=0.35)	ns (log_2=-0.03)	Th17	-	Th17 *Irf4*$^{-/-}$	differentiated cells: Th17 WT/*Irf4*$^{-/-}$, Treg WT/*Irf4*$^{-/-}$
KPCT	*Prkcq*	Th17 enriched (log_2=2.24)	Th17 enriched (log_2=0.70)	Th17, Treg	-	ns	naïve cells: Th17 WT/*Irf4*$^{-/-}$, Treg WT/*Irf4*$^{-/-}$
KTN1	*Ktn1*	Core (log_2=0.04)	ns (log_2=-0.30)	-	-	ns	differentiated cells: Th17 WT/*Irf4*$^{-/-}$, Treg WT/*Irf4*$^{-/-}$

Protein name	Gene name	Interactome log_2(Th17/Treg)	Proteome	ChIP-seq (Promoter)	ChIP-seq (Motif)	*Irf4*$^{-/-}$ analysis (*Irf4*$^{-/-}$ vs WT D3)	*Irf4*$^{-/-}$ analysis (D0 vs D3)
LAR4B	*Larp4b*	Treg enriched (log_2=-1.95)	ns (log_2=-0.20)	Th17	-	ns	differentiated cells: Th17 WT/*Irf4*$^{-/-}$, Treg WT/*Irf4*$^{-/-}$
LARP4	*Larp4*	Treg enriched** (log_2=-0.95)	ns (log_2=-0.50)	Treg	-	Th17 *Irf4*$^{-/-}$, Treg *Irf4*$^{-/-}$	differentiated cells: Th17 WT/*Irf4*$^{-/-}$, Treg WT/*Irf4*$^{-/-}$
LARP7	*Larp7*	Core (log_2=0.06)	ns (log_2=-0.03)	-	-	ns	ns
LAS1L	*Las1l*	Core (log_2=0.10)	ns (log_2=0.28)	-	-	ns	differentiated cells: Th17 WT/*Irf4*$^{-/-}$, Treg WT/*Irf4*$^{-/-}$
LAT1	*Slc7a5*	Treg enriched** (log_2=-0.76)	Treg enriched (log_2=-1.46)	Th17	-	Treg WT	differentiated cells: Th17 WT/*Irf4*$^{-/-}$, Treg WT/*Irf4*$^{-/-}$
LC7L2	*Luc7l2*	Core (log_2=-0.06)	ns (log_2=-0.02)	Th17, Treg	-	ns	ns
LCP2	*Lcp2*	Th17 enriched (log_2=0.96)	ns (log_2=0.39)	Th17	-	ns	differentiated cells: Th17 *Irf4*$^{-/-}$
LRC8C	*Lrrc8c*	Th17 enriched** (log_2=1.20)	Th17 enriched (log_2=0.53)	Th17, Treg	-	ns	differentiated cells: Th17 WT/*Irf4*$^{-/-}$, Treg WT/*Irf4*$^{-/-}$
LRCH3	*Lrch3*	Th17 enriched (log_2=0.63)	ns (log_2=0.01)	Th17, Treg	-	Th17 WT	ns
LRRF1	*Lrrfip1*	Core (log_2=0.11)	ns (log_2=0.21)	Th17	-	ns	differentiated cells: Th17 WT
LSM6	*Lsm6*	Core (log_2=-0.01)	ns (log_2=0.08)	Th17	-	ns	naïve cells: Th17 WT/*Irf4*$^{-/-}$, Treg WT/*Irf4*$^{-/-}$
MALT1	*Malt1*	Th17 enriched** (log_2=2.03)	Th17 enriched (log_2=1.29)	Th17, Treg	-	Treg WT	differentiated cells: Th17 WT/*Irf4*$^{-/-}$, Treg WT/*Irf4*$^{-/-}$
MARK2	*Mark2*	Th17 enriched** (log_2=1.27)	ns (log_2=0.39)	Th17, Treg	-	ns	ns
MBD2	*Mbd2*	Th17 enriched (log_2=0.62)	ns (log_2=0.19)	Th17	-	ns	ns
MBD3	*Mbd3*	Core (log_2=-0.16)	ns (log_2=-0.04)	Th17	-	ns	differentiated cells: Th17 WT/*Irf4*$^{-/-}$, Treg WT/*Irf4*$^{-/-}$
MCES	*Rnmt*	Core (log_2=-0.02)	ns (log_2=-0.01)	Th17	-	ns	ns
MCMBP	*Mcmbp*	Core (log_2=0.03)	ns (log_2=0.04)	Th17	-	Th17 *Irf4*$^{-/-}$	differentiated cells: Th17 *Irf4*$^{-/-}$, Treg WT/*Irf4*$^{-/-}$
MDC1	*Mdc1*	Core (log_2=-0.49)	ns (log_2=-0.33)	Th17, Treg	-	ns	differentiated cells: Treg WT
MED1	*Med1*	Core (log_2=0.18)	ns (log_2=0.09)	Th17	-	ns	differentiated cells: Th17 *Irf4*$^{-/-}$, Treg *Irf4*$^{-/-}$
MED12	*Med12*	Th17 enriched (log_2=1.97)	Th17 enriched (0 log_2=.73)	Th17	-	ns	ns
MED23	*Med23*	Core (log_2=0.39)	ns (log_2=-0.02)	Th17	-	ns	differentiated cells: Th17 *Irf4*$^{-/-}$
MEMO1	*Memo1*	Treg enriched (log_2=-0.67)	ns (log_2=-0.40)	Th17	-	ns	differentiated cells: Th17 WT/*Irf4*$^{-/-}$, Treg WT/*Irf4*$^{-/-}$
MIA2	*Mia2*	Core (log_2=-0.43)	ns (log_2=-0.14)	-	-	ns	differentiated cells: Th17 *Irf4*$^{-/-}$, Treg WT
MINT	*Spen*	Core (log_2=0.12)	ns (log_2=0.33)	-	-	ns	ns
MORC3	*Morc3*	Core (log_2=-0.04)	ns (log_2=-0.30)	Th17	-	ns	naïve cells: Th17 WT
MOV10	*Mov10*	Treg enriched (log_2=-2.68)	Treg enriched (log_2=-0.99)	Th17, Treg	-	Th17 *Irf4*$^{-/-}$	differentiated cells: Th17 *Irf4*$^{-/-}$, Treg WT/*Irf4*$^{-/-}$
MPRI	*Igf2r*	Th17 enriched** (log_2=4.44)	Th17 enriched (log_2=1.29)	-	-	ns	differentiated cells: Th17 WT/*Irf4*$^{-/-}$, Treg WT/*Irf4*$^{-/-}$
MRE11	*Mre11*	Core (log_2=-0.25)	ns (log_2=-0.30)	Th17	-	ns	differentiated cells: Th17 WT/*Irf4*$^{-/-}$, Treg WT/*Irf4*$^{-/-}$

Protein name	Gene name	Interactome log_2(Th17/Treg)	Proteome	ChIP-seq (Promoter)	ChIP-seq (Motif)	*Irf4*$^{-/-}$ analysis (*Irf4*$^{-/-}$ vs WT D3)	*Irf4*$^{-/-}$ analysis (D0 vs D3)
MSH2	*Msh2*	Core (log_2=0.11)	ns (log_2=0.18)	Th17	-	ns	differentiated cells: Th17 WT/*Irf4*$^{-/-}$, Treg WT/*Irf4*$^{-/-}$
MSH6	*Msh6*	Core (log_2=-0.05)	ns (log_2=0.04)	Th17	-	ns	differentiated cells: Th17 WT/*Irf4*$^{-/-}$, Treg WT/*Irf4*$^{-/-}$
MTA1	*Mta1*	Core (log_2=0.12)	ns (log_2=-0.10)	-	-	ns	differentiated cells: Th17 WT/*Irf4*$^{-/-}$, Treg WT/*Irf4*$^{-/-}$
MTA2	*Mta2*	Th17 enriched (log_2=0.59)	ns (log_2=0.21)	-	-	ns	differentiated cells: Th17 WT
MTA3	*Mta3*	Core (log_2=0.27)	ns (log_2=-0.07)	-	-	ns	differentiated cells: Th17 WT, Treg WT/*Irf4*$^{-/-}$
MTOR	*Mtor*	Core (log_2=-0.15)	ns (log_2=0.09)	Th17, Treg	-	ns	ns
MTREX	*Mtrex*	Core (log_2=-0.07)	ns (log_2=0.00)	-	-	ns	ns
MTSS1	*Mtss1*	Th17 enriched (log_2=1.12)	ns (log_2=0.48)	Th17	-	Th17 WT, Treg WT	differentiated cells: Th17 WT naïve cells: Th17 *Irf4*$^{-/-}$
NAB2	*Nab2*	Th17 enriched** (log_2=0.93)	Th17 enriched (log_2=0.68)	-	-	Th17 WT	differentiated cells: Th17 WT/*Irf4*$^{-/-}$, Treg WT/*Irf4*$^{-/-}$
NACC1	*Nacc1*	Th17 enriched (log_2=0.60)	ns (log_2=0.10)	-	-	ns	differentiated cells: Th17 WT/*Irf4*$^{-/-}$, Treg *Irf4*$^{-/-}$
NBN	*Nbn*	Core (log_2=-0.46)	ns (log_2=-0.36)	Th17	-	ns	differentiated cells: Th17 *Irf4*$^{-/-}$, Treg WT/*Irf4*$^{-/-}$
NCBP1	*Ncbp1*	Core (log_2=0.15)	ns (log_2=0.03)	-	-	ns	ns
NCOA2	*Ncoa2*	Core (log_2=0.09)	ns (log_2=-0.04)	Th17, Treg	-	ns	ns
NCOA3	*Ncoa3*	Core (log_2=0.16)	ns (log_2=0.05)	Th17	-	ns	differentiated cells: Treg *Irf4*$^{-/-}$
NCOR1	*Ncor1*	Th17 enriched (log_2=0.50)	ns (log_2=0.14)	-	-	ns	ns
NCOR2	*Ncor2*	Th17 enriched (log_2=1.18)	ns (log_2=0.28)	-	-	ns	ns
NEK9	*Nek9*	Treg enriched (log_2=-0.53)	ns (log_2=-0.22)	-	-	ns	ns
NELFA	*Nelfa*	Core (log_2=0.46)	ns (log_2=0.29)	Th17, Treg	-	ns	differentiated cells: Th17 WT
NELFB	*Nelfb*	Core (log_2=0.49)	ns (log_2=0.45)	Th17	-	Th17 WT	differentiated cells: Th17 WT
NELFD	*Nelfcd*	Th17 enriched (log_2=0.55)	ns (log_2=0.24)	-	-	ns	differentiated cells: Th17 WT
NELFE	*Nelfe*	Core (log_2=0.15)	ns (log_2=0.19)	Th17, Treg	-	Th17 WT	differentiated cells: Th17 WT
NFAC2	*Nfatc2*	Core (log_2=0.08)	ns (log_2=0.22)	Th17	-	ns	ns
NFKB1	*Nfkb1*	Core (log_2=-0.46)	Treg enriched (log_2=-0.67)	-	TRANSFAC: Th17, Treg	ns	differentiated cells: Th17 WT/*Irf4*$^{-/-}$, Treg WT/*Irf4*$^{-/-}$
NFKB2	*Nfkb2*	Core (log_2=-0.16)	ns (log_2=-0.40)	-	-	ns	differentiated cells: Th17 WT/*Irf4*$^{-/-}$, Treg WT/*Irf4*$^{-/-}$
NIPA	*Nipa*	Core (log_2=-0.03)	ns (log_2=-0.05)	-	-	ns	differentiated cells: Treg WT
NIPBL	*Nipbl*	Th17 enriched (log_2=0.71)	ns (log_2=-0.21)	Th17, Treg	-	ns	ns
NOL9	*Nol9*	Treg enriched (log_2=-0.53)	ns (log_2=0.06)	-	-	ns	differentiated cells: Th17 WT/*Irf4*$^{-/-}$, Treg *Irf4*$^{-/-}$
NONO	*Nono*	Core (log_2=-0.11)	ns (log_2=0.11)	Th17	-	ns	ns

Protein name	Gene name	Interactome log_2(Th17/Treg)	Proteome	ChIP-seq (Promoter)	ChIP-seq (Motif)	*Irf4*$^{-/-}$ analysis (*Irf4*$^{-/-}$ vs WT D3)	*Irf4*$^{-/-}$ analysis (D0 vs D3)
NR2C2	*Nr2c2*	Core (log_2=0.39)	ns (log_2=-0.19)	Th17, Treg	TRANSFAC: Th17, Treg MEME: Treg	ns	naïve cells: Th17 *Irf4*$^{-/-}$
NSMA3	*Smpd4*	Core (log_2=-0.16)	ns (log_2=-0.37)	-	-	ns	differentiated cells: Th17 WT/*Irf4*$^{-/-}$, Treg WT/*Irf4*$^{-/-}$
NSUN2	*Nsun2*	Core (log_2=0.07)	ns (log_2=-0.01)	-	-	ns	differentiated cells: Th17 WT/*Irf4*$^{-/-}$, Treg WT/*Irf4*$^{-/-}$
NUB1	*Nub1*	Core (log_2=0.03)	ns (log_2=-0.05)	Th17, Treg	-	ns	differentiated cells: Th17 WT/*Irf4*$^{-/-}$, Treg WT/*Irf4*$^{-/-}$
NUP50	*Nup50*	Core (log_2=0.22)	ns (log_2=-0.02)	Th17	-	ns	differentiated cells: Th17 WT/*Irf4*$^{-/-}$, Treg WT/*Irf4*$^{-/-}$
NVL	*Nvl*	Core (log_2=-0.16)	ns (log_2=-0.22)	Th17, Treg	-	ns	differentiated cells: Th17 WT/*Irf4*$^{-/-}$, Treg WT/*Irf4*$^{-/-}$
NXF1	*Nxf1*	Core (log_2=0.19)	ns (log_2=0.15)	-	-	ns	ns
OGT1	*Ogt*	Th17 enriched** (log_2=0.71)	ns (log_2=0.45)	-	-	ns	differentiated cells: Th17 WT/*Irf4*$^{-/-}$, Treg WT/*Irf4*$^{-/-}$
P4R3A	*Ppp4r3a*	Core (log_2=0.36)	ns (log_2=0.19)	-	-	ns	differentiated cells: Th17 WT/*Irf4*$^{-/-}$, Treg *Irf4*$^{-/-}$
P66A	*Gatad2a*	Th17 enriched (log_2=0.76)	ns (log_2=0.10)	Th17, Treg	-	ns	differentiated cells: Th17 WT/*Irf4*$^{-/-}$, Treg WT
P66B	*Gatad2b*	Core (log_2=0.26)	ns (log_2=-0.11)	Th17, Treg	-	ns	differentiated cells: Th17 WT/*Irf4*$^{-/-}$, Treg WT/*Irf4*$^{-/-}$
PAF1	*Paf1*	Core (log_2=0.26)	ns (log_2=0.04)	-	-	ns	ns
PAK2	*Pak2*	Core (log_2=-0.35)	ns (log_2=-0.10)	Th17	-	ns	ns
PAPOA	*Papola*	Core (log_2=0.06)	ns (log_2=0.10)	-	-	ns	ns
PARP3	*Parp3*	Th17 enriched (log_2=0.58)	ns (log_2=0.32)	-	-	ns	naïve cells: Th17 WT/*Irf4*$^{-/-}$, Treg WT/*Irf4*$^{-/-}$
PARP9	*Parp9*	Core (log_2=-0.39)	ns (log_2=0.06)	Th17, Treg	-	Treg *Irf4*$^{-/-}$	differentiated cells: Th17 *Irf4*$^{-/-}$, Treg *Irf4*$^{-/-}$
PARVG	*Parvg*	Th17 enriched (log_2=0.89)	ns (log_2=0.38)	-	-	ns	differentiated cells: Treg *Irf4*$^{-/-}$
PAXI1	*Paxip1*	Treg enriched (log_2=-1.07)	ns (log_2=-0.27)	-	-	ns	ns
PB1	*Pbrm1*	Core (log_2=0.21)	ns (log_2=-0.21)	-	-	ns	differentiated cells: Th17 WT
PCM1	*Pcm1*	Th17 enriched (log_2=0.52)	ns (log_2=-0.35)	Th17	-	ns	differentiated cells: Th17 WT/*Irf4*$^{-/-}$, Treg WT/*Irf4*$^{-/-}$
PDIP3	*Poldip3*	Core (log_2=0.21)	ns (log_2=-0.29)	-	-	ns	naïve cells: Th17 WT, Treg WT
PDS5A	*Pds5a*	Core (log_2=0.06)	ns (log_2=-0.42)	-	-	ns	ns
PDS5B	*Pds5b*	Core (log_2=0.28)	ns (log_2=-0.23)	Th17	-	ns	naïve cells: Treg WT/*Irf4*$^{-/-}$
PEBB	*Cbfb*	Core (log_2=0.35)	ns (log_2=0.10)	Th17	-	ns	ns
PFD6	*Pfdn6*	Core (log_2=0.04)	ns (log_2=-0.28)	-	-	ns	differentiated cells: Th17 WT/*Irf4*$^{-/-}$, Treg WT/*Irf4*$^{-/-}$
PHF8	*Phf8*	Th17 enriched (log_2=1.09)	ns (log_2=0.23)	Th17	-	ns	ns
PHOCN	*Mob4*	Core (log_2=0.44)	ns (log_2=-0.25)	-	-	ns	ns
PI4KA	*Pi4ka*	Core (log_2=0.43)	ns (log_2=0.00)	Th17	-	ns	ns

Protein name	Gene name	Interactome log_2(Th17/Treg)	Proteome	ChIP-seq (Promoter)	ChIP-seq (Motif)	*Irf4*$^{-/-}$ analysis (*Irf4*$^{-/-}$ vs WT D3)	*Irf4*$^{-/-}$ analysis (D0 vs D3)
PLRG1	*Plrg1*	Core (log_2=0.33)	ns (log_2=-0.02)	Th17, Treg	-	ns	ns
PML	*Pml*	Th17 enriched** (log_2=1.18)	Th17 enriched (log_2=1.08)	Th17, Treg	-	Th17 WT	differentiated cells: Th17 WT naïve cells: Treg WT/*Irf4*$^{-/-}$
PNKP	*Pnkp*	Core (log_2=-0.04)	ns (log_2=0.12)	Th17, Treg	-	Th17 WT	naïve cells: Th17 WT/*Irf4*$^{-/-}$, Treg WT/*Irf4*$^{-/-}$
PP1R8	*Ppp1r8*	Core (log_2=0.14)	ns (log_2=0.11)	Th17, Treg	-	ns	ns
PP4R2	*Ppp4r2*	Core (log_2=0.32)	ns (log_2=0.20)	-	-	ns	differentiated cells: Th17 WT/*Irf4*$^{-/-}$, Treg WT/*Irf4*$^{-/-}$
PP6R1	*Ppp6r1*	Treg enriched (log_2=-0.55)	ns (log_2=-0.20)	Th17	-	ns	naïve cells: Th17 WT
PP6R3	*Ppp6r3*	Core (log_2=0.22)	ns (log_2=0.03)	Th17	-	ns	differentiated cells: Th17 WT/*Irf4*$^{-/-}$, Treg WT
PPIL1	*Ppil1*	Core (log_2=-0.01)	ns (0.19)	Th17	-	ns	differentiated cells: Th17 WT/*Irf4*$^{-/-}$, Treg WT/*Irf4*$^{-/-}$
PPIL2	*Ppil2*	Th17 enriched (log_2=0.78)	Th17 enriched (log_2=0.62)	-	-	ns	ns
PPIL4	*Ppil4*	Core (log_2=0.32)	ns (log_2=0.14)	Th17	-	ns	naïve cells: Th17 WT/*Irf4*$^{-/-}$, Treg WT/*Irf4*$^{-/-}$
PPIP1	*Pstpip1*	Th17 enriched** (log_2=1.60)	Th17 enriched (log_2=1.63)	Treg	-	Th17 WT	differentiated cells: Th17 WT naïve cells: Treg WT/*Irf4*$^{-/-}$
PPWD1	*Ppwd1*	Core (log_2=0.01)	ns (log_2=0.00)	-	-	ns	ns
PR40A	*Prpf40a*	Core (log_2=0.23)	ns (log_2=0.02)	-	-	ns	ns
PRC2C	*Prrc2c*	Core (log_2=-0.16)	ns (log_2=0.20)	Th17, Treg	-	ns	differentiated cells: Th17 WT/*Irf4*$^{-/-}$, Treg *Irf4*$^{-/-}$
PRP17	*Cdc40*	Th17 enriched (log_2=1.04)	ns (log_2=0.18)	Th17	-	ns	ns
PSB4	*Psmb4*	Core (log_2=0.14)	ns (log_2=-0.14)	Th17	-	ns	ns
PSB7	*Psmb7*	Core (log_2=0.15)	ns (log_2=-0.10)	Th17	-	ns	differentiated cells: Th17 WT/*Irf4*$^{-/-}$, Treg WT/*Irf4*$^{-/-}$
PSMD9	*Psmd9*	Core (log_2=-0.16)	ns (log_2=0.13)	Th17	-	ns	differentiated cells: Th17 WT/*Irf4*$^{-/-}$, Treg WT
PSPC1	*Pspc1*	Core (log_2=-0.29)	ns (log_2=-0.13)	Th17	-	ns	ns
PTN2	*Ptpn2*	Core (log_2=0.29)	ns (log_2=0.29)	Th17	-	Th17 WT	differentiated cells: Th17 WT/*Irf4*$^{-/-}$, Treg WT
PTPA	*Ptpa*	Core (log_2=-0.22)	ns (log_2=0.07)	Th17, Treg	-	ns	naïve cells: Th17 *Irf4*$^{-/-}$, Treg WT/*Irf4*$^{-/-}$
PUM2	*Pum2*	Core (log_2=-0.22)	ns (log_2=0.16)	-	-	ns	differentiated cells: Th17 *Irf4*$^{-/-}$
PUR4	*Pfas*	Core (log_2=-0.14)	ns (log_2=-0.03)	Th17	-	ns	ns
PUR8	*Adsl*	Treg enriched (log_2=-0.68)	ns (log_2=-0.18)	Th17, Treg	-	ns	ns
PYRG1	*Ctps1*	Treg enriched** (log_2=-1.17)	ns (log_2=-0.40)	Th17	-	ns	differentiated cells: Th17 WT/*Irf4*$^{-/-}$, Treg WT/*Irf4*$^{-/-}$
QKI	*Qki*	Treg enriched (log_2=-0.65)	ns (log_2=-0.36)	Th17	-	ns	differentiated cells: Th17 WT/*Irf4*$^{-/-}$, Treg WT/*Irf4*$^{-/-}$
RAD50	*Rad50*	Core (log_2=-0.02)	ns (log_2=-0.24)	Th17, Treg	-	ns	differentiated cells: Th17 WT/*Irf4*$^{-/-}$, Treg WT/*Irf4*$^{-/-}$

Protein name	Gene name	Interactome log_2(Th17/Treg)	Proteome	ChIP-seq (Promoter)	ChIP-seq (Motif)	*Irf4*$^{-/-}$ analysis (*Irf4*$^{-/-}$ vs WT D3)	*Irf4*$^{-/-}$ analysis (D0 vs D3)
RANB3	*Ranbp3*	Core (log_2=0.00)	ns (log_2=0.19)	Th17, Treg	-	ns	ns
RASL3	*Rasal3*	Th17 enriched (log_2=0.69)	ns (log_2=0.28)	Th17	-	ns	ns
RAVR1	*Raver1*	Core (log_2=0.26)	ns (log_2=0.11)	-	-	ns	naïve cells: Th17 *Irf4*$^{-/-}$
RBBP4	*Rbbp4*	Core (log_2=0.35)	ns (log_2=0.14)	Treg	-	ns	differentiated cells: Th17 WT, Treg WT/*Irf4*$^{-/-}$
RBBP6	*Rbbp6*	Core (log_2=-0.03)	ns (log_2=0.04)	Th17	-	ns	differentiated cells: Th17 WT
RBBP7	*Rbbp7*	Core (log_2=0.11)	ns (log_2=0.03)	-	-	ns	differentiated cells: Th17 WT/*Irf4*$^{-/-}$, Treg WT/*Irf4*$^{-/-}$
RBM10	*Rbm10*	Core (log_2=0.25)	ns (log_2=0.14)	-	-	ns	ns
RBM12	*Rbm12*	Core (log_2=0.04)	ns (log_2=0.09)	Th17	-	ns	ns
RBM14	*Rbm14*	Core (log_2=0.08)	ns (log_2=0.02)	Th17	-	ns	ns
RBM5	*Rbm5*	Th17 enriched (log_2=0.67)	ns (log_2=0.49)	Th17, Treg	-	ns	ns
RBM7	*Rbm7*	Core (log_2=-0.29)	ns (log_2=0.21)	-	-	ns	differentiated cells: Th17 *Irf4*$^{-/-}$, Treg WT
RCOR1	*Rcor1*	Core (log_2=0.44)	ns (log_2=0.12)	Th17	-	ns	ns
RD23B	*Rad23b*	Core (log_2=0.39)	ns (log_2=0.16)	Th17	-	ns	ns
REQU	*Dpf2*	Core (log_2=0.34)	ns (log_2=-0.11)	-	-	ns	ns
RFX1	*Rfx1*	Core (0.42)	ns (log_2=0.15)	Th17	TRANSFAC: Th17, Treg	ns	naïve cells: Treg *Irf4*$^{-/-}$
RHG01	*Arhgap1*	Th17 enriched (log_2=0.55)	Th17 enriched (log_2=0.52)	Treg	-	ns	naïve cells: Th17 WT/*Irf4*$^{-/-}$, Treg WT/*Irf4*$^{-/-}$
RHG30	*Arhgap30*	Th17 enriched (log_2=0.59)	Th17 enriched (log_2=0.51)	Th17, Treg	-	Th17 WT	naïve cells: Treg *Irf4*$^{-/-}$
RING2	*Rnf2*	Core (log_2=0.23)	ns (log_2=-0.16)	-	-	ns	ns
RIPK1	*Ripk1*	Core (log_2=-0.42)	ns (log_2=0.08)	Th17	-	ns	differentiated cells: Th17 WT/*Irf4*$^{-/-}$, Treg WT/*Irf4*$^{-/-}$
RIPR2	*Ripor2*	Th17 enriched** (log_2=5.26)	Th17 enriched (log_2=2.14)	Th17	-	Th17 WT	naïve cells: Th17 WT/*Irf4*$^{-/-}$, Treg WT/*Irf4*$^{-/-}$
RORG	*Rorc*	Th17 enriched** (log_2=8.56)	Th17 enriched (log_2=9.38)	Th17	-	Th17 WT	differentiated cells: Th17 WT/*Irf4*$^{-/-}$
RPAP3	*Rpap3*	Core (log_2=0.28)	ns (log_2=0.34)	-	-	ns	differentiated cells: Th17 WT/*Irf4*$^{-/-}$, Treg WT/*Irf4*$^{-/-}$
RPB1	*Polr2a*	Core (log_2=0.31)	ns (log_2=0.11)	-	-	ns	ns
RPR1B	*Rprd1b*	Core (log_2=0.28)	ns (log_2=0.33)	Treg	-	ns	naïve cells: Th17 WT/*Irf4*$^{-/-}$, Treg WT/*Irf4*$^{-/-}$
RRP44	*Dis3*	Core (log_2=0.16)	ns (log_2=-0.09)	-	-	ns	ns
RTF1	*Rtf1*	Core (log_2=0.25)	ns (log_2=0.17)	-	-	ns	ns
RUNX1	*Runx1*	Th17 enriched (log_2=0.54)	ns (log_2=-0.04)	Th17, Treg	-	ns	naïve cells: Th17 WT/*Irf4*$^{-/-}$, Treg WT
RUNX3	*Runx3*	Core (log_2=0.07)	ns (log_2=-0.18)	Th17, Treg	-	Treg *Irf4*$^{-/-}$	differentiated cells: Treg *Irf4*$^{-/-}$
S23IP	*Sec23ip*	Core (log_2=0.03)	ns (log_2=0.07)	Th17, Treg	-	ns	differentiated cells: Th17 WT/*Irf4*$^{-/-}$, Treg WT/*Irf4*$^{-/-}$
SAE1	*Sae1*	Treg enriched (log_2=-0.59)	ns (log_2=-0.12)	Th17	-	ns	ns
SAFB1	*Safb*	Core (log_2=-0.02)	ns (log_2=0.06)	Th17	-	ns	ns

Protein name	Gene name	Interactome log_2(Th17/Treg)	Proteome	ChIP-seq (Promoter)	ChIP-seq (Motif)	*Irf4*$^{-/-}$ analysis (*Irf4*$^{-/-}$ vs WT D3)	*Irf4*$^{-/-}$ analysis (D0 vs D3)
SAFB2	*Safb2*	Th17 enriched (log_2=0.79)	ns (log_2=0.13)	-	-	ns	ns
SAMH1	*Samhd1*	Th17 enriched** (1.19)	Th17 enriched (log_2=1.54)	Th17, Treg	-	Th17 WT	naïve cells: Th17 WT/*Irf4*$^{-/-}$, Treg WT/*Irf4*$^{-/-}$
SATB1	*Satb1*	Th17 enriched** (5.44)	Th17 enriched (log_2=4.75)	Th17	TRANSFAC: Th17, Treg	Th17 WT	differentiated cells: Th17 WT naïve cells: Treg WT/*Irf4*$^{-/-}$
SBNO1	*Sbno1*	Th17 enriched (log_2=0.59)	ns (log_2=0.27)	Th17, Treg	-	ns	differentiated cells: Th17 WT/*Irf4*$^{-/-}$, Treg *Irf4*$^{-/-}$
SC16A	*Sec16a*	Core (log_2=-0.16)	ns (log_2=-0.07)	Th17, Treg	-	ns	ns
SCAF8	*Scaf8*	Core (log_2=0.17)	ns (log_2=0.10)	Th17	-	ns	differentiated cells: Th17 *Irf4*$^{-/-}$, Treg WT/*Irf4*$^{-/-}$
SEPT6	*Septin6*	Core (log_2=-0.20)	ns (log_2=-0.10)	Th17, Treg	-	ns	ns
SET1A	*Setd1a*	Core (log_2=0.29)	ns (log_2=0.04)	Th17	-	ns	ns
SETX	*Setx*	Th17 enriched (log_2=2.38)	Th17 enriched (log_2=0.86)	Th17, Treg	-	Th17 WT	differentiated cells: Th17 WT
SF01	*Sf1*	Core (log_2=0.01)	ns (log_2=0.17)	Th17	-	ns	ns
SFPQ	*Sfpq*	Core (log_2=0.10)	ns (log_2=0.15)	Th17	-	ns	ns
SGT1	*Sugt1*	Treg enriched (log_2=-0.53)	ns (log_2=-0.37)	Th17	-	ns	differentiated cells: Th17 WT/*Irf4*$^{-/-}$, Treg WT/*Irf4*$^{-/-}$
SIN3A	*Sin3a*	Core (log_2=0.24)	ns (log_2=-0.09)	Th17	-	ns	ns
SLK	*Slk*	Th17 enriched (log_2=0.70)	ns (log_2=0.29)	-	-	ns	differentiated cells: Th17 WT/*Irf4*$^{-/-}$, Treg WT/*Irf4*$^{-/-}$
SMC5	*Smc5*	Core (log_2=0.26)	ns (log_2=-0.27)	-	-	ns	naïve cells: Th17 WT
SMCA2	*Smarca2*	Core (log_2=-0.06)	ns (log_2=-0.34)	Th17, Treg	-	ns	naïve cells: Th17 WT/*Irf4*$^{-/-}$, Treg WT/*Irf4*$^{-/-}$
SMCA4	*Smarca4*	Th17 enriched (log_2=0.51)	ns (log_2=-0.10)	Th17, Treg	-	ns	ns
SMCE1	*Smarce1*	Core (log_2=0.22)	ns (log_2=0.10)	Th17	-	ns	ns
SMHD1	*Smchd1*	Th17 enriched (log_2=0.50)	ns (log_2=0.20)	Th17	-	ns	ns
SMRC1	*Smarcc1*	Core (log_2=0.36)	ns (log_2=0.01)	Th17, Treg	-	ns	differentiated cells: Th17 WT/*Irf4*$^{-/-}$, Treg WT/*Irf4*$^{-/-}$
SMRC2	*Smarcc2*	Th17 enriched (log_2=0.68)	ns (log_2=0.41)	-	-	ns	naïve cells: Th17 WT/*Irf4*$^{-/-}$, Treg WT/*Irf4*$^{-/-}$
SMRD1	*Smarcd1*	Core (log_2=0.40)	ns (log_2=0.14)	-	-	ns	ns
SMRD2	*Smarcd2*	Core (log_2=0.47)	ns (log_2=0.04)	Th17, Treg	-	ns	ns
SNF5	*Smarcb1*	Core (log_2=0.29)	ns (log_2=0.14)	Th17	-	ns	ns
SNW1	*Snw1*	Core (log_2=0.14)	ns (log_2=-0.03)	Th17	-	ns	ns
SON	*Son*	Th17 enriched (log_2=0.50)	ns (log_2=0.06)	Treg	-	ns	differentiated cells: Th17 WT
SPF45	*Rbm17*	Core (log_2=-0.02)	ns (log_2=-0.19)	Th17	-	ns	differentiated cells: Th17 WT/*Irf4*$^{-/-}$, Treg WT/*Irf4*$^{-/-}$
SPT5H	*Supt5h*	Core (log_2=0.31)	ns (log_2=0.22)	Th17	-	ns	ns
SR140	*U2surp*	Core (log_2=0.03)	ns (log_2=0.06)	Th17	-	ns	differentiated cells: Th17 WT/*Irf4*$^{-/-}$, Treg WT/*Irf4*$^{-/-}$

Protein name	Gene name	Interactome log_2(Th17/Treg)	Proteome	ChIP-seq (Promoter)	ChIP-seq (Motif)	*Irf4*$^{-/-}$ analysis (*Irf4*$^{-/-}$ vs WT D3)	*Irf4*$^{-/-}$ analysis (D0 vs D3)
SRRM2	*Srrm2*	Core (log_2=-0.16)	ns (log_2=0.08)	Th17, Treg	-	ns	differentiated cells: Th17 WT/ *Irf4*$^{-/-}$, Treg WT/ *Irf4*$^{-/-}$
SRRT	*Srrt*	Core (log_2=0.24)	ns (log_2=0.18)	Th17, Treg	-	ns	ns
STA5B	*Stat5b*	Core (log_2=-0.23)	ns (log_2=-0.16)	Th17, Treg	-	ns	differentiated cells: Th17 WT/*Irf4*$^{-/-}$, Treg WT/*Irf4*$^{-/-}$
STAT1	*Stat1*	Treg enriched** (log_2=-0.89)	Treg enriched (log_2=-0.59)	Th17, Treg	TRANSFAC: Th17, Treg MEME: Th17, Treg	ns	differentiated cells: Treg *Irf4*$^{-/-}$
STAT3	*Stat3*	Core (log_2=0.05)	ns (log_2=-0.29)	Th17, Treg	TRANSFAC: Th17, Treg MEME: Th17, Treg	Th17 WT	differentiated cells: Th17 WT/*Irf4*$^{-/-}$, Treg WT/*Irf4*$^{-/-}$
STK10	*Stk10*	Core (log_2=0.34)	ns (log_2=0.07)	Th17	-	ns	naïve cells: Th17 WT/*Irf4*$^{-/-}$, Treg WT/*Irf4*$^{-/-}$
STK4	*Stk4*	Core (log_2=0.18)	ns (log_2=0.20)	Th17, Treg	-	ns	naïve cells: Th17 WT/*Irf4*$^{-/-}$, Treg WT/*Irf4*$^{-/-}$
STXB2	*Stxbp2*	Th17 enriched** (log_2=0.91)	ns (log_2=0.40)	Th17	-	Th17 WT, Treg WT	differentiated cells: Th17 WT, Treg WT
SUFU	*Sufu*	Th17 enriched (log_2=0.58)	Th17 enriched (log_2=0.74)	Th17, Treg	-	Th17 WT	differentiated cells: Th17 WT
SUH	*Rbpj*	Th17 enriched (log_2=0.56)	ns (log_2=0.21)	Th17, Treg	-	Th17 WT	differentiated cells: Th17 WT/*Irf4*$^{-/-}$, Treg WT/*Irf4*$^{-/-}$
SUMO1	*Sumo1*	Core (log_2=-0.10)	ns (log_2=-0.31)	Th17, Treg	-	ns	differentiated cells: Treg WT
SYMC	*Mars1*	Treg enriched (log_2=-0.73)	ns (log_2=-0.30)	Th17	-	ns	differentiated cells: Th17 WT/*Irf4*$^{-/-}$, Treg WT/*Irf4*$^{-/-}$
T2EA	*Gtf2e1*	Treg enriched (log_2=-0.50)	ns (log_2=-0.50)	-	-	ns	differentiated cells: Th17 WT/*Irf4*$^{-/-}$, Treg WT/*Irf4*$^{-/-}$
TACC3	*Tacc3*	Treg enriched (log_2=-1.22)	Treg enriched (log_2=-0.78)	-	-	Th17 *Irf4*$^{-/-}$	differentiated cells: Th17 WT/*Irf4*$^{-/-}$, Treg WT/*Irf4*$^{-/-}$
TAF5	*Taf5*	Core (log_2=0.04)	ns (log_2=-0.04)	Th17, Treg	-	ns	differentiated cells: Treg WT
TAF6	*Taf6*	Core (log_2=-0.25)	ns (log_2=-0.08)	Treg	-	ns	ns
TAF9	*Taf9*	Core (log_2=0.04)	ns (log_2=-0.13)	-	-	ns	ns
TBL1R	*Tbl1xr1*	Core (log_2=0.42)	ns (log_2=-0.23)	Th17, Treg	-	Th17 WT	ns
TBX21	*Tbx21*	Treg enriched** (log_2=-2.46)	Treg enriched (log_2=-2.22)	-	-	Th17 *Irf4*$^{-/-}$	differentiated cells: Th17 *Irf4*$^{-/-}$, Treg WT/*Irf4*$^{-/-}$
TCEA1	*Tcea1*	Treg enriched (log_2=-0.50)	Treg enriched (log_2=-0.60)	Th17, Treg	-	ns	naïve cells: Th17 WT/*Irf4*$^{-/-}$, Treg *Irf4*$^{-/-}$
TCF20	*Tcf20*	Th17 enriched (log_2=1.20)	ns (log_2=-0.13)	-	-	ns	ns
TCF7	*Tcf7*	Th17 enriched** (log_2=1.52)	Th17 enriched (log_2=1.13)	Th17	TRANSFAC: Th17, Treg	Th17 WT	naïve cells: Th17 WT/*Irf4*$^{-/-}$, Treg WT/*Irf4*$^{-/-}$
TCRG1	*Tcerg1*	Core (log_2=0.18)	ns (log_2=0.19)	Th17, Treg	-	ns	ns
TES	*Tes*	Treg enriched** (log_2=-0.88)	Treg enriched (log_2=-0.86)	Th17	-	ns	ns
TF3C4	*Gtf3c4*	Core (log_2=0.36)	ns (log_2=0.09)	Th17	-	ns	ns
TF65	*Rela*	Th17 enriched (log_2=0.51)	ns (log_2=0.42)	Th17	-	ns	ns
TFP11	*Tfip11*	Th17 enriched (log_2=0.68)	ns (log_2=0.31)	Th17	-	ns	ns

Protein name	Gene name	Interactome log_2(Th17/Treg)	Proteome	ChIP-seq (Promoter)	ChIP-seq (Motif)	*Irf4*$^{-/-}$ analysis (*Irf4*$^{-/-}$ vs WT D3)	*Irf4*$^{-/-}$ analysis (D0 vs D3)
THOP1	*Thop1*	Core (log_2=0.35)	ns (log_2=0.00)	-	-	ns	differentiated cells: Th17 WT/*Irf4*$^{-/-}$, Treg WT/*Irf4*$^{-/-}$
TIF1A	*Trim24*	Core (log_2=0.24)	ns (log_2=0.16)	Th17	-	ns	ns
TIF1B	*Trim28*	Core (log_2=0.30)	ns (log_2=0.25)	Th17	-	ns	ns
TIM	*Timeless*	Treg enriched (log_2=-1.08)	ns (log_2=-0.29)	-	-	ns	ns
TLE3	*Tle3*	Th17 enriched** (log_2=0.84)	ns (log_2=0.45)	Th17, Treg	-	ns	ns
TNPO2	*Tnpo2*	Core (log_2=0.06)	ns (log_2=-0.12)	Th17	-	ns	ns
TOM34	*Tomm34*	Treg enriched (log_2=-0.88)	ns (log_2=-0.25)	Th17, Treg	-	ns	ns
TPX2	*Tpx2*	Treg enriched (log_2=-1.75)	Treg enriched (log_2=-1.61)	Th17	-	Th17 *Irf4*$^{-/-}$	differentiated cells: Th17 WT/*Irf4*$^{-/-}$, Treg WT/*Irf4*$^{-/-}$
TRI33	*Trim33*	Core (log_2=-0.20)	ns (log_2=-0.01)	Th17	-	ns	ns
TRIPC	*Trip12*	Core (log_2=-0.36)	Treg enriched (log_2=-0.57)		-	ns	ns
TRM6	*Trmt6*	Core (log_2=-0.30)	ns (log_2=-0.09)	Th17, Treg	-	ns	ns
TRRAP	*Trrap*	Th17 enriched (log_2=0.56)	ns (log_2=0.10)	Th17	-	ns	ns
TT39B	*Ttc39b*	Core (log_2=-0.19)	ns (log_2=-0.32)	Th17, Treg	-	ns	differentiated cells: Th17 WT/*Irf4*$^{-/-}$, Treg WT/*Irf4*$^{-/-}$
TTL12	*Ttll12*	Core (log_2=-0.20)	ns (log_2=0.36)	Th17	-	ns	ns
TXLNA	*Txlna*	Core (log_2=0.25)	ns (log_2=0.33)	Th17	-	Th17 *Irf4*$^{-/-}$	differentiated cells: Th17 WT/*Irf4*$^{-/-}$, Treg WT/*Irf4*$^{-/-}$
UBA6	*Uba6*	Core (log_2=-0.43)	ns (log_2=-0.22)	Th17	-	ns	ns
UBAP2	*Ubap2*	Treg enriched (log_2=-0.70)	ns (log_2=-0.22)	Th17	-	Th17 *Irf4*$^{-/-}$	differentiated cells: Th17 WT/*Irf4*$^{-/-}$, Treg WT/*Irf4*$^{-/-}$
UBE3A	*Ube3a*	Core (log_2=-0.32)	ns (log_2=-0.09)	Th17	-	ns	ns
UBP15	*Usp15*	Core (log_2=-0.36)	ns (log_2=-0.12)	Th17	-	ns	differentiated cells: Th17 WT/*Irf4*$^{-/-}$, Treg WT/*Irf4*$^{-/-}$
UBP4	*Usp4*	Core (log_2=-0.03)	ns (log_2=-0.17)	Th17	-	ns	differentiated cells: Treg WT/*Irf4*$^{-/-}$
UBP7	*Usp7*	Core (log_2=0.27)	ns (log_2=0.12)	-	-	ns	ns
UBR4	*Ubr4*	Core (log_2=-0.17)	ns (log_2=-0.29)	Th17	-	ns	ns
UBR5	*Ubr5*	Core (log_2=0.41)	ns (log_2=0.37)	-	-	ns	differentiated cells: Th17 WT/*Irf4*$^{-/-}$, Treg WT/*Irf4*$^{-/-}$
UBS3A	*Ubash3a*	Core (log_2=-0.20)	ns (log_2=-0.47)	Th17	-	ns	naïve cells: Th17 WT/*Irf4*$^{-/-}$
UBXN7	*Ubxn7*	Core (log_2=0.01)	ns (log_2=-0.22)	Th17	-	ns	ns
USP9X	*Usp9x*	Core (log_2=0.01)	ns (log_2=-0.02)	Th17	-	ns	ns
VAC14	*Vac14*	Core (log_2=-0.33)	ns (log_2=-0.12)	Th17	-	ns	ns
VCIP1	*Vcpip1*	Core (log_2=0.22)	ns (log_2=0.16)	-	-	ns	ns
WAC	*Wac*	Core (log_2=0.34)	ns (log_2=0.32)	Th17	-	ns	differentiated cells: Th17 *Irf4*$^{-/-}$
WAPL	*Wapl*	Core (log_2=0.05)	ns (log_2=0.08)	-	-	ns	ns
WASH1	*Washc1*	Th17 enriched (log_2=2.61)	ns (log_2=-0.06)	Th17, Treg	-	ns	ns

Protein name	Gene name	Interactome log_2(Th17/Treg)	Proteome	ChIP-seq (Promoter)	ChIP-seq (Motif)	*Irf4*$^{-/-}$ analysis (*Irf4*$^{-/-}$ vs WT D3)	*Irf4*$^{-/-}$ analysis (D0 vs D3)
WDR26	*Wdr26*	Core (log_2=0.19)	ns (log_2=0.20)	-	-	ns	differentiated cells: Th17 WT/*Irf4*$^{-/-}$, Treg WT/*Irf4*$^{-/-}$
WDR6	*Wdr6*	Treg enriched (log_2=-0.79)	ns (log_2=0.16)	-	-	ns	differentiated cells: Th17 WT/*Irf4*$^{-/-}$, Treg WT/*Irf4*$^{-/-}$
WRIP1	Wrnip1	Core (log_2=0.46)	ns (log_2=0.02)	Th17, Treg	-	ns	differentiated cells: Th17 WT/*Irf4*$^{-/-}$, Treg WT
XPO4	Xpo4	Core (log_2=-0.04)	ns (log_2=0.04)	-	-	ns	differentiated cells: Th17 *Irf4*$^{-/-}$, Treg WT
XPO5	Xpo5	Core (log_2=-0.13)	ns (log_2=0.12)	-	-	ns	differentiated cells: Th17 WT/*Irf4*$^{-/-}$, Treg WT/*Irf4*$^{-/-}$
XPO7	Xpo7	Core (log_2=-0.16)	ns (log_2=-0.03)	-	-	ns	ns
XPOT	Xpot	Core (log_2=-0.25)	ns (log_2=-0.27)	Th17	-	ns	differentiated cells: Th17 WT/*Irf4*$^{-/-}$, Treg WT/*Irf4*$^{-/-}$
XRCC5	Xrcc5	Core (log_2=-0.39)	ns (log_2=-0.17)	Th17, Treg	-	ns	differentiated cells: Th17 *Irf4*$^{-/-}$, Treg WT/*Irf4*$^{-/-}$
XRN2	Xrn2	Core (log_2=0.04)	ns (log_2=0.00)	Th17, Treg	-	ns	ns
ZBTB1	Zbtb1	Th17 enriched (log_2=1.14)	Th17 enriched (log_2=0.59)	-	-	ns	differentiated cells: Th17 WT, Treg *Irf4*$^{-/-}$
ZC3HE	Zc3h14	Th17 enriched (log_2=0.51)	ns (log_2=-0.15)	-	-	ns	differentiated cells: Treg WT
ZCCHV	Zc3hav1	Core (log_2=0.24)	ns (log_2=0.04)	Th17, Treg	-	ns	ns
ZCH18	Zc3h18	Th17 enriched (log_2=0.65)	ns (log_2=0.11)	Th17	-	ns	ns
ZEP3	Hivep3	Th17 enriched (log_2=2.78)	Th17 enriched (log_2=1.43)	-	-	Th17 WT	differentiated cells: Th17 WT/*Irf4*$^{-/-}$, Treg WT/*Irf4*$^{-/-}$
ZFR	Zfr	Core (log_2=-0.39)	Treg enriched (log_2=-0.53)	Th17	-	ns	differentiated cells: Th17 WT/*Irf4*$^{-/-}$, Treg WT/*Irf4*$^{-/-}$
ZMYM2	Zmym2	Th17 enriched (log_2=0.83)	ns (log_2=0.40)	Th17, Treg	-	Th17 WT	differentiated cells: Th17 *Irf4*$^{-/-}$, Treg *Irf4*$^{-/-}$
ZN592	Znf592	Core (log_2=-0.11)	ns (log_2=-0.17)	-	-	ns	naïve cells: Th17 *Irf4*$^{-/-}$
ZN598	*Znf598*	Treg enriched (log_2=-0.57)	Treg enriched (-0.56)	Th17	-	ns	differentiated cells: Th17 WT/*Irf4*$^{-/-}$, Treg WT/*Irf4*$^{-/-}$
ZN609	*Znf609*	Th17 enriched** (log_2=1.57)	Th17 enriched (log_2=0.50)	Treg	-	ns	differentiated cells: Th17 WT/*Irf4*$^{-/-}$, Treg WT/*Irf4*$^{-/-}$
ZN638	*Znf638*	Core (log_2=0.04)	ns (log_2=-0.01)	Treg	-	ns	ns

S Table 2: Published IRF4 interactors extracted from PSICQUIC and HIPPIE search

Protein name	Species	Type of interaction	Doi/PMID	Author
ARI1A	Homo sapiens	nd	doi: 10.1186/gb-2010-11-5-r72	Wu et al.
ARI1B	Homo sapiens	proximity	doi: 10.1038/s41467-022-28341-5	Helka et al.
ARID2	Homo sapiens	proximity	doi: 10.1038/s41467-022-28341-5	Helka et al.
BC11B	Mus musculus	physical association	doi: 10.1126/science.1228309	Glasmacher et al.
BRD7	Homo sapiens	proximity	doi: 10.1038/s41467-022-28341-5	Helka et al.
CARM1	Homo sapiens	association	doi: 10.1016/j.immuni.2011.06.014	Li et al.
CARM1	Homo sapiens	association, physical association	doi: 10.1016/j.immuni.2011.06.014	Shitao Li et al.
CHD7	Homo sapiens	proximity	doi: 10.1038/s41467-022-28341-5	Helka et al.
DEFI6	Mus musculus	physical association	doi: 10.1084/jem.20111195	Biswas et al.
DEFI6	Homo sapiens	physical association	doi: 10.1016/s0198-8859(03)00024-7	Gupta et al.
EP300	Homo sapiens	proximity	doi: 10.1038/s41467-022-28341-5	Helka et al.
EP300	Homo sapiens	nd	doi: 10.1186/gb-2010-11-5-r56	Wu et al.
FOXP3	Mus musculus	physical association	doi:10.1038/nature07674IM-17819	Zheng et al.
IKZF1	Homo sapiens	predictive, confidence: High	doi: 10.1038/gene.2012.10	C-M Fang et al
IRF4	Homo sapiens	physical association	doi: 10.4049/jimmunol.175.10.6570	Lehtonen et al.
IRF4	Mus musculus	association	doi: 10.1038/nature11530	Li et al.
IRF4	Homo sapiens	physical association	doi: 10.1016/j.ccr.2007.08.011	Saito et al.
IRF4	Homo sapiens	physical association	doi: 10.1038/nature07064	Shaffer et al.
IRF4	Homo sapiens	predictive, confidence: Low	doi: 10.1073/pnas.0504226102	Kiri Honma et al.
IRF4	Homo sapiens	predictive, confidence: High	doi: 10.4049/jimmunol.175.10.6570	Lehtonen et al.
IRF4	Homo sapiens	predictive, confidence: Low	doi: 10.1093/nar/gki1001	Ch. A Ortmann et al.
IRF4	Homo sapiens	predictive, confidence: Low	doi: 10.1128/JVI.01876-14	Caline G Matar et al.
IRF4	Homo sapiens	predictive; confidence: Low	doi: 10.1371/journal.pone.0022628	Simanta Pathak et al.
IRF8	Mus musculus	physical association	PMID: 10590072	F Rosenbauer et al.
IRF8	Homo sapiens	physical association	doi: 10.4049/jimmunol.168.12.6224	Meraro et al.
JUNB	Mus musculus	association	doi: 10.1038/nature11530	Li et al.
KDM6A	Homo sapiens	proximity	doi: 10.1038/s41467-022-28341-5	Helka et al.
KMT2D	Homo sapiens	proximity	doi: 10.1038/s41467-022-28341-5	Helka et al.
NCOA3	Homo sapiens	proximity	doi: 10.1038/s41467-022-28341-5	Helka et al.
NCOR2	Homo sapiens	proximity	doi: 10.1038/s41467-022-28341-5	Helka et al.
NFAC2	Mus musculus	physical association	doi: 10.1084/jem.20011128	Rengarajan et al.
NFAC2	Homo sapiens	physical association	doi: 10.1084/jem.20011128	Rengarajan et al.
NFAC2	Homo sapiens	physical association	doi: 10.4049/jimmunol.169.6.3120	Sharma et al.
NFAC2	Homo sapiens	nd	doi: 10.1186/gb-2010-11-5-r80	Wu et al.
NFKB1	Mus musculus	physical association	doi: 10.1084/jem.191.8.1281	Grumont et al.
NFKB1	Homo sapiens	physical association	doi: 10.4049/jimmunol.175.10.6570	Lehtonen et al.
NFKB1	Homo sapiens	physical association	doi: 10.4049/jimmunol.169.6.3120	Sharma et al.
NFKB1	Homo sapiens	nd	doi: 10.1186/gb-2010-11-5-r58	Wu et al.
NFKB1	Homo sapiens	predictive, confidence: Low	doi: 10.4049/jimmunol.175.10.6570	Lehtonen et al.
NFKB1	Homo sapiens	predictive, confidence: Low	doi: 10.4049/jimmunol.169.6.3120	Sharma et al.
NIPBL	Homo sapiens	proximity	doi: 10.1038/s41467-022-28341-5	Helka et al.
PAXI1	Homo sapiens	proximity	doi: 10.1038/s41467-022-28341-5	Helka et al.
PB1	Homo sapiens	proximity	doi: 10.1038/s41467-022-28341-5	Helka et al.
REQU	Homo sapiens	proximity	doi: 10.1038/s41467-022-28341-5	Helka et al.
RUNX3	Homo sapiens	predictive, confidence: Low	doi: 10.1002/eji.201040570	Yonghao Cao et al.
SATB1	Homo sapiens	proximity	doi: 10.1038/s41467-022-28341-5	Helka et al.
SMCA2	Homo sapiens	proximity	doi: 10.1038/s41467-022-28341-5	Helka et al.
SMCA4	Homo sapiens	nd	doi: 10.1186/gb-2010-11-5-r86	Wu et al.
SMCE1	Homo sapiens	nd	doi: 10.1186/gb-2010-11-5-r83	Wu et al.
SMRC1	Homo sapiens	nd	doi: 10.1186/gb-2010-11-5-r59	Wu et al.
SMRC2	Homo sapiens	nd	doi: 10.1186/gb-2010-11-5-r70	Wu et al.
SMRD1	Homo sapiens	nd	doi: 10.1186/gb-2010-11-5-r60	Wu et al.
SNF5	Homo sapiens	nd	doi: 10.1186/gb-2010-11-5-r62	Wu et al.
STAT1	Homo sapiens	association	doi: 10.1186/gb-2007-8-3-r39	Vastrik et al.
STAT3	Homo sapiens	physical association	doi: 10.1038/s41598-018-35109-9	Chen et al.
STAT3	Mus musculus	colocalization	doi: 10.1016/j.immuni.2009.10.008	Hyokjoon Kwon et al.
SUFU	Homo sapiens	direct interaction	doi: 10.15252/msb.202110584	Benz et al.
T2EA	Homo sapiens	nd	doi: 10.1186/gb-2010-11-5-r81	Wu et al.
TCF20	Homo sapiens	proximity	doi: 10.1038/s41467-022-28341-5	Helka et al.
TF65	Homo sapiens	physical association	doi: 10.4049/jimmunol.175.10.6570	Lehtonen et al.
TF65	Homo sapiens	physical association	doi: 10.1016/j.ccr.2007.08.011	Saito et al.
TF65	Homo sapiens		doi: 10.1186/gb-2010-11-5-r66	Wu et al.
UBP4	Homo sapiens	affinity chromatography technology, enzymatic study	doi: 10.3892/ijmm.2017.3087	Guo et al.
ZN609	Homo sapiens	proximity	doi: 10.1038/s41467-022-28341-5	Helka et al.

S Table 3: Literature curated genes with critical influence for Th17 development or function

Gene name	Gene type	Effect	PMID	Evidence	Experimental Data
Ahr	TF	positive	18362915, 18362914	deficiency	Th17 ChIP-seq, Th17 *Irf4*$^{-/-}$ analysis
Batf	TF	positive	19578362	deficiency	Th17 ChIP-seq, Th17 *Irf4*$^{-/-}$ analysis
Bcl3	TF	negative	20622172	deficiency	Th17 ChIP-seq
Bcl6	TF	negative	19628815, 19631565, 20212093	deficiency	Th17 ChIP-seq
Ccl20	chemokine	positive	19050256, 18025126	ligand deficiency, recombinant protein, neutralizing antibody to receptor	Th17 ChIP-seq
Ccr6	cell surface	positive	19050256, 18025126	deficiency, neutralizing antibody	Th17 ChIP-seq
Cd28	cell surface	positive, negative	16200068, 19333372	ligand deficiency, blocking antibody	Th17 ChIP-seq, Th17 *Irf4*$^{-/-}$ analysis
Csf2	cytokine	positive-function	21516112, 21516111	deficiency	-
Ctla4	cell surface	negative	19457253	blocking antibody	Th17 ChIP-seq, Th17 *Irf4*$^{-/-}$ analysis
Ddit3	TF	negative	20974859	overexpression	-
Def6	other	negative, positive	19062315, 19915062	deficiency	Th17 ChIP-seq
Ebi3	cytokine	negative	18412165, 22387555	deficiency	-
Ets1	TF	negative	17967903	deficiency	Th17 ChIP-seq
Fabp5	other	positive	19494286	deficiency	Th17 ChIP-seq, Th17 *Irf4*$^{-/-}$ analysis
Foxo1	TF	negative	20467422	deficiency	Th17 ChIP-seq
Foxp3	TF	negative	18368049, 18585065, 18849990	overexpression	-
Fyn	kinase	Positive	22539787	deficiency	Th17 ChIP-seq
Gfi1	TF	negative	19188499	deficiency	Th17 ChIP-seq
Hif1a	TF	positive	21708926	deficiency	Th17 ChIP-seq
Icos	cell surface	positive	16200068	deficiency	Th17 ChIP-seq
Ifngr1	cytokine receptor	negative	16200070	deficiency	Th17 ChIP-seq
Il10	cytokine	negative-function	21511184	deficiency	Th17 ChIP-seq
Il17a	cytokine	positive	16785554, 18264110, 16200068, 16982811, 18025225	deficienty, transgenic overexpression, recombinant protein, neutralizing antibody	Th17 ChIP-seq
Il17f	cytokine	positive	18411338, 16982811, 18025225	deficiency, cytokine administration, neutralizing antibody	Th17 ChIP-seq, Th17 *Irf4*$^{-/-}$ analysis
Il1r1	cytokine receptor	positive	16818675	deficiency	Th17 ChIP-seq
Il21	cytokine	positive	17581588, 17581589, 17581537	deficiency, in vitro assay	Th17 ChIP-seq
Il22	cytokine	positive	18202747, 16982811	neutralizing antibody, cytokine administration	Th17 ChIP-seq
Il23r	cytokine receptor	positive	17030949, 15657292, 14662908	ligand deficiency	Th17 ChIP-seq
Il7r	cytokine receptor	positive	20062065, 20861865	deficiency, antagonsim	Th17 ChIP-seq
Il9	cytokine	negative-function	21360526, 21674475	deficiency	Th17 ChIP-seq
Inpp5d	phosphatase	positive	19542365	deficiency	Th17 ChIP-seq

Gene name	Gene type	Effect	PMID	Evidence	Experimental Data
Irak4	kinase	positive	19542468	deficiency	Th17 ChIP-seq
Irf4	TF	positive	17676043	deficiency	Th17 ChIP-seq, Th17 *Irf4*$^{-/-}$ analysis
Itgb2	integrin	Positive	22025301	antibody blocking	Th17 ChIP-seq, Th17 *Irf4*$^{-/-}$ analysis
Itk	kinase	positive	19818650	deficiency	Th17 ChIP-seq, Th17 *Irf4*$^{-/-}$ analysis
Jak2	kinase	positive	16622035	inhibitor	Th17 ChIP-seq
Jak3	kinase	positive	20696842	jak inhibitor	Th17 ChIP-seq
Ksr1	kinase	positive	20875416	deficiency	Th17 ChIP-seq
Lif	cytokine	negative	19342884, 21835648	soluble factor	Th17 ChIP-seq
Lta	cell surface	positive-function	19561618	depleting/blocking antibody	Th17 ChIP-seq, Th17 *Irf4*$^{-/-}$ analysis
Maf	TF	positive, negative	19098919, 16200068	overexpression, deficiency	Th17 ChIP-seq
Map3k14	kinase	positive	19411637, 21807870	deficiency	Th17 ChIP-seq
Mapk14	kinase	positive	2030482, 21791428	inhibitor	Th17 ChIP-seq, Th17 *Irf4*$^{-/-}$ analysis
Ndfip1	other	Negative	22403444	deficiency	Th17 ChIP-seq, Th17 *Irf4*$^{-/-}$ analysis
Nkfb1	TF	negative	20383124, 19234210	deficiency	-
Nfkbiz	TF	positive	20383124	deficiency	Th17 ChIP-seq
Nr2f6	TF	negative	18701084	deficiency	-
Pparg	TF	negative	19737866	deficiency	Th17 ChIP-seq
Ptger4	cell surface	positive	20566843	deficiency	Th17 ChIP-seq
Rara	TF	positive, negative	21419664, 17569825, 17951529	vitamin a insufficiency, ligand activation	Th17 ChIP-seq
Rbpj	TF	positive	20231432	deficiency	Th17 ChIP-seq, Th17 *Irf4*$^{-/-}$ analysis
Rel	TF	positive	21940679	deficiency	Th17 ChIP-seq, Th17 *Irf4*$^{-/-}$ analysis
Rel	TF	Positive	22006976	deficiency	Th17 ChIP-seq, Th17 *Irf4*$^{-/-}$ analysis
Rheb	GTPase	positive	21358638	deficiency	Th17 ChIP-seq
Rora	TF	positive	18164222	deficiency	Th17 ChIP-seq
Rorc	TF	positive	16990136	deficiency	Th17 ChIP-seq, Th17 *Irf4*$^{-/-}$ analysis
Runx1	TF	positive	18849990	knock-down	Th17 ChIP-seq
Sigirr	other	Negative	20060329	deficiency	Th17 ChIP-seq
Smad3	TF	negative	20548029	deficiency	Th17 ChIP-seq
Socs1	signalling	positive	18322180	deficiency	Th17 ChIP-seq
Socs3	signalling	negative	16698929	deficiency	Th17 ChIP-seq
Stat1	TF	negative	16200070, 20974984	deficiency	Th17 ChIP-seq
Stat3	TF	positive	17277312, 17878325	deficiency	Th17 ChIP-seq, Th17 *Irf4*$^{-/-}$ analysis
Stat5a	TF	negative	17363300, 21278738		Th17 ChIP-seq, Th17 *Irf4*$^{-/-}$ analysis
Stim1	other	positive	21061435	deficiency	Th17 ChIP-seq, Th17 *Irf4*$^{-/-}$ analysis
Tbx21	TF	negative	16200068, 16200070, 20974984	deficiency	Th17 *Irf4*$^{-/-}$ analysis
Tcf7	TF	negative	21935461, 21339363	deficiency	Th17 ChIP-seq, Th17 *Irf4*$^{-/-}$ analysis
Tec	kinase	positive	20870948	deficiency	Th17 ChIP-seq

Gene name	Gene type	Effect	PMID	Evidence	Experimental Data
Tgfbr2	cytokine receptor	positive	16998492, 17481928	dominant negative, ligand deficiency	Th17 ChIP-seq
Tnf	cytokine	positive-function	18039949	Blocking TNFR-Ig fusion protein	Th17 ChIP-seq
Traf6	signalling	negative	20351308	deficiency	Th17 ChIP-seq
Txk	kinase	positive	19818650	deficiency	Th17 ChIP-seq
Vdr	TF	negative	20974859, 20886077, 1617111	ligand activation	Th17 ChIP-seq
Tnfrsf8	cell surface	positive	20639486	deficiency	Th17 ChIP-seq

S Table 4: Literature curated genes with critical influence for Treg development or function

Gene name	Doi	Experimental Data
Areg	doi: 10.1016/j.celrep.2017.08.068	-
Batf	doi: 10.1172/JCI130426	-
Cd83	https://doi.org/10.1038/ni1437	Treg ChIP-seq
Ctla4	https://doi.org/10.1038/ni1437, doi: 10.1016/j.it.2015.04.006, doi: 10.1172/JCI130426	Treg ChIP-seq, Treg *Irf4*$^{-/-}$ analysis
Ebi3	doi: 10.1016/j.celrep.2017.08.068, https://doi.org/10.1038/ni1437	-
Entpd1	https://doi.org/10.1038/ni1437	Treg *Irf4*$^{-/-}$ analysis
Eos	doi: 10.1016/j.it.2015.04.006	Treg *Irf4*$^{-/-}$ analysis
Fgl2	https://doi.org/10.1038/ni1437	Treg ChIP-seq
Foxp3	https://doi.org/10.1038/ni1437, doi: 10.1016/j.it.2015.04.006, https://doi.org/10.1016/j.immuni.2007.09.010	Treg *Irf4*$^{-/-}$ analysis
Gata3	doi: 10.1016/j.it.2015.04.006	Treg ChIP-seq
Gbp1	https://doi.org/10.1038/ni1437	-
Ggt1	https://doi.org/10.1038/ni1437	-
Gpr83	https://doi.org/10.1038/ni1437	-
Gzmb	https://doi.org/10.1038/ni1437	Treg ChIP-seq
Icos	doi: 10.1016/j.celrep.2017.08.068, doi: 10.1172/JCI130426	Treg ChIP-seq, Treg *Irf4*$^{-/-}$ analysis
Ikzf2 (Helios)	https://doi.org/10.1038/ni1437, doi: 10.1172/JCI130426	Treg ChIP-seq
Il10	doi: 10.1016/j.celrep.2017.08.068, https://doi.org/10.1038/ni1437	Treg ChIP-seq
Il1rl1	doi: 10.1016/j.celrep.2017.08.068, https://doi.org/10.1038/ni1437	Treg ChIP-seq
Il2ra (Cd25)	https://doi.org/10.1038/ni1437, doi: 10.1016/j.it.2015.04.006, doi: 10.1172/JCI130426	Treg ChIP-seq, Treg *Irf4*$^{-/-}$ analysis
Il7r (Cd127)	https://doi.org/10.1038/ni1437	Treg ChIP-seq
Irf4	doi: 10.1016/j.it.2015.04.006	Treg ChIP-seq, Treg *Irf4*$^{-/-}$ analysis
Itgae	https://doi.org/10.1016/j.immuni.2007.09.010, https://doi.org/10.1038/ni1437	Treg ChIP-seq, Treg *Irf4*$^{-/-}$ analysis
Itgb8	https://doi.org/10.1038/ni1437	-
Klrg1	https://doi.org/10.1038/ni1437	-
Lef1	doi: 10.1016/j.it.2015.04.006	Treg ChIP-seq
Lycat	https://doi.org/10.1038/ni1437	Treg *Irf4*$^{-/-}$ analysis
Nrn1	https://doi.org/10.1038/ni1437	Treg ChIP-seq
Nt5e	doi: 10.1016/j.celrep.2017.08.068, https://doi.org/10.1016/j.immuni.2007.09.010	Treg ChIP-seq, Treg *Irf4*$^{-/-}$ analysis
Pde3b	https://doi.org/10.1038/ni1437	Treg ChIP-seq
Prdm1	doi: 10.1016/j.celrep.2017.08.068.	Treg ChIP-seq
Satb1	doi: 10.1016/j.it.2015.04.006	Treg ChIP-seq
Socs2	https://doi.org/10.1038/ni1437	Treg *Irf4*$^{-/-}$ analysis
Tigit	doi: 10.1016/j.celrep.2017.08.068.	Treg ChIP-seq
Tnfrsf18	https://doi.org/10.1038/ni1437, doi: 10.1172/JCI130426	Treg ChIP-seq, Treg *Irf4*$^{-/-}$ analysis
Tnfrsf4	https://doi.org/10.1038/ni1437, doi: 10.1172/JCI130426	Treg ChIP-seq
Tnfrsf8	https://doi.org/10.1038/ni1437	Treg ChIP-seq
Tnfrsf9	https://doi.org/10.1038/ni1437, doi: 10.1172/JCI130426	Treg ChIP-seq, Treg *Irf4*$^{-/-}$ analysis

DANKSAGUNG